

**MICRONEEDLES ASSISTED IONTOPHORETIC TRANSDERMAL DELIVERY
OF DRUGS**

by

Kasturi Pawar

A Dissertation submitted to the Graduate Faculty of
Auburn University
in partial fulfillment of the
requirements for the Degree of
Doctor of Philosophy

Auburn, Alabama
December 14, 2013

Keywords: Transdermal, Microneedles, Iontophoresis, Lipophilicity, Nanoemulsion

Copyright 2013 by Kasturi Pawar

Approved by

Jayachandra B. Ramapuram, Chair, Associate Professor, Pharmacal Sciences
Daniel L. Parsons, Professor, Pharmacal Sciences
William R. Ravis, Professor, Pharmacal Sciences
C. Randall Clark, Professor, Pharmacal Sciences
Steve R. Duke, Associate Professor, Chemical Engineering

ABSTRACT

Topical/transdermal delivery offers an attractive alternative to oral and parenteral delivery in terms of non-invasiveness, administration and termination of dose and drug stability etc. However, the excellent barrier system of skin limits the number of drugs that can be delivered in therapeutic quantities to the site of action. Various approaches such as iontophoresis (ITP), microneedles (MN), chemical permeation enhancers, phonophoresis and synthesis of lipophilic analogues have been used to increase drug permeation across skin. ITP and MN have shown promising results in enhancing the topical transdermal delivery. Further, the combination of ITP and MN (ITP+MN) has shown additive or synergistic effects on transdermal drug delivery.

The effect of lipophilicity of drug on permeation across skin has been well reported. However, this effect has not been studied under the influence of ITP in microporated skin. Further, the effect of the lipophilicity of delivery vehicle on the transdermal delivery across microporated skin has not been reported. Thus, this dissertation focuses on studying the effect of lipophilicity of drug as well as the delivery vehicle on the skin permeation of drug across microporated skin under the influence of ITP.

To investigate the effect of drug's lipophilicity on its delivery across skin under the influence of ITP and MNs, we selected four model beta blocker drugs, propranolol, acebutolol, atenolol and sotalol, with similar molecular weights and pKa values but varied lipophilicity. The skin permeation of these drugs was studied under the influence of MNs, ITP and their

combination across dermatomed human skin. Both ITP and MNs enhanced the skin permeation of hydrophilic as well as lipophilic drugs when used alone. However the combination strategy showed synergistic enhancement for the delivery of hydrophilic drugs. This was attributed to the creation of aqueous channels by MNs that improved the delivery for hydrophilic drugs more than lipophilic drugs.

To investigate the effect of lipophilicity/polarity of the delivery vehicle on drug permeation across human skin, we formulated a nanoemulsion using fatty acids of varied lipophilicity, Caproic acid (C₆), Caprylic acid (C₈), Capric acid (C₁₀) and Lauric acid (C₁₂), for the delivery of a hydrophilic peptide molecule, Proline-Lysine-Valine (KPV). The polarity of the lipids had a significant influence on the delivery of KPV. A parabolic relationship was observed between hydrocarbon chain length and skin permeation rate. Both normal and microporated skin showed similar relationship with the hydrocarbon chain length, indicating that there is no influence of MN on this behavior. Further, the skin retention data of KPV indicated that the deposition of KPV enhanced with the lipophilicity of the fatty acid chain length.

ACKNOWLEDGMENTS

As I reach towards the culmination of my doctoral program, I would like to extend my heartiest gratitude to everyone, who provided me the kind support in one way or the other during this wonderful journey. I would like to dedicate my work to my parents, because of whose unconditional love, care and belief in me, I was able to reach this far and accomplish my desire of pursuing the doctoral degree.

I feel privileged to express my immense gratitude towards Dr. Jayachandra Babu Ramapuram, my mentor, for believing in my abilities and providing me with this opportunity. I am also indebted to him for his guidance, constant motivation and support, patience and freedom in lab to carry out the work. I am grateful to my committee members, Dr. Daniel Parsons, Dr. William Ravis, Dr. Randall Clark and Dr. Steve Duke, for their constant support and guidance throughout my doctoral studies.

I extend my sincere thanks to my collaborator, Dr. Chandra Sekhar Kolli for his valuable inputs and guidance for my research work. My special thanks to Dr. Forrest Smith, Dr. Vijay Rangari, Dr. Ram Gupta and Dr. Oldarin Fasina for providing their facilities and help to carry out my studies. I would like to thank Dr. Kevin Huggins for serving as an outside reader for my dissertation.

I am especially grateful to Dr. Sateesh Sathigari for not only teaching me various techniques in lab, but also for his immense help, in and outside the lab, and valuable inputs in my research work. Thanks are also due to my wonderful lab mates and friends, Julia, Li,

Mohammad, Philip and Haley for creating a joyous and cheerful lab ambience. Thanks would be a small word to express my gratitude towards Sharmila ma'am for her unconditional love, care and support. I am indebted to her for considering me as a family member and providing me a home away from home. I owe special thanks to Dr. Vanisree Mulabagal for her care, support and valuable suggestions for my research work. I also thank all my friends in Auburn for the wonderful time I spent during my stay here that has left an inerasable imprint on my heart.

Last but not the least, a very heartfelt thanks to my parents and family without whom I would not have achieved all this. I express deep sense of gratitude towards them for their great sacrifices, unreleting love and blessings, and for being the wind beneath my wings that helped me reach this far and will take me forward through the rest of my life.

TABLE OF CONTENTS

ABSTRACT	ii
ACKNOWLEDGEMENTS	iv
LIST OF FIGURES	xiii
LIST OF TABLES	xvi
1. INTRODUCTION	1
1.1 The skin.....	1
1.2 Topical/transdermal delivery	2
1.3 Iontophoresis assisted drug delivery	3
1.4 Factors affecting iontophoretic flux	5
1.4.1 Donor drug concentration	5
1.4.2 Effect of current strength	5
1.4.3 Effect of pH	6
1.4.4 Effect of ionic strength and presence of other ions	6
1.4.5 Types of electrodes used	7
1.4.6 Type of skin	8
1.5 Microneedles assisted drug delivery	8
1.5.1 Poke with patch delivery	9
1.5.2 Coat and poke	9
1.5.3 Poration followed by dissolving/soluble microneedles	10
1.5.4 Poration with hollow microneedles	10

1.6	Combination of iontophoresis and microneedles	11
1.7	References	13
2.	MATERIALS FOR TOPICAL NANOPARTICLE DELIVERY SYSTEMS	29
2.1	Abstract.....	29
2.2	Introduction	29
2.3	Polymeric materials in the formulation of nanoparticles	32
2.3.1	Chitosan	32
2.3.2	Poly(α) esters	35
2.3.3	Polyalkylcyanoacrylates (PACAS).....	41
2.3.4	Polyamidoamines (PAMAMs, dendritic polymers)	42
2.4	Solid and liquid lipids in the formulation of nanoparticles.....	45
2.4.1	Glyceride esters	47
2.4.2	Waxes	52
2.5	Stability of nanoparticles	57
2.5.1	Electrostatic stabilization.....	57
2.5.2	Steric stabilization.....	58
2.6	Toxicity of nanoparticles	60
2.7	Summary	62
2.8	Acknowledgements	64
2.9	References	64
3.	LIPIDS FOR TOPICAL NANOEMULSION DELIVERY SYSTEMS	99
3.1	Abstract	99
3.2	Introduction	99
3.3	Factors affecting drug permeation enhancement across the skin by nanoemulsions	101

3.3.1	Amount of drug	101
3.3.2	Type and amount of surfactant	101
3.3.3	Amount of water	103
3.3.4	Penetration enhancers	104
3.4	Permeation pathways for drug delivery by nanoemulsions	105
3.5	Lipid materials in the formulation of nanoemulsions	106
3.5.1	Vegetable oils	107
3.5.2	Fatty acids and alcohols	109
3.5.3	Glycerides and fatty acid esters	115
3.6	Conclusions	120
3.7	References	120
4.	EFFECT OF LIPOPHILICITY ON MICRONEEDLES-MEDIATED IONTOPHORETIC TRANSDERMAL DELIVERY ACROSS HUMAN SKIN <i>IN VITRO</i>	158
4.1	Abstract	158
4.2	Introduction	159
4.3	Experimental	161
4.3.1	Materials	161
4.3.2	Preparation of drug solution	162
4.3.3	Skin permeation studies	162
4.3.4	Drug extraction from skin	163
4.3.5	Iontophoresis	163
4.3.6	Microporation	164
4.3.7	Combination of iontophoresis and microporation	164
4.3.8	Analytical method	164

4.3.9 Data analysis	165
4.4 Results	165
4.4.1 Passive delivery	166
4.4.2 Iontophoresis.....	166
4.4.3 Microneedles.....	167
4.4.5 Combination strategy	167
4.5 Discussion	168
4.6 Conclusions	171
4.7 Acknowledgements	172
4.8 References.....	172
5. STABILITY-INDICATING HPLC ASSAY FOR LYSINE-PROLINE-VALINE (KPV) IN AQUEOUS SOLUTIONS	186
5.1 Abstract.....	186
5.2 Introduction.....	187
5.3 Experimental	187
5.3.1 Materials	187
5.3.2 Standard and sample preparation	188
5.3.3 Sample preparation and validation of the extraction procedure	186
5.3.4 Instrumentation and HPLC method development	189
5.3.5 Forced degradation studies	190
5.3.5.1 Acid hydrolysis	190
5.3.5.2 Alkaline hydrolysis.....	190
5.3.5.3 Oxidative degradation	190
5.3.5.4 LC/MS analysis of KPV and Lys-Pro-Diketopiperazine (DKP). 189	

5.4 Results	192
5.4.1 Development of HPLC method	192
5.4.2 Validation of analytical method	193
5.4.2.1 System suitability	193
5.4.2.2 Linearity	193
5.4.2.3 Specificity/Forced degradation study and characterization of degradation product	193
5.4.2.4 Accuracy	194
5.4.2.5 Precision.....	195
5.4.2.6 Limit of detection (LOD) and limit of quantitation (LOQ)	195
5.4.2.7 Application to skin homogenate samples	195
5.5 Discussion	196
5.6 Conclusions	197
5.7 Acknowledgements	197
5.8 References	197
6. ENHANCEMENT OF KPV DELIVERY USING IONTOPHORESIS ACROSS MICROPORATED HUMAN SKIN	205
6.1 Abstract.....	205
6.2 Introduction	206
6.3 Materials and methods	207
6.3.1 Materials	207
6.3.2 Skin permeation studies	207
6.3.3 Drug extraction from skin	208
6.3.4 Iontophoresis	208

6.3.5 Microporation studies	209
6.3.6 Combination of iontophoresis and microporation	209
6.3.7 Analytical method	210
6.3.8 Confocal imaging study for KPV	210
6.3.9 Data analysis	211
6.4 Results	211
6.4.1 Influence of current density	211
6.4.2 Influence of KPV concentration	212
6.4.3 Effect of various enhancement strategies	212
6.4.4 Effect of current duration	213
6.4.5 Confocal imaging	214
6.5 Discussion	214
6.6 Conclusions	217
6.7 References	217
7. DEVELOPMENT OF KPV NANOEMULSION FORMULATIONS FOR ENHANCED TOPICAL DELIVERY ACROSS HUMAN SKIN	230
7.1 Abstract	230
7.2 Introduction	231
7.3 Materials and methods	231
7.3.1 Materials	231
7.3.2 Formulation of KPV nanoemulsions	232
7.3.3 Viscosity Determination	232
7.3.4 Particle size and Zeta potential measurement	233
7.3.5 Skin permeation studies	233

7.3.6 Drug extraction from skin	234
7.3.7 Microporation studies	234
7.3.8 Analytical method	235
7.3.9 Data analysis	235
7.4 Results	235
7.4.1 Effect of hydrocarbon chain length of lipids on skin permeation of KPV	236
7.4.2 Effect of hydrocarbon chain length of lipids on skin retention of KPV	237
7.5 Discussion	237
7.6 Conclusions	240
7.7 References	240
8. SUMMARY AND FUTURE DIRECTIONS	248
Appendix: Journal Publications and Conference Presentations	251

LIST OF FIGURES

Figure 1.1: Pathways of drug transport across skin	27
Figure 1.2: Skin permeation enhancement techniques	27
Figure 1.3: Typical iontophoretic set up	28
Figure 1.4: Various ways of drug delivery using microneedles	28
Figure 2.1 Schematic representations of different topical solid nanoparticle systems	95
Figure 2.2 Permeation pathways for the nanoparticles in the skin	95
Figure 2.3 Structure of chitosan.....	96
Figure 2.4 Structure of PGA	96
Figure 2.5 Structure of PLA.....	96
Figure 2.6 Structure of PLGA.....	97
Figure 2.7 Structure of PCL.....	97
Figure 2.8 Structure of PACA	97
Figure 2.9 Structure of PAMAM monomer (A) and G5-NH ₂ PAMAM dendrimer (B)	98
Figure 2.10 Stabilization techniques used for nanoparticles	98
Figure 3.1 Structures of (a) W/O (b) O/W and (c) bicontinuous microemulsion	157
Figure 3.2 Permeation pathways for drug delivery by nanoemulsion	157
Figure 4.1 Permeation of propranolol HCl across dermatomed human skin.....	184
Figure 4.2 Permeation of acebutolol HCl across dermatomed human skin.....	184
Figure 4.3 Permeation of atenolol HCl across dermatomed human skin	185
Figure 4.4 Permeation of sotalol HCl across dermatomed human skin.....	185

Figure 5.1 HPLC chromatogram of KPV peptide	200
Figure 5.2 Typical calibration plot of lysine-proline-valine (KPV)	201
Figure 5.3 HPLC chromatogram of KPV spiked with proline, valine, proline-valine and lysine-proline	202
Figure 5.4 HPLC analysis of KPV under acidic (A) alkaline (B) and oxidative (C) stress conditions	203
Figure 5.5 LC/MS spectra of KPV degradation product, Lys-Pro-Diketopiperazine formed under stress conditions	204
Figure 6.1 Effect of applied current density on the iontophoretic delivery of KPV (10 mg/mL) across dermatomed human skin.....	226
Figure 6.2 Effect of KPV concentrations on its iontophoretic delivery across dermatomed human skin.....	226
Figure 6.3 Permeation profile for KPV across dermatomed human skin under the influence of iontophoresis across normal and microporated skin.....	227
Figure 6.4 Effect of applied current duration on the iontophoretic delivery of KPV with A) ITP and B) ITP+MN, across dermatomed human skin	228
Figure 6.5 Confocal imaging of skin after treatment with KPV-FITC to locate the depth of micro-pores after MN treatment.....	229
Figure 7.1 Effect of microneedles on the transdermal permeation of various nanoemulsions of KPV across dermatomed human skin. A) Delivery across Normal Skin (PD) B) Delivery across Microneedle Treated Skin (MN).....	245
Figure 7.2 Effect of microneedles on the transdermal flux of various nanoemulsions of KPV across dermatomed human skin. A) Delivery across Normal Skin (PD) B) Delivery across Microneedle Treated Skin (MN).....	246
Figure 7.3 Effect of microneedles on the skin retention of various nanoemulsions of KPV in the dermatomed human skin. A) Delivery across Normal Skin (PD) B) Delivery across Microneedle Treated Skin (MN).....	247

LIST OF TABLES

Table 2.1 Polymer based topical nanoparticles for enhanced skin permeation	85
Table 2.2 Wax and lipid based topical nanoparticles for enhanced skin permeation or epidermal targeting	89
Table 3.1 Lipids used in the formulation of topical and transdermal microemulsions.....	143
Table 4.1 Physicochemical properties and structures of beta blockers	179
Table 4.2 Chromatographic conditions for beta blocker analysis.....	180
Table 4.3 Steady state fluxes, lag times and skin retention data of various beta blockers	181
Table 4.4 Enhancement ratios calculated from the flux data of different beta blocker drugs ..	183
Table 5.1 System suitability parameters of HPLC method for the determination of KPV in aqueous solution	199
Table 5.2 Accuracy of HPLC method for the determination of KPV in aqueous solution	195
Table 5.3 Precision of HPLC method for the determination of KPV in aqueous solution.....	196
Table 6.1 Effect of applied current density and concentration and KPV on the iontophoretic delivery of KPV across dermatomed human skin	221
Table 6.2 Effect of MN and ITP and their combination (ITP+MN) on the permeation of KPV across dermatomed human skin	223
Table 6.3 Effect of current duration on the skin permeation of KPV across normal and microneedles treated human skin	224
Table 7.1 Composition and physical properties of microemulsion formulations of KPV	243
Table 7.2 Flux and skin retention data for various ME formulations of KPV	244

1. INTRODUCTION

1.1 THE SKIN

The skin is the largest human organ of the integumentary system and also an excellent biological barrier against chemical and biological insult.^{1,2} It is about 2 mm in thickness and accounts for nearly 4% of the total body weight. It is composed of three major components: the epidermis, dermis, and subcutaneous fat layer (hypodermis). The epidermis, which is the outermost skin layer, is typically 50-150 μm in thickness and it consists of five histologically distinct layers starting from the inside to the outside: stratum germinativum, stratum spinosum, stratum granulosum, stratum lucidum and stratum corneum. The main barrier for the permeation of drugs across the skin is its outermost layer, the stratum corneum (SC). It is 10 - 20 μm thick and made up of dead keratinized cells called corneocytes, which are embedded in a lipid matrix that renders the membrane practically impermeable to large and hydrophilic molecules. The lipid matrix is composed of multiple bilayers of ceramides, fatty acids, cholesterol and cholesterol esters. These bilayers form regions of semi-crystalline, gel and liquid crystal domains. Followed by the stratum corneum is the viable epidermis which is 50 - 100 μm thick and is avascular. Underneath this is the dermis, which is 1 - 2 mm thick and is highly vascular. It also contains fibroblasts, adipocytes, collagen, sensory nerve endings, sweat glands, some immunologically active cells, nerves, plus dermal lymph and blood capillaries.³⁻⁵

1.2 TOPICAL/TRANSDERMAL DELIVERY

Topical/transdermal delivery represents an attractive alternative to oral and parenteral delivery and offers various advantages. Transdermal delivery can prevent the degradation of active therapeutics by avoiding hepatic first-pass metabolism and the hostile gastrointestinal environment. It is non-invasive in application and provides a multi-day therapy from a single application. Further, it is easy to apply and remove when needed.^{6,7} However, the greatest challenge with transdermal/topical delivery is the limited number of drug molecules that can be effectively delivered through skin in therapeutic quantities. In order for the drug molecule to permeate the skin layers, it has to diffuse through the intracellular lipids and corneocytes in the stratum corneum via a tortuous pathway, which bestows a restriction on the molecular size, structure and lipophilicity requirements of the drug molecules.

The drug can permeate into the skin via three pathways: (a) transcellular, (b) inter/paracellular and (c) trans-appendageal (Figure 1.1). Transcellular route involves sequential partitioning of the drug in the cell and intercellular lipids while it traverses down the skin layers, whereas inter/paracellular route involves movement of drug molecules through the lipid pathways between the cells. Trans-appendageal pathway involves movement of molecules through skin appendages such as hair follicles and sweat glands.⁸ Thus, for a drug molecule to permeate through skin layers via any of these pathways it should have optimal lipophilicity and molecular weight, which reduces the number of drug candidates qualifying for topical/transdermal delivery. Thus in order to increase the range of number of therapeutic molecules for delivery through skin, three types of permeation enhancing techniques is used: Physical approach, chemical approach and biochemical approach. Physical approach includes stripping or hydration of stratum corneum, ITP or phonophoresis, heat or thermal energy

abrasion, and microneedles application. Chemical enhancement involves synthesis of lipophilic analogues, delipidization of stratum corneum, and administration of chemical skin permeation enhancers. Biochemical approach involves synthesizing bioconvertible prodrugs and co-administration of skin metabolism inhibitors (Figure 1.2). The ITP and microneedles techniques have shown encouraging results for various drugs that are difficult-to-deliver across skin and thus, are gaining large popularity among the scientific community.

1.3 IONTOPHORESIS ASSISTED DRUG DELIVERY

Iontophoresis is a second-generation permeation enhancement technique.⁷ It involves facilitated delivery of ions of soluble salt of drug under an externally applied current.⁹ It is based on the general principle of electricity i.e. like repels like. Thus, in order to deliver a positively charged drug (cation), it is placed under a negatively charged electrode (cathode), and vice-versa.¹⁰ The iontophoretic mechanism comprises several processes for moving molecules across the skin: molecular diffusion, electromigration and electroosmosis. Electromigration is the movement of charged ionic species in response to the applied electric field and this is the primary process in delivering charged drugs. Electroosmosis, on the other hand, is the induced solvent flow due to the movement of charged species. This process is useful for delivering both charged and neutral drugs.¹¹ The contribution and dominance from these processes during drug delivery has been studied by various researchers.¹²⁻¹⁴ A schematic of a typical iontophoretic set up is depicted in Figure 1. 3.

An iontophoretic device includes a power source and two electrode compartments. The drug is often in its salt formulation (D^+A^-). The ionized molecule (D^+) and its counter ion (A^-) are placed in the donor compartment bearing the same charge (e.g. a positively charged drug

such as lidocaine would be placed in the anodal compartment). The receptor compartment contains biologically acceptable cations (C^+) and anions (A^-), and is placed at a distal site on the skin.^{11,15} Generally silver/silver chloride is used as an anode and cathode, respectively. Once the current is applied, the electric field imposes a direction on the movement of the ions present due to which the positive charges in the anodal compartment move towards the cathode and anions move in the opposite direction. This is known as electromigratory movement. The drug ions migrate together with the cationic ions into the skin, endogenous anions, mostly chloride; migrate from the body into the donor reservoir.¹⁶ In the cathodal chamber, Cl^- ions are released from the electrode since for maintaining the electroneutrality, it is required that either an anion is lost from the cathodal chamber or that a cation enters the chamber from the skin.

The predominant pathway of iontophoretic transport is via skin appendages (hair follicles and sweat glands); however the extracellular routes across the SC also contribute to enhanced drug delivery.¹⁷ The main advantage of ITP is that drug delivery is directly proportional to the amount of electrical potential applied, thus considerably reducing the inter- and intra-subject variability. Further, ITP offers an opportunity for programmable drug delivery to tailor the dosage regimen based on an individual.^{11,18-20} It has an advantage in terms of effectively delivering both ionized and unionized drugs. In addition, it also enables continuous or pulsatile delivery and systemic or local delivery of drugs, depending upon the dosage regimen.^{21,22} Thus, ITP is highly effective in delivering polar and high molecular weight compounds. However, since ITP does not primarily alter the skin barrier itself, it is limited to ionizable as well as unionizable drug molecules with molecular weights $<10,000$ Daltons.^{16,23,24} Further, the maximum amount of current that can be used is limited to 0.5 mA, as beyond this limit the skin may develop allergic and irritant reactions.

1.4 FACTORS AFFECTING IONTOPHORETIC FLUX

1.4.1 DONOR DRUG CONCENTRATION

Generally a linear relationship is observed between the donor drug concentration and iontophoretic flux, as seen from many studies reported in literature for drugs like metoprolol,²⁵ diclofenac sodium,²⁶ rotigotine²⁷ and ketorolac.²⁸ However, beyond a certain point, the flux plateaus and any further increase in the concentration does not increase the flux.^{29,30} This is attributed to the charge saturation of the aqueous conducting pathways of skin.³¹ This indicates that the concentrations and mobilities of competing ions play an important role, and thus, the physicochemical properties of the drug should be taken into account. In some cases, even a more complex relationship is observed between the drug concentration and iontophoretic flux values. Some lipophilic drugs, such as propranolol, nafarelin and leuprolide, which showed a reduction in drug delivery when the concentration was increased beyond a certain point.³²⁻³⁵ This was attributed to the alteration in the permselectivity of the skin. In the absence of competing ions, in the case of lidocaine hydrochloride²⁹ or R-apomorphine hydrochloride,³⁰ the iontophoretic flux was found to be independent of the donor drug concentration.

1.4.2 EFFECT OF CURRENT STRENGTH

In general, in the case of small molecules and peptides, the electromigratory contribution to iontophoretic flux is linearly proportional to the applied current, provided the respective ion concentrations are kept constant. Various literature reports show that a linear relationship exists between the apparent flux and current for a number of drugs such as ketorolac,²⁸ gonadotropin releasing hormone (LHRH) and its analogues,³⁶ methyl phenidate hydrochloride,³⁷ thyrotropin releasing hormone,³⁸ verapamil,³⁹ sodium diclofenac⁴⁰ etc. The maximum current that can be

used in humans is $0.5\text{mA}/\text{cm}^2$ as beyond this, it causes irritation reactions and damage to the skin.¹⁵

1.4.3 EFFECT OF pH

pH of the donor solution has a substantial effect on iontophoretic drug delivery. Most drugs have a broad pH range for their solubility and stability for iontophoretic delivery. However, optimal drug delivery and biocompatibility are usually limited to a narrow range of donor solution pH. Since the skin has an iso-electric point of pH 4,⁴¹ the pH of the donor solution influences the permselectivity of the skin. Above pH 4, the carboxylic acid moieties in the skin becomes ionized which favors and increases the anodal iontophoretic flux for cationic drugs.¹³ The pH of the donor solution also affects the ionization of the drug itself and a weakly basic drug is ionized to a lower extent at a pH higher than its pKa and will not permeate.⁴²

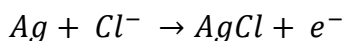
1.4.4 EFFECT OF IONIC STRENGTH AND PRESENCE OF OTHER IONS

It is desirable in ITP for the drug ion to carry maximum charge across the membrane for enhanced delivery. Addition of a salt is necessary for the electrochemical reaction in the ITP and drug delivery. However, an increase in ionic strength decreases drug delivery, since the extraneous ions now compete with the drug ions for carrying the charge.⁴³ The buffering agents used in ITP are a main source of co-ions. They are generally more mobile and smaller in size as compared to the drug ions, thus they dominate the penetration into the skin and cause a decrease in transdermal flux of the drug. Several literature reports indicate the effect of extraneous ions due to buffers and salts on drug delivery. For example, ketorolac showed increased flux with decrease in ionic strength.²⁸ Increase in the concentration of HEPES buffer decreased salicylic

acid flux across human skin.⁴⁴ 9-desglycinamide and 8-arginine-vasopressin,⁴⁵ salmon calcitonin⁴⁶ and leuprolide⁴⁷ showed a higher flux occurring at low electrolyte concentration.

1.4.5 TYPES OF ELECTRODES USED

Electrodes are used in ITP to serve as the bridge between the electric circuit and the two reservoirs, and to carry out the electrochemical reaction. An ideal electrode system must meet a variety of performance, compatibility and physical requirements. The electrodes used could be non-consumable or consumable based on whether they get depleted in the process. Although the non-consumable electrodes made up of stainless steel or platinum are advantageous for lasting long, they can release metal ions through direct oxidation at the anode or indirectly by the creation of a caustic environment at the cathode. Further, platinum electrodes cause hydrolysis of water resulting in significant alteration of pH of the solution. Thus, the preferred electrodes are consumable ones made of silver and silver-chloride serving as anode and cathode, respectively, since they do not change the pH (like sharp decreases in pH have been seen with platinum electrodes). The only disadvantage of silver/silver chloride electrodes is the consumption and accumulation of chloride ions at the anode and cathode, respectively.⁴⁸⁻⁵⁰ Since the electrochemical reaction for silver electrodes occur at voltages lower than that necessary for the electrolysis of water, the electrodes do not react with water and cause any side effects such as acid-induced skin burns due to the proton created at the anode site. The following reactions occur at the anode.⁵¹



The final product is silver chloride, which forms on the surface of the silver anode. It is electrically neutral and practically insoluble, and, therefore, it does not generate species that compete with cationic drugs for delivery.⁵²

1.4.6 TYPE OF SKIN

Type of skin and skin condition also affects drug delivery by ITP. *In vivo* studies have shown that skin from different areas of human body have different effects on passive diffusion of drugs. The rank order for passive delivery is abdomen>forearm> instep >heel>planter for all subjects. In addition, it is reported that passive diffusion occurred maximally from the area with numerous hair follicle and lesser in area with thickest stratum corneum.⁵³

ITP technology is in use at commercial level and there are several products available on market such as, Lidosite[®], Iomed Phoresor[®] II, E-Trans, Activadose[®] II, OcuPhor[™] and Dupel[®].

1.5 MICRONEEDLES ASSISTED DRUG DELIVERY

MN technology is a third generation enhancement strategy.⁵⁴ It involves temporary physical disruption of the stratum corneum barrier using micron-sized needles. The concept of using these small needles of up to a few hundred microns to breach the stratum corneum was first proposed by Henry et al.⁵⁵ The MN pierce across the epidermis and sometimes into the superficial dermis and create micron-scale aqueous conduits for drug transport into the skin.⁵⁶ The pores created are in the nanometer range and are big enough for macromolecules to pass through, but small enough not to cause any discomfort or damage of clinical significance.⁵⁷ Further, an *in vivo* study proved that this technology is painless since the MN reach only up to the epidermis/superficial dermis and the pain sensory nerve endings are located in the papillary

(upper) dermis along side the capillaries and lymphatic vessels.⁵⁸ MN can be comprised of various materials such as metal, titanium, silicon, polymer, glass, ceramic and sugars.⁵⁶

There are four different ways of delivering drugs using MN technology as shown in Figure 1.4: 1) poke with patch, 2) coat and poke, 3) poration followed by dissolving MN and 4) poration with hollow MN.

1.5.1 POKE WITH PATCH DELIVERY

In this method, first solid MN are applied on to the skin to create the microchannels and then removed. This is followed by the application of a patch containing drug so that the drug can diffuse through the created microchannels.^{54,59} Various drugs and macromolecules have been delivered using this technology such as oligonucleotides,⁶⁰ insulin,⁶¹ desmopressin,⁶² naltrexone,⁶³ deoxynucleic acid⁶⁴ etc. The advantages with this technique are that extended release of the drugs can be achieved using the patch system and no pump or encapsulation/coating process is required. However no precise dosing can be achieved.

1.5.2 COAT AND POKE

This approach involves using solid MN that are coated with the drug solution, hence once poked; they deliver the drug into the viable skin layers. These drug-coated microneedle arrays are, just as in the “poke with patch” approach but in a single-unit drug delivery system. Drugs such as desmopressin,⁶² calcein, vitamin B and bovine serum albumin,⁶⁵ immunotherapeutics,⁶⁶ ovalbumin,⁶⁷ lidocaine⁶⁸ etc. are delivered efficiently using this technique. The advantage of this method is that the microneedle strength is retained after coating. Further, no patch or pump is required and precise dosing can be achieved. However, only a small dose can be coated onto the

MN, thus it is not an efficient technique for large dose drugs. Further, the coating may result in reduction of microneedle sharpness/penetration ability.

1.5.3 PORATION FOLLOWED BY DISSOLVING/SOLUBLE MICRONEEDLES

This technique has the drug encapsulated in the microneedle matrix made of polymers or sugars.^{56,69} Various materials used to synthesize dissolving MN include carboxymethyl cellulose,⁷⁰ chondroitin sulfate,⁷¹⁻⁷³ dextrin,⁷⁴⁻⁷⁶ poly vinyl pyrrolidones,^{77,78} PVA,^{79,80} polylactide co-glycolide,^{81,82} fibroin⁸³ and sugars^{84,85} etc.

Biodegradable MN dissolve/degrade in the skin after application, thereby releasing the incorporated drugs. The main advantage with this technique is that precise and sustained delivery up to months can be achieved by choosing a suitable polymer.⁸⁶ Furthermore, since these MN eventually dissolve/disappear, there is no risk of bio-hazardous sharp waste. However, it suffers from disadvantages such as limited drug loading ability and impaired microneedle strength and penetration ability.⁶⁹ Various compounds have been delivered using dissolving or soluble MN including calcein and bovine serum albumin,⁸² erythropoietin,⁷⁶ insulin,⁸⁷ lysozyme,⁷⁰ model drug, sulforhodamine B,⁷⁹ influenza vaccine,⁷⁸ recombinant human growth hormone and desmopressin.⁸⁸

1.5.4 PORATION WITH HOLLOW MICRONEEDLES

In contrast to the solid MN discussed above, hollow MN offer the possibility of delivering drugs through the interior of well-defined needles by diffusion or, for more rapid rates of delivery, by force/pressure-driven flow. Hence, the mechanism of this technique is delivery via the “poke and flow” approach. The advantage of this technique is that the dose of the desired

drug in solution can be more easily controlled according to the need of the patient. The main disadvantage of this technique is that the flow rates are normally quite low (50 - 300 nL/min).⁵⁷ At the same time the drug solution may clog the bore. In addition, the strength of the MN may get impaired due to the hollow nature and there is an increased risk of leakage for arrays.⁶⁹ Efficient delivery of drugs such as insulin,⁸⁹ lidocaine,⁹⁰ nicotine derivatives,^{91,92} influenza vaccine^{93,94} etc were achieved using hollow MN systems. Further, the hollow MN system for intradermal influenza vaccines is commercially available under the trade name, BD Soluvia™ (Becton Dickinson, NJ, USA).^{95,96}

1.6 COMBINATION OF IONTOPHORESIS AND MICRONEEDLES

As reported and reviewed by various researchers, combining more than one permeation enhancement technique can result in additive or synergistic delivery of drugs across the skin.⁹⁷⁻¹⁰⁰ Combination of ITP and MN has provided encouraging results in maximizing drug delivery for various drugs such as salbutamol,¹⁰¹ prochlorperazine edisylate,¹⁰² calcein and human growth hormone,¹⁰³ deuterated water and fluorescein isothiocyanate – dextran complex,¹⁰⁴ ropinirole hydrochloride,²⁴ methotrexate,⁹⁹ leuprolide,¹⁰⁵ etc.

Recently nanoparticulate carriers such as polymeric nanospheres, nanocapsules, dendrimers, solid lipid nanoparticles (SLNs) and nanostructured lipid carriers (NLCs) have been utilized in an attempt to alter the skin barrier and deliver the drug and cosmetic actives of interest. The advantages with nanoparticulate delivery are that in addition to their direct effects on the skin barrier, due to their small size, they also provide an occlusive barrier resulting in hydration and better permeation of drugs. Various vaccines, macromolecules and other therapeutic moieties have been delivered transdermally and topically using particulate drug

carrier systems with the use of either passive delivery or permeation enhancement techniques.^{104,106-111}

It is reported in literature that the combination of ITP and MN can result in additive or synergistic effects on drug delivery; however the effect of lipophilicity, an inherent property of the drug molecule, on the skin permeation has not been studied on microporated skin or under the influence of ITP or the combination of the two.

Thus, the aim of our study was to investigate the effect of lipophilicity of drugs on their iontophoretic delivery through microporated skin. The outcome of this study could provide an insight into the versatility of this combination approach for enhancing the transdermal delivery of molecules. Further, in a separate study, we also investigated the effect of polarity of lipid vehicles in a nano-size formulation under the influence of MN. The effect of chain length and polarity of fatty acids on skin permeation of drugs has been evaluated by several researchers.¹¹²⁻¹¹⁷ However, the effect of lipophilicity or polarity of the lipid on the skin permeation of drugs across microporated skin has not been reported. Thus, in the second study, we developed nanoemulsion formulations of a model peptide, Proline-Lysine-Valine (KPV) using fatty acids of varied polarity to evaluate the effect of chain length on KPV permeation in microporated human skin.

1.7 REFERENCES

1. Cevc G, Vierl U. 2010. Nanotechnology and the transdermal route: A state of the art review and critical appraisal. *J Control Release* 141(3):277-299
2. Hadgraft J. 2001. Modulation of the barrier function of the skin. *Skin Pharmacol Appl Skin Physiol* 14 Suppl 1 72-81.
3. Barry BW. 2004. Breaching the skin's barrier to drugs. *Nat Biotechnol* 22(2):165-167
4. Morrow DIJ, McCarron PA, Woolfson AD, Donnelly RF. 2007. Innovative Strategies for Enhancing Topical and Transdermal Drug Delivery. *The Open Drug Delivery Journal* 1 36-59.
5. Barry BW, Williams AC. 1995. Permeation enhancement through skin. In *Encyclopedia of Pharmaceutical Technology*; Swarbrick J, Boylan JC, Ed.; Marcel Dekker: New York; pp:449–493.
6. Paudel KS, Milewski M, Swadley CL, Brogden NK, Ghosh P, Stinchcomb AL. 2010. Challenges and opportunities in dermal/transdermal delivery. *Ther Deliv* 1(1):109-131.
7. Prausnitz MR, Langer R. 2008. Transdermal drug delivery. *Nat Biotechnol* 26(11):1261-1268.
8. Naik A, Kalia YN, Guy RH. 2000. Transdermal drug delivery: overcoming the skin's barrier function. *Pharm Sci Technolo Today* 3(9):318-326.
9. Guy RH. 2010. Transdermal drug delivery. In *Handbook of Experimental Pharmacology*; M Schäfer-Korting, Ed.; Springer: Berlin; pp.399-410.
10. Singh P, Maibach HI. 1996. Iontophoresis: an alternative to the use of carriers in cutaneous drug delivery. *Adv Drug Deliv Rev* 18(379-394).

11. Phipps JB, Padmanabhan RV, Lattin GA. 1989. Iontophoretic delivery model inorganic and drug ions. *J Pharm Sci* 78(5):365–369.
12. Abla N, Naik A, Guy RH, Kalia YN. 2005. Contributions of electromigration and electroosmosis to peptide iontophoresis across intact and impaired skin. *J Control Release* 108(2-3):319-330
13. Marro D, Kalia YN, Delgado-Charro MB, Guy RH. 2001. Contributions of electromigration and electroosmosis to iontophoretic drug delivery. *Pharm Res* 18(12):1701-1708
14. Sieg A, Guy RH, Delgado-Charro MB. 2004. Electroosmosis in transdermal iontophoresis: implications for noninvasive and calibration-free glucose monitoring. *Biophys J* 87(5):3344-3350.
15. Kalia YN, Naik A, Garrison J, Guy RH. 2004. Iontophoretic drug delivery. *Adv Drug Deliv Rev* 56(5):619-658.
16. Wang Y, Thakur R, Fan Q, Michniak B. 2005. Transdermal iontophoresis: combination strategies to improve transdermal iontophoretic drug delivery. *Eur J Pharm Biopharm* 60(2):179-191.
17. Essa EA, Bonner MC, Barry BW. 2002. Human skin sandwich for assessing shunt route penetration during passive and iontophoretic drug and liposome delivery. *J Pharm Pharmacol* 54(11):1481-1490.
18. Bellantone NH, Rim S, Francoeur ML, Rasadi B. 1986. Enhanced percutaneous absorption via iontophoresis, I: evaluation of an in vitro system and transport of model compounds. *Int J Pharm* 30(1):63-72

19. Burnette RR, Ongpipattanakul B. 1987. Characterization of the permselective properties of excised human skin during iontophoresis. *J Pharm Sci* 76(10):765-773
20. Singh P, Maibach HI. 1996. Iontophoresis: an alternative to the use of carriers in cutaneous drug delivery. *Adv Drug Deliv Rev* 18(3):379–394.
21. Williams AC, Barry BW. 1991. Terpenes and the lipid-protein-partitioning theory of skin penetration enhancement. *Pharm Res* 8(1):17-24
22. Williams AC, Barry BW. 1992. Skin absorption enhancers. *Crit Rev Ther Drug Carrier Syst* 9(3-4):305-353.
23. Kalaria DR, Patel P, Patravale V, Kalia YN. 2012. Comparison of the cutaneous iontophoretic delivery of rasagiline and selegiline across porcine and human skin in vitro. *Int J Pharm* 438(1-2):202-208.
24. Singh ND, Banga AK. 2013. Controlled delivery of ropinirole hydrochloride through skin using modulated iontophoresis and microneedles. *J Drug Target* 21(4):354-366.
25. Thysman S, Preat V, Roland M. 1992. Factors affecting iontophoretic mobility of metoprolol. *J Pharm Sci* 81(7):670-675.
26. Koizumi T, Kakemi M, Katayama K, Inada H, Sudeji K, Kawasaki M. 1990. Transfer of diclofenac sodium across excised guinea pig skin on high-frequency pulse iontophoresis. II. Factors affecting steady-state transport rate. *Chem Pharm Bull (Tokyo)* 38(4):1022-1023.
27. Nugroho AK, Li GL, Danhof M, Bouwstra JA. 2004. Transdermal iontophoresis of rotigotine across human stratum corneum in vitro: influence of pH and NaCl concentration. *Pharm Res* 21(5):844-850.

28. Tiwari SB, Udupa N. 2003. In vitro iontophoretic transport of ketorolac: synthetic membrane as a barrier. *Drug Deliv* 10(3):161-168.
29. Marro D, Kalia YN, Delgado-Charro MB, Guy RH. 2001. Optimizing iontophoretic drug delivery: identification and distribution of the charge-carrying species. *Pharm Res* 18(12):1709-1713.
30. van der Geest R, van Laar T, Gubbens-Stibbe JM, Bodde HE, Danhof M. 1997. Iontophoretic delivery of apomorphine. II: An in vivo study in patients with Parkinson's disease. *Pharm Res* 14(12):1804-1810.
31. Sanderson JE, de Riel S, Dixon R. 1989. Iontophoretic delivery of nonpeptide drugs: formulation optimization for maximum skin permeability. *J Pharm Sci* 78(5):361-364.
32. Delgado-Charro MB, Guy RH. 1995. Iontophoretic delivery of nafarelin across the skin. *Int J Pharm* 117(2):165-172
33. Delgado-Charro MB, Rodríguez-Bayón AM, Guy RH. 1995. Iontophoresis of nafarelin: Effects of current density and concentration on electrotransport in vitro. *J Control Release* 35(1):35-40
34. Hirvonen J, Guy RH. 1997. Iontophoretic delivery across the skin: electroosmosis and its modulation by drug substances. *Pharm Res* 14(9):1258-1263
35. Hoogstraate AJ, Srinivasan V, Sims SM, Higuchi WI. 1994. Iontophoretic enhancement of peptides: behaviour of leuprolide versus model permeants. *J Control Release* 31(1):41-47.
36. Miller LL, Kolaskie CJ, Smith GA, Rivier J. 1990. Transdermal iontophoresis of gonadotropin releasing hormone (LHRH) and two analogues. *J Pharm Sci* 79(6):490-493.

37. Singh P, Boniello S, Liu P, Dinh S. 1999. Transdermal iontophoretic delivery of methylphenidate HCl in vitro. *Int J Pharm* 178(1):121-128.
38. Burnette RR, Marrero D. 1986. Comparison between the iontophoretic and passive transport of thyrotropin releasing hormone across excised nude mouse skin. *J Pharm Sci* 75(8):738-743.
39. Wearley L, Jue-Chen L, Chien YW. 1989. Iontophoresis-facilitated transdermal delivery of verapamil I. In vitro evaluation and mechanistic studies. *J Control Release* 8(3):237–250.
40. Hui X, Anigbogu A, Singh P, Xiong G, Poblete N, Liu P, Maibach HI. 2001. Pharmacokinetic and local tissue disposition of [14C]sodium diclofenac following iontophoresis and systemic administration in rabbits. *J Pharm Sci* 90(9):1269-1276.
41. Luzardo-Alvarez A, Rodriguez-Fernandez M, Blanco-Mendez J, Guy RH, Delgado-Charro MB. 1998. Iontophoretic permselectivity of mammalian skin: characterization of hairless mouse and porcine membrane models. *Pharm Res* 15(7):984-987.
42. Subedi RK, Oh SY, Chun MK, Choi HK. 2010. Recent advances in transdermal drug delivery. *Arch Pharm Res* 33(3):339-351.
43. Dixit N, Bali V, Baboota S, Ahuja A, Ali J. 2007. Iontophoresis- An Approach for Controlled Drug Delivery: A Review. *Curr Drug Deliv* 4(1):1-10.
44. Yoshida NH, Roberts MS. 1995. Prediction of cathodal iontophoretic transport of various anions across excised skin from different vehicles using conductivity measurements. *J Pharm Pharmacol* 47(11):883-890.
45. Craane-van Hinsberg WH, Bax L, Flinterman NH, Verhoef J, Junginger HE, Bodde HE. 1994. Iontophoresis of a model peptide across human skin in vitro: effects of

- iontophoresis protocol, pH, and ionic strength on peptide flux and skin impedance. *Pharm Res* 11(9):1296-1300.
46. Morimoto K, Iwakura Y, Nakatani E, Miyazaki M, Tojima H. 1992. Effects of proteolytic enzyme inhibitors as absorption enhancers on the transdermal iontophoretic delivery of calcitonin in rats. *J Pharm Pharmacol* 44(3):216-218.
 47. Lu MF, Lee D, Carlson R, Subba Rao G, Hui HW, Adjei L, Herrin M, Sundberg D, Hsu L. 1993. The Effects of Formulation Variables on Iontophoretic Transdermal Delivery of Leuprolide to Humans. *Drug Dev Ind Pharm* 19(13):1557-1571.
 48. Delgado-Charro MB, Guy RH. 2003. Iontophoresis: Applications in drug delivery and noninvasive monitoring. In *Transdermal drug delivery*, Guy RH, Hadgraft J, Ed.; New York: Marcel Dekker; pp:199-225.
 49. Anigbogu AN, Maibach HI. 2004. Iontophoresis. In *Dermatotoxicology*, Zhai H, Maibach HI, Ed.; Boca Raton: CRC Press; pp:151-180
 50. Singh P, Liu P, Dinh SM. 2001. Facilitated transdermal delivery by iontophoresis. In *Topical Absorption of Dermatological Products*, Bronaugh RL, Maibach HI, Ed.; New York: Marcel Dekker; pp:334-355.
 51. Phipps JB, Scott ER, Gyory JRP, Padmanabhan RV. 2002. In *Encyclopedia of Pharmaceutical Technology*, Swarbrick J, Boylan P, Ed.; New York: Marcel Dekker; pp:1578-1588.
 52. Scott ER, Phipps JB, Gyory JRP, Padmanabhan RV. 2000. Electrotransport systems for transdermal delivery:A practical implementation of iontophoresis. In *Handbook of pharmaceutical controlled release society*, Wise DL, Ed.; New York: Marcel Dekker; pp:617-660.

53. Roberts MS, Favretto WA, Meyer A, Reckmann M, Wongseelashote T. 1982. Topical bioavailability of methyl salicylate. *Aust N Z J Med* 12(3):303-305.
54. Banga AK. 2009. Microporation applications for enhancing drug delivery. *Expert Opin Drug Deliv* 6(4):343-354.
55. Henry S, McAllister DV, Allen MG, Prausnitz MR. 1998. Microfabricated microneedles: a novel approach to transdermal drug delivery. *J Pharm Sci* 87(8):922-925.
56. Kim YC, Park JH, Prausnitz MR. 2012. Microneedles for drug and vaccine delivery. *Adv Drug Deliv Rev* 64(14):1547-1568.
57. Prausnitz MR. 2004. Microneedles for transdermal drug delivery. *Adv Drug Deliv Rev* 56(5):581-587.
58. Kaushik S, Hord AH, Denson DD, McAllister DV, Smitra S, Allen MG, Prausnitz MR. 2001. Lack of pain associated with microfabricated microneedles. *Anesth Analg* 92(2):502-504.
59. Sivamani RK, Liepmann D, Maibach HI. 2007. Microneedles and transdermal applications. *Expert Opin Drug Deliv* 4(1):19-25.
60. Lin W, Cormier M, Samiee A, Griffin A, Johnson B, Teng CL, Hardee GE, Daddona PE. 2001. Transdermal delivery of antisense oligonucleotides with microprojection patch (Macroflux) technology. *Pharm Res* 18(12):1789-1793.
61. Martanto W, Davis SP, Holiday NR, Wang J, Gill HS, Prausnitz MR. 2004. Transdermal delivery of insulin using microneedles in vivo. *Pharm Res* 21(6):947-952.
62. Cormier M, Johnson B, Ameri M, Nyam K, Libiran L, Zhang DD, Daddona P. 2004. Transdermal delivery of desmopressin using a coated microneedle array patch system. *J Control Release* 97(3):503-511.

63. Banks SL, Pinninti RR, Gill HS, Crooks PA, Prausnitz MR, Stinchcomb AL. 2008. Flux across [corrected] microneedle-treated skin is increased by increasing charge of naltrexone and naltrexol in vitro. *Pharm Res* 25(7):1677-1685.
64. Chabri F, Bouris K, Jones T, Barrow D, Hann A, Allender C, Brain K, Birchall J. 2004. Microfabricated silicon microneedles for nonviral cutaneous gene delivery. *Br J Dermatol* 150(5):869-877.
65. Gill HS, Prausnitz MR. 2007. Coated microneedles for transdermal delivery. *J Control Release* 117(2):227-237.
66. Chen X, Prow TW, Crichton ML, Jenkins DW, Roberts MS, Frazer IH, Fernando GJ, Kendall MA. 2009. Dry-coated microprojection array patches for targeted delivery of immunotherapeutics to the skin. *J Control Release* 139(3):212-220.
67. Matriano JA, Cormier M, Johnson J, Young WA, Buttery M, Nyam K, Daddona PE. 2002. Macroflux microprojection array patch technology: a new and efficient approach for intracutaneous immunization. *Pharm Res* 19(1):63-70.
68. Zhang Y, Brown K, Siebenaler K, Determan A, Dohmeier D, Hansen K. 2012. Development of lidocaine-coated microneedle product for rapid, safe, and prolonged local analgesic action. *Pharm Res* 29(1):170-177.
69. van der Maaden K, Jiskoot W, Bouwstra J. 2012. Microneedle technologies for (trans)dermal drug and vaccine delivery. *J Control Release* 161(2):645-655.
70. Lee JW, Park JH, Prausnitz MR. 2008. Dissolving microneedles for transdermal drug delivery. *Biomaterials* 29(13):2113-2124.

71. Ito Y, Hagiwara E, Saeki A, Sugioka N, Takada K. 2007. Sustained-release self-dissolving micropiles for percutaneous absorption of insulin in mice. *J Drug Target* 15(5):323-326
72. Ito Y, Hasegawa R, Fukushima K, Sugioka N, Takada K. 2010. Self-dissolving micropile array chip as percutaneous delivery system of protein drug. *Biol Pharm Bull* 33(4):683-690
73. Ito Y, Ohashi Y, Saeki A, Sugioka N, Takada K. 2008. Antihyperglycemic effect of insulin from self-dissolving micropiles in dogs. *Chem Pharm Bull (Tokyo)* 56(3):243-246.
74. Ito Y, Hagiwara E, Saeki A, Sugioka N, Takada K. 2006. Feasibility of microneedles for percutaneous absorption of insulin. *Eur J Pharm Sci* 29(1):82-88
75. Ito Y, Murakami A, Maeda T, Sugioka N, Takada K. 2008. Evaluation of self-dissolving needles containing low molecular weight heparin (LMWH) in rats. *Int J Pharm* 349(1-2):124-129.
76. Ito Y, Yoshimitsu J, Shiroyama K, Sugioka N, Takada K. 2006. Self-dissolving microneedles for the percutaneous absorption of EPO in mice. *J Drug Target* 14(5):255-261.
77. Sullivan SP, Murthy N, Prausnitz MR. 2008. Minimally invasive protein delivery with rapidly dissolving polymer microneedles. *Adv Mater* 20(5):933-938.
78. Sullivan SP, Koutsonanos DG, Del Pilar Martin M, Lee JW, Zarnitsyn V, Choi SO, Murthy N, Compans RW, Skountzou I, Prausnitz MR. 2010. Dissolving polymer microneedle patches for influenza vaccination. *Nat Med* 16(8):915-920.

79. Chu LY, Prausnitz MR. 2011. Separable arrowhead microneedles. *J Control Release* 149(3):242-249.
80. Wendorf JR, Ghartey-Tagoe EB, Williams SC, Enioutina E, Singh P, Cleary GW. 2011. Transdermal delivery of macromolecules using solid-state biodegradable microstructures. *Pharm Res* 28(1):22-30.
81. Park JH, Allen MG, Prausnitz MR. 2005. Biodegradable polymer microneedles: Fabrication, mechanics and transdermal drug delivery. *J Control Release* 104(1):51–66.
82. Park JH, Allen MG, Prausnitz MR. 2006. Polymer microneedles for controlled-release drug delivery. *Pharm Res* 23(5):1008-1019.
83. You X, Chang JH, Ju BBK, Pak JJ. 2011. Rapidly dissolving fibroin microneedles for transdermal drug delivery. *Materials Science and Engineering: C* 31(8):1632–1636.
84. Martin CJ, Allender CJ, Brain KR, Morrissey A, Birchall JC. 2012. Low temperature fabrication of biodegradable sugar glass microneedles for transdermal drug delivery applications. *J Control Release* 158(1):93-101
85. Miyano T, Tobinaga Y, Kanno T, Matsuzaki Y, Takeda H, Wakui M, Hanada K. 2005. Sugar micro needles as transdermic drug delivery system. *Biomed Microdevices* 7(3):185-188.
86. Park JH, Choi SO, Kamath R, Yoon YK, Allen MG, Prausnitz MR. 2007. Polymer particle-based micromolding to fabricate novel microstructures. *Biomed Microdevices* 9(2):223-234.
87. Migalska K, Morrow DI, Garland MJ, Thakur R, Woolfson AD, Donnelly RF. 2011. Laser-engineered dissolving microneedle arrays for transdermal macromolecular drug delivery. *Pharm Res* 28(8):1919-1930.

88. Fukushima K, Ise A, Morita H, Hasegawa R, Ito Y, Sugioka N, Takada K. 2011. Two-layered dissolving microneedles for percutaneous delivery of peptide/protein drugs in rats. *Pharm Res* 28(1):7-21.
89. Davis SP, Martanto W, Allen MG, Prausnitz MR. 2005. Hollow Metal Microneedles for Insulin Delivery to Diabetic Rats. *IEEE Transactions On Biomedical Engineering* 52(5):909-915.
90. Gupta J, Denson DD, Felner EI, Prausnitz MR. 2012. Rapid local anesthesia in humans using minimally invasive microneedles. *Clin J Pain* 28(2):129-135.
91. Sivamani RK, Stoeber B, Liepmann D, Maibach HI. 2009. Microneedle penetration and injection past the stratum corneum in humans. *J Dermatolog Treat* 20(3):156-159
92. Sivamani RK, Stoeber B, Wu GC, Zhai H, Liepmann D, Maibach H. 2005. Clinical microneedle injection of methyl nicotinate: stratum corneum penetration. *Skin Res Technol* 11(2):152-156.
93. Alarcon JB, Hartley AW, Harvey NG, Mikszta JA. 2007. Preclinical evaluation of microneedle technology for intradermal delivery of influenza vaccines. *Clin Vaccine Immunol* 14(4):375-381
94. Mikszta JA, Dekker JP, 3rd, Harvey NG, Dean CH, Brittingham JM, Huang J, Sullivan VJ, Dyas B, Roy CJ, Ulrich RG. 2006. Microneedle-based intradermal delivery of the anthrax recombinant protective antigen vaccine. *Infect Immun* 74(12):6806-6810.
95. Atmar RL, Patel SM, Keitel WA. 2010. Intanza®: a new intradermal vaccine for seasonal influenza. *Expert Rev Vaccines* 9(12):1399-1409

96. Eizenberg P, Booy R, Naser N, Mason G, Stambouliau D, Weber F. 2011. Acceptance of Intanza(R) 9 mug intradermal influenza vaccine in routine clinical practice in Australia and Argentina. *Adv Ther* 28(8):640-649.
97. Cross SE, Roberts MS. 2004. Physical enhancement of transdermal drug application: is delivery technology keeping up with pharmaceutical development? *Curr Drug Deliv* 1(1):81-92
98. Karande P, Mitragotri S. 2009. Enhancement of transdermal drug delivery via synergistic action of chemicals. *Biochim Biophys Acta* 1788(11):2362-2373
99. Vemulapalli V, Yang Y, Friden PM, Banga AK. 2008. Synergistic effect of iontophoresis and soluble microneedles for transdermal delivery of methotrexate. *J Pharm Pharmacol* 60(1):27-33.
100. Daugimont L, Baron N, Vandermeulen G, Pavselj N, Miklavcic D, Jullien MC, Cabodevila G, Mir LM, Preat V. 2010. Hollow microneedle arrays for intradermal drug delivery and DNA electroporation. *J Membr Biol* 236(1):117-125.
101. Nolan LM, Corish J, Corrigan OI, Fitzpatrick D. 2007. Combined effects of iontophoretic and chemical enhancement on drug delivery. II. Transport across human and murine skin. *Int J Pharm* 341(1-2):114-124
102. Kolli CS, Xiao J, Parsons DL, Babu RJ. 2012. Microneedle assisted iontophoretic transdermal delivery of prochlorperazine edisylate. *Drug Dev Ind Pharm* 38(5):571-576.
103. Kumar V, Banga AK. 2012. Modulated iontophoretic delivery of small and large molecules through microchannels. *Int J Pharm* 434(1-2):106-114.

104. Wu XM, Todo H, Sugibayashi K. 2007. Enhancement of skin permeation of high molecular compounds by a combination of microneedle pretreatment and iontophoresis. *J Control Release* 118(2):189-195.
105. Sachdeva V, Zhou Y, Banga AK. 2013. In vivo transdermal delivery of leuprolide using microneedles and iontophoresis. *Curr Pharm Biotechnol* 14(2):180-193.
106. Saupe A, Wissing SA, Lenk A, Schmidt C, Muller RH. 2005. Solid lipid nanoparticles (SLN) and nanostructured lipid carriers (NLC) -- structural investigations on two different carrier systems. *Biomed Mater Eng* 15(5):393-402
107. Schafer-Korting M, Mehnert W, Korting HC. 2007. Lipid nanoparticles for improved topical application of drugs for skin diseases. *Adv Drug Deliv Rev* 59(6):427-443
108. Lawson LB, Freytag LC, Clements JD. 2007. Use of nanocarriers for transdermal vaccine delivery. *Clin Pharmacol Ther* 82(6):641-643
109. Baroli B. 2010. Penetration of nanoparticles and nanomaterials in the skin: fiction or reality? *J Pharm Sci* 99(1):21-50
110. Castro GA, Orefice RL, Vilela JM, Andrade MS, Ferreira LA. 2007. Development of a new solid lipid nanoparticle formulation containing retinoic acid for topical treatment of acne. *J Microencapsul* 24(5):395-407
111. McAllister DV, Wang PM, Davis SP, Park JH, Canatella PJ, Allen MG, Prausnitz MR. 2003. Microfabricated needles for transdermal delivery of macromolecules and nanoparticles: fabrication methods and transport studies. *Proc Natl Acad Sci USA* 100(24):13755-13760

112. Aungst BJ, Rogers NJ, Shefter E. 1986. Enhancement of naloxone penetration through human skin in vitro using fatty acids, fatty alcohols, surfactants, sulfoxides and amides. *Int J Pharm* 33(1-3):225–234
113. Chien YW, Xu HL, Chiang CC, Huang YC. 1988. Transdermal controlled administration of indomethacin. I. Enhancement of skin permeability. *Pharm Res* 5(2):103-106
114. Ibrahim SA, Li SK. 2010. Efficiency of fatty acids as chemical penetration enhancers: mechanisms and structure enhancement relationship. *Pharm Res* 27(1):115-125
115. Kandimalla K, Kanikkannan N, Andega S, Singh M. 1999. Effect of fatty acids on the permeation of melatonin across rat and pig skin in-vitro and on the transepidermal water loss in rats in-vivo. *J Pharm Pharmacol* 51(7):783-790
116. Kim MJ, Doh HJ, Choi MK, Chung SJ, Shim CK, Kim DD, Kim JS, Yong CS, Choi HG. 2008. Skin permeation enhancement of diclofenac by fatty acids. *Drug Deliv* 15(6):373-379
117. Warner KS, Li SK, Higuchi WI. 2001. Influences of alkyl group chain length and polar head group on chemical skin permeation enhancement. *J Pharm Sci* 90(8):1143-1153.

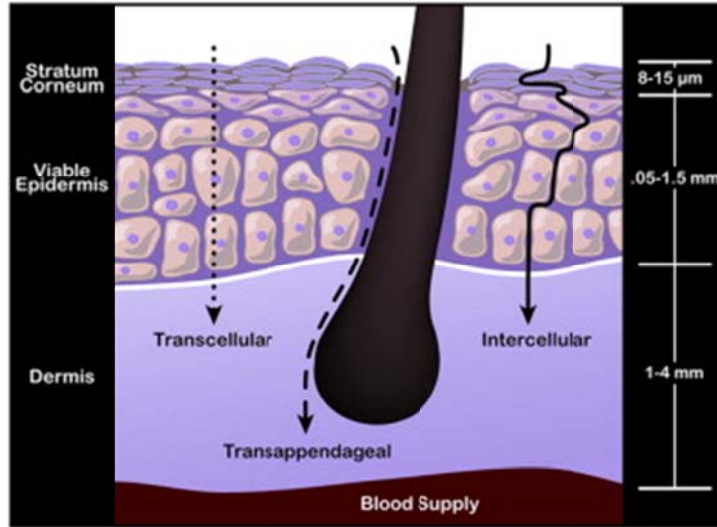


Figure 1.1: Pathways of drug transport across skin⁶

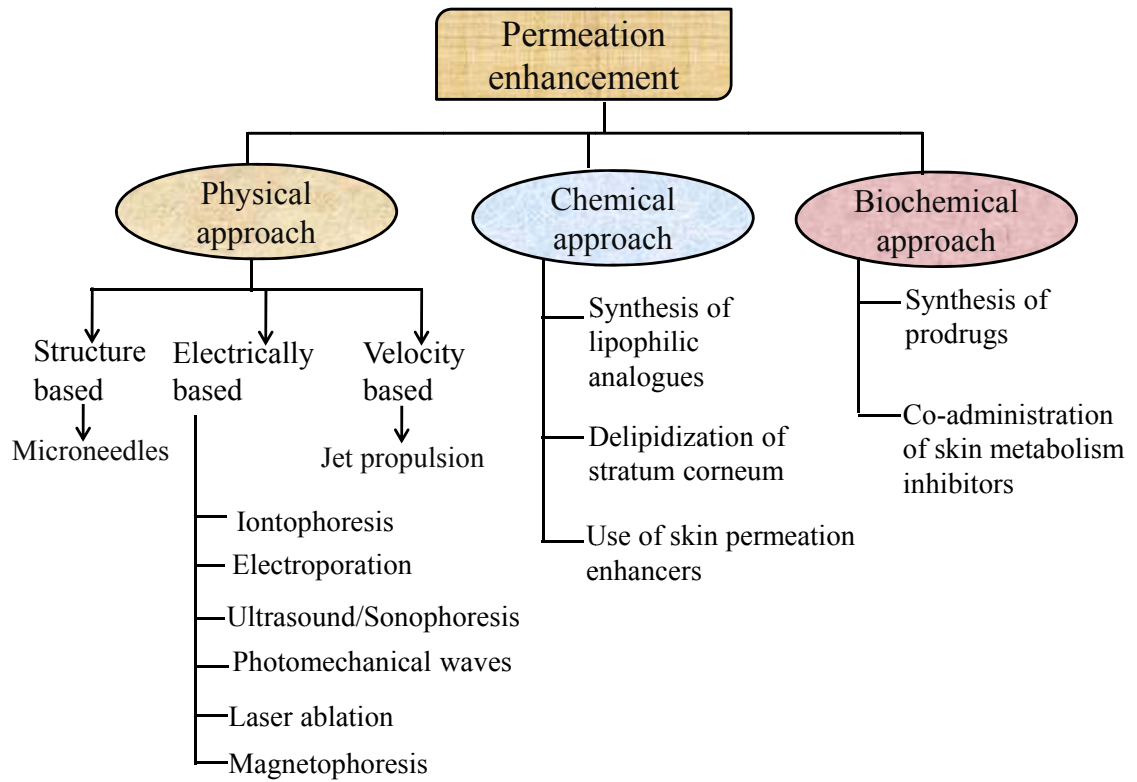


Figure 1.2: Skin permeation enhancement techniques

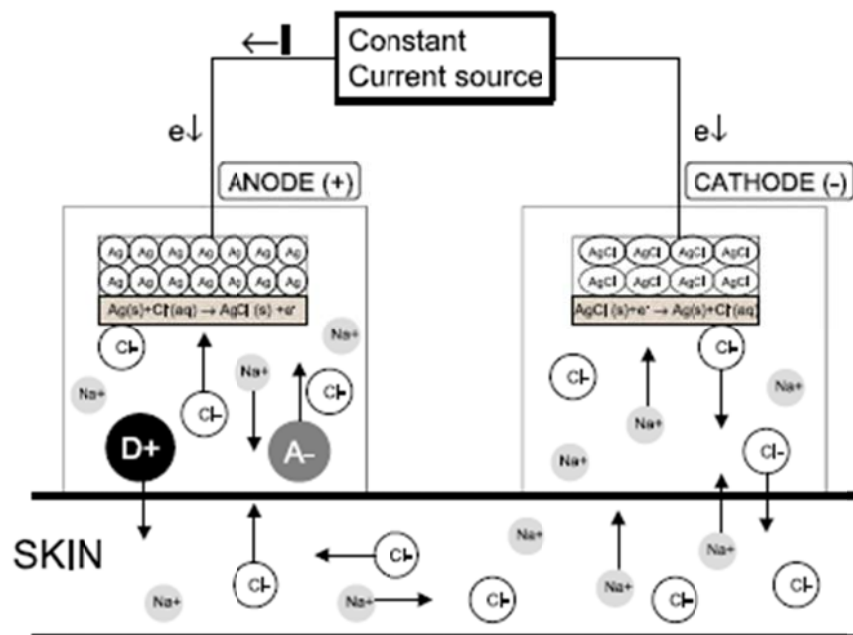


Figure 1.3: Typical iontophoretic set up¹⁶

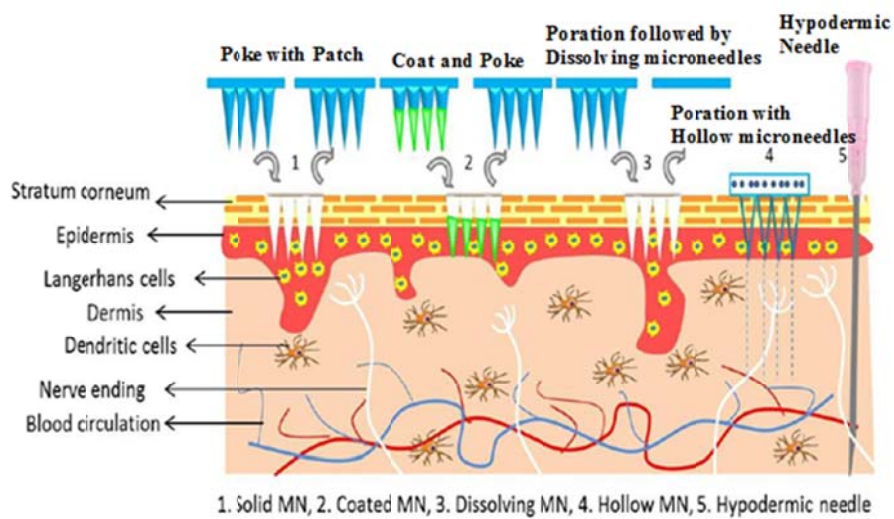


Figure 1.4: Various ways of drug delivery using microneedles⁵⁵

2. MATERIALS FOR TOPICAL NANOPARTICLE DELIVERY SYSTEMS

2.1 ABSTRACT

The delivery of drugs and cosmetic actives to the skin by nanoparticle formulations has a number of advantages over conventional formulations. They offer protection of incorporated active compounds against chemical degradation, more flexibility in modulating the release of the compound, allow the use of well tolerated excipients and feasibility of large scale production. The materials used in the nanoparticle synthesis and formulation can influence product stability, active ingredient properties and its delivery to the intended site of action. This review describes the characteristics and application of various polymeric and lipid materials in the preparation of nanoparticles for topical and transdermal drug delivery.

2.2 INTRODUCTION

The skin is the largest organ in the human body and its principal function is to defend the body from external environment. It regulates body temperature through blood circulation and perspiration. In addition it serves as a barrier for entry of chemicals, biological agents and microorganisms. Upon dermal exposures, chemical and biological agents can enter the skin but these are neutralized by immunological and anti-microbial responses of the skin by its cellular and enzymatic systems. The large surface area and easy accessibility of the skin offers a convenient route for delivery of drugs and cosmetic actives for local or systemic effects. Unfortunately the barrier nature of stratum corneum, the outermost skin layer, prevents

percutaneous absorption of drugs in therapeutic quantities. The stratum corneum is made up of dead keratinized cells (corneocytes) which are embedded in a lipid matrix. The lipid is composed of multiple bilayers of ceramides, fatty acids, cholesterol and cholesterol esters.¹ These bilayers form regions of semi-crystalline, gel and liquid crystal domains. Skin penetration occurs via intercellular route (across the lipid), transcellular route (across the corneocytes) and transappendageal route (via hair follicles and associated sebaceous glands and sweat ducts). Various methods have been applied to enhance drug absorption such as 1) drug-vehicle interactions leading to increased drug solubility and skin permeation 2) skin penetration enhancers to reversibly modify the barrier function of stratum corneum, 3) partial by-pass of stratum corneum barrier by microporation (using microneedle array) or ablation with heat, 4) electrically assisted methods such as ITP, electroporation, magnetoporesis and ultrasound 5) vesicles and particulates such as liposomes and analogs to modify the skin barrier.² Recently nanoparticulate carriers such as polymeric nanospheres, nanocapsules, dendrimers, solid lipid nanoparticles (SLNs) and nanostructured lipid carriers (NLCs) as shown in Figure 2.1, have been utilized in an attempt to reversibly modulate the skin barrier and provide novel delivery systems for the drug and cosmetic actives of interest.³⁻⁸ In addition to their direct effects on the skin barrier, nanoparticles also can provide better occlusive barrier on the skin. Due to the small size, they can have closer contact on the skin than the conventional formulations and provide better occlusion.⁹ The transepidermal water loss is prevented leading to water accumulation and swelling of corneocytes. This facilitates nanoparticle migration and deposition in the stacked cell layers of stratum corneum. Skin penetration or retardation of nanoparticles or their components is dependent on the size, composition and physicochemical properties of the materials used in the preparation of nanoparticles.

The entry of nanomaterials into skin is limited by stratum corneum nanoporosity and gradients. The most important requirements of the permeant for transdermal absorption are: dimensions (size), oil-water partition coefficient, and the surface charges of the permeant. Only lipophilic and unionized compounds that have the size less than 600 Daltons can be considered as the best candidates for transdermal delivery.^{10,11} Based on the nanoporosity of stratum corneum, only those agents with size less than 36 nm are able to diffuse through lipidic or aqueous channels.¹²⁻¹⁵ Other researchers report that polymeric nanoparticles with an average diameter < 100 nm accumulate in the SC and skin appendages (sebaceous glands and hair follicles).¹⁶⁻¹⁹ It appears that trans-follicular penetration may be used by those agents whose dimensions are below the follicular openings (< 200 nm) and able to disperse themselves into sweat or sebum.¹² Figure 2.2 shows the permeation pathways for the nanoparticles in the skin. The nanoparticles are generally dispersed in aqueous solutions, gels or creams (or related formulations). The particles are generally charged to improve dispersion stability against aggregation (discussed under stability section). Several different polymers, waxes, solid lipids and oils are used in the formulation of solid nanoparticles. The material properties are critical in the nanoparticle formulation as these have direct influence on the release properties, size and surface charges and topical permeability. This review describes various polymers and lipids and their use in the formulation of topical nanoparticles. The influence of composition of nanoparticles on drug stability and skin permeability are described.

2.3 POLYMERIC MATERIALS IN THE FORMULATION OF NANOPARTICLES

Polymeric nanoparticles are of two types, nanocapsules and nanospheres. Polymeric nanocapsules are submicron colloidal particles with a core surrounded by a polymeric shell, where the drug or active is confined to core. The core can be a polymer or a lipid. These are prepared by two basic methods, interfacial polymerization around the core particle or interfacial nanodeposition of a preformed polymer.^{20,21} Nanospheres are made up of a homogeneous matrix of polymer in which the drug or active ingredient is dissolved or dispersed uniformly in the matrix. These are generally prepared by interfacial polymerization, emulsion polymerization or solvent deposition.^{22,23} Various biocompatible and biodegradable polymers such as chitosan, poly α -esters (polylactide, polylactide-co-glycolide, polycaprolactone), polycyanoacrylates and polyamidoamines have been utilized in the formulation of nanoparticles for topical and transdermal drug delivery. Table 2.1 summarizes various polymer based nanoparticles for topical and transdermal delivery.

2.3.1 CHITOSAN

It is the second most abundant natural biopolymer after cellulose. It is a linear polymer of randomly distributed β -(1-4)-linked D-glucosamine and N-acetyl-D-glucosamine units (Figure 2.3). It forms a structural element of crustaceans and insects especially protective shells of crabs and shrimp. It is obtained by exhaustive deacetylation of chitin (> 60%). It is semi-crystalline in nature and the degree of crystallinity depends on the degree of deacetylation.²⁴ Crystallinity is maximum for both chitin (0% deacetylation) and fully deacetylated (i.e. 100%) chitosan. Minimum crystallinity can be obtained at intermediate degrees of deacetylation. Owing to its stable crystalline structure, chitosan is normally insoluble in aqueous solutions above pH 7.

However, in dilute acids, the free amino groups are protonated and the molecules become fully soluble below pH 5. The pH dependent solubility provides a convenient means of processing it under mild conditions.²⁵ The primary amino group of chitosan due to protonation under acidic conditions (amine pKa, 6.3) provides cationic property to the polymer, which is an advantage in terms of ion pairing with various anionic moieties.²⁶ Chitosan has several advantages such as biocompatibility, stability, ease of sterilization and susceptibility to enzymatic degradation. In addition, it is non-toxic and non-immunogenic unlike other polysaccharides and therefore it is used for several drug delivery applications.²⁷

Chitosan enhances permeation across skin by altering the secondary structure of keratin. It also increases the water content in stratum corneum and cell membrane fluidity. Further, due to its positive charge, chitosan depolarizes the negatively charged cell membrane thus decreasing the membrane potential driving the drug inside skin.²⁸⁻²⁹

Chitosan nanoparticles have been used for the topical gene delivery, skin burn and wound healing applications. It forms stable complexes with a plasmid DNA and the additives such as salt, serum and sodium dodecyl sulfate did not affect their stability.³⁰ Plasmid DNA - condensed chitosan nanoparticles, and plasmid DNA-coated on pre-formed cationic chitosan/carboxymethylcellulose (CMC) nanoparticles were utilized for genetic immunization in mice.³¹ Chitosan enhanced intracellular delivery of genes for the expression of encoded proteins. These systems produced detectable and quantifiable levels of luciferase expression in mouse skin indicating the possibility of topical delivery of plasmid DNA in the form of nanoparticles. Chitosan forms a stable nanocomposite with cytomegalovirus promoting DNA due to electrostatic attraction. Addition of poly- γ -glutamic acid (γ -PGL) to the above complex helps to produce “compact and denser” nanoparticles. When bombarded with a gene gun, the skin

penetration depth in mice for the “compact and denser” nanoparticles was significantly higher as compared to nanoparticles without γ -PGL.³² Nanoparticles of chitosan and small interfering RNA for natriuretic peptide receptor A (siNPRA) as a transdermal cream for the treatment of asthma was developed.³³ The topical cream containing imiquimod was mixed with chitosan nanoparticles containing siNPRA. siNPRA was successfully delivered to lungs upon topical application in mice. The transdermal siNPRA as chitosan nanoparticles showed reduced airway hyper responsiveness, eosinophilia, lung histopathology and pro-inflammatory cytokines.

The hydrolytic products of chitosan such as N-acetyl glucosamine, which is an essential component of dermal tissues help in recovering the tissue faster resulting in a scar-less tissue repair.³⁴ Furthermore, chitosan has antibacterial and hemostatic properties due to its stimulatory effects on macrophages and neutrophils.^{35,36} Due to these properties, chitosan can be used in tissue engineering and wound healing applications. Chitosan based nanoparticle delivery system was developed for enhanced intracellular delivery of prolidase in the fibroblasts. The enzymatic activity was restored due to the intracellular uptake and release of prolidase from chitosan nanoparticles. Chitosan protected the enzyme from degradation and helped permeating into the skin tissue and released the enzyme in its active form across the cell membrane.³⁷ Electrospun chitin nanofibers have been utilized for wound healing and skin regeneration. The cellular response for chitin nanofibers was higher than chitosan microfibrillar matrices. Further, chitin coated with extracellular matrix proteins (eg: Type I collagen) promoted cell attachment and spreading of human keratinocytes and fibroblasts on the nanowoven matrices. The enhanced cell spreading was due to the high surface area (of nanoparticulate chitosan) available for cell attachment, growth and proliferation.³⁸

The chemical stability of acyclovir was enhanced by incorporation into chitosan nanoparticles. Furthermore, the nanoparticles with higher chitosan content have higher surface charge density that provided stronger interaction with the cell surface than nanoparticles with lower chitosan content.²⁹

2.3.2 POLY(α) ESTERS

Most common polymers in this class include polylactide (PLA), polyglycolide (PGA), polylactide-co-glycolide (PLGA) and polycaprolactone (PCL). These are thermoplastic polymers and constitute hydrolytically labile aliphatic ester linkages in their backbone. Theoretically all polyesters are biodegradable because they undergo fragmentation at the ester bonds. Practically only short chain aliphatic polyesters degrade over the time frame as required by biomedical applications. They undergo degradation by bulk-erosion mechanism.³⁹

PGA is a cyclic di-ester dimer of polyglycolic acid (Figure 2.4). PGA has 45 - 55% crystallinity and thus possesses a high tensile strength and excellent mechanical properties. It has a T_g in the range of 35 - 40°C and melting point above 200°C. It degrades by bulk erosion within a period of 6 - 12 months and the hydrolytic product; glycine is either excreted in urine or converted to carbon dioxide and water. Because of its faster degradation, acidic products and low solubility, its use in biomedical applications is limited.³⁴

PLA is a cyclic di-ester dimer of polylactic acid (Figure 2.5). It occurs in two optically active forms, D and L isomers, out of which L isomer is a naturally occurring form. The degree of crystallinity depends upon the molecular weight of the polymer. Poly(L-lactide) has a crystallinity of around 37%, a glass transition temperature (T_g) in the range of 60 - 65°C and a melting point in the range of 173 - 178°C. It degrades slowly compared to PGA and may take up

to 6 years for total resorption *in vivo*. The α -methyl group of PLA makes it more hydrophobic than PGA. The hydrophobicity is responsible for limited accessibility for the aqueous physiological fluids into polymer matrix. On the other hand, the racemic form, poly(DL-lactide) is a completely amorphous polymer with a T_g of around 57°C. Because of lack of crystallinity, DL-poly(lactide) has lower tensile strength compared to poly(L-lactide).³⁴ PLA undergoes bulk hydrolysis of the ester bonds in the polymer backbone and the degradation product, lactic acid gets converted into water and carbon dioxide via Krebs's cycle.⁴⁰

Paclitaxel loaded methoxy poly(ethylene glycol)-block-poly (D,L-lactic acid) nanoparticles for transdermal delivery were prepared.⁴¹ Fluorescence microscopy measurements indicate that the nanoparticles can penetrate the skin not only via appendage routes including sweat ducts and hair follicles but also via compact structures of stratum corneum and epidermal routes. On the other hand, lipophilic dye studies (Nile red and coumarin - 6) indicate that PLA nanoparticles were accumulated preferentially in the hair follicles.⁴² The dyes diffused and permeated to epidermal cells, and accumulated in the sebaceous glands. Absence of intracellular spotted fluorescence in the epidermal cells of the skin cryo-sections suggested that the particles did not reach viable epidermis.

PLGA is a copolymer of PLA and PGA (Figure 2.6). It is synthesized by means of ring opening polymerization (ROP) of PLA and PGA. Both L-lactide and DL-lactide can be used for polymerization. PLGA is amorphous in nature with a T_g in the range of 40 - 60°C. It degrades by hydrolysis of its ester linkages. The rate of degradation depends on lactide/glycolide ratio, molecular weight of the polymer and shape and structure of the polymer matrix. The composition containing 1:1 of PLA and PGA was shown to be hydrolytically unstable and the resistance to hydrolysis increases with either end of the copolymer composition range.⁴³ The

biodegradability and release properties of the PLGA can be modified by altering the lactide/glycolide ratio. More commonly PLGA with 1:1 lactide:glycolide ratio was used in topical nanoparticle formulations.⁴⁴⁻⁴⁸

PLGA nanoparticles were utilized for topical delivery of variety of drugs including anti-inflammatory agents, anticancer agents and macromolecules. The skin permeation behavior of PLGA encapsulated flufenamic acid nanoparticles across human skin was studied. Drug accumulation in the deeper skin layers and transport across human epidermis were delayed for the nanoencapsulated drug compared to the free drug at incubation times less than 12 h. In contrast, after longer incubation times, the nanoencapsulated drug showed significantly enhanced transport and accumulation of flufenamic acid. Multiphoton fluorescence microscopy showed that the nanoparticles were homogeneously distributed on the skin surface but no nanoparticles were detected within or between the corneocytes.⁴⁵ PLGA nanoparticle formulation loaded with insulin-protamine complex was studied for transdermal drug delivery.⁴⁹ Encapsulation of insulin-protamine complex in PLGA matrix prevented protein degradation and improved physical stability. Nanoparticles showed permeation into the viable epidermis and dermis with deposition concentrated around the hair follicles and sebaceous glands. PLGA nanoparticles were also investigated as carriers for iontophoretic delivery of peptide therapeutics. The skin permeation of triptorelin from PLGA nanoparticles was enhanced by iontophoretic transport. Higher drug loading was achieved for nanoparticles due to the ionic interaction between arginyl and histidyl residues of triptorelin and carboxylic acid moieties of PLGA. These particles when suspended in a positively charged surfactant solution of cetyltributylammoniumbromide, enhanced iontophoretic delivery of triptorelin.⁵⁰

PLGA has been studied for delivery of various photosensitizers for photodynamic therapy (PDT). PLGA nanoparticles of benzopsoralen⁴⁴ or bacteriochlorophyll-a⁵¹ were used in combination with long-wave ultra violet radiation (commonly known as PUVA therapy). The direct contact of photosensitizers can be avoided via encapsulation in the nanoparticles. The nanoparticles provided enhanced delivery of photosensitizers across different macrophage cell lines. The particles were also found to be phagocytosed and localized inside the mitochondria of the target cells for PUVA therapy. PLGA nanoparticle formulation loaded with Zinc (II) Phthalocyanine (ZnPc) was used for PDT. The stability and photodynamic efficacy of ZnPc was improved as found from studies on P388-D1 neoplastic cell lines. Due to hydrophobic nature, ZnPc nanoparticles can get intracellularly localized specifically in mitochondria, lysosomal compartment and cytoplasmic membrane and after irradiation with UVA light, generate reactive singlet oxygen species and free radicals leading to cell death.⁴⁷ Nanospheres of PLGA loaded with 4, 5', 8-Trimethylpsoralen (TMP) into PLGA for topical delivery for treatment of psoriasis. PLGA nanospheres improved the drug penetration in the skin and decreased the TMP permeation through the skin avoiding the percutaneous transport, thus maintaining its topical activity. This was due to the high affinity of the hydrophobic PLGA nanospheres for the hydrophobic proteins present in the skin structures.⁵²

PLGA in combination with chitin was evaluated for tissue engineering applications. Min et al.⁴⁶ demonstrated the use of composite matrix of PLGA/chitin (chitin nanoparticles embedded in a PLGA nanofiber matrix). The results indicate that PLGA/chitin composite matrix is a better candidate than PLGA matrix for normal human keratinocytes and fibroblasts in terms of cell adhesion and spreading. Generally, PLGA is combined with polyethylene glycol (PEG) to obtain a diblock or a triblock co-polymer. PEG confers the hydrophilic nature to the polymer thus

preventing it from recognition from macrophages and degradation. Stracke et al.⁴⁸ performed in depth investigations on imaging of the dermal penetration of nanoparticle-borne drugs. They report that PLGA nanoparticles do not penetrate the skin but remain on the skin surface based on covalently bound fluorescence marker studies. The nanoparticles may be taken up or destroyed close to the skin surface releasing the drug for diffusion into the skin layers. The lack of penetration of particles may be attributed the larger size (average diameter around 300 nm) of the particles.

Polycaprolactone (PCL) is another polyester type polymer, which is highly hydrophobic, non-toxic and biodegradable in nature.⁵³ It is obtained by ROP of a relatively cheap monomeric unit “ ϵ -caprolactone”. The structure of PCL includes a relatively polar ester group and five non-polar methylene groups in a repeating order (Figure 2.7).⁵⁴ Amongst the family of polyesters, PCL has excellent mechanical properties and slow biodegradability leading to slow diffusion and sustained release of drugs.⁵⁵ It has a melting point of $\sim 60^{\circ}\text{C}$, depending on the crystallite state; it has a T_g of $\sim -60^{\circ}\text{C}$. The crystallinity varies with the molecular weight.⁵⁶ Degradation of PCL involves non-enzymatic, random hydrolysis in physiological conditions due to the presence of hydrolytically labile aliphatic ester linkages in the macromolecular main chain; however due to the high degree of crystallinity and hydrophobicity, the degradation is much slower compared to other polyesters. PCL is much more resistant to chemical hydrolysis than other polyesters.⁵³ PCL has an advantage over PLA and PGA that it does not give rise to acidic degradation products as the resulting acidic environment may hamper the release pattern of drugs or adversely affect the antigenicity in case of vaccines.⁵⁷ Due to achiral nature, PCL is far from offering the range of properties and versatility as that of PLA and is difficult to modulate its properties by alteration in polymeric chain configuration.⁵⁸

PCL is generally co-polymerized with lactides or glycolides or converted into a block copolymer with PEG, to yield a rapidly degrading polymer.⁵⁹ The skin permeation behavior of minoxidil loaded poly(ϵ -caprolactone)-block-poly(ethylene glycol) nanoparticles was studied in hairy and hairless guinea pig skin. Only in the case of hairy skin, the permeation was found to be dependent on the size of the nanoparticles; the smaller size particles accumulating more in the skin leading to greater penetration rates across the skin. It was suggested that the nanoparticles were absorbed by follicular penetration via the shunt routes such as skin appendages.⁶⁰

Alvarez-Roman et.al⁶¹ studied the enhancement of topical delivery of a highly lipophilic sunscreen agent, octyl methoxycinnamate (OMC) in PCL nanoparticles. High drug loading was achieved for OMC due to the lipophilicity of the polymer. Nanoparticles significantly enhanced the penetration of OMC across the stratum corneum layers to elicit the photo-protective activity with minimal or negligible penetration into the deeper tissues of the skin, avoiding systemic toxicity. Rastogi et al.⁶² developed self-assembled PCL polymersomes (polymer vesicles) for epidermal targeting for the treatment of melanomas and basal cell carcinomas. The particles were located in the furrows in the stratum corneum and also in the hair follicles. Presence of fluorescence in the inner-corneocyte space in stratum corneum was attributed to the deformable nature of the particles, which result in formation of small vesicles while traversing through the narrow and tortuous hydrophilic pathways. It is also suggested that some transient pores in the epidermis may be self-formed due to the force generated while the vesicles pass through them. Choi et al.⁶³ prepared nanofibers of PCL immobilized with human epidermal growth factor (rh-EGF) for wound healing treatment of diabetic ulcers in mice. Chemical conjugation of the protein to nanofibers prevents the degradation of protein by proteases at the wound sites.

2.3.3 POLYALKYLCYANOACRYLATES (PACAS)

These can be synthesized by polymerization of various alkyl cyanoacrylate monomers with different alkyl ($C_1 - C_{10}$) chain lengths (Figure 2.8). They have remarkable adhesive properties along with the ability to retard bleeding. For this reason, they were initially utilized as surgical glues and skin adhesives.⁶⁴ Dermabond[®] (2-octyl cyanoacrylate) is a popular liquid skin adhesive used as topical skin adhesive to close wounds. PACAs are one of the fastest degrading polymers having degradation time ranging from few hours to few days. PACA is unstable at the carbon - carbon sigma bond on polymer backbone which is hydrolytically sensitive due to the high inductive activation of methylene hydrogen atoms by the electron withdrawing neighboring groups.⁶⁵ In aqueous environment, PACA degrades by hydrolytic scission of the polymer chain. They are quite stable in acidic medium ($pH < 2$) but they degrade very fast in alkaline pH (few hours). The degradation rates of these polymers depends on the length of the alkyl side groups.⁶⁶

The skin permeation of indomethacin in poly(n-butyl cyanoacrylate) (PNBCA) nanocapsules in a Pluronic F-127 gel, was higher than Pluronic F-127. It was apparent that the thin smooth film of nanocapsule formulation gradually disappeared from the skin over a time proving that the nanoparticles penetrated the stratum corneum and the epidermis. Confocal laser scanning microscopy images revealed that rhodamine loaded PNBCA nanocapsules penetrated into different skin regions.⁶⁷ Similarly, nanoparticles of poly{[α -maleic anhydride- ω -methoxy-poly(ethylene glycol)]-co-(Ethyl cyanoacrylate) graft copolymer loaded with tetrahydropalmatine (THP) were found to have accumulated in rat skin via appendageal and epidermal routes.⁶⁸ In addition, ethylcyanoacrylate nanoparticles and poly(butylcyanoacrylate) were found to be potential drug carriers for topical drug delivery.^{69,70} Further, cyanoacrylic

nanoparticles containing phthalocyanines and naphthalocyanines for photodynamic treatment of tumors was described.²²

2.3.4 POLYAMIDOAMINES (PAMAMS, DENDRITIC POLYMERS)

These are unique drug delivery carriers because they are nanosized (1 - 10 nm) hyperbranched, and monodisperse polymers.⁷¹ They are synthesized typically by stepwise and iterative two-step reaction sequences by Michael addition of primary amine to methyl acrylates.⁷² This macromolecular architecture of “dense star” polymers are called as dendrimers and unlike classical polymers, these dendrimers allows a precise control of high degree of molecular uniformity, narrow molecular weight distribution, specific size and shape characteristics, and a highly functionalized terminal surface which can be utilized to attach the drug molecules. Dendrimers are classified by generation, which refers to the number of repeated branching cycles that are performed during its synthesis. The structure of generation 5 dendrimer is shown in Figure 2. 9. More commonly G4-NH₂ and G5-NH₂ dendrimers were investigated for topical and transdermal delivery applications. In solid state, PAMAMs exhibit partially crystalline nature owing to their regular structure with a melting temperature of 80 - 120°C, however the cyclic structures may exhibit a melting point of as high as 270°C (with decomposition). Free bases of PAMAMs do not have much higher thermal stability and generally starts decomposing at 140°C.⁷³ PAMAMs are principally degradable in water due to the hydrolyzable amidic bonds in their main chain along with nucleophilic ter-aminic functions in the β -position.⁷⁴

PAMAMs have been utilized for solubility enhancement of poorly soluble drugs via molecular encapsulation and covalent and non-covalent interactions. These polymers have high

surface charge density due to the presence of multiple ionizable groups which can be utilized to attach the drugs electrostatically. Also, each macromolecule of PAMAM can undergo multivalent interactions with drug and biological membranes, depending on the available surface groups and thus dendrimers are more efficient compared to the conventional complexing agents which can attach the drugs only in 1:1 stoichiometric ratio. PAMAMs present the drug to skin in a more diffusible form and increase its permeability across the skin.⁷⁵

Transdermal delivery of indomethacin in G4-OH and G4-NH₂ dendrimer solutions was studied. Skin permeation was higher for G4-NH₂ dendrimers than G4-OH and G4.5-NH₂ dendrimers. This was attributed to increased solubility of indomethacin due to better molecular encapsulation of drug in G4-NH₂ dendrimer and also electrostatic bonding between amino groups of dendrimer and carboxylic acid groups of drug. No electrostatic bonding occurred between G4.5-NH₂ dendrimer and the drug as both have net negative charge at physiological pH. G4-OH did not enhance the solubility due to weak hydrogen bonding with drug.⁷⁶ In another study, skin permeation was enhanced for 5-fluorouracil (5-FU) when pretreated with G4-NH₂ dendrimer as compared to co-treatment of drug and dendrimer in various vehicles. The dendrimers along with isopropyl myristate showed higher permeation than in other solvents (mineral oil and phosphate buffer). It was postulated that the dendrimers penetrated the stratum corneum and interacted with polar head groups of ceramides and free fatty acids present in skin.⁷⁷ Further, the effect of dendrimer surface charge, generation and concentration on skin permeation of 5-FU was evaluated. The skin partitioning and permeation was higher for G4-NH₂ than G4-OH and G3.5-COOH.⁷⁸ Similarly skin permeation and bioavailability of non-steroidal anti-inflammatory drugs (NSAIDs) such as ketoprofen and diflunisal was enhanced by G5-dendrimers. The cationic charges on the surface of dendrimers caused by primary amino groups

that modified the skin barrier property facilitated the permeation of NSAIDs/PAMAM dendrimer complex.⁷⁹

G2-NH₂ dendrimers containing 5-aminolevulonic acid (5-ALA) in 1:18 molecular ratio were synthesized and studied for intracellular delivery on PAM 212 cells (naturally transformed murine keratinocytes). Encapsulation of highly hydrophilic 5-ALA into dendrimers improved the drug payload and delivered 5-ALA efficiently into the cells for porphyrin synthesis. The 5-ALA dendrimer complex showed better intracellular delivery.⁸⁰ Dendrimers also demonstrated greater uptake by cells by macropinocytosis, a non-receptor-mediated endocytosis, leading to an increased intracellular drug delivery.⁸¹ Delivery of a hydrophilic, ionizable drug, tamsulosin was investigated in a polyhydroxyalkanoate (PHA)-based matrix system with the addition of G3-NH₂ dendrimers. Dendrimers demonstrated a weak skin permeation enhancement of tamsulosin on dendrimer pretreated skin. This may be because of the change in the space group and orientation of the drug in the PHA matrix. However, transdermal system achieved the clinically required amount of tamsulosin permeating through the skin.⁸²

Transfection of epidermal cells mediated by solid-phase dendrimer/DNA membrane system has been reported using G5-NH₂, G7-NH₂ and G9-NH₂ dendrimers.⁸³ Complexes of cationic dendrimers and DNA were coated or incorporated on PLGA or collagen/fibronectin-based bioerodable membranes. Florescent proteins were employed to detect the efficiency of transfection. It was found that dendrimer/DNA complexes can dissociate from PLGA matrix while retaining transfectional ability. All dendrimer/DNAs complexes showed increased transgene expression compared to non-complexed DNA.

Mecke et al.⁸⁴ reported the mechanism of three different dendrimers, G7-NH₂ and G7-COOH and core-shell dendrimers (G7-NH₂ as core and G5-COOH as shell) in enhancing the

skin permeation. Dendrimers were shown to create pores or craters in the lipid bilayers which may enhance the skin permeation. The pores formed by G7-dendrimers were due to the removal of lipids and formation of dendrimer-lipid aggregates whereas core-shell dendrimers, due to their irregular cluster surface, were unable to remove lipids from bilayers and form pores. They instead displayed a strong affinity for already existing bilayers defects and adsorption on it. The pore formation was observed for both amine- and carboxyl-capped dendrimers, thus indicating that the net charge of the dendrimers is not the sole feature determining their interaction with the lipid membranes. Increasing the concentration of dendrimers may result in instability and complete disruption of lipid bilayers.

2.4 SOLID AND LIQUID LIPIDS IN THE FORMULATION OF NANOPARTICLES

Polymeric topical nanoparticles offer several advantages but they suffer from limitations such as poor drug loading, physical instability and expensive scale-up methods and residues of the organic solvents used in the production process.^{85,86} Lipid based nanoparticles (SLNs and NLCs) serve as an alternative to polymeric nanoparticles which have several advantages. Similar to polymeric materials, lipids protect the active ingredient against chemical degradation and are flexible for modulating the drug release.⁸⁷ In addition; they are composed of physiological and compatible lipids that stay solid at room and body temperature. The production method avoids organic solvents and it is feasible to scale up and sterilize the product at large scale.⁸⁸ Lipid nanoparticles are generally produced by high pressure homogenization and these have an usual size range of 50 - 200 nm which ensure close contact with the skin and enhance the drug partitioning into the stratum corneum.⁸⁷ The best advantage of lipid nanoparticles is that the diffusion coefficient of the drug is lowered and therefore these serve as sustained release drug

carriers. The small lipid particles enter the lipid domains of corneocytes and hair follicles and provide slow release of drug enabling epidermal targeting.

By definition, lipids are a group of organic compounds containing fatty acids and their derivatives. They are somewhat amphiphilic in nature due to the presence of lipophilic and hydrophilic groups in the structure. They are identified and characterized by their fatty acid composition, melting temperature, hydrophilic-lipophilic balance (HLB) values and solubility in non-polar organic solvents. The melting temperature of lipids increases with increase in the hydrocarbon chain length or the molecular weight. The melting point also decreases with the increase in the unsaturation of the fatty acid.⁸⁹

SLNs have been introduced to the literature in 1990s as a novel carrier system for drug and cosmetic active ingredients. SLNs are derived from o/w nanoemulsions replacing the liquid lipid (oil) by a lipid being solid at room and body temperatures. The important property of the lipid is that the particle matrix is in a solid state, its melting temperature can be adjusted by the choice of the lipid. The nanodispersion obtained by homogenization under high pressure is stabilized by the addition of surfactants such as poloxamer and polysorbates.⁹⁰ SLNs can be stable for years. The compact crystalline structure of the lipid (eg, tristearin) of the SLNs can lead to poor drug incorporation efficiencies. The poor drug loading capacity of SLNs is due to the limited space for the drug within the crystalline lattice. To overcome this problem, a liquid lipid (eg, oils such as caprylic/capric triglycerides) is blended with the solid lipid to produce NLCs. These nanostructures possess imperfections and defects in the crystalline structure of the solid lipid. The NLCs also remain solid at room and body temperatures, a relatively high amount of liquid lipid (oil) can be blended by choosing a lipid with a high melting point. The consistency of NLCs in fact stand in between SLNs and nanoemulsions (Reviewed in Muller et al.).⁹¹ Although

both SLNs and NLCs provide long term physical stability, NLCs provide higher encapsulation efficiency whereas SLN provides higher occlusivity and skin hydration effects due to the solid rigid core of particles.⁴ Both SLNs and NLCs are widely used in topical and transdermal delivery of drugs and cosmetic active ingredients.^{92,7} The lipids used in the formulation of SLNs and NLCs can be classified into two major groups according to their composition, Glyceride esters and Waxes. Table 2.2 summarizes various lipid based materials used in the formulation of nanoparticles for topical delivery.

2.4.1 GLYCERIDE ESTERS

Glyceride esters are trans-esterification products of glycerol and fatty acids to render the lipid more hydrophilic. Esterification also modifies physical characteristics such as melting point and HLB of the resulting glycerides. Some of the commonly used lipids in this class include caprylic/capric triglyceride, glyceryl behenate, glyceryl tripalmitate etc.

Caprylic/capric triglyceride is clear, slightly yellowish oil which has mixed glyceride esters of saturated coconut and palm kernel oil-derived caprylic and capric fatty acids. It is highly refined oil possessing excellent oxidation stability with a longer shelf life. It is referred to as caprylic/capric triglyceride oil or medium chain triglyceride (MCT) oil because it has primarily the medium chain caprylic (8 carbons) and capric (10 carbons) acids that make up the bulk of the oil. It is commercially available as Miglyol[®] 810 and 812. Miglyol[®] 810 and 812 differ only in C₈/C₁₀-ratio. Glyceryl behenate (Tribehenin; Glycerol Tribehenin or Glyceryl Tridocosanoate), is an off-white powder, which is a glyceryl ester of behenic acid. It is a mixture of 12 - 18% mono-, 52 - 54% di- and 28 - 32% triglycerides. It has a melting point of 72°C. It is commercially available as Compritol[®] 888 ATO. Glyceryl tripalmitate (tripalmitin) is available

as white, flakes and is a triglyceride of palmitic acid. It has a melting point of $\sim 65^{\circ}\text{C}$. It is commercially available as Dynasan[®] 116.

Caprylic/capric triglycerides are used along with solid lipids (e.g., glyceryl behenate) in the preparation of NLCs. The NLC formulations of glyceryl behenate-caprylic/capric triglyceride loaded with indomethacin, ketorolac, ketoprofen and naproxen for local delivery to skin are reported.⁹³⁻⁹⁵ These NLCs accumulated in the horny layer and provided sustained release of the drugs and thereby reduced the penetration of drug into deeper skin layers. The decreased penetration across skin barrier for nanoparticles can be described by the higher chemical affinity and thus partial “sequestration” of drug by lipid matrix preventing its diffusion and permeation through stratum corneum. In addition, NLC formulation of glyceryl behenate and caprylic/capric triglyceride augmented adhesion of the particles to stratum corneum because of its analogy to skin composition.

Nanocapsules of caprylic/capric triglyceride coated with PCL for prolonged topical delivery of nimesulide are reported.⁹⁶ This formulation provided highest skin accumulation levels for nimesulide than the nanosphere formulation without the lipid phase or the nanoemulsion formulation without the coating polymer. It is speculated that the longer residence time of the nanocapsule formulation facilitates better skin accumulation of the drug in the skin layers. In another study, a nanoparticle formulation for improving chemical stability of tretinoin is reported.⁹⁷ Tretinoin-loaded nanocapsules were formulated with a capric/caprylic triglyceride mixture as a core lipid and PCL as a coating polymer to improve the photo stability of tretinoin. The nanoemulsion formulation did not appreciably improve the photostability of tretinoin which indicates the significance of polymer coating to protect the tretinoin in the core. This phenomenon of enhancing the stability is owed to the crystallinity of the polymer which has the

ability to reflect and scatter UV radiation. Similarly, nanoemulsion (caprylic/capric triglycerides and lecithin or oleylamine) coated with hydrophilic silica for skin targeting of drugs such as retinol was reported.^{98,99} The silica coating served as a barrier to avoid skin contact and irritation and also improved dermal delivery of retinol.

Glyceryl behenate nanoparticles loaded with retinol and retinyl palmitate for epidermal drug targeting are reported. High retinol concentrations were found in the upper skin layers following application of SLN preparations, whereas the deeper regions showed only very low retinol levels.¹⁰⁰ Similarly, glyceryl behenate SLNs loaded with vitamin A showed higher amounts of drug localized into the upper skin layers and slowly released into the viable epidermis in a sustained manner.¹⁰¹ Glyceryl behenate nanoparticles offer good drug encapsulation for retinol owing to less ordered lattice structure than of beeswax or cetyl palmitate.¹⁰² When compared to different lipids such as glyceryl tripalmitate, cetyl palmitate and solid paraffin, glyceryl behenate showed superior entrapment and stability of sensitive retinoid molecules in the lipid matrix. Further, the encapsulation efficiency increased with increase in the lipophilicity of drugs in the order retinyl palmitate > retinol > tretinoin.¹⁰³

Glyceryl behenate or glyceryl palmitostearate microparticles containing juniper oil demonstrate that entrapment of the volatile oil in SLNs protects the oil from oxidative degradation. Nanoparticles based on glyceryl behenate exhibited long term physical stability than glyceryl palmitostearate which may be due to the higher ratio of monoglycerides present in latter that resulted in increase in particle size and physical instability.¹⁰⁴

SLN formulations of glyceryl behenate for enhanced topical delivery of some anti-fungal compounds are reported.^{105,106} Glyceryl behenate SLNs produced less ordered crystal lattices and amorphous regions in the crystal lattice which contributed to the higher drug loading for

miconazole nitrate. In addition, inclusion of propylene glycol increased drug solubility in the lipid which further enhanced the drug loading. These SLNs facilitated the transfer and accumulation of particles in the stratum corneum due to their lipoidal nature. Glyceryl behenate SLNs, and NLCs with α -tocopherol as liquid lipid containing ketoconazole were prepared. The drug loading and photo stability of NLC formulation was superior as compared to SLN.

Glyceryl behenate SLN formulation of prednicarbate was compared with SLNs made with glyceryl palmitostearate, hydrogenated coco-glycerides and cetyl palmitate. Higher entrapment efficiencies were obtained in glyceryl behenate formulations due to high lipophilicity (log P 4.02) of prednicarbate.¹⁰⁷ The encapsulation efficiency of SLNs can be very high and often exceeds 90% with highly lipophilic agents such as cyproterone acetate,¹⁰⁸ clobetasol¹⁰⁹ and econazole.¹¹⁰ For prednicarbate, the drug was localized in the epidermis to reduce the risk of deeper tissue absorption leading to skin atrophy by the inhibition of fibroblasts.¹¹¹

Lidocaine SLNs of a mixture of glyceryl behenate and glyceryl palmitostearate in contrast demonstrated higher entrapment efficiency than NLC formulation composed of caprylic/capric triglyceride. This was attributed to the fact that increased liquid lipid load was not very well accommodated in the solid lipid and thus gets expelled out.¹¹²

A series of fatty acid esters (C_{13} - C_{23}) of isopropanol were synthesized and formulated in lipid nanoparticles based on glyceryl palmitostearate. The drug loading efficiency and skin permeation of econazole nitrate, chosen as a lipophilic model drug, were evaluated. A parabolic correlation between skin permeation and chain length of the fatty esters present in the lipid nanoparticles was observed. The maximum flux of drug was observed for the nanoparticles containing C_{17} – C_{19} esters, suggesting that these formulations may constitute a potential carrier for topical delivery of econazole nitrate.¹¹³

SLNs of glyceryl palmitostearate and NLCs made with glyceryl palmitostearate and squalene loaded with different psoralens [(8-methoxypsoralen (8-MOP), 5-methoxypsoralen (5-MOP), TMP] are reported.¹¹⁴ Squalene increased drug loading and skin permeability of NLCs. The skin permeation of psoralens increased in the order 8-MOP > 5-MOP > TMP.

Stecova et al.¹⁰⁸ evaluated nanoparticles (SLN and NLC) and nanoemulsions for the delivery of cyproterone acetate (CPA) for topical acne treatment. Glyceryl palmitostearate was used as solid lipid whereas oleic acid or caprylic/capric triglycerides were as liquid lipids. The nanoparticles were stabilized by Poloxamer 188. The permeation studies demonstrated that SLN and NLCs provided up to 4-fold higher levels of CPA in epidermis than a conventional cream or nanoemulsion. With SLN formulation, epidermal targeting of the drug was observed whereas for NLC, the drug was not confined with the outermost layer but reached to sebocytes and dermal papilla cells. This high level of permeation for SLN and NLC may be attributed to their close contact with superficial tight junctions of corneocyte clusters and furrows between corneocyte islands from where the drug may slowly be released over a period of several hours. Additionally, the drug dissolved or finely dispersed within the lipid matrix of the nanoparticles or attached to their surfaces may facilitate drug dissolution within epidermal lipids.¹⁰⁸ Glyceryl palmitostearate SLNs loaded with triamcinolone acetonide in a carbopol gel was studied for enhanced transdermal iontophoretic delivery. The synergistic effect of ITP and carbopol gel allowed the use of SLN carbopol gel as a vehicle for transdermal iontophoretic drug delivery.¹¹⁵

Isotretinoin loaded glyceryl palmitostearate SLNs provided epidermal targeting and reduced systemic uptake of tretinoin. The SLN formulation minimized the direct skin contact thereby skin irritation was prevented.¹¹⁶ SLN formulation of glyceryl tripalmitate significantly improved the stability of coenzyme Q₁₀ by forming a super cooled melt. At higher drug loadings,

coenzyme Q₁₀ melted in the matrix and decreased the crystallization temperature of lipid preventing its crystallization, thus the blend of lipid and drug formed a eutectic mixture and remained as a supercooled melt at room temperature.¹¹⁷ Furthermore, glyceryl tripalmitate SLN formulation of podophyllotoxin for the treatment of genital warts is reported.¹¹⁸ Encapsulation of drug into nanoparticles reduced its systemic side effects and severe skin irritation due to minimal contact of the free drug with skin. Drug formulations stabilized by poloxamer/soyabean lecithin (P-SLN) and polysorbate 80 (T-SLN) were compared in terms of skin permeation. Both P-SLN and T-SLN were successful in preventing the systemic absorption of drug, however, P-SLN showed increased accumulation of drug in skin layers compared to T-SLN due to small particle size of P-SLN that provided more occlusive effect favoring the accumulation of drug. Polyoxyl 40 hydrogenated castor oil and glyceryl behenate based SLNs with an outer hydrogel (Carbopol 940) matrix for improved skin targeting (dermal delivery) of podophyllotoxin was reported.¹¹⁹ Furthermore, a coating of silica on the surface of SLNs enhanced the penetration of drug into skin from dermal delivery to transdermal delivery.

Clotrimazole loaded SLN and NLC formulations of glyceryl tripalmitate and caprylic/capric triglycerides were reported.¹²⁰ Entrapment into both SLN and NLC formulations increased the dermal bioavailability and stability of drug as well as reduced its side effect such as local irritation. The drug melted into the lipid matrix and dispersed molecularly in between fatty acid chains, forming supercooled melt.

2.4.2 WAXES

The term wax generally refers to a substance, which is a plastic solid at room temperature and a liquid of low viscosity above its melting point. These are simple ester of a monohydric

long-chain fatty alcohol and a long chain fatty acid. It may contain free hydroxyl groups within the molecule or free fatty acid function. Beeswax is a natural wax obtained from the honey bees. Its main components are palmitate, palmitoleate, hydroxyl palmitate and oleate esters of long chain (C_{30} - C_{32}) aliphatic alcohols. It melts at 62 to 64°C and on heating above 85°C, discoloration occurs. Carnauba wax (Brazil wax or palm wax) is obtained from the leaves of Brazilian palm tree as a yellow to brown, hard, brittle lustrous wax. It contains mainly C_{16} to C_{20} fatty acid esters of C_{30} to C_{34} fatty alcohols (85%), accompanied by small amounts of free acids and alcohols, hydrocarbons and resins. It has highest melting point (~82°C) amongst the natural waxes. Cetyl Palmitate is a white, crystalline wax and is available commercially as Cutina wax or Precifac[®] ATO. Due to the solid nature of the waxes, they are used as solid lipids in the formulation of nanoparticles.

It is important to know the thermal characteristics, crystal habit, texture, and appearance of a new lipid matrix when determining its suitability for use in pharmaceutical applications. The performance of SLNs depends on the type and concentration of the lipid. Glyceryl monostearate (monostearin) SLNs demonstrated remarkably lower permeation rate and greater reservoir effect in the epidermis compared to bees wax for betamethasone 17-valerate. On the other hand, the beeswax SLNs failed to show controlled release properties and drug localizing effects.¹²¹ This is due to highly packed crystal order structure of beeswax that expels the drug upon solidification.¹²² Higher drug loading or encapsulation efficiency can be achieved by an admixture of theobroma oil and beeswax lipid matrix. The transformation of alpha crystals to a more stable beta crystalline state of theobroma oil in beeswax produced a “disordered matrix” and “microstructures” in the lipid structure to accommodate more drug in the matrix.¹²³ The

crystallinity of beeswax can be modified by heterolipid (Phospholipon[®] 90G or Goat Fat) that offers a way of improving the drug incorporation efficiency of nanoparticles.¹²⁴

An admixture of PEG with beeswax has is commercially available as Apifil[®] (waxy solid pellets of PEG-8 Beeswax). It is non-ionic and hydrophilic with self-emulsifying properties and has a melting point between 59°C to 70°C.¹²⁵ The combination of solid lipid and liquid lipid results in a less-ordered crystalline structure to accommodate more drug and better drug delivery due to balanced lipophilic and hydrophilic properties of Apifil[®].¹²⁶

Carnauba wax has been frequently used in the formulation of SLNs or NLCs. Inorganic sunscreens such as titanium dioxide (TiO₂) were enclosed inside or bonded with carnauba wax - decyl oleate nanoparticles for synergistically enhancing the UV protection properties. Carnauba wax contains 2- or 3-hydroxy, 3,4-dihydroxy and 4-dihydroxy substituted cinnamic acids, p-methoxycinnamic aliphatic diesters and p-hydroxycinnamic aliphatic diesters, which are known to be effective sunscreen agents. The sunscreen effect is based on their UV absorption property which is attributed to the conjugated double bonds of their chemical structures. Carnauba wax and its constituents (ethanolic extract) were coated on the surface of TiO₂ nanoparticles under high pressure homogenization. The surface contact between organic molecules possessing double conjugated systems such as the cinnamates and hydrophobic TiO₂ demonstrated a synergistic increase in the UV absorption capacity of both species. This adsorption was particularly favored by the use of a solid matrix composed of saturated fatty acids, which provided a medium for the fixation of the organic molecules onto the surface of the TiO₂ crystals.¹²⁷

Nanoparticles based on carnauba wax and decyl oleate for the dispersion of inorganic sunscreens (barium sulfate, strontium carbonate and TiO₂) in aqueous media were reported.

These mixed lipid matrices showed a promising system for the delivery of UV protecting agents across the skin.¹²⁸ A cDNA coding nucleic acid for keratinocyte growth factor- 1 (KGF-I) for wound healing was formulated as nanoparticles containing caprylic/capric triglycerides oils including carnauba wax and adenosine. The formulation has conventional ingredients which do not affect the skin barrier function or cause abrasion but are able to permeate the skin due to the small size range (10 - 85 nm) of the particles to deliver the nucleic acid.¹²⁹ Hybrid lipid-based particles composed of hydrogenated castor oil and glyceryl monostearate loaded with silanized TiO₂ and caffeine for treatment of skin diseases such as psoriasis and skin cancer has been reported. A synergistic effect for UV-protection with TiO₂ and caffeine which has protective effects against UV-B radiation, anticellulite activity and photoaging prevention capacity was observed. Reduction of the crystallinity of glyceryl monostearate was due to hydrogenated castor oil leading to imperfections in the crystal lattice. These crystal defects improved drug loading and UV protecting effect. It was also observed that the obtained lipid mixture was non-toxic with some skin hydrating effects.¹³⁰

Cetyl palmitate forms a stable colloidal carrier or NLC when used in combination with caprylic/capric triglycerides. It was not completely recrystallized to a solid state in association with the oil at various ratios indicating its ability to form stable NLC structures. The particle size and crystallinity of γ -oryzanol loaded cetyl palmitate nanoparticles decreases with an increase in caprylic/capric triglyceride content. The drug lipid interaction studies indicate that γ -oryzanol was associated with the liquid lipid content, enabling readily releasable drug in the NLC system.¹³¹ Studies on cetyl palmitate – Labrasol® (oil) based NLCs for topical delivery of coenzyme Q₁₀ indicate that the crystallinity decreases as the quantity of the oil is increased confirming the enhanced disturbance and irregularity in the lipid matrix due to incorporation of

oil. The skin permeation of coenzyme Q₁₀ shows a biphasic pattern with an initial fast release followed by a slow and prolonged release to maintain the Q₁₀ concentrations in the skin.¹³²

In a similar study, SLNs made with cetyl palmitate or bees wax containing retinol possessed good physical stability but lacked sufficient drug encapsulation in the solidified state. These differences were attributed in part to different crystal packing. Less ordered crystal lattices favor successful drug inclusion, as in the case of glyceryl monostearate and glyceryl behenate SLN. The highly ordered crystal packing of wax SLN comprising beeswax or cetyl palmitate, for instance, leads to drug expulsion, but also to superior physical stability.¹⁰² Cutanova Nanorepair Q₁₀ cream is the first commercial cosmetic product containing NLCs made with a lipid matrix of cetyl palmitate and caprylic/capric triglycerides. This formulation provides increased occlusive behavior due to dense packing of small particles on the skin leading to enhanced skin penetration of Q₁₀ into stratum corneum.¹³³ It has been demonstrated for cetyl palmitate SLNs that the existence of a solid particle matrix with a particle size in the nanometer range is a prerequisite to form a semisolid dispersion having the appropriate consistency for topical application. Particle size reduction from micro- to nano- size has resulted in an 80 - fold increase of the elastic modulus. Thus, it is evident that the presence of a solid matrix in nanometer range is important to provide a semisolid consistence for the topical preparation.¹³⁴

The influence of oil content in the NLCs prepared with cetyl palmitate and caprylic/capric triglycerides on physicochemical properties of formulation and skin distribution of nanoparticles was evaluated. Increasing the oil content upto 20% increased the viscosity and thus size of nanoparticles but decreased after that which may be due to the expulsion of excess oil by the lipid matrix during crystallization process with the excess oil accumulating at the surface of nanoparticles. NLCs provided higher occlusion than corresponding nanoemulsion

formulations, however, increasing the oil quantity led to decrease in occlusivity which may be attributed to the decreased viscosity of formulation. Permeation studies indicate epidermal targeting of nanoparticles (as indicated by the deposition of Nile red) due to occlusive effect of nanoparticles. Nanoparticles with lower oil content deposited more dye into stratum corneum, viable epidermis and superficial dermis whereas nanoparticles with higher oil content deposited the dye only into stratum corneum and upper viable epidermis.¹³⁵

2.5 STABILITY OF NANOPARTICLES

Stability of nanoparticles in a formulation is affected by several factors. In liquid medium, nanoparticles undergo Brownian motion which is inversely proportional to the particle size. Further in presence of excess electrolytes the nanoparticles tend to destabilize due to compression of the diffuse layer leading to reduction in zeta potential.¹³⁹ In addition to these issues the type and molecular weight of polymer, storage temperature, and storage medium also affect the stability of nanoparticles. In solid state, nanoparticles undergo aggregation due to van der Waals attractive forces, as the potential barrier between the particles is very small.¹⁴⁰ A schematic of approaches to stabilize nanoparticles is shown in Figure 2.10. Further, stabilization techniques specific to each polymer are reported.¹⁴¹

2.5.1 ELECTROSTATIC STABILIZATION

Repulsion occurs with the particles bearing the same electrical surface charge. Charged or ionic additives are added to the particles so that they attain a definite surface charge to repel from each other. These charges retard the attractive forces because of high surface free energy of the small particles.¹⁴² The repulsive forces also counterbalance the van der Waals attraction

forces between particles and provide them Coulombic repulsion. Anionic or cationic compounds can be adsorbed on to particle surface to form a charged layer. To maintain electroneutrality, an equal number of counterions will surround the particle to form an electrical double layer. In liquid media, when two such particles approach each other, the mutual repulsion of these double layers surrounding the particles occurs between them to prevent aggregation.¹⁴³ The extent of adsorption and degree of repulsion generated depend on factors such as: the pH and the solid fraction of nanoparticle suspension, structure and molecular weight of the stabilizer, and surface charge of nanoparticles. Anionic polymers (partially hydrolyzed polyacrylamide, sodium dodecyl sulfate), cationic polymers [polyamines, poly(dimethylaminoethyl methacrylate) and polyethyleneimine], nonionic polymers (polyacrylamide, methylcellulose, polyvinyl alcohol and polyethylene oxide) and amphoteric polymers [partially hydrolyzed poly(acrylamide-co-dimethylaminoethyl methacrylate)] can be used as electrostatic stabilizers.¹⁴⁴ Since this mechanism relies on the separation of ionic charges, it is mainly relevant in the systems of high polarity. The major disadvantage of this technique is its sensitivity with respect to surface charge (pH) and salt concentration. Thus it is only applicable to dilute systems. Also, once agglomerated, it is difficult to re-disperse the particles.¹⁴⁵

2.5.2 STERIC STABILIZATION

In steric stabilization, the contact between adjacent nanoparticles is physically avoided due to steric hindrance. This physical hindrance is achieved by attaching macromolecules to the surfaces of the colloidal particles either by physical adsorption or chemical bonding of polymer molecules or by adding polymer molecules to the dispersion medium in order to prevent the aggregation of colloidal particles. In contrast to electrostatic stabilization, steric stabilization is

not affected by a variation of pH or salt concentration thus making it more advantageous than the former.¹⁴⁶ The polymers used for steric stabilization are of high molecular weight, generally > 10,000 Daltons. One of the requirements is that the polymer should form a dense coating and adsorb uniformly enough to screen the attractive forces between the particles. An appropriate solvent or dispersion medium should be used in order to solvate the particles to form an extended shielding layer on the particles to prevent van der Waals attractive forces.¹⁴⁷ The polymers utilized for steric stabilization include polyoxyethylene, polyvinyl alcohol, polyacrylic acid, polyvinyl pyrrolidone, polyvinyl acetate and polymethyl methacrylate.¹⁴²

The combination of electrostatic and steric stabilization is called as electrosteric stabilization. This occurs when stabilizing polymers are attached to a charged surface of the colloidal particle. When a second particle approaches, both electrostatic repulsion and steric restriction would prevent the particles from aggregation.¹⁴⁵

Other methods such as freeze drying of nanoparticles using cryoprotectants or pH adjustment can also improve the stability of nanoparticles. Various cryoprotectants used in freeze drying process include glucose, sucrose, lactose, trehalose, maltose, poloxamer 188, glycine, alanine and polyvinyl pyrrolidone. These act as spacers in between the polymer particles to prevent their aggregation¹⁴⁸⁻¹⁵⁰ whereas surfactants and certain polymers form a hydrophilic layer around nanoparticles avoiding aggregation.¹⁴⁸ The stability of freeze dried polymers may be attributed to the low content of residual water which prevent the hydrolysis of ester groups in polyester polymers.¹⁴¹

2.6 TOXICITY OF NANOPARTICLES

Based on the literature information on topical and transdermal delivery of nanomaterials, it is well known that penetration of intact nanoparticles through skin and reaching blood circulation is negligible. Similarly, insoluble nanoparticles used in sunscreens do not penetrate into/or through human skin to induce any local or systemic adverse health effects. Therefore, the potential human skin and systemic exposure from nanosized formulations should be rated similar to those of solutions of the respective ingredients (Reviewed in Nohynek et al.).¹⁵¹

On the other hand, several studies demonstrate that nanoparticles can penetrate and reach epidermis and hair follicles. These include polymeric nanoparticles,^{41,49,60} SLNs,^{116,108} quantum dots,¹⁵² fullerene nanoparticles¹⁵³ and latex nanoparticles.¹⁵⁴ Skin exposure to nanoparticles can occur from the use of topical creams, gels and other drug and cosmetic treatments containing nanoparticles. Due to their small size and unique physicochemical properties, nanoparticles are rendered biologically more active than structures of the same chemical make-up, which is apparent by the inflammatory, oxidant, and anti-oxidant capacities described for nanocarrier systems.¹⁵⁵⁻¹⁵⁷ Once in the epidermis, nanoparticles can reach the lymphatic system and regional lymph, and from there they can translocate to the systemic vasculature and reach major organs and tissues including brain, kidney, heart, liver, bone marrow, spleen and nervous system. The nanoparticles interact with the cells resulting in increased oxidative stress, inflammatory cytokine production and cell death.

Currently there are about 27 cosmetic products on the market containing lipid nanoparticles and many other products are under clinical trials.⁹² As the applications of engineered nanoparticles are increasing, there is a need to recognize their potential toxicities. In

order to understand the properties of nanoparticles that affect their biological response, a comprehensive material characterization is required.¹⁵⁸

High-throughput screening methods can be utilized to understand the interaction behavior looking at the ROS production, cell viability, cell stress, particle uptake studies, cell morphology and phenotyping.¹⁵⁹ Particle size, shape and surface modification influences particle uptake and biological responses.¹⁶⁰ Marquis et al.¹⁶¹ reviewed the different analytical techniques that can be utilized to assess nanoparticle toxicity. The *in vitro* nanoparticle uptake, localization into cells and nanoparticle-cell interactions can be visualized by Transmission electron microscopy (TEM) or fluorescence spectroscopy. In some cases, dynamic light scattering (DLS) is used in conjunction with TEM to analyze the size of the nanoparticles. Qualitative elemental analysis techniques such as electron-dispersive X-ray analysis (EDS) and electron energy loss spectroscopy (EELS) in conjunction with TEM can provide the nanoparticle composition. Elemental analysis of internalized nanoparticles can be best done by inductively coupled plasma atomic emission spectroscopy (ICP-AES). A novel technique known as video-enhanced differential interference contrast (VEDIC) microscopy is also been used for nanoparticle uptake studies. The *in vitro* toxicity can be assessed with various cell-based assays whereas the *in vivo* toxicity can be determined by fluorescence imaging and scintillation counting.

With the risks associated with the applications of nanomaterials, numerous prominent bodies have been established to perform the risk assessment of nanomaterials. These include the National Nanotech Initiative (NNI), the Innovation Medicines (IM) for Europe Platform, the European Nanomedicine Technology (ENT), the International Life Sciences Institute (ILSI) Research Foundation/Risk Science Institute Nanomaterial Toxicity Screening Working Group, the International Association of Nanotechnology's Nomenclature and Terminology

Subcommittee, and the American National Standards Institute Nanotechnology Standard Panel (ANSI-NSP). Currently, a NanoTechnology Interest Group (NTIG) formed by US Food and Drug Administration is regulating the nanotechnological products.¹⁶²

2.7 SUMMARY

Topical nanoparticles utilized various polymers and lipids to study the influence of composition of nanoparticles on the drug stability and skin permeability of drugs and cosmetic actives.

The cationic nature of chitosan nanoparticles provides them good cell permeability characteristics. Chitosan also interacts with keratin and alters the barrier properties of stratum corneum to increase the skin permeability of various compounds. Due to its cationic nature, it forms stable complexes with many DNA molecules to improve their physical and chemical stability, which makes this polymer suitable for DNA delivery applications. Its inherent property of cell attachment and proliferation helps in quick restoring the damaged cells. Chitosan also possesses antibacterial and hemostatic property which makes it suitable for skin burn and wound healing applications. The biodegradability and release properties of PLGA can be modulated by altering lactide/glycolide ratio. More commonly PLGA with 1:1 lactide:glycolide ratio was used in topical nanoparticle formulations. PLGA nanoparticles accumulate in hair follicles and sebaceous glands to provide sustained drug delivery. In addition, PLGA provided stability and intracellular delivery of photosensitizers in the PUVA therapy. Although, PCL has excellent mechanical properties and biodegradability, owing to the high degree of crystallinity and hydrophobicity, it is less biocompatible with soft tissue which limits the use of this polymer for further clinical applications. Polyacrylate polymers produce ultrafine particles which can adsorb

both hydrophilic and lipophilic drugs. These particles can improve topical and transdermal delivery of drugs. PAMAM polymers (dendrimers) are particularly suitable for molecular encapsulation of drugs by covalent and non-covalent interactions leading to increased drug solubility and high drug loading. Mostly generation 4 and 5 dendrimers are used for transdermal applications. These help to present the drug to the skin in the solubilized form and increase its permeability. Further, they interact with ceramides and fatty acids and enhance skin permeation.

Glyceryl behenate is mostly used in combination with caprylic/capric triglycerides to form NLCs. These are commonly used for enhancing physical and chemical stability of susceptible actives. These nanoparticles are particularly suitable for enhancing the skin deposition of drugs such as NSAIDs because of their intimate contact with stratum corneum and similar composition to skin lipids. Glyceryl behenate based nanoparticles were particularly used for stabilizing retinol and retinyl palmitate in the topical products. Glyceryl behenate can offer high drug loadings for lipophilic actives ($\text{Log } P > 3.0$). Glyceryl tripalmitate and glyceryl palmitostearate based nanoparticles were mostly used for topical delivery of anti-acne or UV protection applications due to their accumulation in the upper layers of skin. These nanoparticles are also useful for minimizing their skin irritation and systemic absorption to reduce systemic toxicity.

Bees wax and carnauba wax are not utilized well due to their poor drug loading capacity, because of their highly ordered crystal lattice structures. However, incorporation of liquid lipids induces crystal defects and increases drug loading for their use in transdermal and topical delivery. They are mostly used for topical delivery of UV-protecting actives or sunscreens due to inherent anti-UV activity owing to the presence of double conjugated systems such as the

cinnamates that enhance the UV-protection. Cetyl palmitate is mostly used for epidermal targeting due to its occlusive effect and accumulation into skin structures.

2.8 ACKNOWLEDGEMENT

We would like to acknowledge the financial assistance and research resources of Auburn University, School of Pharmacy. Authors have no conflicts of interests directly relevant to the content of this article.

2.9 REFERENCES

1. Barry BW, Williams AC. 1995. Permeation enhancement through skin. In Encyclopedia of Pharmaceutical Technology; Swarbrick, J, Boylan, JC, Ed.; Marcel Dekker: New York; pp: 449– 493.
2. Barry BW. 2001. Novel mechanisms and devices to enable successful transdermal drug delivery. *Eur J Pharm Sci* 14(2):101-114.
3. Lawson LB, Freytag LC, Clements JD. 2007. Use of nanocarriers for transdermal vaccine delivery. *Clin Pharmacol Ther* 82(6):641-643.
4. Saupe A, Wissing SA, Lenk A, Schmidt C, Müller RH. 2005. Solid lipid nanoparticles (SLN) and nanostructured lipid carriers (NLC) - structural investigations on two different carrier systems. *Biomed Mater Eng* 15(5):393-402.
5. Schäfer-Korting M, Mehnert W, Korting HC. 2007. Lipid nanoparticles for improved topical application of drugs for skin diseases. *Adv Drug Deliv Rev* 59(6):427-443.

6. Souto EB, Almeida AJ, Müller RH. 2007. Lipid Nanoparticles (SLN[®], NLC[®]) for Cutaneous Drug Delivery: Structure, Protection and Skin Effects. *J Biomed Nanotechnol* 3(4):317-331.
7. Souto EB, Müller RH. 2008. Cosmetic features and applications of lipid nanoparticles (SLN[®], NLC[®]). *Int J Cosmet Sci* 30(3):157-165.
8. Wu X, Guy RH. 2009. Applications of nanoparticles in topical drug delivery and in cosmetics. *J Biomed Nanotechnol* 19(6):371-384.
9. Müller RH, Mäder K, Gohla S. 2000. Solid lipid nanoparticles (SLN) for controlled drug delivery - a review of the state of the art. *Eur J Pharm Biopharm* 50(1):161-177.
10. Hadgraft J, Lane ME. 2005. Skin permeation: The years of enlightenment. *Int J Pharm* 305(1-2):2-12.
11. Prausnitz MR, Mitragotri S, Langer R. 2004. Current status and future potential of transdermal drug delivery. *Nat Rev Drug Discov* 3(2):115-124.
12. Baroli B. 2010. Penetration of nanoparticles and nanomaterials in the skin: fiction or reality? *J Pharm Sci* 99(1):21-50.
13. Bouwstra JA, Ponc M. 2006. The skin barrier in healthy and diseased state. *Biochim Biophys Acta* 1758(12):2080-2095.
14. Potts RO, Francoeur ML. 1991. The influence of stratum corneum morphology on water permeability. *J Invest Dermatol* 96(4):495-499.
15. Vogt A, Combadiere B, Hadam S, Stieler KM, Lademann J, Schaefer H, Autran B, Sterry W, Blume-Peytavi U. 2006. 40 nm, but not 750 or 1,500 nm, nanoparticles enter epidermal CD1a⁺ cells after transcutaneous application on human skin. *J Invest Dermatol* 126(6):1316-1322.

16. Castro GA, Orefice RL, Vilela JM, Andrade MS, Ferreira LA. 2007. Development of a new solid lipid nanoparticle formulation containing retinoic acid for topical treatment of acne. *J Microencapsul* 24(5):395-407.
17. Chourasia R, Jain SK. 2009. Drug targeting through pilosebaceous route. *Curr Drug Targets* 10(10):950-967.
18. Toll R, Jacobi U, Richter H, Lademann J, Schaefer H, Blume-Peytavi U. 2004. Penetration profile of microspheres in follicular targeting of terminal hair follicles. *J Invest Dermatol* 123(1):168-176.
19. Wu X, Griffin P, Price GJ, Guy RH. 2009. Preparation and in vitro evaluation of topical formulations based on polystyrene-poly-2-hydroxyl methacrylate nanoparticles. *Mol Pharm* 6(5):1449-1456.
20. Couvreur P, Barratt G, Fattal E, Legrand P, Vauthier C. 2002. Nanocapsule technology: a review. *Crit Rev Ther Drug Carrier Syst* 19(2):99-134.
21. Sarkar AB, Kestur U, Kochak GM. 2009. Interfacially assembled carbohydrate nanocapsules: a hydrophilic macromolecule delivery platform. *J Biomed Nanotechnol* 5(5):456-463.
22. Labib A, Lenaerts V, Chouinard F, Leroux JC, Ouellet R, van Lier JE. 1991. Biodegradable nanospheres containing phthalocyanines and naphthalocyanines for targeted photodynamic tumor therapy. *Pharm Res* 8(8):1027-1031.
23. Pinto Reis C, Neufeld RJ, Ribeiro AJ, Veiga F. 2006. Nanoencapsulation I. Methods for preparation of drug-loaded polymeric nanoparticles. *Nanomedicine* 2(1):8-21.
24. Dodane V, Vilivalam VD. 1998. Pharmaceutical applications of chitosan. *Pharmaceutical Science & Technology Today* 1(6):246-253.

25. Francis Suh JK, Matthew HWT. 2000. Application of chitosan-based polysaccharide biomaterials in cartilage tissue engineering: a review. *Biomaterials* 21(24):2589-2598.
26. Berth G, Dautzenberg H, Peter MG. 1998. Physico-chemical characterization of chitosans varying in degree of acetylation. *Carbohydr Polym* 36(2-3):205-216.
27. Muzzarelli RAA, Muzzarelli C. 2005. Chitosan Chemistry: Relevance to the Biomedical Sciences. In *Polysaccharides I, structure, characterization and use*; Heinze T, Ed.; Springer: Heidelberg; pp: 151-209.
28. He W, Guo X, Xiao L, Feng M. 2009. Study on the mechanisms of chitosan and its derivatives used as transdermal penetration enhancers. *Int J Pharm* 382(1-2):234-243.
29. Hasanovic A, Zehl M, Reznicek G, Valenta C. 2009. Chitosan-tripolyphosphate nanoparticles as a possible skin drug delivery system for aciclovir with enhanced stability. *J Pharm Pharmacol* 61(12):1609-1616.
30. MacLaughlin FC, Mumper RJ, Wang J, Tagliaferri JM, Gill I, Hinchcliffe M, Rolland AP. 1998. Chitosan and depolymerized chitosan oligomers as condensing carriers for in vivo plasmid delivery. *J Control Release* 56(1-3):259-272.
31. Cui Z, Mumper RJ. 2001. Chitosan-based nanoparticles for topical genetic immunization. *J Control Release* 75(3):409-419.
32. Lee PW, Peng SF, Su CJ, Mi FL, Chen HL, Wei MC, Lin HJ, Sung HW. 2008. The use of biodegradable polymeric nanoparticles in combination with a low-pressure gene gun for transdermal DNA delivery. *Biomaterials* 29(6):742-751.
33. Wang X, Xu W, Mohapatra S, Kong X, Li X, Lockey RF, Mohapatra SS. 2008. Prevention of airway inflammation with topical cream containing imiquimod and small interfering RNA for natriuretic peptide receptor. *Genet Vaccines Ther* 6(7):1-9.

34. Nair LS, Laurencin CT. 2007. Biodegradable polymers as biomaterials. *Prog Polym Sci* 32(8-9):762-798.
35. Peluso G, Petillo O, Ranieri M, Santin M, Ambrosic L, Calabró D, Avallone B, Balsamo G. 1994. Chitosan-mediated stimulation of macrophage function. *Biomaterials* 15(15):1215-1220.
36. Usami Y, Okamoto Y, Takayama T, Shigemasa Y, Minami S. 1998. Chitin and chitosan stimulate canine polymorphonuclear cells to release leukotriene B4 and prostaglandin E2. *J Biomed Mater Res* 42(4):517-522.
37. Colonna C, Conti B, Perugini P, Pavanetto F, Modena T, Dorati R, Iadarola P, Genta I. 2008. Ex vivo evaluation of prolidase loaded chitosan nanoparticles for the enzyme replacement therapy. *Eur J Pharm Biopharm* 70(1):58-65.
38. Noh HK, Lee SW, Kim JM, Oh JE, Kim KH, Chung CP, Choi SC, Park WH, Min BM. 2006. Electrospinning of chitin nanofibers: Degradation behavior and cellular response to normal human keratinocytes and fibroblasts. *Biomaterials* 27(21):3934-3944.
39. Perrin DE, English JP. Polyglycolide and Polylactide. 1997. In *Handbook of biodegradable polymers*; Domb AJ, Kost J, Wiseman DM, Ed.; Harwood academic publishers: Amsterdam; pp:3-28.
40. Maurus PB, Kaeding CC. 2004. Bioabsorbable implant material review. *Oper Tech Sports Med* 12(3):158-160.
41. Li J, Zhai Y, Zhang B, Deng L, Xu Y, Dong A. 2008. Methoxy poly(ethylene glycol)-block-poly(D,L-lactic acid) copolymer nanoparticles as carriers for transdermal drug delivery. *Polymer International* 57(2):268-274.

42. Rancan F, Papakostas D, Hadam S, Hackbarth S, Delair T, Primard C, Verrier B, Sterry W, Blume-Peytavi U, Vogt A. 2009. Investigation of polylactic acid (PLA) nanoparticles as drug delivery systems for local dermatotherapy. *Pharm Res* 26(8):2027-2036.
43. Middleton JC, Tipton AJ. 2000. Synthetic biodegradable polymers as orthopedic devices. *Biomaterials* 21(23):2335-2346.
44. Gomes AJ, Faustino AS, Lunardi CN, Lunardi LO, Machado AE. 2007. Evaluation of nanoparticles loaded with benzopsoralen in rat peritoneal exudate cells. *Int J Pharm* 332(1-2):153-160.
45. Luengo J, Weiss B, Schneider M, Ehlers A, Stracke F, König K, Kostka KH, Lehr CM, Schaefer UF. 2006. Influence of nanoencapsulation on human skin transport of flufenamic acid. *Skin Pharmacol Physiol* 19(4):190-197.
46. Min B-M, You Y, Kim JM, Lee SJ, Park WH. 2004. Formation of nanostructured poly(lactic-co-glycolic acid)/chitin matrix and its cellular response to normal human keratinocytes and fibroblasts. *Carbohydr Polym* 57(3):285-292.
47. Ricci-Junior E, Marchetti JM. 2006. Preparation, characterization, photocytotoxicity assay of PLGA nanoparticles containing zinc (II) phthalocyanine for photodynamic therapy use. *J Microencapsul* 23(5):523-538.
48. Stracke F, Weiss B, Lehr CM, König K, Schaefer UF, Schneider M. 2006. Multiphoton microscopy for the investigation of dermal penetration of nanoparticle-borne drugs. *J Invest Dermatol* 126(10):2224-2233.

49. Wang F, Chen Y, Benson HAE. 2008. Formulation of nano and micro PLGA particles of the model peptide insulin: preparation, characterization, stability and deposition in human skin. *The Open Drug Delivery Journal* 2:1-9.
50. Nicoli S, Santi P, Couvreur P, Couarraze G, Colombo P, Fattal E. 2001. Design of triptorelin loaded nanospheres for transdermal iontophoretic administration. *Int J Pharm* 214(1-2):31-35.
51. Gomes AJ, Lunardi LO, Marchetti JM, Lunardi CN, Tedesco AC. 2005. Photobiological and ultrastructural studies of nanoparticles of poly(lactic-co-glycolic acid)-containing bacteriochlorophyll-a as a photosensitizer useful for PDT treatment. *Drug Deliv* 12(3):159-164.
52. Lboutounne H, Guillaume YC, Michel L, Makki S, Humbert P, Millet J. 2004. Study and development of encapsulated forms of 4, 5, 8-Trimethylpsoralen for topical drug delivery. *Drug Dev Res* 61(2):86-94.
53. Ponsart S, Coudane J, Vert M. 2000. A novel route to poly(ϵ -caprolactone)-based copolymers via anionic derivatization. *Biomacromolecules* 1(2):275-281.
54. Wei X, Gong C, Gou M, Fu S, Guo Q, Shi S, Luo F, Guo G, Qiu L, Qian Z. 2009. Biodegradable poly(ϵ -caprolactone)-poly(ethylene glycol) copolymers as drug delivery system. *Int J Pharm* 381(1):1-18.
55. Raghavan D. 1995. Characterization of biodegradable plastics. *Polym Plast Technol Eng* 34(1):41-63.
56. Gunatillake P, Mayadunne R, Adhikari R. 2006. Recent developments in biodegradable synthetic polymers. *Biotechnol Annu Rev* 12:301-347.

57. Perrin DE, English JP. 1997. Polycaprolactone. In Handbook of biodegradable polymers; Domb AJ, Kost J, Wiseman DM, Ed.; Harwood academic publishers: Amsterdam; pp:63-78.
58. Pitt GG, Gratzl MM, Kimmel GL, Surles J, Sohindler A. 1981. Aliphatic polyesters II. The degradation of poly (DL-lactide), poly ([epsilon]-caprolactone), and their copolymers in vivo. *Biomaterials* 2(4):215-220.
59. Xu P, Tang H, Li S, Ren J, Van Kirk E, Murdoch WJ, Radosz M, Shen Y. 2004. Enhanced stability of core-surface cross-linked micelles fabricated from amphiphilic brush copolymers. *Biomacromolecules* 5(5):1736-1744.
60. Shim J, Seok Kang H, Park WS, Han SH, Kim J, Chang IS. 2004. Transdermal delivery of mixnoxidil with block copolymer nanoparticles. *J Control Release* 97(3):477-484.
61. Alvarez-Roman R, Naik A, Kalia YN, Guy RH, Fessi H. 2004. Enhancement of topical delivery from biodegradable nanoparticles. *Pharm Res* 21(10):1818-1825.
62. Rastogi R, Anand S, Koul V. 2009. Flexible polymerosomes-An alternative vehicle for topical delivery. *Colloids Surf B Biointerfaces* 72(1):161-166.
63. Choi JS, Leong KW, Yoo HS. 2008. In vivo wound healing of diabetic ulcers using electrospun nanofibers immobilized with human epidermal growth factor (EGF). *Biomaterials* 29(5):587-596.
64. Fattal E, Peracchia MT, Couvreur P. 1997. Poly(alkylcyanoacrylates). In Handbook of biodegradable polymers; Domb AJ, Kost J, Wiseman DM, Ed.; Harwood academic publishers: Amsterdam; pp:183-202.

65. Nair LS, Laurencin CT. 2006. Polymers as biomaterials for tissue engineering and controlled drug delivery. *Adv Biochem Eng/Biotechnol* 102:47-90.
66. Piskin E. 2002. Biodegradable polymers in medicine. In *Journal of Biomaterials Science, Polymer Edition*; Piskin E, Ed.; Kluwer academic publishers: Dordrecht; pp:321-378.
67. Miyazaki S, Takahashi A, Kubo W, Bachynsky J, Loebenberg R. 2003. Poly n-butylcyanoacrylate (PNBCA) nanocapsules as a carrier for NSAIDs: in vitro release and in vivo skin penetration. *J Pharm Pharm Sci* 6(2):238-245.
68. Xing J, Deng L, Li J, Dong A. 2009. Amphiphilic poly{[alpha-maleic anhydride-omega-methoxy-poly(ethylene glycol)]-co-(ethyl cyanoacrylate)} graft copolymer nanoparticles as carriers for transdermal drug delivery. *Int J Nanomedicine* 4:227-232.
69. Diaz-Torres R, Castano VM, Ganem-Quintanar A, Quintanar-Guerrero D, Rodriguez-Romo S. 2005. Oscillations in the kinetics of ethylcyanoacrylate nanoparticles intended as skin drug carriers. *Nanotechnology* 16:2612–2618.
70. Simeonova M, Velichkova R, Ivanova G, Enchev V, Abrahams I. 2003. Poly(butylcyanoacrylate) nanoparticles for topical delivery of 5-fluorouracil. *Int J Pharm* 263(1-2):133-140.
71. Khandare J, Haag R. 2010. Pharmaceutically used polymers: principles, structures, and applications of pharmaceutical delivery systems. *Handb Exp Pharmacol* 197:221-250.

72. Lee JW, Kim JH, Kim BK. 2006. Synthesis of azide-functionalized PAMAM dendrons at the focal point and their application for synthesis of PAMAM-like dendrimers. *Tetrahedron Lett* 47(16):2683-2686.
73. Danusso F, Ferruti P. 1970. Synthesis of tertiary amine polymers. *Polymer* 11(2):88-113.
74. Bignotti F, Sozzani P, Ranucci E, Ferruti P. 1994. NMR studies, molecular characterization, and degradation behavior of poly(amido amine)s. 1. poly(amido amine) deriving from the polyaddition of 2-Methylpiperazine to 1,4-Bis(acryloyl)piperazine. *Macromolecules* 27(24):7171-7178.
75. Loftsson T, Masson M. 2001. Cyclodextrins in topical drug formulations: theory and practice. *Int J Pharm* 225(1-2):15-30.
76. Chauhan AS, Sridevi S, Chalasani KB, Jain AK, Jain SK, Jain NK, Diwan PV. 2003. Dendrimer-mediated transdermal delivery: enhanced bioavailability of indomethacin. *J Control Release* 90(3):335-343.
77. Venuganti VV, Perumal OP. 2008. Effect of poly(amidoamine) (PAMAM) dendrimer on skin permeation of 5-fluorouracil. *Int J Pharm* 361(1-2):230-238.
78. Venuganti VV, Perumal OP. 2009. Poly(amidoamine) dendrimers as skin penetration enhancers: Influence of charge, generation, and concentration. *J Pharm Sci* 98(7):2345-2356.
79. Yiyun C, Na M, Tongwen X, Rongqiang F, Xueyuan W, Xiaomin W, Longping W. 2006. Transdermal delivery of nonsteroidal anti-inflammatory drugs mediated by polyamidoamine (PAMAM) dendrimers. *J Pharm Sci* 96(3):595-602.

80. Battah SH, Chee CE, Nakanishi H, Gerscher S, MacRobert AJ, Edwards C. 2001. Synthesis and biological studies of 5-aminolevulinic acid-containing dendrimers for photodynamic therapy. *Bioconjug Chem* 12(6):980-988.
81. Battah S, Balaratnam S, Casas A, O'Neill S, Edwards C, Battle A, Dobbin P, MacRobert AJ. 2007. Macromolecular delivery of 5-aminolaevulinic acid for photodynamic therapy using dendrimer conjugates. *Mol Cancer Ther* 6(3):876-885.
82. Wang Z, Itoh Y, Hosaka Y, Kobayashi I, Nakano Y, Maeda I, Umeda F, Yamakawa J, Kawase M, Yag K. 2003. Novel transdermal drug delivery system with polyhydroxyalkanoate and starburst polyamidoamine dendrimer. *J Biosci Bioeng* 95(5):541-543.
83. Bielinska AU, Yen A, Wu HL, Zahos KM, Sun R, Weiner ND, Baker JR, Jr., Roessler BJ. 2000. Application of membrane-based dendrimer/DNA complexes for solid phase transfection in vitro and in vivo. *Biomaterials* 21(9):877-887.
84. Mecke A, Uppuluri S, Sassanella TM, Lee D-K, Ramamoorthy A, Baker JJR, Orr BG, Banaszak Holl MM. 2004. Direct observation of lipid bilayer disruption by poly(amidoamine) dendrimers. *Chem Phys Lipids* 132(1):3-14.
85. Zhang J, Purdon CH, Smith EW. 2006. Solid Lipid Nanoparticles for Topical Drug Delivery. *American Journal of Drug Delivery* 4(4):215-220.
86. Zweers MLT, Engbers GHM, Grijpma DW, Feijen J. 2004. In vitro degradation of nanoparticles prepared from polymers based on DL-lactide, glycolide and poly(ethylene oxide). *J Control Release* 100(3):347-356.

87. Müller RH, Radtke M, Wissing SA. 2002. Solid lipid nanoparticles (SLN) and nanostructured lipid carriers (NLC) in cosmetic and dermatological preparations. *Adv Drug Deliv Rev* 54(Supplement 1):S131-S155.
88. Saupe A, Rades T. 2006. Solid Lipid Nanoparticles. In *Nanocarrier Technologies: Frontiers of nanotherapy*; Mozafari MR, Ed.; Springer: Dordrecht; pp:41-50.
89. Jannin V, Musakhanian J, Marchaud D. 2008. Approaches for the development of solid and semi-solid lipid-based formulations. *Adv Drug Deliv Rev* 60(6):734-746.
90. Korting HC, Schäfer-Korting M. 2010. Carriers in the topical treatment of skin disease. *Handb Exp Pharmacol* 197:435-468.
91. Müller RH, Petersen RD, Hommoss A, Pardeike J. 2007. Nanostructured lipid carriers (NLC) in cosmetic dermal products. *Adv Drug Deliv Rev* 59(6):522-530.
92. Pardeike J, Hommoss A, Müller RH. 2009. Lipid nanoparticles (SLN, NLC) in cosmetic and pharmaceutical dermal products. *Int J Pharm* 366(1-2):170-184.
93. Puglia C, Blasi P, Rizza L, Schoubben A, Bonina F, Rossi C, Ricci M. 2008. Lipid nanoparticles for prolonged topical delivery: an in vitro and in vivo investigation. *Int J Pharm* 357(1-2):295-304.
94. Puglia C, Filosa R, Peduto A, de Caprariis P, Rizza L, Bonina F, Blasi P. 2006. Evaluation of alternative strategies to optimize ketorolac transdermal delivery. *AAPS PharmSciTech* 7(3):64.
95. Ricci M, Puglia C, Bonina F, Giovanni CD, Giovagnoli S, Rossi C. 2005. Evaluation of indomethacin percutaneous absorption from nanostructured lipid carriers (NLC): in vitro and in vivo studies. *J Pharm Sci* 94(5):1149-1159.

96. Alves MP, Scarrone AL, Santos M, Pohlmann AR, Guterres SS. 2007. Human skin penetration and distribution of nimesulide from hydrophilic gels containing nanocarriers. *Int J Pharm* 341(1-2):215-220.
97. Ourique AF, Pohlmann AR, Guterres SS, Beck RCR. 2008. Tretinoin-loaded nanocapsules: Preparation, physicochemical characterization, and photostability study. *Int J Pharm* 352(1-2):1-4.
98. Eskandar NG, Simovic S, Prestidge CA. 2009. Nanoparticle coated submicron emulsions: sustained in-vitro release and improved dermal delivery of all-trans-retinol. *Pharm Res* 26(7):1764-1775.
99. Eskandar NG, Simovic S, Prestidge CA. 2010. Mechanistic insight into the dermal delivery from nanoparticle-coated submicron O/W emulsions. *J Pharm Sci* 99(2):890-904.
100. Jennings V, Gysler A, Schäfer-Korting M, Gohla SH. 2000. Vitamin A loaded solid lipid nanoparticles for topical use: occlusive properties and drug targeting to the upper skin. *Eur J Pharm Biopharm* 49(3):211-218.
101. Pople PV, Singh KK. 2006. Development and evaluation of topical formulation containing solid lipid nanoparticles of vitamin A. *AAPS PharmSciTech* 7(4):91.
102. Jennings V, Gohla S. 2000. Comparison of wax and glyceride solid lipid nanoparticles (SLN[®]). *Int J Pharm* 196(2):219-222.
103. Jennings V, Gohla SH. 2001. Encapsulation of retinoids in solid lipid nanoparticles (SLN). *J Microencapsul* 18(2):149-158.

104. Gavini E, Sanna V, Sharma R, Juliano C, Usai M, Marchetti M, Karlsen J, Giunchedi P. 2005. Solid lipid microparticles (SLM) containing juniper oil as anti-acne topical carriers: preliminary studies. *Pharm Dev Technol* 10(4):479-487.
105. Bhalekar MR, Pokharkar V, Madgulkar A, Patil N, Patil N. 2009. Preparation and evaluation of miconazole nitrate-loaded solid lipid nanoparticles for topical delivery. *AAPS PharmSciTech* 10(1):289-296.
106. Souto EB, Müller RH. 2005. SLN and NLC for topical delivery of ketoconazole. *J Microencapsul* 22(5):501-510.
107. Maia CS, Mehnert W, Schäfer-Korting M. 2000. Solid lipid nanoparticles as drug carriers for topical glucocorticoids. *Int J Pharm* 196(2):165-167.
108. Stecová J, Mehnert W, Blaschke T, Kleuser B, Sivaramakrishnan R, Zouboulis CC, Seltmann H, Korting HC, Kramer KD, Schäfer-Korting M. 2007. Cyproterone acetate loading to lipid nanoparticles for topical acne treatment: particle characterisation and skin uptake. *Pharm Res* 24(5):991-1000.
109. Hu FQ, Yuan H, Zhang HH, Fang M. 2002. Preparation of solid lipid nanoparticles with clobetasol propionate by a novel solvent diffusion method in aqueous system and physicochemical characterization. *Int J Pharm* 239(1-2):121-128.
110. Sanna V, Gavini E, Cossu M, Rassa G, Giunchedi P. 2007. Solid lipid nanoparticles (SLN) as carriers for the topical delivery of econazole nitrate: in-vitro characterization, ex-vivo and in-vivo studies. *J Pharm Pharmacol* 59(8):1057-1064.
111. Maia CS, Mehnert W, Schaller M, Korting HC, Gysler A, Haberland A, Schäfer-Korting M. 2002. Drug targeting by solid lipid nanoparticles for dermal use. *J Drug Target* 10(6):489-495.

112. Pathak P, Nagarsenker M. 2009. Formulation and evaluation of lidocaine lipid nanosystems for dermal delivery. *AAPS PharmSciTech* 10(3):985-992.
113. Sanna V, Mariani A, Caria G, Sechi M. 2009. Synthesis and evaluation of different fatty acid esters formulated into Precirol ATO-Based lipid nanoparticles as vehicles for topical delivery. *Chem Pharm Bull* 57(7):680-684.
114. Fang JY, Fang CL, Liu CH, Su YH. 2008. Lipid nanoparticles as vehicles for topical psoralen delivery: Solid lipid nanoparticles (SLN) versus nanostructured lipid carriers (NLC). *Eur J Pharm Biopharm* 70(2):633-640.
115. Liu W, Hu M, Liu W, Xue C, Xu H, Yang X. 2008. Investigation of the carbopol gel of solid lipid nanoparticles for the transdermal iontophoretic delivery of triamcinolone acetonide acetate. *Int J Pharm* 364(1):135-141.
116. Liu J, Hu W, Chen H, Ni Q, Xu H, Yang X. 2007. Isotretinoin-loaded solid lipid nanoparticles with skin targeting for topical delivery. *Int J Pharm* 328(2):191-195.
117. Bunjes H, Drechsler M, Koch MH, Westesen K. 2001. Incorporation of the model drug ubidecarenone into solid lipid nanoparticles. *Pharm Res* 18(3):287-293.
118. Chen H, Chang X, Du D, Liu W, Liu J, Weng T, Yang Y, Xu H, Yang X. 2006. Podophyllotoxin-loaded solid lipid nanoparticles for epidermal targeting. *J Control Release* 110(2):296-306.
119. Chen H, Xiao L, Du D, Mou D, Xu H, Yang X. 2010. A facile construction strategy of stable lipid nanoparticles for drug delivery using a hydrogel-thickened microemulsion system. *Nanotechnology* 21(1):1-9.

120. Souto EB, Müller RH. 2006. Investigation of the factors influencing the incorporation of clotrimazole in SLN and NLC prepared by hot high-pressure homogenization. *J Microencapsul* 23(4):377-388.
121. Zhang J, Purdon C, Smith E. 2006. Solid lipid nanoparticles for topical drug delivery. *Am J Drug Deliv* 4(4): 215-220.
122. Manjunath K, Reddy JS, Venkateswarlu V. 2005. Solid lipid nanoparticles as drug delivery systems. *Methods Find Exp Clin Pharmacol* 27(2):127-144.
123. Attama AA, Schicke BC, Müller-Goymann CC. 2006. Further characterization of theobroma oil-beeswax admixtures as lipid matrices for improved drug delivery systems. *Eur J Pharm Biopharm* 64(3):294-306.
124. Attama AA, Müller-Goymann CC. 2008. Effect of beeswax modification on the lipid matrix and solid lipid nanoparticle crystallinity. *Colloids Surf A Physicochem Eng Asp* 315(1-3):189-195.
125. Pardeike J, Hommoss A, Müller RH. 2009. Lipid nanoparticles (SLN, NLC) in cosmetic and pharmaceutical dermal products. *Int J Pharm* 366(1-2):170-184.
126. Ruktanonchai U, Bejrapha P, Sakulkhu U, Opanasopit P, Bunyaphatsara N, Junyaprasert V, Puttipatkhachorn S. 2009. Physicochemical characteristics, cytotoxicity, and antioxidant activity of three lipid nanoparticulate formulations of alpha-lipoic acid. *AAPS PharmSciTech* 10(1):227-234.
127. Villalobos-Hernández JR, Müller-Goymann CC. 2006. Sun protection enhancement of titanium dioxide crystals by the use of carnauba wax nanoparticles: The synergistic interaction between organic and inorganic sunscreens at nanoscale. *Int J Pharm* 322(1-2):161-170.

128. Villalobos-Hernández JR, Müller-Goymann CC. 2005. Novel nanoparticulate carrier system based on carnauba wax and decyl oleate for the dispersion of inorganic sunscreens in aqueous media. *Eur J Pharm Biopharm* 60(1):113-122.
129. Edelson J, Kotyla T, Zhang B. 2008. Nucleic acid nanoparticles and uses thereof for treatment of skin disorders. In Organization WIP, editor World Intellectual Property Organization, ed., WIPO patent WO2008151022: Anterios, Inc. p 90.
130. García-González CA, Sousa ARSd, Argemí A, Periago AL, Saurina J, Duarte CMM, Domingo C. 2009. Production of hybrid lipid-based particles loaded with inorganic nanoparticles and active compounds for prolonged topical release. *Int J Pharm* 382(1-2):296-304.
131. Anantachaisilp S, Smith SM, Treetong A, Pratontep S, Puttipipatkachorn S, Ruktanonchai UR. 2010. Chemical and structural investigation of lipid nanoparticles: drug-lipid interaction and molecular distribution. *Nanotechnology* 21(12):1-11.
132. Teeranachaideekul V, Souto EB, Junyaprasert VB, Müller RH. 2007. Cetyl palmitate-based NLC for topical delivery of Coenzyme Q10 - Development, physicochemical characterization and in vitro release studies. *Eur J Pharm Biopharm* 67(1):141-148.
133. Pardeike J, Schwabe K, Müller RH. 2010. Influence of nanostructured lipid carriers (NLC) on the physical properties of the Cutanova Nanorepair Q10 cream and the in vivo skin hydration effect. *Int J Pharm* 396(1-2):166-173.
134. Lippacher A, Müller RH, Mäder K. 2002. Semisolid SLNTM dispersions for topical application: influence of formulation and production parameters on viscoelastic properties. *Eur J Pharm Biopharm* 53(2):155-160.

135. Teeranachaideekul V, Boonme P, Souto EB, Müller RH, Junyaprasert VB. 2008. Influence of oil content on physicochemical properties and skin distribution of Nile red-loaded NLC. *J Control Release* 128(2):134-141.
136. Junyaprasert VB, Teeranachaideekul V, Souto EB, Boonme P, Müller RH. 2009. Q10-loaded NLC versus nanoemulsions: Stability, rheology and in vitro skin permeation. *Int J Pharm* 377(1-2):207-214.
137. Wissing SA, Müller RH. 2002. Solid lipid nanoparticles as carrier for sunscreens: in vitro release and in vivo skin penetration. *Journal of Controlled Release* 81(3):225-233.
138. Bhaskar K, Anbu J, Ravichandiran V, Venkateswarlu V, Rao YM. 2009. Lipid nanoparticles for transdermal delivery of flurbiprofen: formulation, in vitro, ex vivo and in vivo studies. *Lipids Health Dis* 8(6):1-15.
139. Zimmermann E, Müller RH. 2001. Electrolyte- and pH-stabilities of aqueous solid lipid nanoparticle (SLN) dispersions in artificial gastrointestinal media. *Eur J Pharm Biopharm* 52(2):203-210.
140. Iijima M, Kamiya H. 2009. Surface modification for improving the stability of nanoparticles in liquid media. *KONA Powder and Particle Journal* 11(4):1-7.
141. Lemoine D, Francois C, Kedzierewicz F, Preat V, Hoffman M, Maincent P. 1996. Stability study of nanoparticles of poly(ϵ -caprolactone), poly(D,L-lactide) and poly(D,L-lactide-co-glycolide). *Biomaterials* 17(22):2191-2197.
142. Kuchibhatla SV, Karakoti AS, Seal S. 2005. Colloidal stability by surface modification. *J Miner Met Mater Soc* 57(12):52-56.

143. Gracia L, Chowdhry BZ, Snowden MJ. 2006. Stabilization of colloids by polymers. In Encyclopedia of surface and colloid science; Somasundaran P, Ed.; Taylor and Francis: New York. pp:5775-5787.
144. Falkiewicz MJ. 1988. Theory of suspensions. In Pharmaceutical dosage forms- Disperse systems; Liberman HA, Rieger MM and Banker GS, Ed.; Marcel Dekker: New York; pp:13-48.
145. Tiraferri A, Chen KL, Sethi R, Elimelech M. 2008. Reduced aggregation and sedimentation of zero-valent iron nanoparticles in the presence of guar gum. *J Colloid Interface Sci* 324(1-2):71-79.
146. Kaldasch J, Senge B. 2009. Shear thickening in polymer stabilized colloidal suspensions. *Colloid Polym Sci* 287(12):1481-1485.
147. Dutta J, Hofmann H. 2003. Self-organization of colloidal nanoparticles. In Encyclopedia of Nanoscience and Nanotechnology; Nalwa HS, Ed.; American Scientific Publishers: California; pp:1-23.
148. Layre AM, Couvreur P, Richard J, Requier D, Ghermani NE, Gref R. 2006. Freeze-Drying of Composite Core-Shell Nanoparticles. *Drug Dev Ind Pharm* 32(7):839-846.
149. Ohshima H, Miyagishima A, Kurita T, Makino Y, Iwao Y, Sonobe T, Itai S. 2009. Freeze-dried nifedipine-lipid nanoparticles with long-term nano-dispersion stability after reconstitution. *Int J Pharm* 377(1-2):180-184
150. Saez A, Guzmán M, Molpeceres J, Aberturas MR. 2000. Freeze-drying of polycaprolactone and poly(D,L-lactic-glycolic) nanoparticles induce minor particle size changes affecting the oral pharmacokinetics of loaded drugs. *Eur J Pharm Biopharm* 50(3):379-387.

151. Nohynek GJ, Dufour EK, Roberts MS. 2008. Nanotechnology, cosmetics and the skin: is there a health risk? *Skin Pharmacol Physiol* 21(3):136-149.
152. Ryman-Rasmussen JP, Riviere JE, Monteiro-Riviere NA. 2006. Penetration of intact skin by quantum dots with diverse physicochemical properties. *Toxicol Sci* 91(1):159-165.
153. Rouse JG, Yang J, Ryman-Rasmussen JP, Barron AR, Monteiro-Riviere NA. 2007. Effects of mechanical flexion on the penetration of fullerene amino acid-derivatized peptide nanoparticles through skin. *Nano Lett* 7(1):155-160.
154. Kohli AK, Alpar HO. 2004. Potential use of nanoparticles for transcutaneous vaccine delivery: effect of particle size and charge. *Int J Pharm* 275(1-2):13-17.
155. Curtis J, Greenberg M, Kester J, Phillips S, Krieger G. 2006. Nanotechnology and nanotoxicology: a primer for clinicians. *Toxicol Rev* 25(4):245-260
156. Gwinn MR, Vallyathan V. 2006. Nanoparticles: health effects - pros and cons. *Environ Health Perspect* 114(12):1818-1825.
157. Oberdörster G, Oberdörster E, Oberdörster J. 2005. Nanotoxicology: an emerging discipline evolving from studies of ultrafine particles. *Environ Health Perspect* 113(7):823-839.
158. Kunzmann A, Andersson B, Thurnherr T, Krug H, Scheynius A, Fadeel B. 2011. Toxicology of engineered nanomaterials: Focus on biocompatibility, biodistribution and biodegradation. *Biochimica et Biophysica Acta* 1810(3):361-373.
159. Jones CF, Grainger DW. 2009. In vitro assessments of nanomaterial toxicity. *Adv Drug Deliv Rev* 61(6):438-456.

160. Verma A, Stellacci F. 2010. Effect of surface properties on nanoparticle-cell interactions. *Small* 6(1):12-21.
161. Marquis BJ, Love SA, Braun KL, Haynes CL. 2009. Analytical methods to assess nanoparticle toxicity. *Analyst* 134(3):425-439.
162. Chan VS. 2006. Nanomedicine: An unresolved regulatory issue. *Regul Toxicol Pharmacol* 46(3):218-224.

Table 2.1 Polymer based topical nanoparticles for enhanced skin permeation

Polymer system	Active drug /marker	Application	Model
Chitosan	Plasmid DNA for luciferase expression ³¹	Genetic immunization	Female BALB/c mice
CMC	Prolidase (enzyme) ³⁷	Improved intracellular delivery of prolidase	Cultured human skin fibroblasts
	SiRNA for natriuretic peptide receptor A (SiNPRA) ³³	To protect siNPRA from enzymatic degradation in the treatment of bronchitis.	Ovalbumin sensitized BALB/c mice, and nude mice
	Aciclovir ²⁹	Enhanced chemical stability of acyclovir	Excised porcine skin
Chitin nanofibers ³⁸	-	Chitin coated with extracellular matrix proteins (eg: Type I collagen) promoted cell attachment and spreading on the nanowoven matrices	Human keratinocytes and fibroblasts
CS - γ PGL	DNA ³²	γ -PGL provides more compact and dense nanoparticles for better skin penetration	Female BALB/c mice
PEDLLA	Paclitaxel ⁴¹	PEDLLA nanoparticles enlarge the skin pores and get accumulated into hair follicles and sweat ducts	Excised rat skin

PLGA	Flufenamic acid ⁴⁵	Degradation of polymer results in decrease in pH to provide unionized drug for better skin penetration	Surgical human skin
	Bovine insulin ⁴⁹	To improve the stability and skin permeability of insulin	Surgical human skin
	Benzopsoralen (BP) ⁴⁴	To reduce irritation and phototoxicity of BP	Exudate of rat peritoneal cells
	Zinc Phthalocyanine (ZnPc) ⁴⁷	To improve the stability of ZnPC for PDT	Macrophagic cell lines (P388-D1)
	Bacteriochlorophyll -a (BCA) ⁵¹	To improve the stability of BCA for PDT	Macrophagic cell lines (P388-D1)
	Triptorelin ⁵⁰	To improve drug loading in the iontophoretic delivery of triptorelin	Porcine ear skin
	4,5,8-Trimethyl-psoralen (TMP) ⁵²	To improve the stability of TMP for PDT	Surgical human skin
	PCL	Minoxidil ⁶⁰	Nanoparticles accumulated in furrows of stratum corneum, sweat ducts and hair follicles for better permeation of minoxidil
Octyl methoxycinnamate ⁶		Flexible, deformable and fragmentable polymersomes (nanocarrier) which	Excised porcine ear skin

	2	penetrate furrows of stratum corneum and hair follicles.	
	Human epidermal growth factor (rh-EGF) ⁶³	Immobilization of rh-EGF on to nanofibers provides its stability and sustained release for the proliferation and expression of keratinocytes in diabetic wound healing	Female C57BL/6 mice
PACA	Indomethacin ⁶⁷	PACA nanoparticles modify the lipid organization in the stratum corneum for better penetration.	Excised rat skin
	Tetrahydropalmatine (THP) ⁶⁸	For better penetration into stratum corneum and skin appendages	Excised rat skin
Polyamido- amines (Dendrimers)	Indomethacin ⁷⁶	Molecular encapsulation of indomethacin improves its solubility and skin partitioning	Male Wistar Rats
	Tamsulosin hydrochloride (TH) ⁸²	Addition of dendrimer to polyhydroxy alkanolate matrix synergistically enhanced the permeation of TH	Shed snake skin
	Ketoprofen or Diflunisal ⁷⁹	The dendrimer - drug complex enhances solubilization and skin permeation of the drug	Excised rat skin
G7-Dendrimer ⁸⁴	-	Dendrimers create pores or craters in the lipid bilayers due to removal of lipids and formation of dendrimer-lipid aggregates.	Supported lipid bilayer

CS: Chitosan, CMC: Carboxy methyl cellulose, γ PGL: poly- γ -glutamic acid, PEDLLA: Methoxy poly(ethylene glycol)-block-poly(D,Llactic acid), PLGA: Poly(lactide-co-glycolide), PCL: Polycaprolactone, PACA: Poly(alkyl cyanoacrylates)

Table 2.2 Wax and lipid based topical nanoparticles for enhanced skin permeation or epidermal targeting

Lipid system	Active drug /marker	Application	Model
Waxes			
Apifil [®] + Miglyol [®] 812	Alpha-lipoic acid (ALA) ¹²⁶	Miglyol [®] 812 improves drug loading, solubility and the stability of ALA	Polyether-sulfone membrane (MW cut off 500,000)
Bees wax + Theobroma oil ¹²³	-	Stable beta crystals of theobroma oil produced a “disordered matrix” and “microstructures” which is expected to improve drug loading in the wax.	-
Bees wax + (Phospholipon [®] 90G) 124	-	Imperfections in the crystal lattices induced by Phospholipon [®] 90G in the wax which is expected to improve the drug loading in the wax	-
Carnauba wax + Decyl oleate	Inorganic salts ¹²⁸	Wax and its constituents (cinnamates) with inorganic salts synergistically increase UV-protection effect	-
Carnauba wax and its	Titanium Dioxide	The wax (which contains cinnamates)	-

ethanolic extract (cinnamates) + Decyl oleate	(TiO ₂) ¹²⁷	when coated on titanium dioxide synergistically increases UV- protection effect	
Precifac [®] ATO + Miglyol [®] 812	Coenzyme Q ₁₀ ^{132,136,133}	Miglyol [®] 812 improves drug loading, chemical stability and skin permeation of Q ₁₀	Excised human skin
Precifac [®] ATO	Oxybenzone ¹³⁷	Longer retention times on the skin provides higher sunscreen effect	Transpore tape
Precifac [®] ATO + Miglyol [®] 812	Nile red ¹³⁵	Nanoparticles with lower Miglyol [®] 812 (oil) content favored epidermal targeting.	Excised human skin
Glycerides			
Caprylic/capric triglycerides mixture + poly-ε- caprolactone	Tretinoin ⁹⁷	The polymeric layer surrounding the lipid NPs prevents photodegradation of tretinoin	-
Compritol [®] 888 ATO	Prednicarbate ¹¹¹	The drug localization in epidermis reduces the risk of deeper tissue absorption leading to skin atrophy by the inhibition of fibroblasts	Excised human skin and reconstruct ed epidermis
	Vitamin A	The lipidic nature of SLN helps the	Human

	palmitate ¹⁰¹	drug localized in skin for epidermal targeting.	cadaver skin
	Retinol ¹⁰²	Water evaporation induces polymorphic transition in the lipid matrix of NP leading to drug expulsion. As the expelled drug is poorly water soluble, the thermodynamic activity of the drug increases resulting in higher diffusion across the skin layers.	Excised porcine skin
Compritol [®] 888 ATO + Precirol [®] ATO 5	Lidocaine ¹¹²	Lipid matrix encapsulates higher amounts of drug. The SLNs penetrate and get mixed with the lipids in the SC forming a reservoir for sustained release for local effects.	Hairless Guinea pig skin (both <i>in vitro</i> and <i>in vivo</i>)
Compritol [®] 888 ATO + Precirol [®] ATO 5 + propylene glycol	Miconazole nitrate ¹⁰⁵	Propylene glycol enhances solubility and thereby drug loading in the SLNs. The SLNs localize in the skin layers for sustained release and epidermal targeting.	Human cadaver skin
Compritol [®] 888 ATO + α -tocopherol	Ketoconazole ¹⁰⁶	Improved photo stability of drug due to incorporation into lipid nanoparticles	-

Compritol [®] 888 ATO + Miglyol [®] 812	Indomethacin ⁹⁵	Miglyol [®] 812 increases drug loading in the lipid matrix. Drug penetrates the lipid in the stratum corneum by “partial sequestration”.	Excised human skin
	Ketoprofen and Naproxen ⁹³	Miglyol [®] 812 increases drug loading in the lipid matrix. This system provides epidermal targeting and lesser drug reaching systemic circulation.	Surgical human skin
	Ketorolac ⁹⁴	Higher chemical affinity and partial “sequestration” of drug by lipid matrix prevents its permeation through stratum corneum	Excised human skin
Precirol [®] ATO 5 + Miglyol [®] 812	Cyproterone acetate ¹⁰⁸	Precirol [®] ATO 5 increases drug loading in the lipid matrix. Localized drug deposition and epidermal targeting.	Surgical human skin
Precirol [®] ATO 5 + stearic acid	Triamcinolone acetone acetate ¹¹⁵	Improved drug loading, stability and electric conductance suitable for iontophoretic delivery of the drug.	Porcine ear skin
Precirol [®] ATO 5	Isotretinoin ¹¹⁶	Direct skin contact and systemic uptake of the drug were avoided. Also SLNs accumulate in the epidermis to	Excised rat skin

		provide skin targeting.	
	Econazole nitrate ¹¹³	Disorganization of structured lipids of stratum corneum enhances skin permeation.	Porcine ear skin
	Psoralens ¹¹⁴	NLCs (Precirol [®] ATO 5 + squalene) provided significantly higher skin permeation than SLNs (Precirol [®] ATO 5 alone).	Female nude mice skin
Dynasan [®] 116	Clotrimazole ¹²⁰	SLNs provided enhanced chemical stability for the drug than NLCs	-
	Coenzyme Q10 ¹¹⁷	Formation of supercooled melt inside the lipid enhances chemical stability of drug	-
Tripalmitin	Podophyllotoxin ¹¹⁸	Small size of nanoparticles provides epidermal targeting	Porcine skin
Lumulse [®] GMS-K + Cutina [®] HR	TiO ₂ (silanized) and caffeine ¹³⁰	Cutina [®] HR improves TiO ₂ loading in the lipid matrix	-
Glyceryl monostearate (Monostearin)	Betamethasone 17-valerate ¹²¹	Monostearin nanoparticles show lower permeation rate and greater reservoir effect in the epidermis than beeswax nanoparticles	Human skin
Dynasan [®] 114 + Captex [®] 355	Flurbiprofen ¹³⁸	Captex [®] 355 improves drug loading in the lipid matrix for enhanced skin	Excised rat skin

permeation

Apifil[®]: Polyethylene glycol-8-Beeswax, Captex[®] 355: Caprylic/capric triglycerides; Compritol[®] 888 ATO: Glyceryl Behenate; Cutina[®] HR: Hydrogenated castor oil; Dynasan[®] 114: Trimyristin; Lumulse[®] GMS-K: Glyceryl monostearate; Miglyol[®] 810/812: Caprylic/capric triglycerides; Phospholipon[®] 90G: Phosphatidyl choline; Precifac[®] ATO: Cetyl palmitate; Precirol[®] ATO 5: Glyceryl palmitostearate; Dynasan[®] 116: Glyceryl tripalmitate

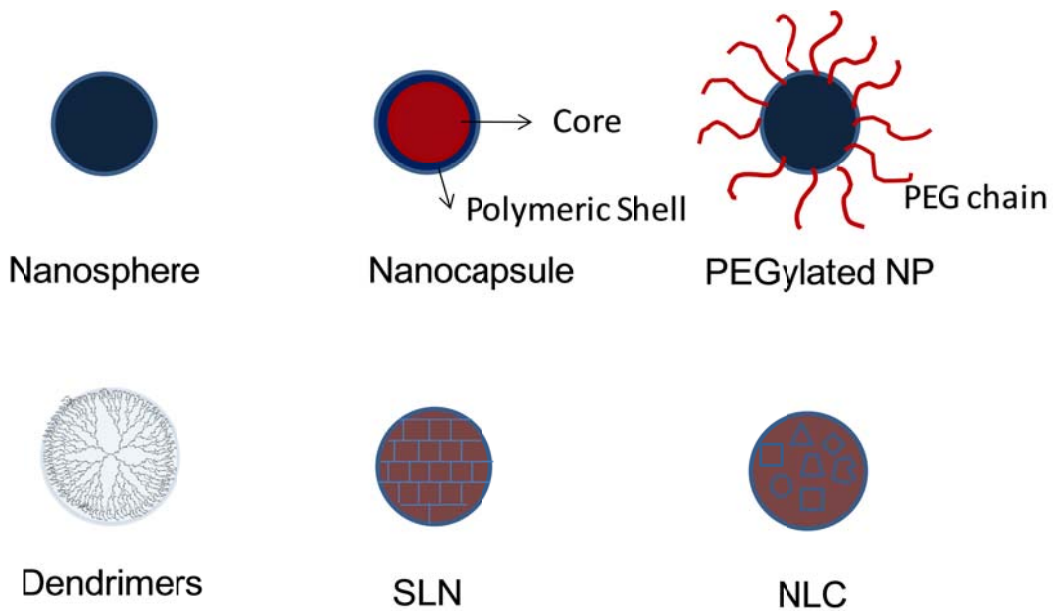


Figure 2.1 Schematic representations of different topical solid nanoparticle systems

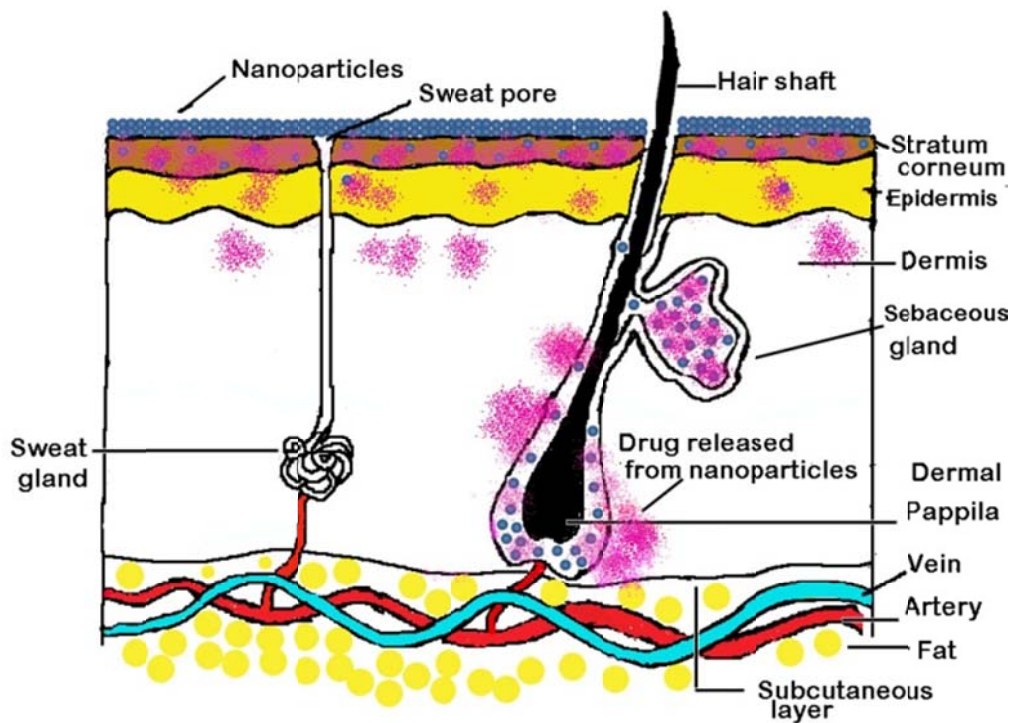


Figure 2.2 Permeation pathways for the nanoparticles in the skin

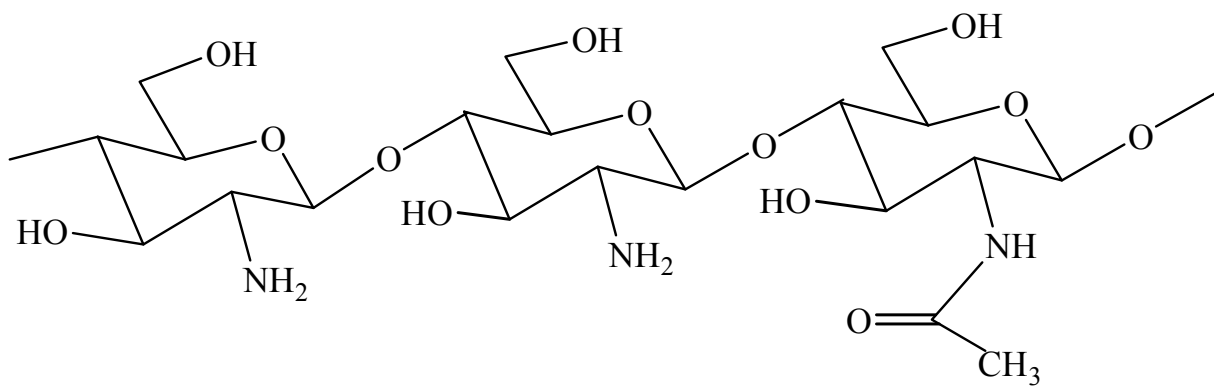


Figure 2.3 Structure of chitosan

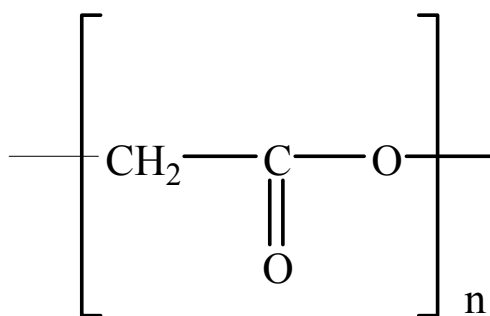


Figure 2.4 Structure of PGA

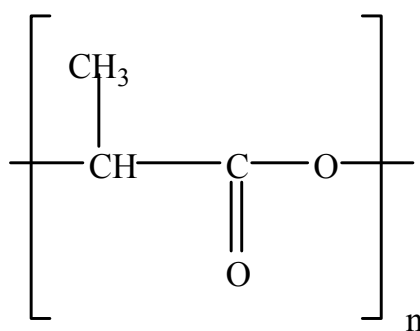


Figure 2.5 Structure of PLA

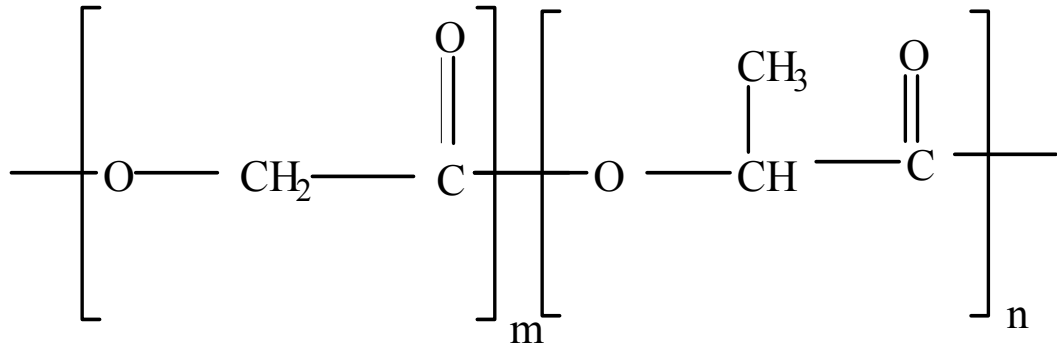


Figure 2.6 Structure of PLGA

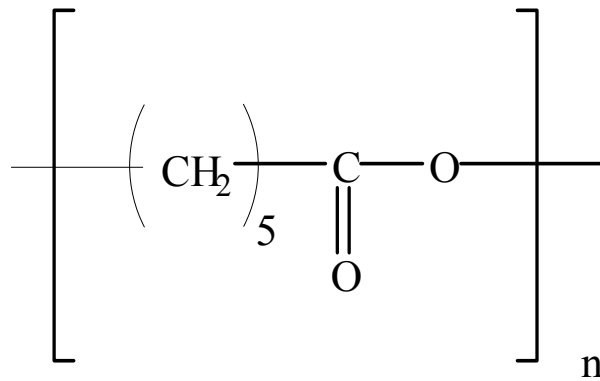


Figure 2.7 Structure of PCL

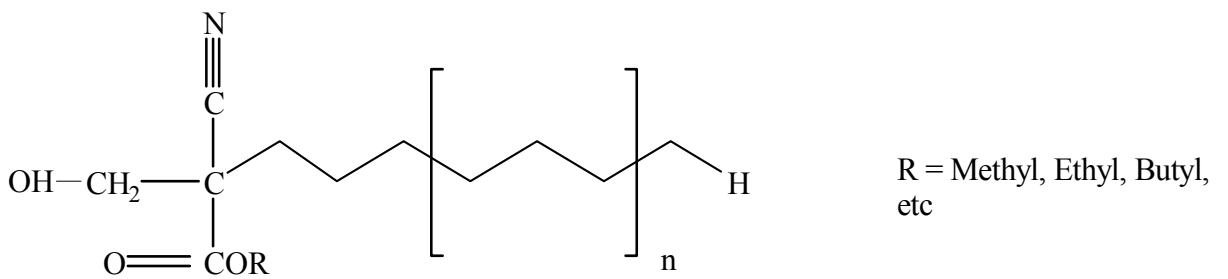


Figure 2.8 Structure of PACA

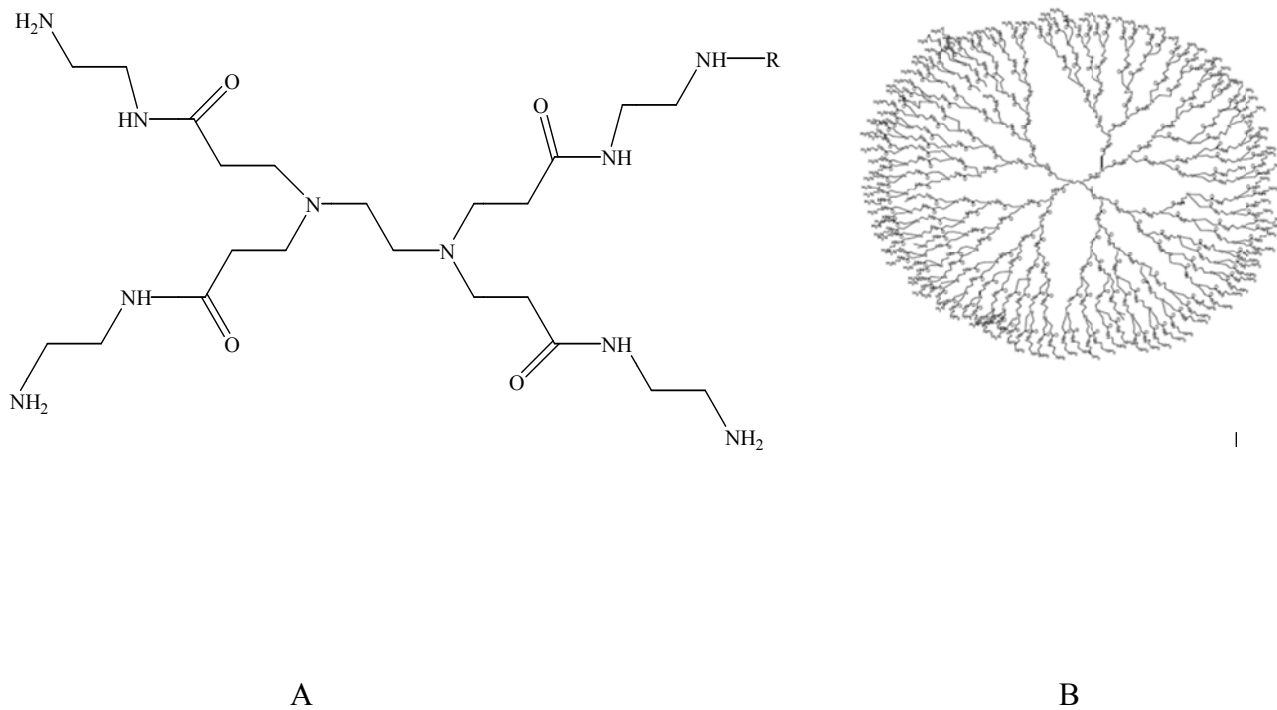


Figure 2.9 Structure of PAMAM monomer (A) and G5-NH₂ PAMAM dendrimer (B)

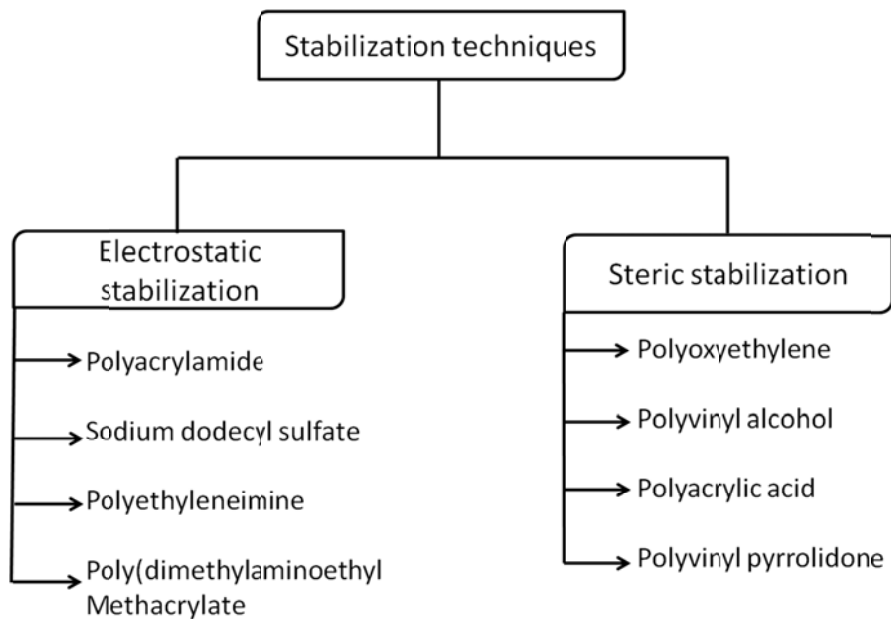


Figure 2.10 Stabilization techniques used for nanoparticles

3. LIPIDS FOR TOPICAL MICROEMULSION DELIVERY SYSTEMS

3.1 ABSTRACT

Over the past few decades, microemulsions have gained significant scientific attention due to their unique features such as high solubilization capacity, spontaneity of formation, enhanced thermodynamic stability, ability to load both hydrophilic and hydrophobic drug molecules, enhanced stability of the encapsulated therapeutic molecule, and high diffusion/absorption rates. Further, they have applications in dermal and epidermal targeting for various skin disorders. The materials used in the microemulsion formulation can greatly influence the *in vitro* and *in vivo* performance of the therapeutic moiety. This review describes various lipid materials used in the preparation of microemulsions for topical and transdermal drug delivery.

3.2 INTRODUCTION

Drug delivery to or through the skin offers various advantages over oral and parenteral routes in terms of non-invasiveness and convenience for drugs for local and systemic effects.¹⁻³ However, the natural protective barrier nature of the skin poses a challenge to deliver drugs in therapeutic quantities. The skin has a multilayered structure with an outermost layer, the stratum corneum (SC), followed by the viable epidermis, dermis and subcutaneous tissue. The SC is made up of dead keratinized cells (corneocytes) embedded in a lipid matrix. The lipid matrix is composed of ceramides, fatty acids, cholesterol and cholesterol esters, organized in tightly

stacked sheets. The unique structural features of the SC provide excellent barrier properties to skin for drug absorption.^{1,4,5}

Thus, to achieve percutaneous absorption of drugs in therapeutic concentrations, the barrier property of the skin must be compromised. Over the last few decades, colloidal carriers such as microemulsions and vesicular particulate carriers (niosomes, transferosomes, liposomes and ethosomes) were used as drug carriers for topical and transdermal delivery and these systems have been extensively reviewed in the literature.⁶⁻¹² Out of these systems, microemulsions have evolved as a potential drug delivery system because of their ability to penetrate the deeper layers of the skin. Microemulsions are quaternary (or pseudo-quaternary) systems composed of water, oil, and surfactant and/or cosurfactant mixture. They are transparent, optically isotropic systems. The globule size ranges from 10 nm – 100 nm. Due to their nanometer size range, microemulsions are often termed as nanoemulsions. They offer various advantages in terms of their high solubilization capacity, spontaneity of formation, improved thermodynamic stability, ability to entrap both hydrophilic and hydrophobic drug molecules, enhanced stability of the encapsulated actives, and high diffusion/absorption rates.^{4,13-16} Microemulsions can be categorized into water-in-oil (w/o), oil-in-water (o/w), and bicontinuous phase systems (Figure 3.1). W/O microemulsions contain water droplets embedded in oil as continuous phase whereas O/W microemulsions have oil droplets dispersed in water as a continuous phase. The third category of bicontinuous phase systems forms when the system contains similar amounts of oil and water as continuous domains separated by surfactant-rich interfaces. This article mainly discusses physicochemical and pharmaceutical properties and applications of various lipid materials used as the oil phase in the formulation of microemulsions.

3.3 FACTORS AFFECTING DRUG PERMEATION ENHANCEMENT ACROSS THE SKIN BY MICROEMULSIONS

Permeation enhancement of microemulsions depends on various factors such as

3.3.1 AMOUNT OF DRUG

Since microemulsions have a high solubilization capacity for both lipophilic and hydrophilic drugs, they can take up large payloads of the active ingredient. The large amount of drug incorporated in the internal phase leads to development of a concentration gradient between the internal and external phase increasing the thermodynamics of the drug and providing an impetus for the diffusion of drug from the internal phase into the skin layers. Kemken et al.¹⁷ reported high thermodynamic activity leading to improved pharmacodynamic effect in a rabbit model for bupranolol supersaturated microemulsions. Similarly, Chen et al.¹⁸ and Hua et al.¹⁹ reported high thermodynamic activity and flux owing to high drug content and solubilization potential of microemulsion formulations for triptolide and vinpocetine, respectively.

3.3.2 TYPE AND AMOUNT OF SURFACTANT

Another crucial parameter in the formulation of microemulsions is the choice of surfactant. The type as well as the content of surfactant greatly affects the drug solubilization and skin permeation. An ideal surfactant should favor microemulsification of the oil and possess good solubilization potential for the active therapeutic agent. Various types of surfactants have been reported in the literature for their use in the formulation of topical/transdermal microemulsions. Different surfactants can be used based on the type of microemulsion formulation such as oil in water or water in oil. Broadly the surfactants can be classified as of

natural or synthetic origin. The synthetic surfactants are further divided into anionic, cationic, non-ionic and zwitterionic (amphoteric). The natural surfactants are preferred over synthetic ones due to their excellent biocompatibility and tolerability by the body.²⁰⁻²² These include zwitterionic phospholipids such as lecithin, and non-ionic sugar surfactants, such as alkyl glucosides and alkyl esters. Further, the non-ionic class of synthetic surfactant is preferred over the anionic or cationic surfactants, as the latter are reported to be harsh on the skin. The anionic and cationic surfactants solubilize the lipid membranes and essential low molecular weight nitrogenous components from the epidermis that are responsible for the binding of water to the stratum corneum and for providing elasticity and flexibility to the skin. Further, they lead to skin irritation reactions.²³⁻²⁶ The synthetic anionic class of surfactants is alkyl sulphonates and the only surfactant of this class which has pharmaceutical acceptability is aerosol OT (AOT) or dioctyl sodium sulfosuccinate (DOSS).^{27,28} It is mainly used in the formulation of water in oil microemulsions and has limited applications due to adverse reactions on skin as explained before. The cationic class of surfactants includes cetyltrimethylammonium bromide and dimethyl-dioctadecyl-ammonium-bromide. These are equally skin irritant and more cytotoxic than the anionic class of surfactants and, thus, are not very commonly used for the preparation of microemulsions for topical use. The least irritant and thus most widely used category of synthetic surfactants is non-ionic which includes polysorbates, sorbitan esters, poloxamers, polyoxyethylene alkyl ethers, polyoxyethylene-castor oil derivatives, alkyl polyglucosides, polyglycolized glycerides, etc. Among these surfactants, sucrose esters,^{29,30} alkyl polyglycosides,³¹⁻³³ polyglycolized glycerides³³⁻³⁵ and phospholipids^{36,37} additionally act as penetration enhancers due to their effect on stratum corneum lipids.

The quantity of surfactant also plays an important role in drug delivery through microemulsions. An inverse relationship exists between the amount of surfactant and drug permeation since a large amount of surfactant reduces the thermodynamic activity of the system hampering drug diffusion. This phenomenon of reduced drug delivery due to high surfactant content is also reported by various research groups.^{18,19,38}

3.3.3 AMOUNT OF WATER

A linear correlation was found between the amount of water in the microemulsion system and drug permeation.³⁹ The water in the microemulsion is utilized in two ways: some of the water molecules are involved in the hydration of the polar head groups of the surfactant molecule whereas the rest of the water hydrates the stratum corneum enhancing the partitioning and diffusivity of drug inside the skin layers. At low water concentrations, all water molecules are used in hydrating the polar heads of the surfactant molecule leaving no free water available for hydrating the stratum corneum, thus affecting the permeation. This phenomenon is important for delivery of both lipophilic as well as hydrophilic drugs. Thus, the difference in the water content/hydration between the microemulsion system and skin provides a strong force to push the drug molecules across skin layers, as seen for the lecithin microemulsion system for the delivery of tetracaine hydrochloride.⁴⁰ Enhanced drug delivery with an increased amount of water phase was also reported by other groups.⁴¹⁻⁴³ In addition, the spontaneous and continuously fluctuating interfaces and the small particle size but high density of droplets of the microemulsion system confers high mobility to the drug molecules further enhancing their diffusion across the skin.¹⁶

3.3.4 PENETRATION ENHANCERS

The lipid phase (oil), such as vegetable oil, fatty acids/alcohols and glycerides, can itself act as a skin penetration enhancer due to similar polarity with the stratum corneum lipids. Fixed oils such as soybean oil, enhanced the permeation of camphor, menthol and methyl salicylate topically for the treatment of arthritis, muscle pain and minor joint pain.⁴⁴ Incorporation of the drugs into a hydrogel-thickened microemulsion system using soybean oil enhanced the flux by 1.24-fold for camphor and 1.38-fold for menthol and methyl salicylate. This enhancement was due to the high solubility of the drugs and development of a concentration gradient between the microemulsion droplets and stratum corneum that acts as the impetus for drug diffusion. Further, the small droplet size enhanced the thermodynamic activity resulting in higher drug delivery across the skin. Penciclovir was efficiently delivered through an oleic acid microemulsion formulation with 3.5-fold higher drug delivery than a commercial cream formulation.⁴⁵ Terbinafine HCl microemulsion using medium chain triglycerides oil for topical antifungal treatment. 1% drug had a 1.4-fold higher flux and 1.3- and 2.2- fold higher skin retention as compared to the commercial creams Basiscreme DAC and Lamisil[®] Crème, respectively.⁴⁶

Apart from the oil phase, there are numerous other compounds that are used as penetration enhancers. These include alcohols/glycols (ethanol, benzyl alcohol, lauryl alcohol, pentanol, propylene glycols and glycerol), dimethyl sulfoxide, pyrrolidones, surfactants, terpenes (carvone and anise oil), etc. These penetration enhancers interact with the stratum corneum and reversibly decrease the barrier properties of the skin.^{29,47} Ethanol containing microemulsions increase the delivery of indomethacin,⁴⁸ estradiol,^{49,50} nadifloxacin,⁵¹ penciclovir,⁴⁵ diclofenac diethylammonium,⁵² etc. Pyrrolidones have been used to enhance the permeation of lidocaine, estradiol and diltiazem⁵³ and itraconazole.⁵⁴ Non-ionic surfactants such as sorbitan monolaurate

and its ethoxylate derivative polysorbate 20 have been investigated as penetration enhancers for the delivery of 5-fluorouracil and antipyrine, benzocaine, salicylic acid and its sodium salt, flufenamic acid, etc.⁵⁵⁻⁵⁷ Various microemulsion formulations using polysorbates have enhanced drug diffusion across the skin layers for drugs such as ³H-inulin, ¹⁴C-tranexamic acid,⁵⁸ quercetin dihydrate,⁵⁹ triptolide,¹⁸ etc. Diethyleneglycol monoethyl ether (Transcutol[®]) is widely used in microemulsion formulations as a penetration enhancer, co-solvent or surfactant. It increased the transdermal delivery of several drugs, alone or in combination with suitable co-solvents such as polyethylene glycol, propylene glycol, and ethanol.⁶⁰⁻⁶³ Several drugs have been successfully delivered in a microemulsion formulation via the transdermal route using Transcutol[®] such as quercetin,⁶⁴ sodium diclofenac,⁶⁵ vinpocetin,⁶⁶ aceclofenac,⁶⁷ silymarin,⁶⁸ babchi oil (*Psoralea corylifolia*),⁶⁹ hydrocortisone acetate,⁷⁰ terbinafine,⁷¹ and testosterone.⁷² The mechanism of action of permeation enhancement of dimethyl sulfoxide (DMSO) has been reported.^{4,73} Confocal Raman Spectroscopy study revealed that DMSO strongly interacts with the stratum corneum lipid components, modifying them from their predominant all *trans* gel phase to a *trans-gauche* liquid crystalline phase. Further, it modifies the keratin conformation from α -helical to β -pleated sheet, thus perturbing the barrier and enhancing drug permeation across the skin layers.⁷⁴ DMSO enhanced the flux significantly ($798.5 \mu\text{g}/\text{cm}^2$) for 5% acyclovir from microemulsion formulations as compared to marketed cream, Herpex[®] ($763.2 \mu\text{g}/\text{cm}^2$) and polyethylene ointment ($751 \mu\text{g}/\text{cm}^2$) across mice skin.⁷⁵

3.4 PERMEATION PATHWAYS FOR DRUG DELIVERY BY MICROEMULSIONS

Based on the partition coefficient, the drug is distributed between the aqueous and oil phases of the microemulsion. Various permeation pathways in the skin for the microemulsion

system are shown in Figure 3.2. One of the pathways is diffusion of the excess drug in the external/continuous phase of the microemulsion due to the high thermodynamic activity and concentration gradient across the SC. In addition, due to the dynamic nature of the microemulsion, the droplets collide and interact with the SC leading to the development of a concentration gradient thus enhancing drug delivery.⁷⁶ Hydration further helps in widening of the weaker intercellular junctions of the corneocytes leading to creation of transcutaneous channels for enhanced drug permeation. In addition, the components of the microemulsion such as oil, surfactant/co-surfactant, and solvent enhance drug delivery, either by solubilizing into the SC lipids and perturbing the barrier membrane, or by extracting the SC lipids thereby decreasing the resistance for drug diffusion and creating voids in between the lipid network.^{53,77} Another mechanism of permeation enhancement is that the components of microemulsions such as oleic acid, tween 20 and Transcutol[®] can cause disruption of the tight SC lipid network by the formation of preferential hydrogen bonding of their oxygen moiety with ceramide head groups, thereby breaking the hydrogen bonds between the lipid bilayers.⁷⁸

3.5 LIPID MATERIALS IN THE FORMULATION OF MICROEMULSIONS

The oil or lipid phase in the microemulsion plays an important role as it influences the selection of the rest of the components. Thus, the choice of the oil phase is a critical parameter for the formulation. Generally, the oil/lipid phase with a large microemulsion region or maximum solubilization capability for the drug is selected. At the same time, the ability to facilitate emulsification of the lipid also needs to be considered. As the hydrocarbon chain length increases, the polarity of the fatty acid decreases, thus increasing its solubilization capacity for lipophilic drugs. However, emulsification of the oil becomes difficult as the chain length

increases.⁷⁹ It is difficult to achieve both the advantages of excellent solubilization potential and ease of emulsification in a single oil system. Thus, the choice of the oil phase is often a compromise between these two goals. In many cases, a combination of oil phases is used to achieve the desired solubilization and ease of emulsification. Various lipids are used as the oil phase for microemulsion formulations in topical and transdermal delivery (Table 3.1).

3.5.1 VEGETABLE OILS

Vegetable oils or fixed oils are fatty acid glycerides that are derived from plant source. Almond oil, castor oil, coconut oil, olive oil and peanut oil have been approved by the US Food and Drug Administration (FDA) for use in topical emulsions. These are not commonly used as the oil phase for topical/transdermal microemulsion formulations. The mechanism of action of permeation enhancement by these vegetable oils includes interaction and extraction/fluidization of the lipids in the bilayer membrane of the stratum corneum. This decreases the resistance to permeation for drugs across the skin.⁸⁰⁻⁸⁷

Soybean oil is more commonly used in microemulsion preparations as compared to the other oils. In permeation studies across porcine skin, a microemulsion formulation with soybean oil demonstrated higher permeation (5%) in 30 min compared to microemulsion formulations containing tributyrin (2.5%) and Miglyol[®] (3%). In addition, it also gave a higher permeation than the control gel (0.5%) composed of mixture of paraffin oil, the emulsifiers Eumulgin[®] O5 and Eumulgin[®] O10, and water. The higher permeation of the soybean oil microemulsion was attributed to lecithin, the main phospholipid in soybean oil which has a high affinity for epidermal tissues.⁸⁸ Carrageenan thickened microemulsions had a positive influence on drug permeation for all microemulsion formulations compared to non-thickened ones. The

formulation with Miglyol[®] showed higher permeation (9%) than formulations with tributyrin (7%), soybean oil (8%) and carrageenan thickened control gel (8%). This enhanced permeation was due to the good skin adhesive properties of carrageenan. Water in oil microemulsions containing diclofenac sodium were studied for *in-vitro* drug release across an artificial cellulose membrane.⁸⁹ Use of propanol as a co-surfactant showed a higher flux (0.059 mg/cm²/h) than formulations containing ethanol (0.04 mg/cm²/h) or iso-propyl alcohol (0.038 mg/cm²/h). The higher water content (10%) of the propanol formulation solubilized diclofenac sodium better compared to formulations containing ethanol (4.5%) and isopropyl alcohol (6.3%), increasing the concentration gradient that acts as the driving force for diffusion across the skin. The high water content also provides better hydration of the stratum corneum leading to improved drug delivery. Microemulsions for the topical delivery of flurbiprofen for anti-inflammatory action are reported by Fang et al.⁹⁰ Addition of 3% oleic acid as a permeation enhancer to soybean oil enhanced the flux by 1.5-fold across rat skin compared to a control solution of flurbiprofen in double distilled water. Hosmer et al.⁹¹ investigated the effect of surfactant concentration on the skin permeation of progesterone and adenosine from the microemulsion formulations. Microemulsions with low concentrations of the surfactant blend (polysorbate 80: medium chain mono- and di-glycerides: propylene glycol) with respect to the oil and water phase (surfactant blend:oil:water::47:20:33) was compared with microemulsion with high amounts of surfactants (surfactant blend:oil:water::63:14:23) for topical delivery. Both low and high surfactant content microemulsions displayed enhanced drug delivery as compared to control formulations. For progesterone, the low and high surfactant showed approx. 4.5- and 4.8-fold higher flux across porcine skin compared to the control solution of drug in soybean oil. For adenosine, the low and high surfactant content greatly enhanced drug delivery compared to the control solution in

soybean oil. The flux for microemulsions with low and high surfactant blend was 0.031 $\mu\text{g}/\text{cm}^2/\text{hr}$ and 0.036 $\mu\text{g}/\text{cm}^2/\text{hr}$ whereas no drug was detected in the receptor for the control sample.

Use of olive oil for microemulsion formulations has been reported for the delivery of a high molecular weight, water soluble marker, inulin, in water in oil microemulsion system.⁵⁸ The microemulsion formulation was compared with corresponding micellar dispersions and aqueous controls, for permeation across mice or rat skin. The microemulsion showed a significantly higher inulin transport (5 to 15-fold) than micellar and aqueous solution systems. Microemulsion facilitated the follicular transport of inulin. It was suggested that the microemulsion system had a hydrophilic-lipophilic balance similar to the sebum of the hair follicles. This makes it more compatible with the natural lipid composition and enhances drug solubilization in the aqueous core. Coconut oil,⁹⁰ sheanut oil,⁹² and canola oil⁵⁹ are seldom used in the formulation of topical microemulsions.

3.5.2 FATTY ACIDS AND ALCOHOLS

Fatty acids and alcohols are used in a variety of skin and general healthcare products including moisturizing creams, shaving creams, shampoos and perfumed products. The wide usage of these as topical ingredients indicates that they are non-toxic and considered safe for topical use. Oleic acid, undecylenic acid, cetyl alcohol, stearyl alcohol, and oleyl alcohol are approved for topical use by the US FDA. Medium chain fatty acids ($\text{C}_6 - \text{C}_{12}$) are liquids or semi-solids and long chain fatty acids ($\text{C}_{13} - \text{C}_{24}$) are solids. Some of these are used not only as oil phase in emulsions, but also as skin penetration enhancers. Structurally, fatty acids and alcohols consist of an aliphatic hydrocarbon chain and a terminal carboxyl group or hydroxyl group,

respectively. Fatty alcohols have generally lower melting points and are more polar than the corresponding fatty acids. Fatty acids have been known to disorganize the stratum corneum lipid structure, enhancing the partitioning and permeation of drugs.^{93,94} DSC studies showed the melting endotherm of oleic acid in the lipid portion of the stratum corneum network in conjunction with non-polar compounds. The *cis* double bond at the C₉ position causes a kink in the alkyl chain disrupting the ordered array of the predominantly saturated straight chain skin lipids and fluidizing the lipid regions.^{84,95,96} In addition, the interaction of oleic acid with the stratum corneum lipids can lead to defects and permeable pores in the highly ordered lipid network.^{29,97,98}

Though used as an oil phase, oleic acid is mainly intended as a drug solubilizer and skin penetration enhancer in many studies. Incorporation of vinpocetin in oleic acid microemulsion enhanced its solubility by 2100-fold as compared to water. Surfactant (PEG-8 glyceryl caprylate/caprate) to co-surfactant (purified diethylene glycol monoethyl ether) concentration was optimized for the microemulsion with 1% vinpocetin and 4% oleic acid. Microemulsions with 2:1 surfactant to co-surfactant ratio increased the flux by 3-fold across rat skin compared to a 1:1 ratio. The permeation enhancement of vinpocetin was a combined effect from penetration enhancement properties of oleic acid, increased thermodynamic activity of the microemulsion due to low surfactant content, and stratum corneum hydration due to water content.¹⁹ Oleic acid was used as an oil phase for penciclovir microemulsion systems.⁴⁵ It showed 3.7-, 1.7- and 5.4-fold higher solubility for penciclovir as compared to IPM, ethyl oleate and (medium chain triglyceride) MCT oil. Microemulsion formulation containing oleic acid showed 3.5-fold higher skin permeation than a commercial cream formulation. The higher thermodynamic activity and

ease of mobility of drug molecules in microemulsion formulation due to low viscosity provided the driving force for the drug diffusion across mice skin.

Chen et al. reported transdermal delivery of triptolide in oleic acid microemulsions with varied quantities of oleic acid, surfactant/co-surfactant and drug. The flux of triptolide increased linearly with drug loading and oleic acid content whereas it showed an inverse relationship with surfactant/co-surfactant quantity. Microemulsion formulation with high oleic acid and low surfactant content gave significantly higher permeation ($1.6 \mu\text{g}/\text{cm}^2$ per h) than an aqueous solution of 20% propylene glycol containing the same amount of triptolide ($0.9 \mu\text{g}/\text{cm}^2$ per h). The higher drug content and low surfactant concentration along with the permeation enhancement effect of oleic acid lead to improved drug delivery of triptolide.¹⁸ Estradiol microemulsion formulations were prepared for topical treatment of hormonal insufficiencies. Microemulsion formulations increased estradiol solubility 1400 to 4500-fold compared to PBS solution. Further, the permeation across human cadaver skin was 200 to 700 times higher than a saturated solution of estradiol in PBS. The small droplet size and higher oil phase (Epikuron[®] 200, oleic acid and IPM) content increased the microemulsion droplet density and surface area, which provided close contact with the skin layers resulting in better permeation of estradiol.⁴⁹ Transdermal delivery of testosterone was achieved using microemulsion formulations containing oleic acid. The ratio of surfactant/co-surfactant, i.e. Tween 20 and Transcutol[®] was optimized. The permeation study for the microemulsion formulations were studied across porcine skin. Flux of testosterone was observed to be dependent on oleic acid concentration; the flux reduced when oleic acid content decreased below 16%. Drug concentration also affected the flux across the skin. A direct relationship was observed between the two and higher drug delivery was achieved with highest drug loading. Further the higher thermodynamic activity and enhanced skin

hydration due to low surfactant/co-surfactant ratio (1:1 as compared to 1:3 and 3:1) and high water content improved the drug diffusion. The optimized formulation showed as high as 77- and as low as 3- fold higher skin permeation compared to other microemulsion formulations.⁷² Zhao et al.⁹⁹ studied the effect of various formulation parameters on skin permeation of theophylline from a microemulsion formulation. The content of surfactant mixture affected the skin permeation. Decreasing the content of surfactant mixture of Cremophor[®] RH 40/Labrasol[®] (1:2) from 54% to 30% enhanced the thermodynamic activity of the microemulsions and increased permeation by 1.3-fold. Both 5 and 12% oleic acid content provided similar skin permeation rates. Since 12% of oleic acid caused skin irritation, the content of oleic acid was fixed at 5%. The permeation enhancement increased linearly with the drug loading. Menthol enhanced permeation by 1.4-, 1.3-, 1.75- and 1.9-fold as compared to microemulsions containing cineol, azone, ethanol and no enhancer, respectively. Further, when comparing oral delivery of theophylline solution with same drug content and transdermal delivery of oleic acid microemulsions in rabbits, although the latter had a lower C_{max} and prolonged t_{max} , the AUC for transdermal delivery was 1.7-times higher than that of orally delivered theophylline.

Goebel et al. used linoleic acid in microemulsion formulation as a lipid topical anti-inflammatory and barrier regenerating agent. Compared to commercial cream formulation, microemulsion formulation delivered linoleic acid more efficiently with an almost 2.8-fold higher amount of linoleic acid delivered to the skin.¹⁰⁰ In spite of low solubility of aceclofenac in linoleic acid compared to glycerol triacetate (triacetin) and propylene glycol dicaprylocaprate, the microemulsion formulation provided 5.5-fold higher drug permeation across rat skin compared to a cream formulation composed of oleic acid, Labrasol[®]/Transcutol[®], ethanol and water and containing the same drug loading.¹⁰¹ Less commonly used fatty acids include myristic

acid. Curcumin loaded microemulsions were prepared using myristic acid for dermal targeting for the antimicrobial effect against *Staphylococcus epidermidis* of both myristic acid and curcumin.¹⁰² The viscosity, water content and amount of surfactant affected the physicochemical properties of the microemulsions such as particle size, viscosity and interfacial tension. Isopropyl alcohol acted as a co-surfactant and increased the solubility of myristic acid in the aqueous phase. The amount of surfactant, Pluronic F127, when increased from 0 to 5%, decreased the particle size from 236 ± 108 to 4 ± 1 nm. However, further increase to 10% lead to increased particle size (46.59 ± 3.21). The viscosity increased with surfactant concentration, from 16 to 246.5 cPs for 0 and 10% F127, respectively. However, the permeation of curcumin across porcine skin was highest with 5% F127 due to a high thermodynamic activity, providing 2.5- and 9-fold higher flux than 0% and 10% F127, respectively. Water content played a key role in enhancing the skin accumulation of curcumin. Fatty alcohols were utilized as an oil phase in topical microemulsions systems. Fluconazole microemulsion was investigated for topical antifungal delivery across rat skin.¹⁰³ Lauryl alcohol showed higher solubility for fluconazole as compared to other oils such as glycerides, mineral oil, natural oils, oleic acid, linoleic acid and polyglycolized glycerides. The microemulsions showed 9-fold higher drug permeation than control formulation of a saturated solution of drug in phosphate buffered saline. Diclofenac diethylammonium was formulated as a lauryl alcohol based microemulsion system.⁵² Lauryl alcohol showed the highest solubility and permeation for the drug across rat skin. A 9.7-fold increase in skin permeation was observed with a change in Labrasol[®]/co-ethanol ratio from 5 to 0.5.

Decanol in combination with 1-Dodecanol was used in the formulation of topical miconazole microemulsions.¹⁰⁴ Maximum drug accumulation in skin with minimal permeation is

desirable for the topical effect of miconazole. Effect of particle charge on miconazole skin delivery was evaluated by formulating cationic microemulsions using stearylamine, L-alanine benzyl ester (ALAB) or cetyltrimethylammonium bromide (CTAB). All these agents provided negligible permeation of miconazole across the skin; however they provided a 2-fold higher skin accumulation compared to corresponding non-ionic microemulsions. The high skin accumulation was a result of the favorable interaction of cationic particles with the negatively charged skin. Trotta et al. investigated the influence of counter-ions on the delivery of positively charged, hydrophilic drug, methotrexate across mice skin using decanol as the oil phase for microemulsion formulation. Counter-ions such as, monoethyl phosphate, monodecyl phosphate, monodecyl glycerophosphate, taurodeoxycholate, dodecyl sulfate and dioctyl sulfosuccinate, were evaluated and dodecyl sulfate and dioctyl sulfosuccinate showed a significantly higher drug permeation. This marked increase in drug diffusion was attributed to the enhanced lipophilicity of methotrexate ion-pair complex with dodecyl sulfate or dioctyl sulfosuccinate that facilitated the delivery across the stratum corneum. Solubility of methotrexate in decanol microemulsion was twice that in aqueous solution. Further, the skin permeation was increased by 6-fold as compared to an aqueous solution of methotrexate.¹⁰⁵ Similar results were obtained by Piera et al.¹⁰⁶ for apomorphine delivery through mice skin using mixture of decanol and isopropyl alcohol as the oil phase for the microemulsion. Octanoic acid was added to the microemulsion to form a lipophilic ion-pair with apomorphine, enhancing its delivery across the skin. Further, the high solubilization capacity of the oil phase for apomorphine leads to development of a concentration gradient across the stratum corneum further increasing the drug diffusion.

3.5.3 GLYCERIDES AND FATTY ACID ESTERS

Glycerides and fatty acid esters are the most commonly used oil phases for the preparation of microemulsions for topical delivery. Glycerides are glycerol esters of fatty acids and include monoglycerides, diglycerides and triglycerides. Caprylic/capric acid glycerides, also called medium chain triglycerides, are extensively used for microemulsion preparation. Tributyrin (butyric acid triglyceride) is also used as an oil phase for microemulsion preparation. Fatty acid esters include ethyl oleate, isopropyl myristate, isopropyl palmitate, isostearyl isostearate, cetearyl octanoate and octyl octanoate. The reason for their wide use over vegetable oil or fatty acids/alcohols is their ease of emulsification. Further, some of them also exhibit surfactant-like properties, additionally favoring emulsification and drug solubilization.

Glycerides such as caprylic/capric mono, di, or triglyceride (MCT oil) or mixtures thereof are most commonly used for microemulsion preparation as oil phase. They act on stratum corneum lipids, increasing the partition coefficient and diffusivity of drugs across the skin layers. Glyceryl monooleate is known to extract the ceramides and increase the fluidity of the lipid bilayer membrane.¹⁰⁷ Glycerol triacetate, on the other hand, acts as a cell envelope disordering compound facilitating drug diffusion across the stratum corneum.^{108,109} Lycopene microemulsions for topical applications were developed.¹¹⁰ Mono/diglycerides of capric and caprylic acids (MG) or triglycerides (TG) were used as oil phases in the microemulsion formulation. Lycopene, being highly lipophilic, has difficulty permeating beyond the stratum corneum and into viable epidermal layers. Also, since lycopene is susceptible to oxidation, ascorbic acid was added as an antioxidant. MG and TG increased lycopene delivery across stratum corneum by 6 and 3.6-fold, respectively, as compared to the control solution of lycopene in myvacet oil. Further, delivery to viable epidermal layers (ED) was increased from undetected

(with the control solution) to 173 ng/cm² and 103 ng/cm² using MG and TG, respectively. Electrical resistance of the skin indicated that MG disrupted the skin barrier more effectively than the control or TG.

Oil in water microemulsion using glycerol triacetate for the dermal delivery of progesterone across porcine skin was developed. Addition of silicon dioxide and Pemulen TR 1, a polymeric emulsifier, increased the skin permeation of progesterone as compared to tributyrin microemulsions without polymeric additives by 1.2 and 1.6- fold, respectively. This enhancement was attributed to the increased solubility and skin adhesion of drug by the use of polymers in addition to the permeation enhancement properties of triacetin.¹¹¹

Diazepam submicron emulsion cream using MCT oil was developed. MCT oil provided higher solubility for diazepam than mineral oil and isopropyl myristate.¹¹² Further, microemulsion with MCT oil resulted in smaller globules than with mineral oil or isopropyl myristate. Effect of submicron emulsion (20mg/kg diazepam, topical application) was studied against pentamethylenetetrazole induced convulsions in mice. The effect was compared with a reference, Assival[®] (10 mg/kg diazepam, intraperitoneal administration) large droplets emulsion cream (20mg/kg diazepam, topical application) prepared in same way but homogenized for less time to obtain large globule size. The effect on reducing convulsions was determined by the number of mice deaths in 6 hr. Diazepam submicron emulsion cream showed no deaths of mice in a group of 6 at the end of 6 hr whereas the score was 2 and 6 for large droplet emulsion and Assival[®], respectively. The enhanced drug delivery was due to the incorporation of MCT oil into skin lipid bilayers and disruption of the skin lipid arrangement, which was not observed with the long chain triglycerides – mineral oil and isopropyl myristate. Terbinafine HCl microemulsion formulation using MCT oil was developed for enhanced skin permeation. Microemulsion with

1% drug gave approximately a 1.4-fold higher flux and 1.3 and 2-fold higher skin retention as compared to the commercial creams, Basiscreme DAC and Lamisil[®] Crème, respectively. The high flux and skin retention were due to interaction of MCT oil with the stratum corneum lipids.⁴⁶

Ethyl oleate based microemulsion for the delivery of sucrose, a hydrophilic model molecule, was developed. Various microemulsions based on different amounts of ethyl oleate and surfactant/co-surfactant mixture were prepared. All the microemulsion formulations showed similar skin permeation rates across mice skin. However, all of the formulations showed about 13-fold higher permeation rates as compared to the control aqueous sucrose solution. The extraction of lipid components from stratum corneum by the oil phases was one of the reasons for the increased flux of sucrose. In addition, the partitioning of drug between internal and external phase of the microemulsion and between the internal or external phase of microemulsion and skin, also contributed to the increased permeation.¹¹³

Araujo et al.¹¹⁴ developed ethyl oleate topical microemulsions of 5- aminolevulinic acid for photodynamic therapy. Permeation studies across porcine skin showed an 18, 17 and 583-fold higher delivery for the microemulsion as compared to control solution of 5- aminolevulinic acid in phosphate buffered saline and bicontinuous microemulsion and water in oil microemulsion, respectively.

Ethyl oleate based nanoemulsions of the active alkaloid, evodiamine and rutaecarpine were developed. Encapsulation of the alkaloids in microemulsion formulation enhanced their chemical stability during storage at 25°C for 6 months. Evodiamine and rutaecarpine nanoemulsions showed higher skin permeation rate of 2.6-fold to 11.4-fold and 1.2-fold to 6-fold higher, respectively, than aqueous suspensions. The *in vivo* studies in rats showed the area under

the curve values for evodiamine and rutaecarpine were 1.5-fold and 2.3-fold higher than ointment and 3-fold and 4.2-fold higher than the tincture, respectively. The enhanced delivery was due to the small globule size of microemulsion for both drugs, high drug solubility in the microemulsion components, and the interaction of ethyl oleate with stratum corneum lipids.¹¹⁵

Triptolide in microemulsion formulation was prepared using isopropyl myristate as oil phase. The water in oil microemulsion showed 7 and 3.4-fold higher skin permeation as compared to the control solution of triptolide in a mixture of propylene glycol and water (1:4), and triptolide solid lipid nanoparticle formulation. High solubility in oil phase and partitioning of drug across skin layers were the major reasons for higher delivery through microemulsion formulation.¹¹⁵ Meloxicam microemulsion formulations were prepared with varied quantities of isopropyl myristate (oil) and surfactant/cosurfactant (Tween 80: ethanol: 1:1). Microemulsion with lowest amount of oil and surfactant offered highest flux for meloxicam, with 2.5-fold higher delivery than control formulation containing surfactant and ethanol micelle solution without oil. Reduced concentration of surfactant provides sufficient driving force for the lipophilic drug into the skin layers. Further, the aqueous portion of the microemulsion hydrates the stratum corneum proteins, causing them to swell, disrupting the bilayers and enhancing the drug diffusion.¹¹⁶ Hesperetin microemulsion based on isopropyl myristate was formulated. The optimum formulation showed 3 and 6-fold higher drug permeation across rat skin compared to aqueous suspension and isopropyl myristate suspension, respectively. Isopropyl myristate was used as oil phase for microemulsion formulation of several drugs such as dithranol,¹¹⁷ buspirone HCl,¹¹⁸ triptolide¹¹⁹, nicardipine HCl,¹²⁰ etc.

Isopropyl palmitate was used as an oil phase in the formulation of transdermal nanoemulsions containing lidocaine, tetracaine and dibucaine and their respective hydrochloride

salt forms. In case of base form, oil in water microemulsion permeated better than water in oil microemulsion across human skin. Oil in water microemulsion gave 2.6, 5.9 and 2.5-fold higher flux than water in oil microemulsion for lidocaine, tetracaine and dibucaine, respectively. In case of salt forms, water in oil microemulsion gave 1.14, 1.12 and 1.51-fold higher flux than oil in water microemulsion for lidocaine, tetracaine and dibucaine, respectively. High solubility of free base form in the oil phase provides high concentration gradient across skin layers favoring the partitioning and drug diffusion across the skin. Further, the nano-size droplets of the emulsion facilitate transport of the drug molecule to stratum corneum.¹²¹ Isopropyl myristate based microemulsion gel was formulated for the delivery of indomethacin and diclofenac. Permeation studies across human skin showed that the flux of indomethacin from microemulsion was 5.7-fold higher than control drug solution in isopropyl palmitate. Similarly the flux for diclofenac microemulsion was 3.5-fold higher than control drug solution in isopropyl palmitate.¹²² A highly hydrophilic drug, diphenhydramine was formulated as microemulsions using isopropyl palmitate as oil phase. A model glycolipid, n-hexadecyl-b-D-triethylenglycol-glucopyranoside (GL) was used as penetration enhancer. Microemulsion with GL showed a higher accumulation of drug into dermis followed by epidermis and stratum corneum as compared to the control hydrogel with GL and microemulsion formulation without GL. This indicates that the microemulsion itself had a strong permeation enhancement effect for lidocaine.¹²³

Lidocaine (lipophilic) and prilocaine (hydrophilic) were formulated as microemulsion to investigate the effect of composition of microemulsions on their delivery across rat skin. Microemulsion formulation containing isostearic isostearate demonstrated 4-fold higher skin permeation for lidocaine than conventional oil in water emulsion. On the other hand, prilocaine microemulsion showed 10-fold higher delivery than control hydrogel system. Higher drug

solubility leading to concentration gradient across skin and barrier perturbation due to isostearyl isostearate resulted in higher drug diffusion for lidocaine and prilocaine.¹⁴

3.6 CONCLUSIONS

Over the last few decades microemulsions have evolved as a potential drug delivery system. Their unique characteristics and advantages provide an edge over other colloidal systems. The choice of components for the microemulsion system significantly influences the in-vitro and in-vivo performance of the dosage form. Microemulsions have shown great potential in the area of dermal targeting due to their interaction with and accumulation at the stratum corneum and epidermal layers. This opens new avenues for their use in the treatment of topical skin disorders such as acne, psoriasis, contact dermatitis, etc.

3.7 REFERENCES

1. Barry BW. 2004. Breaching the skin's barrier to drugs. *Nat Biotechnol* 22(2):165-167.
2. Paudel KS, Milewski M, Swadley CL, Brogden NK, Ghosh P, Stinchcomb AL. 2010. Challenges and opportunities in dermal/transdermal delivery. *Ther Deliv* 1(1):109-131.
3. Prausnitz MR, Langer R. 2008. Transdermal drug delivery. *Nat Biotechnol* 26(11):1261-1268.
4. Barry BW, Williams AC. Permeation enhancement through skin. In Swarbrick J, Boylan JC, editors. *Encyclopaedia of Pharmaceutical Technology*. New York: Marcel Dekker; 1995. p. 449 – 493.

5. Morrow DIJ, McCarron PA, Woolfson AD, Donnelly RF. 2007. Innovative Strategies for Enhancing Topical and Transdermal Drug Delivery. *The Open Drug Delivery Journal* 1:36-59.
6. Gasperlin M, Gosenca M. 2011. Main approaches for delivering antioxidant vitamins through the skin to prevent skin ageing. *Expert Opin Drug Deliv* 8(7):905-919.
7. Saupe A, Wissing SA, Lenk A, Schmidt C, Muller RH. 2005. Solid lipid nanoparticles (SLN) and nanostructured lipid carriers (NLC) -- structural investigations on two different carrier systems. *Biomed Mater Eng* 15(5):393-402
8. Schafer-Korting M, Mehnert W, Korting HC. 2007. Lipid nanoparticles for improved topical application of drugs for skin diseases. *Adv Drug Deliv Rev* 59(6):427-443.
9. Souto EB, Muller RH. 2008. Cosmetic features and applications of lipid nanoparticles (SLN, NLC). *Int J Cosmet Sci* 30(3):157-165.
10. Muller RH, Mader K, Gohla S. 2000. Solid lipid nanoparticles (SLN) for controlled drug delivery - a review of the state of the art. *Eur J Pharm Biopharm* 50(1):161-177.
11. Honeywell-Nguyen P, Bouwstra JA. 2005. Vesicles as a tool for transdermal and dermal delivery. *Drug Discovery Today: Technologies* 2(1):67-74.
12. Souto EB, Almeida AJ, Müller RH. 2007. Lipid Nanoparticles (SLN®, NLC®) for Cutaneous Drug Delivery: Structure, Protection and Skin Effects. *Journal of Biomedical Nanotechnology* 3(4):317-331.
13. Rakshit AK, Moulik SP. Physicochemistry of W/O microemulsions: formation, stability and droplet clustering. In Fanun M, editor *Surfactant science series*. Boca Raton: CRC Press; 2009

14. Kreilgaard M. 2002. Assessment of cutaneous drug delivery using microdialysis. *Adv Drug Deliv Rev* 54 Suppl 1:S99-121.
15. Heuschkel S, Goebel A, Neubert RH. 2008. Microemulsions--modern colloidal carrier for dermal and transdermal drug delivery. *J Pharm Sci* 97(2):603-631.
16. Schroeter A, Engelbrecht T, Neubert RH, Goebel AS. 2010. New nanosized technologies for dermal and transdermal drug delivery. A review. *J Biomed Nanotechnol* 6(5):511-528.
17. Kemken J, Ziegler A, Muller BW. 1992. Influence of supersaturation on the pharmacodynamic effect of bupranolol after dermal administration using microemulsions as vehicle. *Pharm Res* 9(4):554-558.
18. Chen H, Chang X, Weng T, Zhao X, Gao Z, Yang Y, Xu H, Yang X. 2004. A study of microemulsion systems for transdermal delivery of triptolide. *J Control Release* 98(3):427-436.
19. Hua L, Weisan P, Jiayu L, Ying Z. 2004. Preparation, evaluation, and NMR characterization of vinpocetine microemulsion for transdermal delivery. *Drug Dev Ind Pharm* 30(6):657-666.
20. Hall DG. 1987. Thermodynamics of micelle formation. In Schick MJ, editor *Non ionic surfactants physical chemistry*. New York: Marcel Dekker; pp:233-296.
21. Lawrence MJ. 1994. Surfactant systems: their use in drug delivery. *Chemical Society Reviews* 23(6):417-424
22. Malmsten M. 2002. Introduction to surfactants. In Malmsten M, editor *Surfactants and Polymers in Drug Delivery*. Pennsylvania: Marcel Dekker; pp:2-8.

23. Somasundaran P. 2006. Encyclopedia of Surface and Colloid Science. In Somasundaram P, editor New York: Taylor & Francis.
24. Tenjarla S. 1999. Microemulsions: an overview and pharmaceutical applications. *Crit Rev Ther Drug Carrier Syst* 16(5):461-521.
25. Effendy I, Maibach HI. 1995. Surfactants and experimental irritant contact dermatitis. *Contact Dermatitis* 33(4):217-225.
26. Rieger MM. 1997. Surfactant science series. In Rieger MM, Rhein LD, editors. *Surfactants in cosmetics*. New York: Marcel Dekker; pp: 519-532.
27. Gupta RR, Jain SK, Varshney M. 2005. AOT water-in-oil microemulsions as a penetration enhancer in transdermal drug delivery of 5-fluorouracil. *Colloids Surf B Biointerfaces* 41(1):25-32.
28. Liu H, Wang Y, Lang Y, Yao H, Dong Y, Li S. 2009. Bicontinuous cyclosporin a loaded water-AOT/Tween 85-isopropylmyristate microemulsion: structural characterization and dermal pharmacokinetics in vivo. *J Pharm Sci* 98(3):1167-1176.
29. Trommer H, Neubert RH. 2006. Overcoming the stratum corneum: the modulation of skin penetration. A review. *Skin Pharmacol Physiol* 19(2):106-121.
30. Okamoto H, Sakai T, Danjo K. 2005. Effect of sucrose fatty acid esters on transdermal permeation of lidocaine and ketoprofen. *Biol Pharm Bull* 28(9):1689-1694.
31. Pakpayat N, Nielloud F, Fortune R, Tourne-Peteilh C, Villarreal A, Grillo I, Bataille B. 2009. Formulation of ascorbic acid microemulsions with alkyl polyglycosides. *Eur J Pharm Biopharm* 72(2):444-452

32. ElMeshad AN, Tadros MI. 2011. Transdermal delivery of an anti-cancer drug via w/o emulsions based on alkyl polyglycosides and lecithin: design, characterization, and in vivo evaluation of the possible irritation potential in rats. *AAPS PharmSciTech* 12(1):1-9.
33. Manconi M, Sinico C, Caddeo C, Vila AO, Valenti D, Fadda AM. 2011. Penetration enhancer containing vesicles as carriers for dermal delivery of tretinoin. *Int J Pharm* 412(1-2):37-46.
34. Mura S, Manconi M, Sinico C, Valenti D, Fadda AM. 2009. Penetration enhancer-containing vesicles (PEVs) as carriers for cutaneous delivery of minoxidil. *Int J Pharm* 380(1-2):72-79
35. Chessa M, Caddeo C, Valenti D, Manconi M, Sinico C, Fadda AM. 2011. Effect of Penetration Enhancer Containing Vesicles on the Percutaneous Delivery of Quercetin through New Born Pig Skin. *Pharmaceutics* 3(3):497-509.
36. Williams AC, Barry BW. 2007. Chemical permeation enhancement. In Touitou E, Barry BW, editors. *Enhancement in Drug Delivery*. Boca Raton: Taylor and Francis; pp:233-254.
37. Kirjavainen M, Monkkonen J, Saukkosaari M, Valjakka-Koskela R, Kiesvaara J, Urtti A. 1999. Phospholipids affect stratum corneum lipid bilayer fluidity and drug partitioning into the bilayers. *J Control Release* 58(2):207-214.
38. Rhee YS, Choi JG, Park ES, Chi SC. 2001. Transdermal delivery of ketoprofen using microemulsions. *Int J Pharm* 228(1-2):161-170.

39. Zhang J, Michniak-Kohn B. 2011. Investigation of microemulsion microstructures and their relationship to transdermal permeation of model drugs: ketoprofen, lidocaine, and caffeine. *Int J Pharm* 421(1):34-44.
40. Changez M, Varshney M, Chander J, Dinda AK. 2006. Effect of the composition of lecithin/n-propanol/isopropyl myristate/water microemulsions on barrier properties of mice skin for transdermal permeation of tetracaine hydrochloride: in vitro. *Colloids Surf B Biointerfaces* 50(1):18-25.
41. Djordjevic L, Primorac M, Stupar M. 2005. In vitro release of diclofenac diethylamine from caprylocaproyl macrogolglycerides based microemulsions. *Int J Pharm* 296(1-2):73-79.
42. Sintov AC, Shapiro L. 2004. New microemulsion vehicle facilitates percutaneous penetration in vitro and cutaneous drug bioavailability in vivo. *J Control Release* 95(2):173-183.
43. Osborne DW, Ward AJ, O'Neill KJ. 1991. Microemulsions as topical drug delivery vehicles: in-vitro transdermal studies of a model hydrophilic drug. *J Pharm Pharmacol* 43(6):450-454.
44. Mou D, Chen H, Du D, Mao C, Wan J, Xu H, Yang X. 2008. Hydrogel-thickened nanoemulsion system for topical delivery of lipophilic drugs. *Int J Pharm* 353(1-2):270-276.
45. Zhu W, Yu A, Wang W, Dong R, Wu J, Zhai G. 2008. Formulation design of microemulsion for dermal delivery of penciclovir. *Int J Pharm* 360(1-2):184-190.

46. Lusiana, Muller-Goymann CC. 2011. Preparation, characterization, and in vitro permeation study of terbinafine HCl in poloxamer 407-based thermogelling formulation for topical application. *AAPS PharmSciTech* 12(2):496-506.
47. Williams AC, Barry BW. 2004. Penetration enhancers. *Adv Drug Deliv Rev* 56(5):603-618.
48. Chen L, Tan F, Wang J, Liu F. 2012. Microemulsion: a novel transdermal delivery system to facilitate skin penetration of indomethacin. *Pharmazie* 67(4):319-323.
49. Peltola S, Saarinen-Savolainen P, Kiesvaara J, Suhonen TM, Urtti A. 2003. Microemulsions for topical delivery of estradiol. *Int J Pharm* 254(2):99-107.
50. Megrab NA, Williams AC, Barry BW. 1995. Oestradiol permeation across human skin, silastic and snake skin membranes: The effects of ethanol/water co-solvent systems. *International Journal of Pharmaceutics* 116, 101–112.
51. Kumar A, Agarwal SP, Ahuja A, Ali J, Choudhry R, Baboota S. 2011. Preparation, characterization, and in vitro antimicrobial assessment of nanocarrier based formulation of nadifloxacin for acne treatment. *Pharmazie* 66(2):111-114.
52. Kweon JH, Chi SC, Park ES. 2004. Transdermal delivery of diclofenac using microemulsions. *Arch Pharm Res* 27(3):351-356.
53. Lee PJ, Langer R, Shastri VP. 2003. Novel microemulsion enhancer formulation for simultaneous transdermal delivery of hydrophilic and hydrophobic drugs. *Pharm Res* 20(2):264-269.
54. Chudasama A, Patel V, Nivsarkar M, Vasu K, Shishoo C. 2011. Investigation of microemulsion system for transdermal delivery of itraconazole. *J Adv Pharm Technol Res* 2(1):30-38.

55. Dalvi UG, Zatz JL. 1982. Effect of skin binding on percutaneous transport of benzocaine from aqueous suspensions and solutions. *J Pharm Sci* 71(7):824-826.
56. Lopez A, Llinares F, Cortell C, Herraiz M. 2000. Comparative enhancer effects of Span20 with Tween20 and Azone on the in vitro percutaneous penetration of compounds with different lipophilicities. *Int J Pharm* 202(1-2):133-140.
57. Hwang CC, Danti AG. 1983. Percutaneous absorption of flufenamic acid in rabbits: effect of dimethyl sulfoxide and various nonionic surface-active agents. *J Pharm Sci* 72(8):857-860.
58. Wu H, Ramachandran C, Weiner ND, Roessler BJ. 2001. Topical transport of hydrophilic compounds using water-in-oil nanoemulsions. *Int J Pharm* 220(1-2):63-75.
59. Vicentini FT, Simi TR, Del Ciampo JO, Wolga NO, Pitol DL, Iyomasa MM, Bentley MV, Fonseca MJ. 2008. Quercetin in w/o microemulsion: in vitro and in vivo skin penetration and efficacy against UVB-induced skin damages evaluated in vivo. *Eur J Pharm Biopharm* 69(3):948-957.
60. Ganem-Quintanar A, Lafforgue C, Falson-Rieg F, Buri P. 1997. Evaluation of the transepidermal permeation of diethylene glycol monoethyl ether and skin water loss. *International Journal of Pharmaceutics* 147:165-171.
61. Watkinson AC, Hadgraft J, Bye A. 1991. Aspects of the transdermal delivery of prostaglandins. *International Journal of Pharmaceutics* 74:229-236.
62. Escobar-Chavez JJ, Quintanar-Guerrero D, Ganem-Quintanar A. 2005. In vivo skin permeation of sodium naproxen formulated in pluronic F-127 gels: effect of Azone and Transcutol. *Drug Dev Ind Pharm* 31(4-5):447-454.

63. Harrison JE, Watkinson AC, Green DM, Hadgraft J, Brain K. 1996. The relative effect of Azone and Transcutol on permeant diffusivity and solubility in human stratum corneum. *Pharm Res* 13(4):542-546.
64. Censi R, Martena V, Hoti E, Malaj L, Di Martino P. 2012. Permeation and skin retention of quercetin from microemulsions containing Transcutol(R) P. *Drug Dev Ind Pharm* 38(9):1128-1133.
65. Escribano E, Calpena AC, Queralt J, Obach R, Domenech J. 2003. Assessment of diclofenac permeation with different formulations: anti-inflammatory study of a selected formula. *Eur J Pharm Sci* 19(4):203-210.
66. Hua L, Weisan P, Jiayu L, Hongfei L. 2004. Preparation and evaluation of microemulsion of vinpocetine for transdermal delivery. *Pharmazie* 59(4):274-278.
67. Shakeel F, Baboota S, Ahuja A, Ali J, Aqil M, Shafiq S. 2007. Nanoemulsions as vehicles for transdermal delivery of aceclofenac. *AAPS PharmSciTech* 8(4):E104.
68. Panapisal V, Charoensri S, Tantituvanont A. 2012. Formulation of microemulsion systems for dermal delivery of silymarin. *AAPS PharmSciTech* 13(2):389-399.
69. Ali J, Akhtar N, Sultana Y, Baboota S, Ahuja A. 2008. Antipsoriatic microemulsion gel formulations for topical drug delivery of babchi oil (*Psoralea corylifolia*). *Methods Find Exp Clin Pharmacol* 30(4):277-285.
70. Fini A, Bergamante V, Ceschel GC, Ronchi C, De Moraes CA. 2008. Control of transdermal permeation of hydrocortisone acetate from hydrophilic and lipophilic formulations. *AAPS PharmSciTech* 9(3):762-768.

71. Barot BS, Parejiya PB, Patel HK, Gohel MC, Shelat PK. 2012. Microemulsion-based gel of terbinafine for the treatment of onychomycosis: optimization of formulation using D-optimal design. *AAPS PharmSciTech* 13(1):184-192.
72. Hathout RM, Woodman TJ, Mansour S, Mortada ND, Geneidi AS, Guy RH. 2010. Microemulsion formulations for the transdermal delivery of testosterone. *Eur J Pharm Sci* 40(3):188-196.
73. Notman R, den Otter WK, Noro MG, Briels WJ, Anwar J. 2007. The permeability enhancing mechanism of DMSO in ceramide bilayers simulated by molecular dynamics. *Biophys J* 93(6):2056-2068.
74. Caspers PJ, Williams AC, Carter EA, Edwards HG, Barry BW, Bruining HA, Puppels GJ. 2002. Monitoring the penetration enhancer dimethyl sulfoxide in human stratum corneum in vivo by confocal Raman spectroscopy. *Pharm Res* 19(10):1577-1580.
75. Shishu, Rajan S, Kamalpreet. 2009. Development of novel microemulsion-based topical formulations of acyclovir for the treatment of cutaneous herpetic infections. *AAPS PharmSciTech* 10(2):559-565.
76. Pappinen S, Urtti A. Microemulsions in topical drug delivery. In Smith EW, Maibach HI, editors. *Percutaneous penetration enhancers*. Boca Raton: Taylor and Francis; 2006.
77. Kogan A, Garti N. 2006. Microemulsions as transdermal drug delivery vehicles. *Advances in Colloid and Interface Science* 123-126:369-385.
78. Hathout RM, Mansour S, Geneidi AS, Mortada ND. 2011. Visualization, dermatopharmacokinetic analysis and monitoring the conformational effects of a

- microemulsion formulation in the skin stratum corneum. *J Colloid Interface Sci* 354(1):124-130.
79. Rosen MJ, Kunjappu JT. 2012. Characteristic features of the surfactants. In Rosen MJ, Kunjappu JT, editors. *Surfactants and interfacial phenomena*. New Jersey: John Wiley and Sons; pp:1-38.
 80. Loftsson T, Petersen DS, Le Goffic F, Olafsson JH. 1997. Unsaturated glycerol monoethers as novel skin penetration enhancers. *Pharmazie* 52(6):463-465.
 81. Bentley MVLB, Kedor ERM, Vianna RF, Collett JH. 1997. The influence of lecithin and urea on the in vitro permeation of hydrocortisone acetate through skin from hairless mouse. *International Journal of Pharmaceutics* 146:255–262
 82. Bonina FP, Montenegro L. 1994. Effects of some non-toxic penetration enhancers on in vitro heparin skin permeation from gel vehicles. *International Journal of Pharmaceutics* 111:191–196.
 83. Barry BW. 1988. Action of skin penetration enhancers-the Lipid Protein Partitioning theory. *Int J Cosmet Sci* 10(6):281-293.
 84. Mahjour M, Mauser B, Rashidbaigi Z, Fawzi MB. 1990. Effect of egg yolk lecithins and commercial soybean lecithins on in vitro skin permeation of drugs. *Journal of Controlled Release* 14:243–252.
 85. Saija A, Tomaino A, Trombetta D, Giacchi M, De Pasquale A, Bonina F. 1998. Influence of different penetration enhancers on in vitro skin permeation and in vivo photoprotective effect of flavonoids. *International Journal of Pharmaceutics* 175:85–94.

86. Yokomizo Y, Sagitani H. 1996. Effects of phospholipids on the in vitro percutaneous penetration of prednisolone and analysis of mechanism by using attenuated total reflectance-Fourier transform infrared spectroscopy. *J Pharm Sci* 85(11):1220-1226.
87. Barry BW. 1991. Lipid-Protein-Partitioning theory of skin penetration enhancement. *Journal of Controlled Release* 15:237-248.
88. Valenta C, Wanka M, Heidlas J. 2000. Evaluation of novel soya-lecithin formulations for dermal use containing ketoprofen as a model drug. *J Control Release* 63(1-2):165-173.
89. Kantarci G, Ozguney I, Karasulu HY, Arzik S, Guneri T. 2007. Comparison of different water/oil microemulsions containing diclofenac sodium: preparation, characterization, release rate, and skin irritation studies. *AAPS PharmSciTech* 8(4):E91.
90. Fang JY, Leu YL, Chang CC, Lin CH, Tsai YH. 2004. Lipid nano/submicron emulsions as vehicles for topical flurbiprofen delivery. *Drug Deliv* 11(2):97-105.
91. Hosmer J, Reed R, Bentley MV, Nornoo A, Lopes LB. 2009. Microemulsions containing medium-chain glycerides as transdermal delivery systems for hydrophilic and hydrophobic drugs. *AAPS PharmSciTech* 10(2):589-596.
92. Marku D, Wahlgren M, Rayner M, Sjoo M, Timgren A. 2012. Characterization of starch Pickering emulsions for potential applications in topical formulations. *Int J Pharm* 428(1-2):1-7.
93. Mittal A, Sara UV, Ali A, Aqil M. 2009. Status of fatty acids as skin penetration enhancers-a review. *Curr Drug Deliv* 6(3):274-279.

94. Babu RJ, Singh M, Kanikkannan N. 2005. Fatty alcohols and fatty acids. In Smith E, Maibach HI, editors. *Percutaneous Penetration Enhancers*. New York: CRC Press; pp:137-158.
95. Golden GM, McKie JE, Potts RO. 1987. Role of stratum corneum lipid fluidity in transdermal drug flux. *J Pharm Sci* 76(1):25-28.
96. Moghadam SH, Saliyaj E, Wettig SD, Dong C, Ivanova MV, Huzil JT, Foldvari M. 2013. Effect of chemical permeation enhancers on stratum corneum barrier lipid organizational structure and interferon alpha permeability. *Molecular pharmaceutics* XXX.
97. Francoeur ML, Golden GM, Potts RO. 1990. Oleic acid: its effects on stratum corneum in relation to (trans)dermal drug delivery. *Pharm Res* 7(6):621-627.
98. Benson HA. 2005. Transdermal drug delivery: penetration enhancement techniques. *Curr Drug Deliv* 2(1):23-33.
99. Zhao X, Liu JP, Zhang X, Li Y. 2006. Enhancement of transdermal delivery of theophylline using microemulsion vehicle. *Int J Pharm* 327(1-2):58-64.
100. Goebel AS, Schmaus G, Neubert RH, Wohlrab J. 2012. Dermal peptide delivery using enhancer molecules and colloidal carrier systems--part I: carnosine. *Skin Pharmacol Physiol* 25(6):281-287.
101. Yang JH, Kim YI, Kim KM. 2002. Preparation and evaluation of aceclofenac microemulsion for transdermal delivery system. *Arch Pharm Res* 25(4):534-540.
102. Liu CH, Huang HY. 2012. Antimicrobial activity of curcumin-loaded myristic acid microemulsions against *Staphylococcus epidermidis*. *Chem Pharm Bull (Tokyo)* 60(9):1118-1124.

103. Patel MR, Patel RB, Parikh JR, Solanki AB, Patel BG. 2009. Effect of formulation components on the in vitro permeation of microemulsion drug delivery system of fluconazole. *AAPS PharmSciTech* 10(3):917-923.
104. Peira E, Carlotti ME, Trotta C, Cavalli R, Trotta M. 2008. Positively charged microemulsions for topical application. *Int J Pharm* 346(1-2):119-123.
105. Trotta M, Pattarino F, Gasco MR. 1996. Influence of counter ions on the skin permeation of methotrexate from water--oil microemulsions. *Pharm Acta Helv* 71(2):135-140.
106. Peira E, Scolari P, Gasco MR. 2001. Transdermal permeation of apomorphine through hairless mouse skin from microemulsions. *Int J Pharm* 226(1-2):47-51.
107. Amar-Yuli I, Aserin A, Garti N. Interfacial reactivity at liquid crystal interfaces. In Amar-Yuli I, Garti N, editors. *Nanotechnologies for solubilization and delivery in foods and cosmetics pharmaceuticals*. Lancaster, PA: DEStech Publications Inc.; 2012.
108. Deshpanday NA, Ebert CD, Quan D, Venkateshwaran S. 1998. Triacetin as a penetration enhancer for transdermal delivery of a basic drug. In Office USPaT, editor, ed., US: Theratech, Inc, Ebert DC
109. Heiber EW, Patel CD, Venkateshwaran S. 1993. The use of glycerin in moderating transdermal drug delivery. In Office USPaT, editor, ed., US: Theratech, Inc.
110. Lopes LB, VanDeWall H, Li HT, Venugopal V, Li HK, Naydin S, Hosmer J, Levendusky M, Zheng H, Bentley MV, Levin R, Hass MA. 2010. Topical delivery of lycopene using microemulsions: enhanced skin penetration and tissue antioxidant activity. *J Pharm Sci* 99(3):1346-1357.

111. Biruss B, Valenta C. 2008. The advantage of polymer addition to a non-ionic oil in water microemulsion for the dermal delivery of progesterone. *Int J Pharm* 349(1-2):269-273.
112. Schwarz JS, Weisspapir MR, Friedman DI. 1995. Enhanced transdermal delivery of diazepam by submicron emulsion (SME) creams. *Pharm Res* 12(5):687-692.
113. Delgado-Charro MB, Iglesias-Vilas G, Blanco-Méndez J, López-Quintela MA, Marty JP, Guy RH. 1997. Delivery of a hydrophilic solute through the skin from novel microemulsion systems. *European Journal of Pharmaceutics and Biopharmaceutics* 43:37-42.
114. Araujo LM, Thomazine JA, Lopez RF. 2010. Development of microemulsions to topically deliver 5-aminolevulinic acid in photodynamic therapy. *Eur J Pharm Biopharm* 75(1):48-55.
115. Zhang YT, Zhao JH, Zhang SJ, Zhong YZ, Wang Z, Liu Y, Shi F, Feng NP. 2011. Enhanced transdermal delivery of evodiamine and rutaecarpine using microemulsion. *Int J Nanomedicine* 6:2469-2482.
116. Yuan Y, Li SM, Mo FK, Zhong DF. 2006. Investigation of microemulsion system for transdermal delivery of meloxicam. *Int J Pharm* 321(1-2):117-123.
117. Raza K, Negi P, Takyar S, Shukla A, Amarji B, Katare OP. 2011. Novel dithranol phospholipid microemulsion for topical application: development, characterization and percutaneous absorption studies. *J Microencapsul* 28(3):190-199.
118. Tsai YH, Chang JT, Chang JS, Huang CT, Huang YB, Wu PC. 2011. The effect of component of microemulsions on transdermal delivery of buspirone hydrochloride. *J Pharm Sci* 100(6):2358-2365.

119. Chen H, Mou D, Du D, Chang X, Zhu D, Liu J, Xu H, Yang X. 2007. Hydrogel-thickened microemulsion for topical administration of drug molecule at an extremely low concentration. *Int J Pharm* 341(1-2):78-84.
120. Wu PC, Lin YH, Chang JS, Huang YB, Tsai YH. 2010. The effect of component of microemulsion for transdermal delivery of nicardipine hydrochloride. *Drug Dev Ind Pharm* 36(12):1398-1403.
121. Junyaprasert VB, Boonme P, Songkro S, Krauel K, Rades T. 2007. Transdermal delivery of hydrophobic and hydrophilic local anesthetics from o/w and w/o Brij 97-based microemulsions. *J Pharm Pharm Sci* 10(3):288-298.
122. Dreher F, Walde P, Walther P, Wehrli E. 1997. Interaction of a lecithin microemulsion gel with human stratum corneum and its effect on transdermal transport. *Journal of Controlled Release* 45:131-140.
123. Neubert RH, Schmalfluss U, Wolf R, Wohlrab WA. 2005. Microemulsions as colloidal vehicle systems for dermal drug delivery. Part V: Microemulsions without and with glycolipid as penetration enhancer. *J Pharm Sci* 94(4):821-827.
124. Puranjoti PR, Patil T, Sheth PD, Bommareddy GP, Egbaria DK. 2002. Design and Development of Topical Microemulsion for Poorly Water-Soluble Antifungal Agents. *The Journal of Applied Research* 2:10-19.
125. Derle DV, Sagar BSH, Sagar P. 2006. Microemulsion as a vehicle for transdermal permeation of nimesulide. *Indian Journal of Pharmaceutical Sciences* 68:622-625.
126. Chandra A, Sharma PS, Irchhiaya R. 2009. Microemulsion-based hydrogel formulation for transdermal delivery of dexamethasone. *Asian Journal of Pharmaceutics* 3:30-36.

127. Valenta C, Schultz K. 2004. Influence of carrageenan on the rheology and skin permeation of microemulsion formulations. *J Control Release* 95(2):257-265.
128. Dima S, Popescu M. 2009. Topical Delivery of Diclofenac using Microemulsion Systems. *Roumanian Biotechnological Letters* 13:49-55.
129. Park ES, Cui Y, Yun BJ, Ko IJ, Chi SC. 2005. Transdermal delivery of piroxicam using microemulsions. *Arch Pharm Res* 28(2):243-248.
130. Suppasansatorn P, Nimmannit U, Conway BR, Du L, Wang Y. 2007. Microemulsions as topical delivery vehicles for the anti-melanoma prodrug, temozolomide hexyl ester (TMZA-HE). *J Pharm Pharmacol* 59(6):787-794.
131. Malakar J, Sen SO, Nayak AK, Sen KK. 2011. Development and evaluation of microemulsions for transdermal delivery of insulin. *ISRN Pharm* 2011:1-14.
132. Baboota S, Al-Azaki A, Kohli K, Ali J, Dixit N, Shakeel F. 2007. Development and evaluation of a microemulsion formulation for transdermal delivery of terbinafine. *PDA J Pharm Sci Technol* 61(4):276-285.
133. Al Abood RM, Talegaonkar S, Tariq M, Ahmad FJ. 2013. Microemulsion as a tool for the transdermal delivery of ondansetron for the treatment of chemotherapy induced nausea and vomiting. *Colloids Surf B Biointerfaces* 101:143-151.
134. Gao S, Singh J. 1998. Effect of oleic acid/ethanol and oleic acid/propylene glycol on the in vitro percutaneous absorption of 5-fluorouracil and tamoxifen and the macroscopic barrier property of porcine epidermis. *International Journal of Pharmaceutics* 165:45-55.

135. Hathout RM, Elshafeey AH. 2012. Development and characterization of colloidal soft nano-carriers for transdermal delivery and bioavailability enhancement of an angiotensin II receptor blocker. *Eur J Pharm Biopharm* 82(2):230-240.
136. Kumar S, Talegaonkar S, Negi LM, Khan ZI. 2012. Design and Development of Ciclopirox Topical Nanoemulsion Gel for the Treatment of Subungual Onychomycosis. *Indian Journal of Pharmaceutical Education and Research* 46:303-311.
137. Sabale V, Vora S. 2012. Formulation and evaluation of microemulsion-based hydrogel for topical delivery. *Int J Pharm Investig* 2(3):140-149.
138. Goebel AS, Knie U, Abels C, Wohlrab J, Neubert RH. 2010. Dermal targeting using colloidal carrier systems with linoleic acid. *Eur J Pharm Biopharm* 75(2):162-172.
139. Osborne DW, Ward AJI, O'Neill KJ. 1991. Microemulsions as topical drug delivery vehicles: in-vitro transdermal studies of a model hydrophilic drug. *Journal of Pharmacy and Pharmacology* 43:451–454.
140. Osborne DU, Ward AJI, O'Neill KJ. 1988. Microemulsions as Topical Drug Delivery Vehicles. I. Characterization of a Model System. *Drug Development and Industrial Pharmacy* 14:1203-1219.
141. Trotta M, Pattarino F, Gasco MR. 1996. Influence of counter ions on the skin permeation of methotrexate from water-oil microemulsions. *Pharmaceutica Acta Helvetiae* 71:135–140.
142. Subramanian N, Ghosal SK, Moulik SP. 2004. Topical delivery of celecoxib using microemulsion. *Acta Pol Pharm* 61(5):335-341.

143. Piemi MP, Korner D, Benita S, Marty Jp. 1999. Positively and negatively charged submicron emulsions for enhanced topical delivery of antifungal drugs. *J Control Release* 58(2):177-187.
144. Paolino D, Ventura CA, Nistico S, Puglisi G, Fresta M. 2002. Lecithin microemulsions for the topical administration of ketoprofen: percutaneous adsorption through human skin and in vivo human skin tolerability. *Int J Pharm* 244(1-2):21-31.
145. Alvarez-Figueroa MJ, Delgado-Charro MB, Blanco-Mendez J. 2001. Passive and iontophoretic transdermal penetration of methotrexate. *Int J Pharm* 212(1):101-107.
146. Delgado-Charro MB, Iglesias-Vilas G, Blanco-Méndez J, López-Quintela M, Marty JP, Guy RH. 1997. Delivery of a hydrophilic solute through the skin from novel microemulsion systems. *European Journal of Pharmaceutics and Biopharmaceutics* 43:37-42.
147. Subramanian N, Ghosal SK, Moulik SP. 2005. Enhanced in vitro percutaneous absorption and in vivo anti-inflammatory effect of a selective cyclooxygenase inhibitor using microemulsion. *Drug Dev Ind Pharm* 31(4-5):405-416.
148. Mei Z, Chen H, Weng T, Yang Y, Yang X. 2003. Solid lipid nanoparticle and microemulsion for topical delivery of triptolide. *Eur J Pharm Biopharm* 56(2):189-196.
149. Wilisch IL, Müller-Goymann CC. 1993. Correlation of colloidal microstructure, drug release and permeation through excised human skin. *International Journal of Pharmaceutics* 96:79–84.

150. Rozman B, Gasperlin M, Tinois-Tessoneaud E, Pirot F, Falson F. 2009. Simultaneous absorption of vitamins C and E from topical microemulsions using reconstructed human epidermis as a skin model. *Eur J Pharm Biopharm* 72(1):69-75.
151. Tashtoush BM, Bennamani AN, Al-Taani BM. 2013. Preparation and characterization of microemulsion formulations of nicotinic acid and its prodrugs for transdermal delivery. *Pharm Dev Technol* 18(4):834-843.
152. Kitagawa S, Tanaka Y, Tanaka M, Endo K, Yoshii A. 2009. Enhanced skin delivery of quercetin by microemulsion. *J Pharm Pharmacol* 61(7):855-860.
153. Tsai YH, Lee KF, Huang YB, Huang CT, Wu PC. 2010. In vitro permeation and in vivo whitening effect of topical hesperetin microemulsion delivery system. *Int J Pharm* 388(1-2):257-262.
154. Schmalfusz U.; Neubert R.; Wohlrab W. 1997. Modification of drug penetration into human skin using microemulsions. *Journal of Controlled Release* 46:279-285.
155. Kitagawa S, Yoshii K, Morita SY, Teraoka R. 2011. Efficient topical delivery of chlorogenic acid by an oil-in-water microemulsion to protect skin against UV-induced damage. *Chem Pharm Bull (Tokyo)* 59(6):793-796.
156. Ambade KW, Jadhav SL, Gambhire MN, Kurmi SD, Kadam VJ, Jadhav KR. 2008. Formulation and evaluation of flurbiprofen microemulsion. *Curr Drug Deliv* 5(1):32-41.
157. Ustundag Okur N, Apaydin S, Karabay Yavasoglu NU, Yavasoglu A, Karasulu HY. 2011. Evaluation of skin permeation and anti-inflammatory and analgesic effects of new naproxen microemulsion formulations. *Int J Pharm* 416(1):136-144.

158. Tavano L, Alfano P, Muzzalupo R, de Cindio B. 2011. Niosomes vs microemulsions: new carriers for topical delivery of Capsaicin. *Colloids Surf B Biointerfaces* 87(2):333-339.
159. Ktistis G, Niopas I. 1998. A Study on the In-vitro Percutaneous Absorption of Propranolol from Disperse Systems. *Journal of Pharmacy and Pharmacology* 50:413–418.
160. Luo M, Shen Q, Chen J. 2011. Transdermal delivery of paeonol using cubic gel and microemulsion gel. *Int J Nanomedicine* 6:1603-1610.
161. Cao FH, OuYang WQ, Wang YP, Yue PF, Li SP. 2011. A combination of a microemulsion and a phospholipid complex for topical delivery of oxymatrine. *Arch Pharm Res* 34(4):551-562.
162. Baroli B, López-Quintela MA, Delgado-Charro MB, Fadda AM, Mendez JB. 2000. Microemulsions for topical delivery of 8-methoxsalen. *Journal of Controlled Release* 69:209–218.
163. Alvarez-Figueroa MJ, Blanco-Mendez J. 2001. Transdermal delivery of methotrexate: iontophoretic delivery from hydrogels and passive delivery from microemulsions. *Int J Pharm* 215(1-2):57-65.
164. Yuan JS, Ansari M, Samaan M, Acosta EJ. 2008. Linker-based lecithin microemulsions for transdermal delivery of lidocaine. *Int J Pharm* 349(1-2):130-143.
165. Sintov AC, Botner S. 2006. Transdermal drug delivery using microemulsion and aqueous systems: influence of skin storage conditions on the in vitro permeability of diclofenac from aqueous vehicle systems. *Int J Pharm* 311(1-2):55-62.

166. Elshafeey AH, Kamel AO, Fathallah MM. 2009. Utility of nanosized microemulsion for transdermal delivery of tolterodine tartrate: ex-vivo permeation and in-vivo pharmacokinetic studies. *Pharm Res* 26(11):2446-2453.
167. Lehmann L, Keipert S, Gloor M. 2001. Effects of microemulsions on the stratum corneum and hydrocortisone penetration. *Eur J Pharm Biopharm* 52(2):129-136.
168. Changez M, Chander J, Dinda AK. 2006. Transdermal permeation of tetracaine hydrochloride by lecithin microemulsion: in vivo. *Colloids Surf B Biointerfaces* 48(1):58-66.
169. Podlogar F, Bester Rogac M, Gasperlin M. 2005. The effect of internal structure of selected water-Tween 40-Imwitor 308-IPM microemulsions on ketoprofene release. *Int J Pharm* 302(1-2):68-77.
170. Hashem FM, Shaker DS, Ghorab MK, Nasr M, Ismail A. 2011. Formulation, characterization, and clinical evaluation of microemulsion containing clotrimazole for topical delivery. *AAPS PharmSciTech* 12(3):879-886.
171. Holler S, Valenta C. 2007. Effect of selected fluorinated drugs in a "ringing" gel on rheological behaviour and skin permeation. *Eur J Pharm Biopharm* 66(1):120-126.
172. Getie M, Wohlrab J, Neubert RH. 2005. Dermal delivery of desmopressin acetate using colloidal carrier systems. *J Pharm Pharmacol* 57(4):423-427.
173. Bonina FP, Montenegro L, Scrofani N, Esposito E, Cortesi R, Menegatti E, Nastruzzi C. 1995. Effects of phospholipid based formulations on in vitro and in vivo percutaneous absorption of methyl nicotinate. *Journal of Controlled Release* 34:53-63.

174. Kreilgaard M, Pedersen EJ, Jaroszewski JW. 2000. NMR characterisation and transdermal drug delivery potential of microemulsion systems. *J Control Release* 69(3):421-433.
175. Escribano E, Calpena AC, Queralt J, Obach R, Doménech J. 2003. Assessment of diclofenac permeation with different formulations: anti-inflammatory study of a selected formula. *European Journal of Pharmaceutical Sciences* 19:203-210.

Table 3.1 Lipids used in the formulation of topical and transdermal microemulsions

Vegetable oil	Surfactant/ Co-surfactant	Active drug /marker	Membrane/Skin
Olive oil	Tween 80 and Span 80	³ H-inulin, ¹⁴ C-tranexamic acid ⁵⁸	Mice
	Labrafil M 1944	Ketoconazole ¹²⁴	Durapore®
	CS/Plurol Oleique		membrane
	Tween 80/iso-octanol	Nimesulide ¹²⁵	-
	Egg lecithin/isopropyl alcohol	Dexamethasone ¹²⁶	Rat
	Soybean oil	Brij 97	Sodium fluorescein ¹²⁷
Cremophor EL-Span 80/diethylene glycol monoethyl ether or ethanol or propylene glycol		Indomethacin ⁴⁸	Mice
Brij 58-Span 80/ethanol or propanol or isopropyl alcohol		Diclofenac sodium ⁸⁹	Human
Brij 54 and Span		Diclofenac	Synthetic

	80/ethanol or 1- butanol	sodium ¹²⁸	carboxymethyl cellulose membrane
	Egg lecithin	Flurbiprofen ⁹⁰	Rat
	Polysorbate 80, medium-chain glycerides, and propylene glycol	Progesterone and Adenosine ⁹¹	Porcine
Coconut oil	Egg lecithin	Flurbiprofen ⁹⁰	Rat
Sheanut oil	Starch	Methyl salicylate ⁹²	Porcine
Canola oil	Span 80/Tween 80	Quercetin dihydrate ⁵⁹	Porcine

Fatty acids	Surfactant/ Co-surfactant	Active drug /marker	Membrane/Skin
Oleic acid	Cremophor EL/ethanol	Penciclovir ⁴⁵	Mice
	Tween 80/propylene glycol	Triptolide ¹⁸	Rabbit
	Labrasol [®] /Cremophor [®] RH 40	Ketoprofen ³⁸	Rat
	Labrasol [®] /Transcutol [®]	Terbinafine ⁷¹	Human
	Tween 80/ethanol	Nadifloxacin ⁵¹	Rat
	Tween 20 or Span 80/ethanol	Estradiol ⁴⁹	Human
	Labrasol [®] /ethanol	Piroxicam ¹²⁹	Rat
	Cremophor [®] RH 40/Transcutol [®]	Vinpocetine ⁶⁶	Rat
	Vitamin E TPGS acid hexyl ester ¹³⁰	Temozolomide	Mice
	Tween 80/isopropyl alcohol	Insulin ¹³¹	Mice/Goat
	Tween 20/Transcutol [®]	Testosterone ⁷²	Porcine

	Cremophor [®] RH 40/Labrasol [®]	Theophylline ⁹⁹	Rabbit
	Transcutol [®]	Diclofenac sodium ⁶⁵	Human
	Labrasol [®] /Transcutol [®]	Terbinafine ¹³²	Rat
	Tween 20/polyethylene glycol 400	Ondansetron ¹³³	Rat
	Ethanol or propylene glycol	5-fluorouracil and tamoxifen ¹³⁴	Porcine
	Labrasol [®] /Transcutol [®]	Olmesartan medoxomil ¹³⁵	Porcine
	Tween 80/polyethylene glycol 400	Ciclopirox ¹³⁶	Rat
	Cremophor EL/ethanol	Penciclovir ⁴⁵	Mice
	Tween 80/isopropyl alcohol	Bifonazole ¹³⁷	Rat
Linoleic acid	Lauryl glucoside (Plantacare 1200 UP and cetearyl	Linoleic acid ¹³⁸	Human

	glucoside (Tegocare CG 90)/pentylene glycol	Labrasol [®] /Transcutol [®]	Aceclofenac ¹⁰¹	Rat and Human
Myristic acid	Tween 80 and Pluronic F127		Curcumin ¹⁰²	Porcine
Fatty alcohols				
Lauryl alcohol	Labrasol [®] /ethanol		Diclofenac diethylammoniu m ⁵²	Rat
	Labrasol [®] /ethanol		Fluconazole ¹⁰³	Rat
Capryl Alcohol (Octanol)	Diethyl sodium sulphosuccinate		D-Glucose ¹³⁹	Human
	Diethyl sodium sulphosuccinate		Radiolabeled water [³ H]H ₂ O ¹⁴⁰	Human
Decanol	Lecithin/benzyl alcohol		Methotrexate ¹⁴¹	Mice
Decanol + Isopropyl myristate	Octanoic acid, 1,2 propanediol, sodium hexanoate (or octanoate),		Apomorphine HCl ¹⁰⁶	Mice

	sodium glycocholate		
	(or taurocholate)		
	Epikuron 200/Benzyl		
	alcohol		
Decanol + 1-	Oramix [®] NS 10 or	Miconazole	Porcine
Dodecanol	mixture of lecithin	nitrate ¹⁰⁴	
	and Oramix [®] NS		
	10/PG and 1,2-		
	hexanediol		

Glycerides	Surfactant/ Co-surfactant	Active drug /marker	Membrane/Skin
Caprylic/capric monoglycerides	Brij/propylene glycol	Lycopene ¹¹⁰	Porcine
Caprylic/capric mono-/di- glycerides + propylene glycol dicaprylate/dicaprate	Polysorbate 80	Celecoxib ¹⁴²	Rat
Glyceryl monooleate	Tween 20, Labrasol [®] , polyethylene glycol-40 hydrogenated castor oil (HCO-40 [®])/Transcutol [®]	Silymarin ⁶⁸	Porcine
Triacetin/Glycerol triacetate Tributyrin (butyric acid triglyceride)	Brij 35	Progesterone ¹¹¹	Porcine
Medium chain triglycerides (MCT oil)	Tyloxpol Phospholipids and stearylamine/pol	Diazepam ¹¹² Econazole or Miconazole nitrate ¹⁴³	Mice Rat

	oxamer 188		
	Soybean lecithin/n-butanol	Ketoprofen ¹⁴⁴	Human
	Isopropyl alcohol/dimethyl isosorbide	Terbinafine HCl ⁴⁶	Human
Fatty acid esters	Surfactant/ Co-surfactant	Active drug /marker	Membrane/Skin
Ethyl oleate	Labrasol [®] /Plurol Isostearique [®]	Methotrexate ¹⁴⁵	Porcine
	Labrasol [®] /Plurol isostearique	¹⁴ C-radiolabeled sucrose ¹⁴⁶	Mice
	Labrasol [®] /Plurol oleique	5- Aminolevulinic acid ¹¹⁴	Porcine
	Cremophor EL	Evodiamine and Rutaecarpine ¹¹⁵	Rat
Propylene glycol dicaprylate/dicaprate	Polysorbate 80	Celecoxib ¹⁴⁷	Rat
Isopropyl myristate (IPM)	Tween 80/1,2-propylene glycol	Triptolide ¹⁴⁸	Rat

Tween 85/ethanol	Meloxicam ¹¹⁶	Rat
Lecithin	Fenoprofen acid ¹⁴⁹	Human
Imwitor 308/Tween 40	α -Tocopherol (vitamin E) and Ascorbic acid (vitamin C) ¹⁵⁰	Reconstructed human skin - Episkin [®]
Labrasol [®] + Peceol	Nicotinic acid and its prodrugs ¹⁵¹	Mice
Tween 80/ethanol	Quercetin ¹⁵²	Porcine
Tween 80/Span 80 or Tween 80/Span 20	Hesperetin ¹⁵³	Rat
Tween 80 or Tween 20/Phospholipon 90G or ethanol	Dithranol ¹¹⁷	Mice
Tween 80/Span 20 or Brij 35/Brij 30	Buspirone HCl ¹¹⁸	Rat

Tween 80/Span 20	Diphenhydramin e hydrochloride ¹⁵⁴	Human
Tween 80/propylene glycol	Triptolide ¹¹⁹	Mice
Mixture of Tween 80 and Span 80 and/or Mixture of Tween 80 and Span 20/ethanol	Nicardipine HCl ¹²⁰	Rat
Tween 80/ethanol	Chlorogenic acid ¹⁵⁵	Porcine
Aerosol OT/sorbitan monooleate	Flurbiprofen ¹⁵⁶	Rat
Mixture of Labrasol [®] and Span 80/ethanol or mixture of Labrafil M and Cremophor	Naproxen ¹⁵⁷	Rat

EL/isopropyl alcohol	Tween 80/Span 80	Capsaicin ¹⁵⁸	Rabbit
	Polysorbate 80	Propranolol ¹⁵⁹	Artificial cellulose membrane
	Cremophor	Paeonol ¹⁶⁰	Rat
EL/polyethylene glycol 400	Cremophor RH40/polyethyle ne glycol 400	Oxymatrine ¹⁶¹	Mice
	Lecithin	Fenoprofen acid ¹⁴⁹	Human
	Labrasol [®] /Plurol oleique	Diclofenac diethylamine ⁴¹	-
	AOT (Aerosol- OT or sodium bis (2-ethylhexyl) sulfosuccinate)	5-Fluorouracil ²⁷	Mice
	Tween 80/Span 80/1,2- octanediol	8- Methoxsalen ¹⁶²	Porcine

Tween 80/Span 80/1,2- octanediol	Methorexate ¹⁶³	Porcine
Tween 20/Span 20	Acyclovir ⁷⁵	Mice
Lecithin/pentanol	Lidocaine ¹⁶⁴	Porcine and reconstructed human skin, EpiDerm™ EPI- 200
PEG-40 stearate + glyceryl oleate/tetraglycol	Diclofenac sodium ¹⁶⁵	Rat/mice/porcine
Labrasol®/plurol Diisostearique	Tolterodine tartrate ¹⁶⁶	Human skin
Sucrose laurate L 595 + L 1695/PG or Tagat®S + Plurol oleate® WL 1173	Hydrocortisone ¹⁶ 7	Chorioallantoic membranes from hen's egg and Human skin
Lecithin/n- propanol	Tetracaine HCl ¹⁶⁸	Rat /Mice
Tween	Ketoprofene ¹⁶⁹	Hydrophilic

	40/Imwitor [®] 308		cellulose acetate membrane
	Tween 80/n- butanol	Clotrimazole ¹⁷⁰	Mice/Human
	Isopropranol	Fluconazole, flufenamic acid, flutamide, flumethasone pivalate ¹⁷¹	Porcine
	Tween 80	Lidocaine HCl ⁵³	Human
IPM+Decanol	Epikuron 200	Apomorphine HCl ¹⁰⁶	Mice
Isopropyl palmitate (IPP)	Polysorbate 85 or polyoxyethylene (20) glyceryl monooleate/polo xamer 101 or Tegin 4600	Alprenolol, Atenolol, Bupranolol, Carazolol, Metipranolol, Metoprolol, Penbutolol, Propranolol, Timolol ¹⁷	Rabbit
	Tagat 02/Span 80	Desmopressin acetate ¹⁷²	Human

	Brij 97 and 1- butanol	Lidocaine, Tetracaine and Dibucaine ¹²¹	Human
	Soybean lecithin	Indomethacin and Diclofenac ¹²²	Human
	Glyceryl oleate + Cremophor [®] RH 40/Tetraglycol	Lidocaine ⁴²	Mice
	Tween 80/Span 20	Diphenhydramin e HCl ¹²³	Human
	Soybean lecithin (Epikuron 200)	Methyl nicotinate ¹⁷³	Synthetic mem- brane of cellulose and silicone
Isostearylic isostearate	Labrasol [®] /Plurol Isostearique	Lidocaine and Prilocaine hydrochloride ¹⁷⁴	Rat
	Labrasol [®] /Plurol oleique	Sodium diclofenac ¹⁷⁵	Rat

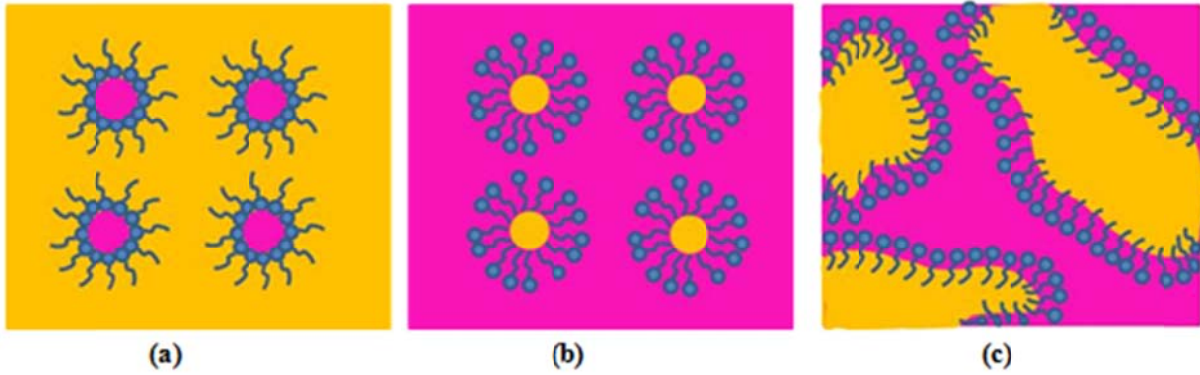


Figure 3.1 Structures of (a) W/O (b) O/W and (c) bicontinuous microemulsion

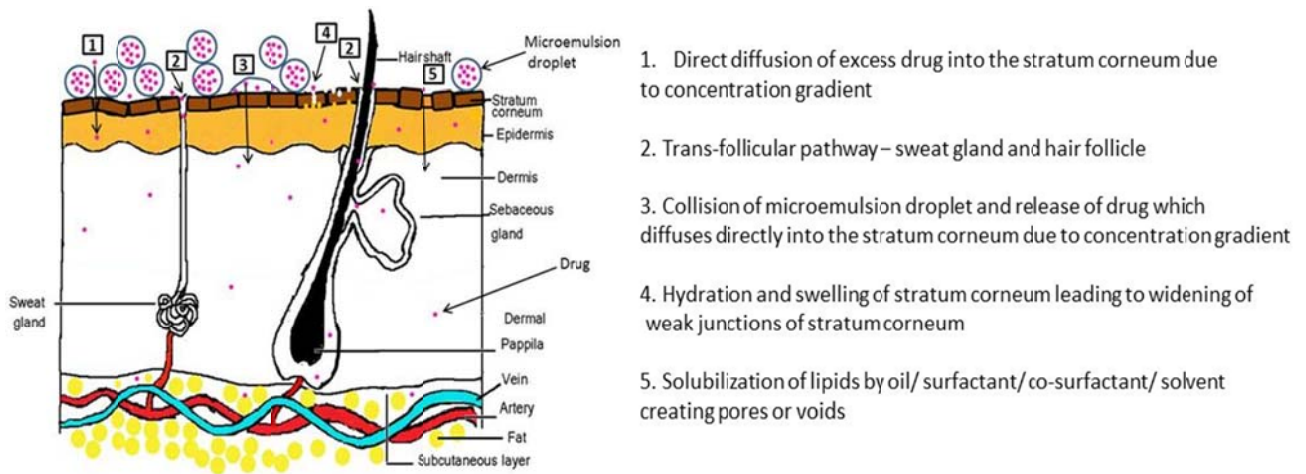


Figure 3.2 Permeation pathways for drug delivery by nanoemulsion

4. EFFECT OF LIPOPHILICITY ON MICRONEEDLE-MEDIATED IONTOPHORETIC TRANSDERMAL DELIVERY ACROSS HUMAN SKIN *IN VITRO*

4.1 ABSTRACT

The effect of lipophilicity of drug on the MN-mediated iontophoretic delivery across dermatomed human skin was studied. Beta blockers with similar pKa but varied log P values were selected as model drugs in this study. ITP or MN, when used independently, increased the transdermal flux of beta blockers as compared to passive delivery (PD). ITP appeared to be the most efficient enhancement method for the beta blockers examined. ITP when applied across the MN treated skin (MN+ITP) resulted in increased transport of beta blockers as compared to PD ($P < 0.001$). The enhancement ratio (ER) for hydrophilic molecules (atenolol and sotalol) was 71- and 78-fold higher for ITP+MN as compared to PD. However, for propranolol (a lipophilic molecule), there was 10-fold increase in the ER as compared to PD. These observations were further substantiated by the skin retention data; an inverse relationship between the skin retention and the hydrophilicity of the drug molecule was observed. The results in the present study point out that the lipophilicity of the molecule plays a significant role on the electrically assisted transdermal delivery of drugs across the microporated skin. Hydrophilic molecules are successfully delivered using the combination strategy than the lipophilic molecules.

4.2 INTRODUCTION

Transdermal delivery is an attractive route for drugs due to the large surface area of the skin. It provides distinct benefits such as non-invasiveness, elimination of hepatic first-pass effect, reduction of systemic side effects, and high patient compliance.^{1,2} However, the outermost skin layer, stratum corneum (SC), poses the main barrier for the permeation of drugs.³ Various permeation enhancement techniques were used to overcome the barrier and increase the delivery of drugs across skin in therapeutic quantities.^{4,5} Some of these include the use of chemical penetration enhancers⁶, ITP⁷ and MN.⁸ Among these, ITP and MN hold promising future as they have shown encouraging results for various drugs that are difficult-to-deliver across skin including biopharmaceutical agents. ITP can be defined as the migration of the solute, either charged or uncharged, across skin, under the influence of an electric current.⁹ While the predominant pathway of iontophoretic transport is through skin appendages (hair follicles and sweat glands), the extracellular routes across the SC also contribute to enhanced drug permeation.¹⁰ As drug delivery is proportionate to the amount of electrical potential applied, ITP offers an opportunity for programmable drug delivery. However, since ITP does not primarily alter the skin barrier itself, it is limited to ionizable as well as un-ionizable drug molecules with molecular weight <10,000 Daltons.¹¹⁻¹³

MN technology utilizes micron-sized needles that typically pierce across the epidermis and sometimes into the superficial dermis creating aqueous pathways for drug transport into the skin.¹⁴ MN can actively drive therapeutic moieties into the skin either as coated or encapsulated cargo when introduced via insertion of solid MN or as convective flow through hollow MN.¹⁵ MN technology has been explored for the delivery of various drugs, nanoparticles, macromolecules and microparticles across skin¹⁶⁻¹⁹ without inducing any pain or discomfort.^{20,21}

The delivery of human growth hormone and desmopressin across hairless rat skin was facilitated by two layered dissolving MN.²² Hollow micro-structured transdermal system (hMTS) provided rapid delivery rates up to 300 $\mu\text{L}/\text{min}$ for liquid formulations of naloxone HCl, human growth hormone, and equine tetanus anti-toxin, in swine.²³ Maltose MN facilitated delivery of a large molecular weight model protein, immunoglobulin G, in solution across hairless rat skin.²⁴

A combination strategy that involves the usage of more than one enhancement technique can result in additive or synergistic delivery of drugs across the skin.²⁵⁻²⁸ ITP or MN acts independently of each other and each of them, used alone, are capable of enhancing skin permeation. ITP applied over MN pre-treated skin has led to significant increase in the transdermal permeation of insulin and a FITC-labeled bovine serum albumin across porcine skin as compared to either MN or ITP alone.²⁹ Though ITP alone was not effective to deliver daniplastim across hairless rat skin, microporation of skin resulted in a 30-fold increase in the permeation under the influence of ITP.³⁰ A combination of MN and ITP for delivery of insulin in a liposomal formulation across rat skin demonstrated a synergistic effect with 713-fold higher permeation than passive delivery (PD) across porcine skin.³¹ Though there are several works that report enhanced skin permeation with combination strategy, none of them investigated the factors that influence this enhancement.

Lipophilicity, which is an inherent property of the drug molecule, plays an important role in the transdermal permeation (such as PD, MN or ITP). As each of these methods has its own limitations when used alone, the use of their combination is becoming increasingly important as an enhancement strategy in the transdermal permeation. The factors that influence the flux when MN and ITP are used in combination have not been investigated well so far. We believe that lipophilicity does play an important role on MN mediated transdermal ITP. Further, skin being

negatively charged at the physiological pH is known to possess perm-selectivity towards positively charged molecules.³²⁻³⁵ Stratum corneum gets breached upon treatment with MN, and this affects its perm-selectivity which in turn could affect the iontophoretic flux.³³ The outcome of this therefore could address this key issue and provide an insight into the versatility of this combination approach for enhancing the transdermal delivery of molecules.

Beta-blockers were used as model molecules to investigate the effect of lipophilicity on the MN mediated ITP. While keeping all other physicochemical parameters such as molecular weight and pKa constant, only log P of the model molecules was varied. Hydrochloride salts of four beta blockers (propranolol, acebutalol, atenolol and sotalol) with similar molecular weight and pKa values but different log P values (Table 4.1) were selected for this study.

4.3 EXPERIMENTAL

4.3.1 MATERIALS

Propranolol HCl was obtained from Letco medical (Decatur, AL, USA). Acebutolol HCl and sotalol HCl were obtained from MP Biomedicals (Solon, OH, USA) and AvaChem scientific (San Antonio, TX, USA) respectively. Atenolol HCl was synthesized in house from atenolol base procured from a commercial source (Letco medical Decatur, AL, USA). The purity of Atenolol HCl was confirmed by NMR and IR spectrometry analyses. Silver wire and silver chloride were purchased from Sigma Aldrich (St. Louis, MO, USA). Sodium chloride, potassium dihydrogen phosphate and triethylamine were purchased from Fisher Scientific (Suwannee, GA, USA).

4.3.2 PREPARATION OF DRUG SOLUTION

The drug solution was prepared by dissolving 100 mg of respective drug in 10 mL of 25mM Tris buffer (pH 7.0). In this solution 43.83 mg of sodium chloride (75 mM) was dissolved to produce a clear solution. Buffer was used to minimize the fluctuations in pH and sodium chloride was included as a source of chloride ions to facilitate the electrochemistry.

4.3.3 SKIN PERMEATION STUDIES

Dermatomed human skin (thickness \sim 0.35 mm) was obtained from Allosource (Cincinnati, OH, USA). To avoid inter-individual variations, the entire skin required for the study was collected from a single donor within 8 h of death and frozen at -70°C until use. *In vitro* studies were performed using vertical Franz diffusion cells (PermeGear, Hellertown, PA, USA). The frozen skin was thawed at ambient temperature for about 30 minutes. It was then cut, rinsed with water, and sandwiched between donor and receptor cells with the epidermis facing the donor cell. The receiver chamber was filled with 5 mL of 25 mM Tris buffer (pH 7.0) and maintained at 37°C with a water circulation jacket that surrounded the cells. The available diffusion area of the skin was 0.64 cm^2 . The donor cell contained 500 μL of drug solution and covered with Parafilm to prevent evaporation. Stirring was maintained in the receptor cells with the help of the magnetic bars throughout the permeation study. At defined intervals, 500 μL aliquots from the receptor cells were collected and replaced with fresh buffer solution. The samples were stored in a refrigerator and analyzed within 24 h. All experiments were performed in 4 replicates.

4.3.4 DRUG EXTRACTION FROM SKIN

At the end of the skin permeation study, the residual drug remaining on the surface of the skin was removed by cotton swabs. The surface was washed with Tris buffer (pH 7.0) and then gently wiped with a cotton swab (Q-tips[®] Uniliver USA, Englewood Cliffs, NJ). A 200 μ L of Tris buffer was then added to the surface and dabbed with a fresh cotton swab. This process of swabbing and dabbing was repeated for five times. Our previous studies ensured complete removal of the drug from the skin surface with this procedure.²⁴ Following the washing procedure, the active diffusion area was isolated with a biopsy punch (George Tiemann & Co, Hauppauge, NY). The collected skin was weighed, minced into pieces and transferred separately into a borosilicate glass vial. To each of these glass vials, 1 mL of Tris buffer was added, sonicated for 15 min and allowed to stand overnight. The next day, samples were sonicated again for 30 min, filtered through 0.45 μ m membrane filter, and the supernatant was analyzed by HPLC.

4.3.5 IONTOPHORESIS

Iontophoretic protocol involved application of a direct current (Keithley Instruments, Inc, Cleveland, Ohio, USA) of 0.4 mA/cm² using Ag as an anode and Ag/AgCl as a cathode. Beta blockers used for the study remain positively charged at the donor cell pH (7.0) and hence delivered from anode (anodal ITP). Electric current was applied for 6 h (iontophoretic phase) and the experiments were continued until 26 h. All the skin permeation studies were conducted using Franz diffusion cells as described earlier in section 4.3.3. Following termination of the permeation experiments, skin extraction studies were continued as described earlier in Section 4.3.4. The drug content in the skin during the current application period was determined in a

separate set of experiments wherein the permeation studies were terminated at 6 h and the residual amount of drug in the skin was determined following procedures detailed in the previous section.

4.3.6 MICROPORATION

Microporation studies involved pretreatment of human skin with solid metallic MN arrays of a Demoroller™ (Dermaoller Deutschland s.a.r.l., Germany). The Dermaroller was run for 20 times on the epidermal surface of the dermatomed human skin and the treated skin was cut to size and mounted over Franz diffusion cells. The *in vitro* permeation and the skin extraction studies were conducted as described in previous sections 4.3.3 and 4.3.4.

4.3.7 COMBINATION OF IONTOPHORESIS AND MICROPORATION

The microporated skin was prepared as described in section 4.3.6 and mounted over Franz diffusion cells. Iontophoresis experiments on microporated skin were performed with a current density of 0.4 mA/cm² using Ag as an anode and Ag/AgCl as a cathode as described in section 4.3.5. The permeation and skin extraction experiments were conducted using Franz diffusion cells as described in Sections 4.3.3 and 4.3.4.

4.3.7 ANALYTICAL METHOD

A HPLC system (Waters Corp., MA, USA) equipped with 717 plus autosampler, 1525 pump, 2998 PDA UV detector and Empower 2 software was used. The HPLC analysis of beta blockers was carried out following a modification of a reported method.³⁶ Samples were eluted on a 4.6 mm x 250 mm Luna C₁₈ analytical column with 5µm silica particles of 100 Å pore size

(Phenomenex, Torrance, CA, USA). The mobile phase A consisted of 15mM potassium dihydrogen phosphate buffer with 1.2% triethylamine, pH adjusted to 3 with orthophosphoric acid while mobile phase B consisted of acetonitrile. The mobile phase ratios for eluting each beta-blocker are given in Table 4.2. The mobile phase was run at a flow rate of 1.0 mL/min and the run time was 15 minutes.

4.3.8 DATA ANALYSIS

All results are presented as mean \pm standard error of mean (SEM). The cumulative amount of drug permeated through a unit area of skin was plotted as a function of time. The steady state flux was calculated from the slope of the linear portion of the plot. The iontophoretic flux and post-iontophoretic flux were obtained from the permeation data between 0 - 6 h and 6 - 26 h, respectively.

The enhancement ratios (ER) were calculated as the ratio between the flux of MN, ITP or ITP+MN experiments and the flux of PD. The lag times were calculated from the x intercept of the linear portion of the skin permeation versus time plot. The amount of drug (μ g) retained in the skin was normalized to per gram of skin. Analysis of variance was performed to determine the level of significance between the means. Mean differences with $P < 0.05$ were considered to be significant.

4.4 RESULTS

The skin permeation profiles of beta blockers are presented in Figures 4.1 – 4.4 with overall transdermal flux shown in the inset of respective figure. The flux values of ITP, post ITP phases and lag times of each permeation study are presented in Table 4.3A and 4.3B,

respectively. The skin retention levels determined at 6 h (end of ITP phase) as well as at 26 h (end of skin permeation study) are presented in Table 4.3C. Enhancement ratios calculated for MN, ITP and ITP+MN permeation studies are presented in Table 4.4.

4.4.1 PASSIVE DELIVERY

The beta blockers used for the study could permeate across the skin well above their level of detection. It is evident from the data (Table 4.3A) that there exists a direct relationship between skin permeation, measured in terms of flux, and log P of drugs investigated. As expected, the permeation increased while the lag time decreased with the log P (Table 4.3B). The skin retention of the drugs immediately following the experiment (26 h) correlated positively with that of permeation data and the residual drug levels in the skin are lower for drugs with low log P (Table 4.3C). The highest flux and skin retention were seen with the most lipophilic drug, propranolol and the values decreased in the order of acebutolol, atenolol and sotalol.

4.4.2 IONTOPHORESIS

The skin permeation following the application of electric current was significantly higher than PD for all the drugs (Figures 4.1 – 4.4). Anodal ITP was very efficient and resulted in a considerable increase in flux for all the beta blockers during the current application period (ITP phase) as compared to PD (Table 4.3A). Following termination of current at 6 h, the flux decreased, but it remained always at a higher level than PD for all the drugs ($P < 0.001$). In contrast to PD, the corresponding lag times observed with ITP were much shorter, and the values decreased with a decrease in the lipophilicity of the drug (Table 4.3B). The skin retentions immediately following termination of the current at 6 h was significantly higher as compared to

26 h retention values for ITP ($P < 0.001$), MN ($P < 0.001$) and PD ($P < 0.001$) for all drugs. There is a direct correlation between skin retention levels and log P of drugs (Table 4.3C).

4.4.3 MICRONEEDLES

Pretreatment of the skin with MN resulted in increased transdermal flux of the beta blockers as compared to the PD ($P < 0.001$) (Figures 4.1 – 4.4). The flux values resulting from MN pretreatment are 6 to 10-fold higher than that of corresponding PD (Table 4.3A). The enhancement ratios with MN (measured as the ratio of the flux of MN to PD) correlated inversely with the lipophilicity of the drug. There was about 10-fold increase in flux for sotalol and atenolol, the hydrophilic molecules investigated, followed by acebutolol (6.5-fold) and propranolol (6.1-fold). The lag times observed were much shorter as compared to their respective PD and the longest lag time was observed with propranolol, the most lipophilic molecule investigated (Table 4.3B). The skin retention of drugs following the completion of permeation study (26 h) decreased with decrease in lipophilicity of the drugs with the retention being highest (1.74 ± 0.10 mg/g) for propranolol and lowest for sotalol (0.22 ± 0.07 mg/g) (Table 4.3C).

4.4.5 COMBINATION STRATEGY

ITP was used in conjunction with MN in the combination strategy, ITP+MN. Except for propranolol, rest of the beta blockers used in the study showed a significant increase in transdermal flux with ITP+MN as compared to ITP alone ($P < 0.01$) (Figures 4.1 – 4.4). The flux values observed with ITP alone and ITP+MN were not significantly different ($P > 0.05$) for propranolol (Table 4.3A). For the comparison purpose, the enhancement is represented as a ratio between transdermal fluxes (6 h) with combination strategy and ITP. The enhancement increased

with a decrease in the log P of the molecule with highest enhancement obtained with sotalol, and no significant enhancement was observed with propranolol. Except for the highly hydrophilic drug - sotalol, the lag times were similar when combined strategy was used as compared to ITP (Table 4.3B). However, they were significantly different when compared to MN used alone. The skin retention for all the drugs analyzed immediately after the termination of the current (6 h), was significantly higher for ITP+MN as compared to ITP or MN used alone (Table 4.3C).

4.5 DISCUSSION

The four model drugs selected for the study are beta blockers which are weak bases with a similar molecular weight, and pKa but with varying lipophilicity (Table 4.1). All the physicochemical parameters for these model drugs are similar with the exception of lipophilicity. These properties make them ideal candidates for studying the effect of lipophilicity on MN mediated transdermal permeation. It should be noted that drugs belonging to this particular class were selected based on their similarities in molecular weight, pKa and no clinical relevance was considered. Beta blockers acquire a positive charge at neutral pH and below; and therefore, were delivered from the anode (anodal delivery). Further, at the pH used for the study, all the drugs remain at least 99% ionized.

The passive transport of beta blockers across dermatomed human skin increased with an increase in the log P values. However, fluxes observed were lowest with PD as compared with the usage of transdermal enhancement strategies (MN, ITP or ITP+MN). This is probably due to higher skin partitioning observed with more lipophilic analogues.³⁷⁻⁴⁰ PD demonstrated higher lag times and low skin retention levels as compared to enhancement strategies (MN or ITP) used alone or in combination (ITP+MN).

Anodal ITP was very effective in delivering drugs across the skin resulting in a 13-fold increase in flux for propranolol (lipophilic drug) and the highest increase in flux for sotalol (hydrophilic drug) was 99-fold higher as compared to respective PD. Since anodal ITP was used, both electro-repulsion and electro-osmosis contribute to the enhanced permeation.⁴¹ During the application of electric current (ITP phase), the flux increase was 10 to 100 fold higher for different drugs. When the current was terminated (post ITP phase) flux values were still 5 to 10 fold greater than PD because of the depot formation in the skin. The depot along with drug from the donor cell contributed to higher post ITP flux as compared to corresponding PD. The ITP flux is inversely related to the lipophilicity of the drug; as the lipophilicity decreased, there was an increase in the flux up to 100 fold. Atenolol and sotalol demonstrated similar flux values owing to their hydrophilic nature. There was also a reduction in the lag time with decrease in the lipophilicity of the drug. In order to understand the mechanism of permeation enhancement, in a separate set of experiments, the skin retention of drugs was determined at 6 h. As can be seen from the data in Table 4.3C, the skin levels were several-fold higher for each drug and the retention is inversely proportional to the log P of the drug. This means that the drug is not bound to the skin and therefore, is readily permeated.

Pretreatment with MN also resulted in increased flux and decreased lag time for all drugs as compared to their respective PD. This is due to creation of micropores for the drug transport across the skin.⁴² However, the magnitude of increase is significantly smaller ($P < 0.001$) as compared to ITP for respective drugs and this observation is consistent with earlier observations^{27,31}. The enhancement ratios with MN increased with decrease in the lipophilicity of the drug (Table 4.4). Typically, drug transport through the microporated skin occurs through micropores as well as the intact stratum corneum. Lipophilic molecules, such as propranolol,

predominantly permeate through the intact stratum corneum as compared to micropores.⁴³ Depending on the lipophilicity, the extent of partitioning into stratum corneum and thus transdermal flux varies. Transappendageal pathway may not contribute significantly to the permeation.⁴¹ A lipophilic molecule, such as propranolol has significant passive permeation and this forms the primary pathway for drug transport. The contribution of microchannels may not be significant in enhancing the drug transport. Furthermore, the area of skin that is disrupted by MN is typically less than 1% and most of the stratum corneum still remains intact.⁴⁴ The passive component therefore effectively contributes in reducing the enhancement ratios of lipophilic drugs. For the hydrophilic drugs, creation of microchannels facilitates increased drug permeation because they provide aqueous pathways of reduced resistance and no partitioning (which is the rate-limiting step for hydrophilic drugs) is required in the disrupted areas over the stratum corneum.^{45,46} For hydrophilic molecules, the enhancement ratios are high because the passive diffusion component is generally low.

MN mediated iontophoretic flux (ITP+MN) during the current application period was significantly higher than ITP alone ($P < 0.001$) for all the drugs except propranolol. Propranolol did not show a significant increase with ITP+MN as compared to ITP alone ($P > 0.05$). Hydrophilic drugs predominantly use aqueous channels (micropores) and appendages for transport across the skin. Under the influence of externally applied electric current across the microporated skin, for hydrophilic molecules, the transport across the micropores increase several folds. However, the same pathways (microchannels) are less significant for the transport of lipophilic molecules and upon application of electric current; there will be only a marginal if any increase in the drug transport. Thus, the present study demonstrates that the combination of ITP+MN may be more useful for hydrophilic compounds. This strategy could be beneficial for

peptides and proteins as many of these are hydrophilic in nature. The larger molecular weight is a limitation for their transport using ITP and microporation can successfully overcome this limitation by creation of additional large aqueous pathways. When ITP is applied across the microporated skin, the hydrophilic molecules are pushed along the aqueous channels resulting in increased drug transport. Electroosmosis associated with anodal ITP might further contribute to the enhanced delivery.⁴⁷

The enhancement for lipophilic molecules is not obvious because they tend to permeate well across the intact stratum corneum. The higher flux for propranolol by PD (compared to other drugs in this study) provides this drug a lower enhancement ratio. The loss of permselectivity appears to play a negligible role in the transdermal transport of beta blockers because MN treatment affects only a small surface area (~1.0%) of the skin surface. Hence breaching of the skin with MN should significantly retain the properties of the intact stratum corneum. Another important consequence of MN pretreatment is the decrease in skin resistance.⁴⁸⁻⁵⁰ This push on charged ionic species across the disrupted stratum corneum with reduced skin resistance also might contribute to enhanced transdermal permeation. Even with the combination strategy, the skin retention is higher with more lipophilic drugs as compared to hydrophilic analogues. The lower skin levels explain the low post iontophoretic fluxes for atenolol and sotalol.

4.6 CONCLUSIONS

The limitations associated with passive transdermal delivery can be overcome by using enhancement strategies and combination of such techniques is becoming increasingly important. The combination of ITP and MN was very effective particularly for hydrophilic molecules as

compared to the lipophilic ones. As the lipophilicity of the molecules increases, the combination strategy becomes less effective and microporation may play a negligible role in enhancing the iontophoretic transdermal delivery.

4.7 ACKNOWLEDGEMENT

The authors acknowledge the financial support provided by NSF award, 1137682. We thank Professor Jack DeRuiter for his help with the physicochemical data and selection of various beta blockers for this study.

4.8 REFERENCES

1. Prausnitz MR, Langer R. 2008. Transdermal drug delivery. *Nat Biotechnol* 26:1261-1268.
2. Brown MB, Traynor MJ, Martin GP, Akomeah FK. 2008. Transdermal drug delivery systems: skin perturbation devices. *Methods Mol Biol* 437:119-139.
3. Guy RH. 2010. Transdermal drug delivery. *Handb Exp Pharmacol* 197:399-410.
4. Herwadkar A, Banga AK. 2012. An update on the application of physical technologies to enhance intradermal and transdermal drug delivery. *Ther Deliv* 3:339-355.
5. Paudel KS, Milewski M, Swadley CL, Brogden NK, Ghosh P, Stinchcomb AL. 2010. Challenges and opportunities in dermal/transdermal delivery. *Ther Deliv* 1:109-131.
6. Karande P, Jain A, Ergun K, Kispersky V, Mitragotri S. 2005. Design principles of chemical penetration enhancers for transdermal drug delivery. *Proc Natl Acad Sci U S A* 102:4688-4693.

7. Kasha PC, Banga AK. 2008. A review of patent literature for iontophoretic delivery and devices. *Recent Pat Drug Deliv Formul* 2:41-50.
8. van der Maaden K, Jiskoot W, Bouwstra J. 2012. Microneedle technologies for (trans)dermal drug and vaccine delivery. *J Control Release*. 161:645-655.
9. Kalia YN, Naik A, Garrison J, Guy RH. 2004. Iontophoretic drug delivery. *Adv Drug Deliv Rev* 56:619-658.
10. Essa EA, Bonner MC, Barry BW. 2002. Human skin sandwich for assessing shunt route penetration during passive and iontophoretic drug and liposome delivery. *J Pharm Pharmacol* 54:1481-1490.
11. Wang Y, Fan Q, Song Y, Michniak B. 2003. Effects of fatty acids and iontophoresis on the delivery of midodrine hydrochloride and the structure of human skin. *Pharm Res* 20:1612-1618.
12. Kalaria DR, Patel P, Patravale V, Kalia YN. 2012. Comparison of the cutaneous iontophoretic delivery of rasagiline and selegiline across porcine and human skin *in vitro*. *Int J Pharm* 438:202-208.
13. Singh ND, Banga AK. 2013. Controlled delivery of ropinirole hydrochloride through skin using modulated iontophoresis and microneedles. *J Drug Target* Epub ahead of print.
14. Kim YC, Park JH, Prausnitz MR. 2012. Microneedles for drug and vaccine delivery. *Adv Drug Deliv Rev* 64:1547-1568.
15. Lee JW, Park JH, Prausnitz MR. 2008. Dissolving microneedles for transdermal drug delivery. *Biomaterials* 29:2113-2124.
16. Goebel AS, Neubert RH, Wohlrab J. 2011. Dermal targeting of tacrolimus using colloidal carrier systems. *Int J Pharm* 404:159-168.

17. McAllister DV, Wang PM, Davis SP, Park JH, Canatella PJ, Allen MG, Prausnitz MR. 2003. Microfabricated needles for transdermal delivery of macromolecules and nanoparticles: fabrication methods and transport studies. *Proc Natl Acad Sci U S A* 100:13755-13760.
18. Migalska K, Morrow DI, Garland MJ, Thakur R, Woolfson AD, Donnelly RF. 2011. Laser-engineered dissolving microneedle arrays for transdermal macromolecular drug delivery. *Pharm Res* 28:1919-1930.
19. Prow TW, Grice JE, Lin LL, Faye R, Butler M, Becker W, Wurm EM, Yoong C, Robertson TA, Soyer HP, Roberts MS. 2011. Nanoparticles and microparticles for skin drug delivery. *Adv Drug Deliv Rev* 63:470-491.
20. Coulman SA, Anstey A, Gateley C, Morrissey A, McLoughlin P, Allender C, Birchall JC. 2009. Microneedle mediated delivery of nanoparticles into human skin. *Int J Pharm* 366:190-200.
21. Sivamani RK, Liepmann D, Maibach HI. 2007. Microneedles and transdermal applications. *Expert Opin Drug Deliv* 4:19-25.
22. Fukushima K, Ise A, Morita H, Hasegawa R, Ito Y, Sugioka N, Takada K. 2011. Two-layered dissolving microneedles for percutaneous delivery of peptide/protein drugs in rats. *Pharm Res* 28:7-21.
23. Burton SA, Ng CY, Simmers R, Moeckly C, Brandwein D, Gilbert T, Johnson N, Brown K, Alston T, Prochnow G, Siebenaler K, Hansen K. 2011. Rapid intradermal delivery of liquid formulations using a hollow microstructured array. *Pharm Res* 28:31-40.
24. Jayachandra Babu R, Ravis WR, Duran SH, Schumacher J, Cox E, Stahl R, Jones K, Jean Lin YJ, Phillip Lee YH, Parsons DL, Portman EM, Brown SC. 2009. Enhancement of

- transdermal delivery of phenylbutazone from liposomal gel formulations through deer skin. *J Vet Pharmacol Ther* 32:388-392.
25. Nolan LM, Corish J, Corrigan OI, Fitzpatrick D. 2007. Combined effects of iontophoretic and chemical enhancement on drug delivery. II. Transport across human and murine skin. *Int J Pharm* 341:114-124.
 26. Karande P, Mitragotri S. 2009. Enhancement of transdermal drug delivery via synergistic action of chemicals. *Biochim Biophys Acta* 1788:2362-2373.
 27. Kolli CS, Xiao J, Parsons DL, Babu RJ. 2012. Microneedle assisted iontophoretic transdermal delivery of prochlorperazine edisylate. *Drug Dev Ind Pharm* 38:571-576.
 28. Kumar V, Banga AK. 2012. Modulated iontophoretic delivery of small and large molecules through microchannels. *Int J Pharm* 434:106-114.
 29. Garland MJ, Caffarel-Salvador E, Migalska K, Woolfson AD, Donnelly RF. 2012. Dissolving polymeric microneedle arrays for electrically assisted transdermal drug delivery. *J Control Release*. 159:52-59.
 30. Katikaneni S, Badkar A, Nema S, Banga AK. 2009. Molecular charge mediated transport of a 13 kD protein across microporated skin. *Int J Pharm* 378:93-100.
 31. Chen H, Zhu H, Zheng J, Mou D, Wan J, Zhang J, Shi T, Zhao Y, Xu H, Yang X. 2009. Iontophoresis-driven penetration of nanovesicles through microneedle-induced skin microchannels for enhancing transdermal delivery of insulin. *J Control Release*. 139:63-72.
 32. Pikal MJ. 2001. The role of electroosmotic flow in transdermal iontophoresis. *Adv Drug Deliv Rev* 46:281-305.

33. Hirvonen J, Guy RH. 1998. Transdermal iontophoresis: modulation of electroosmosis by polypeptide. *J Control Release*. 50:283-289.
34. Sieg A, Guy RH, Delgado-Charro MB. 2004. Electroosmosis in transdermal iontophoresis: implications for noninvasive and calibration-free glucose monitoring. *Biophys J* 87:3344-3350.
35. Morrow DIJ, McCarron PA, Woolfson AD, Donnelly RF. 2007. Innovative Strategies for Enhancing Topical and Transdermal Drug Delivery. *The Open Drug Delivery Journal* 1:36-59.
36. Modamio P, Lastra CF, Montejo O, Marifio EL. 1996. Development and validation of liquid chromatography methods for the quantitation of propranolol, metoprolol, atenolol and bisoprolol: application in solution stability studies. *Int J Pharm* 130:137-140.
37. Abla MJ, Banga AK. 2013. Quantification of skin penetration of antioxidants of varying lipophilicity. *Int J Cosmet Sci* 35:19-26.
38. Cross SE, Magnusson BM, Winckle G, Anissimov Y, Roberts MS. 2003. Determination of the effect of lipophilicity on the *in vitro* permeability and tissue reservoir characteristics of topically applied solutes in human skin layers. *J Invest Dermatol* 120:759-764.
39. Mills PC, Magnusson BM, Cross SE. 2003. Effect of solute lipophilicity on penetration through canine skin. *Aust Vet J* 81:752-755.
40. Yagi S, Nakayama K, Kurosaki Y, Higaki K, Kimura T. 1998. Factors determining drug residence in skin during transdermal absorption: studies on beta-blocking agents. *Biol Pharm Bull* 21:1195-1201.

41. Banga AK. 2006. Therapeutic Peptides and Proteins: Formulation, Processing, and Delivery Systems. In Banga AK, editor Transdermal and topical delivery of therapeutic peptides, 2nd ed., Boca Raton: CRC Press. p 259-290.
42. Banks SL, Pinninti RR, Gill HS, Paudel KS, Crooks PA, Brogden NK, Prausnitz MR, Stinchcomb AL. 2010. Transdermal delivery of naltrexol and skin permeability lifetime after microneedle treatment in hairless guinea pigs. *J Pharm Sci* 99:3072-3080.
43. Wagner H, Kostka KH, Lehr CM, Schaefer UF. 2002. Correlation between stratum corneum/water-partition coefficient and amounts of flufenamic acid penetrated into the stratum corneum. *J Pharm Sci* 91:1915-1921.
44. Kalluri H, Kolli CS, Banga AK. 2011. Characterization of microchannels created by metal microneedles: formation and closure. *AAPS J* 13:473-481.
45. Trommer H, Neubert RH. 2006. Overcoming the stratum corneum: the modulation of skin penetration. A review. *Skin Pharmacol Physiol* 19:106-121.
46. Sachdeva V, Banga AK. 2011. Microneedles and their applications. *Recent Pat Drug Deliv Formul* 5:95-132.
47. Marro D, Kalia YN, Delgado-Charro MB, Guy RH. 2001. Contributions of electromigration and electroosmosis to iontophoretic drug delivery. *Pharm Res* 18:1701-1708.
48. Gupta J, Gill HS, Andrews SN, Prausnitz MR. 2011. Kinetics of skin resealing after insertion of microneedles in human subjects. *J Control Release*. 154:148-155.
49. Yamamoto T, Yamamoto Y. 1976. Electrical properties of the epidermal stratum corneum. *Med Biol Eng* 14:151-158.

50. Prausnitz MR. 1996. The effects of electric current applied to skin: A review for transdermal drug delivery. *Adv Drug Deliv Rev* 18:395–425.

Table 4.1 Physicochemical properties and structures of beta blockers

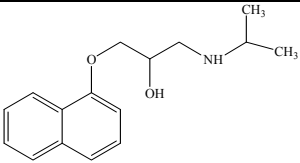
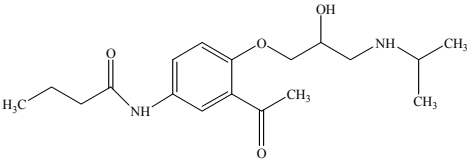
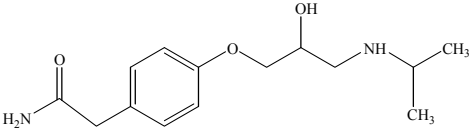
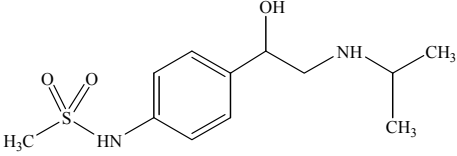
	Molecular weight (free base)	pKa	Log P	Chemical structure
Propranolol	259.35	9.26-9.50	2.58-3.65	
Acebutolol	336.43	9.20-9.40	1.43-1.87	
Atenolol	266.00	9.37-9.63	0.23-0.57	
Sotalol	272.36	9.80 (amine, 8.30 (sulfonamide))	-0.41-0.85	

Table 4.2 Chromatographic conditions for beta blocker analysis

Beta blocker	Mobile phase A (%)*	Mobile phase B (%)**	Detection wavelength (nm)	Retention time (min)
Propranolol	70	30	225	9.5
Acebutolol	80	20	220	7.5
Atenolol	90	10	225	4.7
Sotalol	90	10	230	7.0

*15mM KH_2PO_4 +1.2% triethylamine + H_3PO_4 (to adjust pH to 3.0)

** Acetonitrile

Table 4.3 Steady state fluxes, lag times and skin retention data of various beta blockers

A) Flux

Drug	Flux ($\mu\text{g}/\text{cm}^2/\text{h}$)							
	PD		MN		ITP		ITP+MN	
	0-26 h		0-26 h		0-6 h	6-26 h	0-6 h	6-26 h
Propranolol	5.18 \pm 0.25		31.73 \pm 0.95		66.11 \pm	23.73 \pm	63.67 \pm	34.42 \pm
					5.94***	2.88**	5.13***	3.12**
Acebutolol	2.60 \pm 0.12		16.89 \pm 0.35		171.40 \pm	12.73 \pm	191.40 \pm	24.30 \pm
					11.17***	4.64**	8.75***	5.75**
Atenolol	1.38 \pm 0.13		13.82 \pm 0.63		138.00 \pm	12.06 \pm	169.00 \pm	26.36 \pm
					9.36***	3.43**	7.64***	3.77**
Sotalol	1.33 \pm 0.35		14.16 \pm 1.71		131.20 \pm	12.89 \pm	189.50 \pm	16.89 \pm
					8.40***	3.38**	6.77***	2.25**

P < 0.01; *P < 0.001 versus MN and PD of respective drugs

B) Lag time

Drug	Lag time, h			
	PD	MN	ITP	ITP+MN
Propranolol	4.00	1.94	1.50	1.50
Acebutolol	4.00	1.50	0.50	0.50
Atenolol	8.00	1.00	0.50	0.30
Sotalol	10.00	1.00	0.50	0.30

C) Skin retention levels

Drug	PD (mg of drug /g of skin)	MN (mg of drug /g of skin)	ITP		ITP+MN	
			(mg of drug /g of skin)		(mg of drug /g of skin)	
			6 h	26 h	6 h	26 h
Propranolol	1.67 ± 0.22	1.74 ± 0.10	20.87 ±	4.24 ±	28.82 ±	5.41 ±
			3.71***	1.43**	2.16***	0.43**
Acebutolol	0.67 ± 0.20	1.25 ± 0.30	19.79 ±	2.18 ±	26.77 ±	2.00 ±
			0.88***	0.74**	2.93***	0.30**
Atenolol	0.26 ± 0.05	0.38 ± 0.03	17.34 ±	2.85 ±	20.55 ±	3.50 ±
			2.59***	0.03**	3.71***	0.44**
Sotalol	0.28 ± 0.06	0.22 ± 0.07	9.99 ±	2.42 ±	12.60 ±	2.55 ±
			3.23***	0.44**	1.63***	0.04**

P < 0.01; *P < 0.001 versus MN and PD of respective drugs

Table 4.4 Enhancement ratios calculated from the flux data of different beta blocker drugs

Drug	MN	0-6 h		6-26 h		Total flux	
		ITP	ITP+MN	ITP	ITP+MN	ITP	ITP+MN
Propranolol	6.13 ±	12.76 ±	12.29 ±	4.58 ±	6.64 ±	8.67 ±	9.47 ±
	0.18	1.15	0.99	0.56	0.60**	0.58	0.54
Acebutolol	6.50 ±	65.92 ±	73.62 ±	4.90 ±	9.35 ±	35.41 ±	41.48 ±
	0.13	4.29	3.37**	1.79	2.21**	8.86	2.52
Atenolol	10.01 ±	100.00±	122.46 ±	8.74 ±	19.10±	54.37 ±	70.78 ±
	0.45	6.78	5.54**	2.49	2.73**	9.57	6.66**
Sotalol	10.64 ±	98.65 ±	142.48 ±	9.69 ±	12.70 ±	54.17 ±	77.59 ±
	1.28	6.32	5.09***	2.54	1.69***	8.83	6.55**

P < 0.01; *P < 0.001 versus ITP of respective drugs

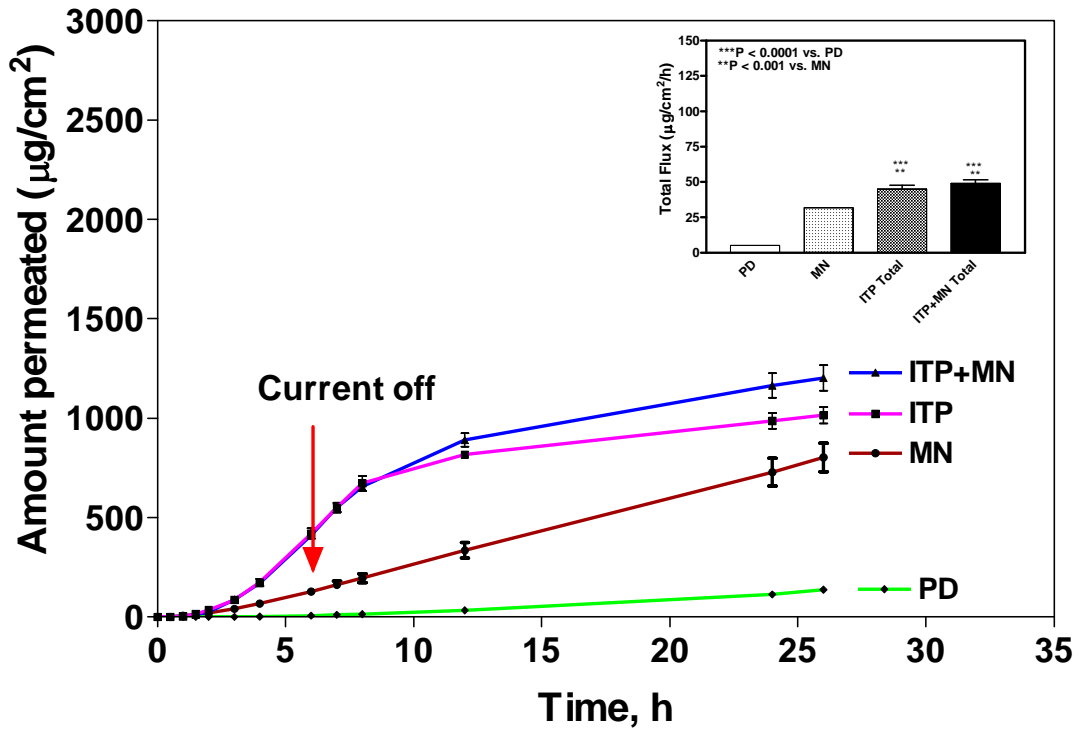


Figure 4.1 Permeation of propranolol HCl across dermatomed human skin

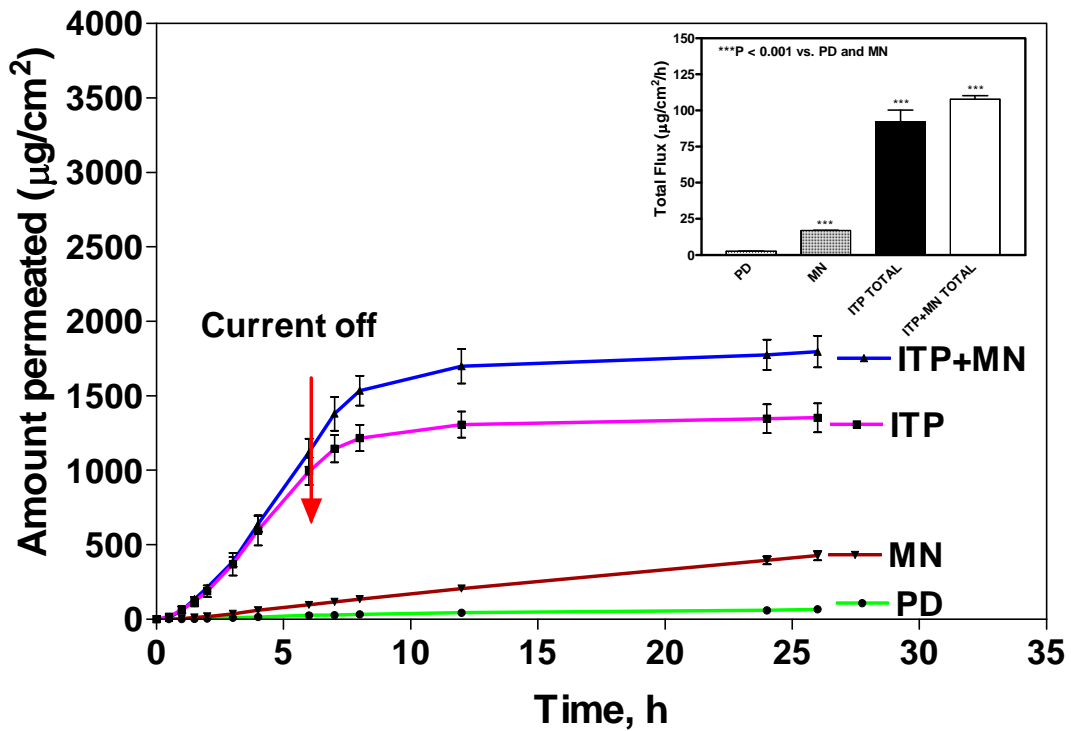


Figure 4.2 Permeation of acebutolol HCl across dermatomed human skin

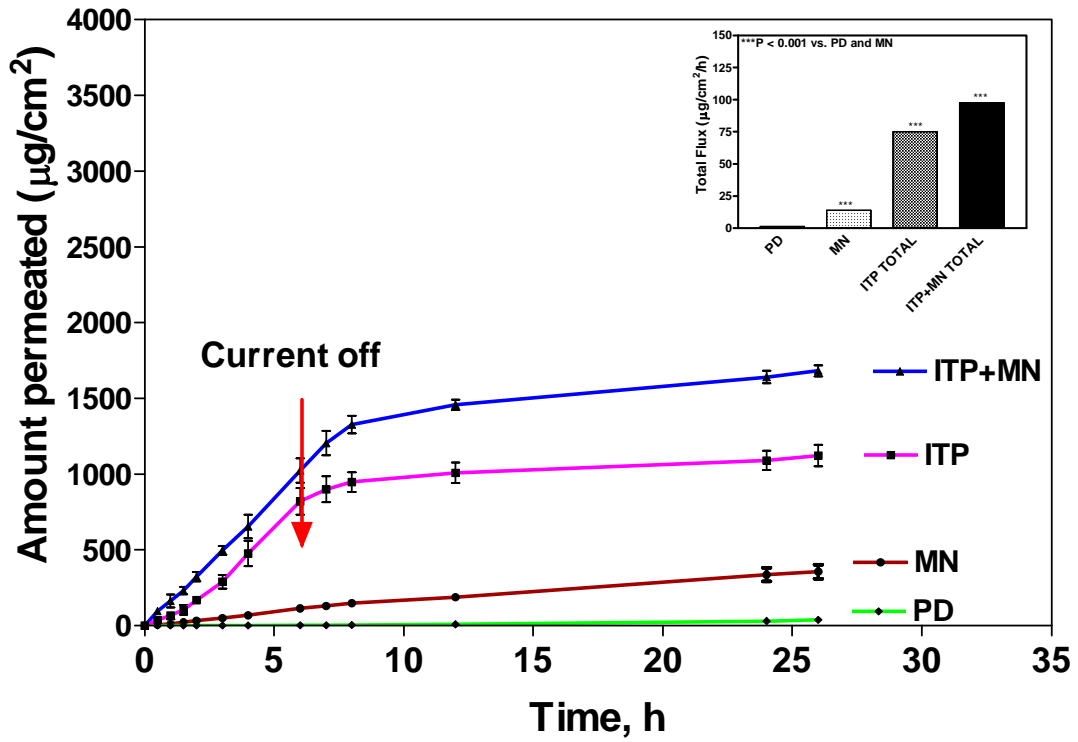


Figure 4.3 Permeation of atenolol HCl across dermatomed human skin

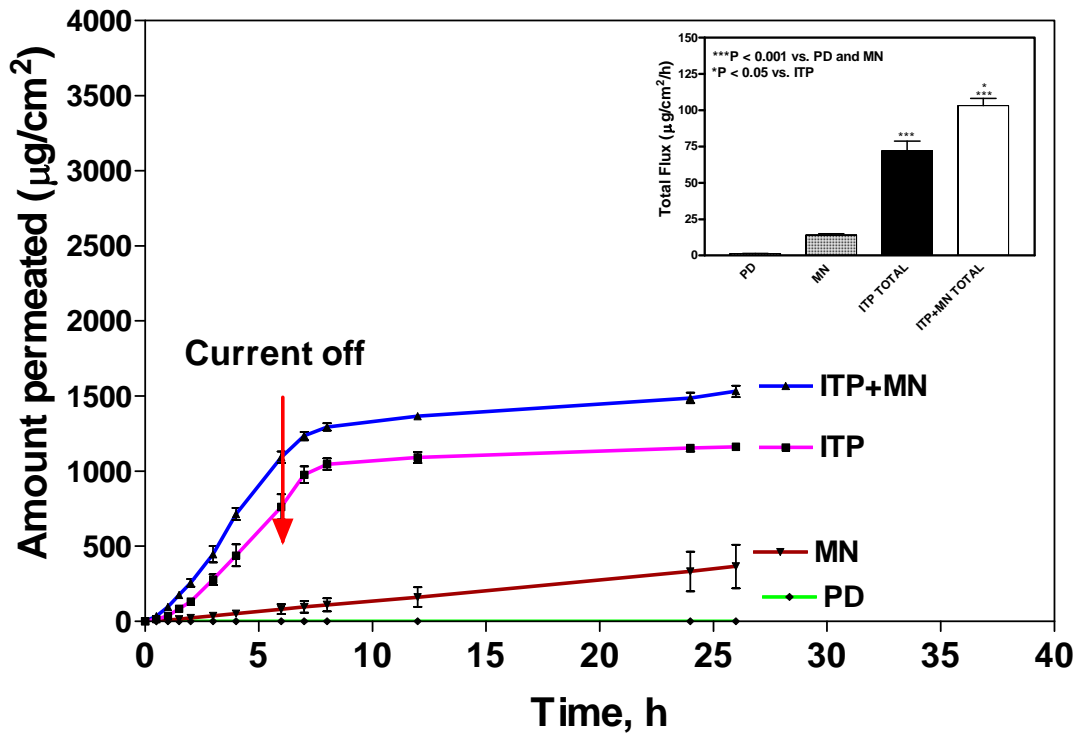


Figure 4.4 Permeation of sotalol HCl across dermatomed human skin

5. STABILITY-INDICATING HPLC ASSAY FOR LYSINE-PROLINE-VALINE (KPV) IN AQUEOUS SOLUTIONS

5.1 ABSTRACT

A simple, sensitive and stability-indicating high performance liquid chromatographic (HPLC) assay method was developed and validated for a bioactive peptide, Lysine-Proline-Valine (KPV) in topical formulations. Chromatographic separation was achieved on a reversed phase Phenomenex C18 column (4.6 mm x 250 mm, packed with 5 μm silica particles) with a gradient mobile phase consisting of 0.1% TFA in water (A) and 0.1% TFA in acetonitrile (B). The proposed HPLC method was validated with respect to accuracy, precision, linearity, repeatability, limit of detection (LOD) and limit of quantitation (LOQ). Calibration curve was linear with a correlation coefficient (r) 0.9999. Relative standard deviation values of accuracy and precision experiments were < 2 . The LOD and LOQ of KPV were 0.01 and 0.25 $\mu\text{g/mL}$, respectively. Under stress conditions (acid, alkali and hydrogen peroxide) KPV yielded Lys-Pro Diketopiperazine as major degradation product which was identified by LC/MS analysis. The developed HPLC method was found to be efficient in separating the active peptide from its degradation products generated under various stress conditions. Also, the validated method was able to separate KPV from other peaks arising from endogenous components of the skin homogenate.

5.2 INTRODUCTION

The anti-inflammatory activity of alpha melanocyte stimulating hormone (α -MSH) is reported to be mediated by its three-amino acid terminal fragment, Lysine-Proline-Valine (KPV).¹ Although KPV lacks the entire sequence motif required for binding to melanocortin receptors (MC-Rs), it still retains almost all of the anti-inflammatory ability of the parent hormone. The advantage of KPV over α -MSH is that it is devoid of the melanotropic effect of α -MSH and thus does not have any effect on the pigment cells.² Moreover, KPV is smaller and chemically more stable as compared to α -MSH.³ These properties make KPV a suitable candidate as an anti-inflammatory agent in topical formulations for the treatment of skin diseases such as psoriasis and contact dermatitis.

A stability-indicating HPLC assay method should be devised for an active chemical substance prior to the formulation development. The analytical method should be able to resolve the degradation products from the active compound. Furthermore, the method needs to be highly selective and specific in order to avoid interferences from endogenous skin components and quantify KPV unambiguously in skin permeation samples. In the current study, we have developed a simple and rapid stability-indicating HPLC assay method for the determination of KPV in a topical formulation. The validated method was applied to determine KPV content in skin homogenate samples and the results have been summarized.

5.3 MATERIALS AND METHODS

5.3.1. MATERIALS

KPV was custom synthesized by Peptides International (Louisville, KY, USA). (HPLC grade), Trifluoroacetic acid (HPLC grade), Hydrochloric acid (12 N) and Sodium hydroxide

pellets (ACS grade) were purchased from VWR International (Suwannee, GA, USA). Hydrogen peroxide (35 wt. % solution in water, stabilized) was purchased from Acros Organics (Fair Lawn, NJ, USA). Valine and proline were obtained from Sigma Aldrich Co (St. Louis, MO). Dermatomed human skin (thickness ~ 0.35 mm) was obtained from Allosource (Cincinnati, OH, USA).

5.3.2 STANDARD AND SAMPLE PREPARATION

All the standard and sample solutions of KPV (aqueous solutions, 100 µg/mL) were prepared and used for the method development and validation procedures. For the skin homogenate sample preparation, the dermatomed human skin (frozen at -80°C, Allosource, Cincinnati, OH, USA) was thawed at ambient temperature for about 30 min. The skin was cut with a biopsy punch (0.64 cm² area), minced with a surgical blade and collected in a glass vial. KPV solutions (1 ml, 100 µg/mL) in Tris buffer, pH 7.0 were added to vials, sonicated for 15 min and incubated overnight at 37°C. After 24 h, the samples were sonicated again for 30 min and filtered through a 0.22 µm membrane filter for analysis by HPLC.

5.3.3 SAMPLE PREPARATION AND VALIDATION OF THE EXTRACTION PROCEDURE

To determine the recovery of KPV from the skin extracts, the skin samples which were not previously in contact with KPV were used. Six skin samples (0.64 cm², representing the active diffusion area) were cut with a biopsy punch. The skin was then minced and collected in individual glass vials. KPV in Tris buffer, pH 7.0 (100 µg/mL) was added to each vial in order to determine the extraction efficiency and KPV retention in the skin. The samples were sonicated for 15 minutes and allowed to equilibrate for 24 h. The samples were again sonicated for 30 minutes and filtered through a 0.22 µm nylon filter and analyzed by HPLC. The KPV recovery

(%) from skin was calculated as the ratio of the amount of KPV extracted from the spiked skin to the amount of KPV extracted from the solution in the absence of skin but processed by the same procedure.

5.3.4. INSTRUMENTATION AND HPLC METHOD DEVELOPMENT

The analysis was performed using an HPLC system (Waters Corp., MA, USA) equipped with an autosampler (model 717 plus), a pump (model 1525) and a PDA detector (model 2998). The system was interfaced to a workstation operated by Empower 2 software. HPLC analysis was performed at room temperature using a reversed-phase C₁₈ column of dimensions 4.6 mm x 250 mm, packed with 5 µm silica particles (Phenomenex, Torrance, CA, USA).

The optimized gradient method consists of 0.1% TFA in water (mobile phase A) and 0.1% TFA in ACN (mobile phase B). The mobile phases were filtered using a 0.22 µm Nylon filter and degassed using sonication prior to use. The chromatographic separation was achieved using a linear gradient from 1% to 30% mobile phase B in 15 min, after which the gradient was reversed to 1% in the following 5 min and equilibrated for 10 min resulting a total run time of 30 min. The flow rate was 1 mL/min and the injection volume was 50 µL. The PDA detector was set at 220 nm for KPV analysis. The proposed method was validated for system suitability and various other parameters such as linearity, accuracy and precision, specificity, and limit of detection and quantification. The system suitability parameters tested were capacity factor (K'), injection repeatability, tailing factor (T), resolution (Rs) and theoretical plate number (N). For linearity, a series of standard aqueous solutions were prepared over a concentration range of 10 – 100 µg/ml of KPV. Linearity of the analytical procedure was evaluated by plotting detector response (peak area) against KPV concentration. Linear regression analysis was applied to calculate the slope, intercept and linear correlation coefficient (*r*). To determine the accuracy,

recovery studies were performed by the standard addition method. Previously analyzed samples of KPV (10 µg/ml) were spiked with additional 50, 100, and 150% KPV standard solutions and the mixtures were analyzed by the proposed method. Recovery (%) and relative standard deviation (RSD) were calculated for each concentration. Precision of the method was determined by repeatability (intraday precision) and intermediate precision (interday precision) of KPV solutions of three different concentrations (10, 40 and 80 µg/ml). In order to estimate the limit of detection (LOD) and limit of quantitation (LOQ) values, the blank sample was injected six times and the peak area of this blank was calculated as noise level. The LOD was calculated as three times the noise level while ten times the noise value gave the LOQ. The validated HPLC method was utilized to analyze KPV content in skin homogenate.

5.3.5. FORCED DEGRADATION STUDIES

Forced degradation studies of KPV in the aqueous solution were conducted under various stress conditions such as acid, alkaline, and oxidative degradation at 70°C. The 0 h sample served as control. Recoveries of KPV in all the reaction solutions were calculated against known concentration of standard KPV solution.

5.3.5.1. Acid hydrolysis

0.5 mL of KPV solution in water (750 µg) was treated with 0.5 mL of 1 N HCl at 70°C for 0, 3, 6, 9 and 24h. Each reaction was terminated by adding 0.5 mL of 1 N NaOH and analyzed by HPLC.

5.3.5.2. Alkaline hydrolysis

0.5 mL of KPV solution in water (750 µg) was treated with 0.5 mL of 1 N NaOH at 70°C for 0, 3, 6, 9 and 24h. Each reaction was terminated by adding 0.5 mL of 1 N HCl and analyzed by HPLC.

5.3.5.3. Oxidative degradation

KPV solution in water (0.5 mL, 750 µg) was treated with hydrogen peroxide (0.5%, v/v) at 70°C for 0, 2, 5, 15, 30, 45 min. The samples were allowed to cool to room temperature and then analyzed by HPLC.

5.3.5.4. LC/MS analysis of KPV and Lys-Pro-Diketopiperazine (DKP)

KPV peptide and its degradation samples were analyzed using an Ultra Performance LC Systems (ACQUITY UPLC, Waters Corp., Milford, MA, USA) coupled with a Quadrupole Time-of-Flight mass spectrometer (Q-TOF Premier) with electrospray ionization (ESI) in ESI⁺-MS mode operated by the MassLynx software (V4.1). Each sample, in water, was injected onto a C₁₈ column (ACQUITY UPLC® BEH C₁₈, 1.7 µm, 2.1 x 50 mm, Waters) with a 150 µL/min flow rate of mobile phase of solution A (95% H₂O, 5% ACN, 0.1% formic acid) and solution B (95% ACN, 5% H₂O, 0.1% formic acid) in a 10 min gradient starting at 95% A to 5% A in 6 min and back to 95% in 8 min. The ion source voltages were set at 3 KV, sampling cone at 37 V and the extraction cone at 3 V. In both modes the source and desolvation temperature were maintained at 120°C and 225°C, respectively, with the desolvation gas flow at 200 L/h. The TOF MS scan was from 200 to 800 *m/z* at 1 s with 0.1 s inter-scan delay using extended dynamic range acquisition with centroid data format. For real time mass calibration, direct infusion of sodium formate solution (10% formic acid/0.1M NaOH/isopropanol at a ratio of 1:1:8) at 1

sec/10 sec to ion source at 1 μ L/min was used. The instrument was calibrated at the time of data acquisition in addition to real time calibration by the lockmass. Mass accuracy at 5 ppm or less was the key for assuring the presence of target molecules. Ion source parameters such as the source temperature (gas and sample cone), mobile phase flow rate, and cone voltage were fixed throughout the study. Ions of interest were analyzed for mass accuracy, elemental composition (using accurate mass measurement of less than 5 ppm error) and isotope modeling to identify the formula.

5.4 RESULTS

5.4.1 DEVELOPMENT OF HPLC METHOD

An isocratic method containing water and ACN resulted in peak fronting, peak broadening, and baseline stabilization issues. Thus a gradient method containing TFA in both mobile phases was applied to resolve these issues. The percentage of TFA was increased from 0.05% to 0.1% to obtain better peak shape. Gradient mobile phase consisting 0.1% TFA (pH 2.0) improved the peak resolution and baseline noise. The method was further optimized by varying the mobile phase gradient (from 1 to 30% to 1 to 59% of mobile phase B in 40 min), column temperature (30, 40 and 50°C), flow rate (1 mL/min and 1.2 mL/min) and/or injection volume (100, 50, 20 μ l). The optimized method uses 1 to 30% mobile phase B in 15 min. followed by reversal to 1% in 5 min and equilibration for 10 min resulting a total run time of 30 min. A typical HPLC chromatogram of KPV is shown in Fig. 5.1.

5.4.2 VALIDATION OF ANALYTICAL METHOD

5.4.2.1. System suitability

System suitability test parameters were monitored to make sure system is working correctly during the analysis. The method performance data including capacity factor (K'), injection repeatability, USP tailing factor (T), resolution (R_s) and USP theoretical plate number (N) are summarized in Table 5.1. All the system suitability parameters were within the acceptable range of recommended analytical guidelines⁴ as shown in Table 5.1.

5.4.2.2. Linearity

The calibration curve constructed from standard aqueous solutions of KPV concentrations ranging from 10-100 $\mu\text{g/mL}$ are shown in Fig. 5.2. The plot is linear with a correlation coefficient (r) of 0.9999 in the concentration range tested.

5.4.2.3. Specificity/Forced degradation study and characterization of degradation product

Prior to forced-degradation study, KPV solution was spiked with its individual and combined constituent amino acids such as proline, valine, lysine, proline-valine and lysine-proline. The chromatographic method clearly resolved these related substances from KPV, again indicating that the specificity/selectivity of the method is achieved (Fig. 5.3). Forced-degradation experiments (acid and alkaline hydrolysis and oxidative degradation by hydrogen peroxide) were carried out on KPV in order to produce possible relevant degradation products and to achieve their chromatographic separation (Fig. 5.4). Under various forced degradation conditions, KPV forms Lys-Pro DKP as one of the major degradation product as shown in Fig. 5.4A, 5.4B and 5.4C. Under basic conditions, KPV produced several non-polar degradation products (DP1, DP2 and DP3) in addition to Lys-Pro DKP (Fig. 4B). When treated with 0.5% hydrogen peroxide, the

reaction was rapid and KPV degraded to Lys-Pro DKP, proline, and valine as shown in Fig. 5.4C.

In order to characterize the major degradation product which was assumed as Lys-Pro DKP, we analyzed the reaction solutions by LC/MS. Loop injections of starting material (KPV) and reaction solutions were subjected to LC/MS analysis as described under experimental section. High resolution MS spectra of KPV showed ion at m/z 384.26 [M+H] corresponding to molecular formula of $C_{18}H_{34}N_5O_4$. The reaction solutions of KPV in hydrogen peroxide were quenched at different time intervals (0, 2, 5, 15, 30 and 45 min) and analyzed by LC/MS. The intense protonated ion at m/z 268.18 (+1) corresponding to the molecular formula $C_{13}H_{22}N_3O_3$ in mass spectra indicated that major degradation product was Lys-Pro DKP and the results are shown in Fig. 5.5. The mass spectra also has shown an ion at m/z 286.12 (+1) that differs in 18 mass units compared to Lys-Pro DKP with a molecular formula of $C_{13}H_{24}N_3O_4$ indicating the formation of linear dipeptide, Lys-Pro. The relative abundance ratio of Lys-Pro DKP and the linear dipeptide, Lys-Pro was 10:1. In addition, the MS spectra also exhibited low abundance ions corresponding to valine. LC/MS analysis of reaction solutions at different time intervals also revealed that the cyclized product Lys-Pro DKP to be decreasing with the increase in the reaction time.

5.4.2.4. Accuracy

To determine the accuracy, recovery studies were performed by the standard addition method. Samples of KPV (10 $\mu\text{g/mL}$) analyzed earlier were spiked with an additional 50, 100 and 150% of KPV standard solutions and analyzed using the proposed method. The experiments were performed in triplicate. The percent recovery values of KPV were in the range of 95.28 to

98.39 and the %RSD values were < 2. The details of accuracy experiments data are presented in Table 5.1.

5.4.2.5. Precision

Precision of the method was determined by repeatability (intra-day precision) and intermediate precision (inter-day precision) of KPV solutions of three different concentrations (10, 40 and 80 µg/mL). The average percent assay of each concentration was between 99.3 and 100.2. The %RSD values obtained were < 0.5 as shown in Table 5.1.

5.4.2.6. Limit of detection (LOD) and limit of quantitation (LOQ)

The limit of detection (LOD) and the limit of quantitation (LOQ) values were calculated at three times and ten times the noise level, respectively. The noise level was calculated as the mean peak area of the blank sample injected six times. The LOD and LOQ values of KPV were 0.01 and 0.25 µg/mL, respectively.

5.4.2.7. Application to skin homogenate samples

The method was applied to determine KPV content in the skin homogenate samples. Six skin homogenate samples spiked with 100 µg/mL KPV solution and incubated overnight at 37 °C were analyzed for KPV. The average percent recovery of KPV in the skin homogenates was 92.15 ± 4.0 . The method was again specific to KPV as its peak was clearly separated from the associated skin constituents and other related substances.

5.5 DISCUSSION

KPV is a small peptide with a molecular weight of 383.49 Da. Charged molecules often exhibit poor retention or secondary interactions with the stationary phase, resulting in a poor peak shape and separation.⁵ Thus, in order to improve peak shape and baseline, TFA was added to the mobile phases. Trifluoroacetic acid (TFA) is a commonly used anionic modifier that forms an ion pair with proteins/peptides, neutralizing the charge and resulting in better peak shape and separation.⁶ Additionally, TFA helps in pH control (buffering) and suppression of adverse ionic interactions between proteins/peptides and silanol groups on the column.⁷ Since KPV exhibits a positive charge at neutral pH, the initial chromatographic studies utilized ACN and water as the mobile phase, each containing 0.05% TFA. The developed HPLC method was able to resolve the degradation products from the main peak of KPV with high resolution and excellent peak shape, confirming that the method is stability indicating. The system suitability parameters for the KPV analytical method were within the acceptable range of their recommended values. The chromatograms from stress studies for KPV indicated that Lys-Pro DKP was the major degradation product at high temperatures. This phenomenon was consistent with the previous reports that at high temperatures, proteins/peptides containing lysine and proline as adjacent amino acids form Lys-Pro DKP.^{8,9} Further, KPV was comparatively more stable at acidic pH while it was susceptible to alkaline and oxidizing conditions leading to the formation of non polar compounds. The developed method also successfully separated the drug peak from the endogenous components in the skin homogenate.

5.6 CONCLUSIONS

The analytical method we developed is the first known RP-HPLC method that can accurately determine KPV in aqueous solutions and skin homogenates. The validated method has been demonstrated to be stability-indicating because it can also separate the degradation products of KPV from the parent KPV. In addition, the current method can also separate KPV from the other peaks arising from endogenous components of the skin homogenate. Furthermore, the validated HPLC method has been demonstrated to have good accuracy, precision, sensitivity, specificity, linearity, reproducibility, repeatability, and robustness. Therefore the method described can be applied for routine analysis of KPV in pharmaceutical formulations.

5.7 ACKNOWLEDGEMENT

The authors acknowledge the financial support provided by NSF-RISE grant, 1137682.

5.8 REFERENCES

1. Luger TA, Scholzen TE, Brzoska T, Böhm M. 2003. New insights into the functions of alpha-msh and related peptides in the immune system. *Ann N Y Acad Sci.* 994:133-140.
2. Brzoska T, Böhm M, Lügering A, Loser K, Luger TA. 2010. Terminal signal: Anti-inflammatory effects of alpha-melanocyte-stimulating hormone related peptides beyond the pharmacophore. *Adv Exp Med Biol.* 68:107-116.
3. Barcellini W, Colombo G, La Maestra L, Clerici G, Garofalo L, Brini AT, Lipton JM, Catania A. 2000. Alpha-melanocyte-stimulating hormone peptides inhibit HIV-1 expression in chronically infected promonocytic u1 cells and in acutely infected monocytes. *J Leukoc Biol.* 68(5):693-699.

4. International Conference on Harmonization of Technical Requirements for the Registration of Pharmaceuticals for Human Use (ICH), Guideline Q2(R1)-Validation of Analytical Procedures: Text and Methodology, ICH secretariat, c/c IFPMA, Geneva, 2005, pp. 1-13.
5. Kiel JS, Morgan SL. 1985. Effects of ionic modifiers on peak shape and retention in reversed phase high performance liquid chromatography. *J Chromatogr A.* 320:313-323.
6. Chen Y, Mehok AR, Mant CT, Hodges RS. 2004. Optimum concentration of trifluoroacetic acid for reversed-phase liquid chromatography of peptides revisited. *J Chromatogr A.* 1043(1):9-18.
7. Shibue M, Mant CT, Hodges RS. 2005. Effect of anionic ion-pairing reagent hydrophobicity on selectivity of peptide separations by reversed-phase liquid chromatography. *J Chromatogr A.* 1080(1):68-75.
8. Kikwai L, Babu RJ, Kanikkannan N, Singh M. 2004. Preformulation stability of Spantide II, a promising topical anti-inflammatory agent for the treatment of psoriasis and contact dermatitis. *J Pharm Pharmacol.* 56(1):19-25.
9. Goolcharran C, Borchardt RT. 1998. Kinetics of diketopiperazine formation using model peptides. *J Pharm Sci.* 87(3):283-288.

Table 5.1 HPLC method validation parameters for KPV in aqueous solutions

System Suitability					
	Capacity factor (K')	%RSD (n=6)	Tailing factor (T)	Resolution (Rs)	Theoretical plate number (N)
Specifications ⁴	> 2.0	≤ 1	≤ 2	> 2	> 2000
Experimental results	2.82	0.89	1.31	2.77	27708
Accuracy					
Conc. KPV spiked (µg/mL)	Theoretical concentration (µg/mL)	Experimental concentration (µg/mL) ± SD*		%Recovery	%RSD
0	10	9.84 ± 0.07		98.39	0.72
5	15	14.36 ± 0.17		95.71	1.16
10	20	19.42 ± 0.17		97.08	0.88
15	25	23.82 ± 0.41		95.28	1.71
Precision					
Theoretical concentration (µg/mL)	Intra-day		Inter-day		
	Experimental concentration (µg/mL) ± SD*	%RSD	Experimental concentration (µg/mL) ± SD*	%RSD	
10	9.99 ± 0.01	0.01	9.97 ± 0.04	0.50	
40	40.05 ± 0.01	0.03	39.96 ± 0.13	0.32	
80	80.02 ± 0.01	0.01	79.48 ± 0.11	0.13	

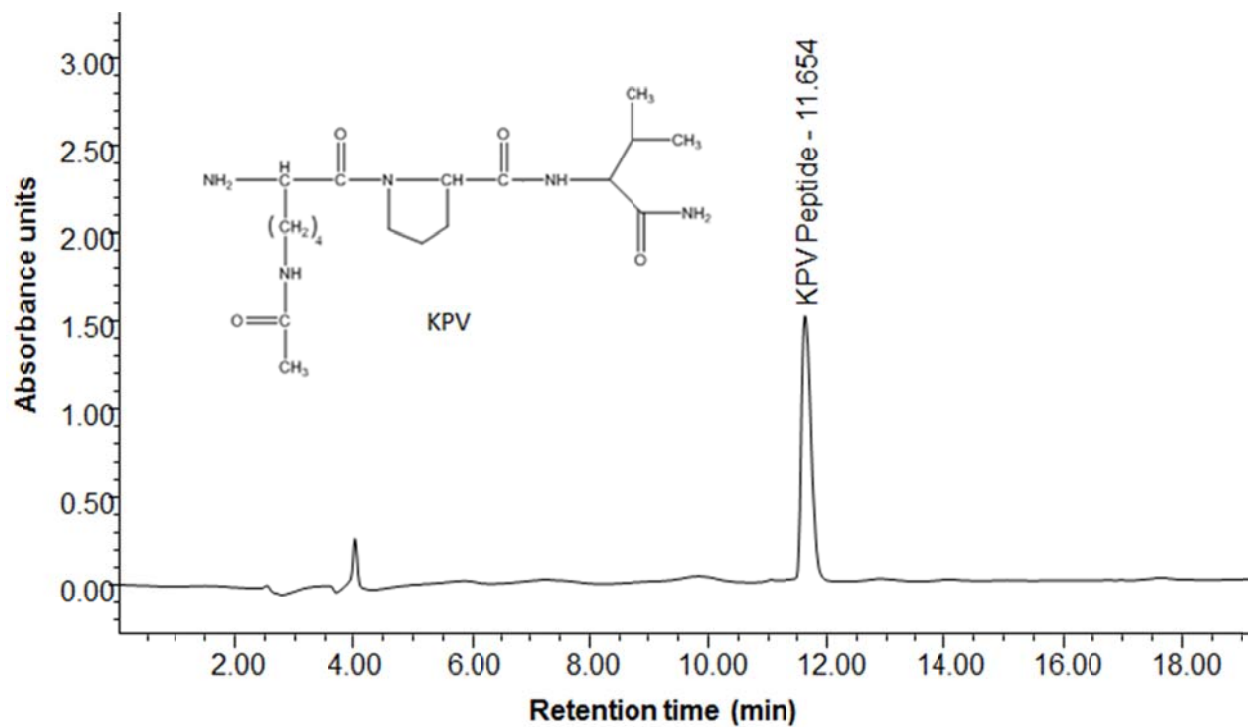


Fig. 5.1 HPLC chromatogram of KPQ peptide

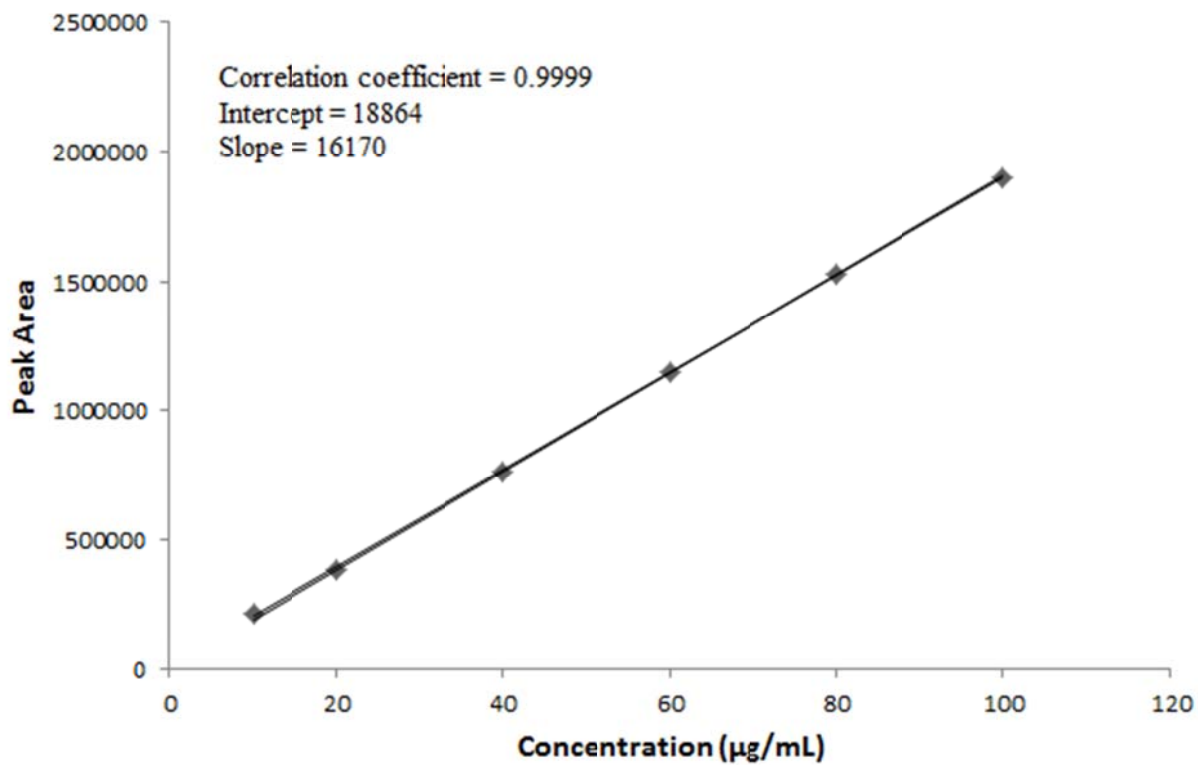


Fig. 5.2 Typical calibration plot of lysine-proline-valine (KPV)

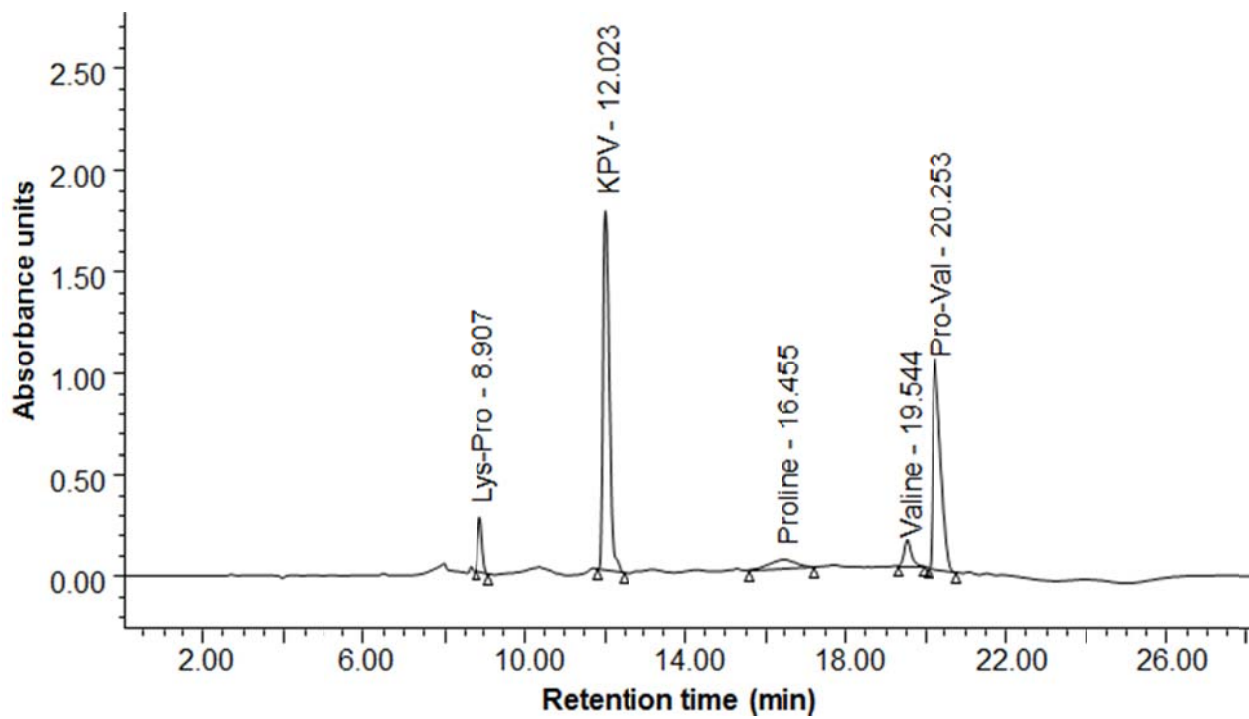


Fig. 5.3 HPLC chromatogram of KPV spiked with proline, valine, proline-valine and lysine-proline

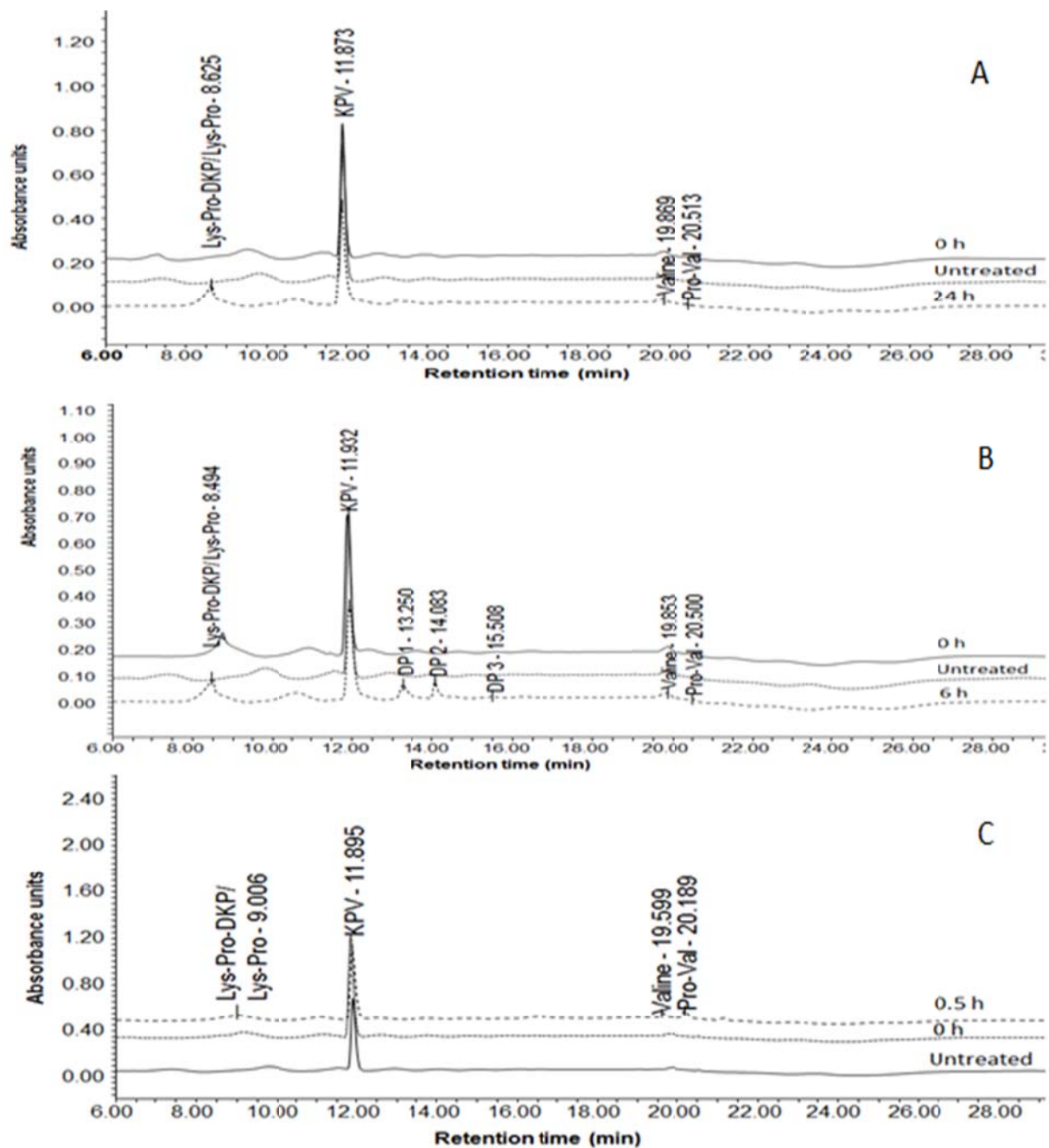


Fig. 5.4 HPLC analysis of KPV under acidic (A) alkaline (B) and oxidative (C) stress conditions

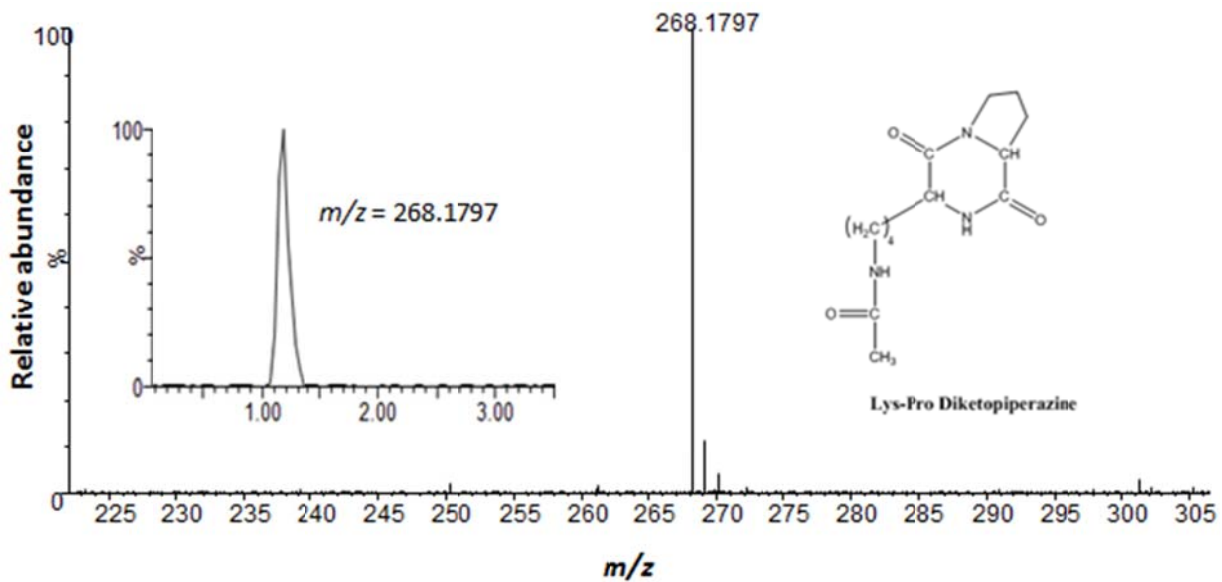


Fig. 5.5 LC/MS spectra of KPV degradation product, Lys-Pro-Diketopiperazine formed under stress conditions

6. ENHANCEMENT OF KPV DELIVERY USING IONTOPHORESIS ACROSS MICROPORATED HUMAN SKIN

6.1 ABSTRACT

A study was performed to improve the transdermal delivery of a C-terminal peptide fragment of α -MSH, KPV, for the treatment of inflammatory disorders such rheumatoid arthritis, psoriasis, and atopic and contact dermatitis. KPV is a highly hydrophilic molecule and thus has poor skin penetration. Various transdermal enhancement strategies such as ITP, MN or their combination were explored to enhance KPV delivery. Since KPV attains a positive charge at pH below 7.0, anodal ITP was employed. The parameters studied included current strength, duration of current application and concentration of KPV. Drug retention in the skin homogenate was also determined. Further, to investigate the permeation pathway of KPV across the skin, confocal microscopy was employed using FITC-labeled KPV. MN, ITP and ITP+MN significantly enhanced skin permeation of KPV ($P < 0.001$) as compared to passive delivery. KPV delivery increased linearly with current density and a 6.7- and 3-fold higher permeation and skin retention was achieved with 0.5 mA/cm^2 as compared to 0.1 mA/cm^2 . Increasing the KPV concentration from 5 mg/mL to 15 mg/mL resulted in a 2.5-fold increase in KPV delivery. Confocal studies indicated that for microporated skin FITC-labeled KPV migrated through the SC, along the microchannels and into the lower epidermal tissue since the fluorescence was observed at a depth

of 100 μm . For passive delivery the fluorescence was observed only on the superficial skin layers.

6.2 INTRODUCTION

Inflammation is the first line of the body's defense and the immune system's response against infection and injury. It involves a series of reactions, such as activation of mast cells or other inflammatory cells, and is primarily mediated by release of neuropeptides such as Substance P, vasoactive intestinal peptide and calcitonin-gene-related peptide from sensory nerves.¹ Current therapies for inflammatory disorders such as psoriasis, atopic and contact dermatitis, and atopic eczema include frequent use of corticosteroids. Chronic use of these drugs produces several local and systemic side effects.^{2,3} α -MSH is a neurohormone with extensive immunomodulatory effects on certain cell types.^{4,5} It exhibits potent anti-inflammatory effects by binding to melanocortin receptors in the skin.⁶ Further, the anti-inflammatory activity of α -MSH is reported to be mediated by the three terminal amino acids, Lysine-Proline-Valine (KPV).^{5,7} KPV lacks the entire sequence motif required for binding to the MC-Rs, but still retains almost all of the anti-inflammatory capacity of the parent hormone.⁸ The inflammatory activity of KPV is suggested to be mediated via inhibition of interleukin (IL)-1 β .⁹ Unlike α -MSH, KPV is free from the melanotropic effects and thus does not cause any pigmentation. Additionally, it is smaller in size and more chemically stable than α -MSH.¹⁰ These attributes make KPV a suitable candidate for the treatment of inflammatory skin disorders.

KPV has a molecular weight of 383.49 Da and an isoelectric point (pI) of 14. It is hydrophilic in nature and hence, poorly permeable across the skin. Enhanced skin permeability of KPV can be attained using permeation enhancement techniques such as ITP and MN.

Additionally, the delivery of KPV can be controlled by optimizing various parameters such as current density, duration of applied current strength and KPV concentration. Thus, the aim of the current study was to investigate the feasibility and optimize the transdermal delivery of KPV. Additionally, the influence of MN pretreatment on the transdermal iontophoretic delivery of KPV was studied.

6.3 MATERIALS AND METHODS

6.3.1 MATERIALS

KPV was obtained from Peptides International (KY, USA). Silver and silver chloride electrodes were purchased from Sigma Aldrich (St. Louis, MO, USA). Sodium chloride, acetonitrile, Trifluoroacetic acid (TFA) and potassium dihydrogen phosphate were purchased from Fisher Scientific (Suwanee, GA, USA). FluoroTagTM FITC conjugation kit was purchased from Sigma-Aldrich Co. (St. Louis, MO, USA). Tris buffer was obtained from VWR International (Suwanee, GA, USA). Dermatomed human skin (thickness ~0.35 mm) was obtained from Allosource (Cincinnati, OH, USA).

6.3.2 SKIN PERMEATION STUDIES

Dermatomed human skin was collected within 8 h of donor death and frozen at -70°C until use. *In vitro* skin permeation studies were performed using vertical static Franz diffusion cells (PermeGear Inc, Bethlehem, PA, USA). The skin was thawed at ambient temperature for 30 minutes after which it was cut, rinsed with water and sandwiched between donor and receptor cells with the epidermis facing the donor cell. The receptor cell contained phosphate buffered saline (PBS) (5 ml, pH 7.4), maintained at 37°C with a water circulation jacket that surrounded

the cell. The available diffusion area of the skin was 0.64 cm². The donor cell contained 10 mg/ml KPV solution in Tris buffer (0.5 ml, pH 7, 25 mM) containing 125 mM sodium chloride. The cell was covered with Parafilm[®] to prevent solvent evaporation. The receptor cells were stirred with magnetic bars at 300 rpm during the study. At regular intervals, 500 µl aliquots from the receptor were collected and replaced with fresh buffer solution pre-equilibrated at 37°C. The samples were stored in a refrigerator and analyzed within 24 h. All experiments were performed in 4 replicates.

6.3.2 DRUG EXTRACTION FROM SKIN

Residual drug in the skin was extracted at the end of the skin permeation study. The drug solution remaining on the surface of the skin was removed using cotton swabs. The surface was washed with Tris buffer (pH 7.0) after which it was gently wiped with a cotton swab (Q-tips[®] Unilever USA, Englewood Cliffs, NJ). Later, 200 µL of Tris buffer was added to the surface and dabbed with a fresh cotton swab. This process of rinsing and dabbing was repeated five times. Following the washing procedure, the active diffusion area was isolated with a biopsy punch (George Tiemann & Co, Hauppauge, NY). The collected skin was weighed, minced into pieces using a scissors and transferred into a borosilicate glass vial. To each vial, 1 mL of Tris buffer was added, sonicated for 15 min and allowed to stand overnight. Then they were re-sonicated for 30 min, filtered through a 0.45 µm membrane filter, and the filtrate was analyzed by HPLC.

6.3.3 IONTOPHORESIS

Iontophoretic protocols involved application of a direct current (Keithley Instruments, Inc, Cleveland, Ohio, USA) of 0.5 mA/cm² using Ag as an anode and Ag/AgCl as a cathode.

Anodal ITP was used. Current was applied for 6 h (iontophoretic phase) and the experiments were continued for 26 h. All skin permeation studies were conducted using Franz diffusion cells as described in section 6.3.2. Current was applied for 1.5, 3.0 and 6.0 h, respectively in three separate sets of experiments, and the experiments were terminated at their respective time points. Upon terminating the permeation experiments, skin extraction studies were performed as described in section 6.3.3.

6.3.5 MICROPORATION STUDIES

Microporation studies involved pretreatment of human skin with solid metallic MN arrays of a Demoroller™ (Dermaoller Deutschland s.a.r.l., Germany). The dermaroller was passed over the epidermal surface of the dermatomed human skin for 20 times and the treated skin was cut to size and mounted over Franz diffusion cells. The *in vitro* permeation and the skin extraction studies were conducted as described in sections 6.3.2 and 6.3.3.

6.3.6 COMBINATION OF IONTOPHORESIS AND MICROPORATION

Microporated skin, prepared as described in section 6.3.5, was mounted over Franz diffusion cells. All skin permeation studies were conducted using Franz diffusion cells as described earlier in section 6.3.2. ITP experiments on microporated skin were performed with a current density of 0.5 mA/cm² using Ag as anode and Ag/AgCl as cathode as described in section 6.3.4. Current was applied for 6 h (iontophoretic phase) and the experiments were continued for 26 h. Current was applied for 1.5, 3.0 and 6.0 h, respectively, in three separate sets of experiments, and the experiments were terminated at their respective time points. Upon

terminating the permeation experiments, skin extraction studies were performed as described in section 6.3.3.

6.3.7 ANALYTICAL METHOD

A HPLC system (Waters Corp., MA, USA) equipped with an autosampler (model 717 plus), a pump (model 1525) and a PDA UV detector (model 2998) was used. The system was interfaced with Empower 2 software for data collection and processing. Samples were eluted on a 4.6 mm x 250 mm Luna C₁₈ analytical column packed with 5 µm silica particles (Phenomenex, Torrance, CA, USA). The method consists of 0.1% TFA in water (mobile phase A) and 0.1% TFA in ACN (mobile phase B). The mobile phases were filtered using 0.2 µm nylon filter and degassed using bath sonication prior to use. Chromatographic separation was achieved using a linear gradient from 1% to 30% mobile phase B in 15 min. after which the gradient was reversed to 1% in 5 min. Then the column was equilibrated with 1% mobile phase for 10 min. The flow rate was 1 mL/min and injection volume was 50 µl. The eluent was monitored with a UV detector at 220 nm.

6.3.8 CONFOCAL IMAGING STUDY FOR KPV

Depth of KPV penetration across the skin was assessed using confocal imaging. KPV, by itself, cannot be visualized under a confocal microscope and, therefore, was conjugated to FITC according to the protocol provided by the manufacturer. Various ratios of FITC: KPV, e.g. 20:1, 30:1, 40:1 and 50:1 were prepared to obtain a conjugate with an absorbance value, $A_{280} > 0.2$. The labeled KPV was isolated from unconjugated KPV using a Sephadex G-25M column. This FITC-labeled KPV solution was then used for skin permeation studies. PD experiments were

performed on normal and microporated skin as described earlier. The skin collected following *in vitro* experiments was blotted and SC surface was thoroughly cleaned using saline and alcohol swabs. The skin samples were placed on a microscope slide and scanned using the confocal microscope. Samples were excited at 488 nm and X–Z sectioning was used to determine the depth of KPV permeation. *In vitro* permeation of FITC labeled KPV across intact skin was used as a negative control.

6.3.9 DATA ANALYSIS

All results are presented as mean \pm standard error of mean (SEM). The cumulative amount of drug permeated through unit area of skin was plotted as a function of time. *In vitro* steady-state permeation flux was calculated from the slope of the linear portion of the plot. Iontophoretic and post-iontophoretic fluxes were calculated from 0 - 6 h and 6 - 26 h permeation data respectively. The average flux from iontophoretic and post iontophoretic phases were calculated and presented as the total flux for ITP experiments. The enhancement ratios (ER) were calculated by dividing the flux of ITP or ITP+MN by the flux of MN. The amount of drug (mg) retained in the skin was normalized to 1 gram of skin. Analysis of variance was performed to determine the level of significance between the means. Mean differences with $P < 0.05$ were considered to be significant.

6.4 RESULTS

6.4.1 INFLUENCE OF CURRENT DENSITY

As shown in Figure 6.1 and Table 6.1A, KPV delivery increased with an increase in the current density. KPV permeation during the current application period (iontophoretic phase)

increased linearly with time. Termination of current at 6 h gradually decreased KPV permeation. The post-iontophoretic fluxes were higher than the corresponding PD values. The magnitude of the post-iontophoretic phase was proportional to the previously applied current density. Table 6.1B provides the corresponding enhancement ratios (ER) of KPV obtained with different current densities. The ER values increased with the current density for the iontophoretic phase, post-iontophoretic phase and total flux. Skin retention (Table 6.1C) was in agreement with the flux data. There was a 3-fold increase in the skin retention as the current density increased from 0.1 to 0.5 mA/cm².

6.4.2 INFLUENCE OF KPV CONCENTRATION

The cumulative amount of KPV permeated versus time as a function of drug concentration is shown in Figure 6.2. There was an increase in the iontophoretic transport of KPV as the concentration of the drug increased. The corresponding steady-state flux values are given in Table 6.1A. A 2.5-fold increase in KPV delivery was observed for both the iontophoretic phase and total flux when the donor concentration increased from 5 to 15 mg/mL ($65.54 \pm 4.62 \mu\text{g}/\text{cm}^2/\text{h}$). The flux values were significantly different at each donor concentration ($P < 0.05$) and a linear correlation was observed ($r^2 = 0.98$). Similar findings were observed for the ER values (Table 6.1B) and skin retention data (Table 6.1C).

6.4.4 EFFECT OF VARIOUS ENHANCEMENT STRATEGIES

Enhancement strategies such as ITP, MN and the combination of ITP and MN (ITP+MN) were employed to improve KPV delivery across skin. Skin permeation of KPV by PD was negligible (Figure 6.3). MN, ITP and ITP+MN significantly enhanced skin permeation of KPV

($P < 0.001$). The steady state flux values are given in Table 6.2A. ITP greatly enhanced the flux for KPV when compared to MN ($P < 0.001$). The flux values with the ITP and MN combination were significantly greater compared to ITP or MN individually ($P < 0.01$). Hence, a synergistic effect was observed when ITP was combined with MN. The ERs for ITP and ITP+MN were 5- and 19-fold greater respectively, compared to MN (Table 6.2B). In addition, the skin retention data (Table 6.2C) indicates that KPV levels obtained with ITP+MN, ITP and MN are much greater compared to PD.

6.4.4 INFLUENCE OF CURRENT DURATION

The influence of current duration on KPV transport across normal skin (ITP) and microporated skin (ITP+MN) was studied. ITP applied for longer durations (1.5, 3 and 6 h) resulted in a proportional increase in KPV skin permeation (Figure 6. 4A). Similarly, for ITP+MN, different durations resulted in increased KPV skin permeation (Figure 6.4B). The increase is significantly higher compared to ITP alone ($P < 0.001$). KPV flux dropped immediately when the current was removed in ITP as well as ITP+MN. It is evident from the data in Table 6.3A that iontophoretic flux is not statistically significantly different at each duration of current application. The cumulative amount of KPV permeated, however, is different but proportional to the duration for which the current is applied. Similar results were obtained with the combination strategy. The flux is higher with MN+ITP compared to ITP for all current durations.

6.4.5 CONFOCAL IMAGING

Following the *in vitro* study with FITC-labeled KPV, the skin sample was imaged at increasing depths from the skin surface (Figure 6.5). Untreated skin served as a negative control and no fluorescence was observed in the lower epidermal tissue. In contrast, for skin subjected to MN treatment, fluorescence was observed in the epidermal tissue. The passive skin samples displayed fluorescence to a depth of 36 μm . The MN treated samples displayed fluorescence for more than 100 μm but only along the microchannels.

6.5 DISCUSSION

Corticosteroids are the first choice to treat inflammatory disorders such as atopic and contact dermatitis, and atopic eczema. However, chronic use can produce severe systemic and local adverse effects. KPV, a C-terminal peptide fragment of α -MSH displays an equal anti-inflammatory effect as the parent molecule. However, it is highly hydrophilic and has poor skin penetration limiting its use as a topical agent. An attempt to measure the aqueous solubility of KPV was unsuccessful since it dissolves in large quantities to produce a gel. KPV displayed negligible skin permeation by PD from its aqueous solution. To enhance the permeation, transdermal enhancement strategies such as ITP, MN or their combination were used. KPV attains a positive charge (+1) at pH below 7.0 and hence anodal ITP was employed. Various factors affecting the permeation of KPV such as current strength, duration of current application and concentration of KPV were studied across normal and microporated skin.

Levels of KPV in the receptor following PD could not be detected by HPLC. Although small in molecular size and weight, the hydrophilic nature of KPV limits its PD permeation across intact skin. Application of current resulted in significantly enhanced permeation of KPV,

probably due to a combination of electrorepulsion and electroosmosis offered by anodal ITP.¹¹ ITP (Figure 6.1, Table 6.1) demonstrated a linear relationship between current density and KPV permeation. Current densities beyond 0.5 mA/cm² have the potential to evoke vascular reactions and skin irritation.^{12,13} In addition; skin retention data depicts maximum drug content at 0.5 mA/cm². A linear relationship existed between KPV delivery and drug concentration. As the drug concentration is increased, drug transport number increased (Figure 6.2) according to the Phipps and Gyori equation¹⁴:

$$J_d = \left(t_d \times \frac{I}{(F \times Z_d)} \right)$$

Where, J_d , t_d and Z_d are the flux, the transport number and the valence of the KPV ion, respectively. I is the applied current density and F is Faraday's constant. Since there was a linear increase in KPV permeation with drug concentration, electro-repulsion is the main mechanism of drug delivery and electro-osmosis plays a minor role. A similar effect was reported by Kolli et al. for selegiline hydrochloride.¹⁵ Additionally, since no plateau effect was observed, the skin concentrations of KPV were within the solubility limits and the ion conducting pathways are not saturated.¹⁶

Another means to improve skin permeation is to reduce the skin barrier resistance. This can be partially overcome by removal of the stratum corneum such as with tape stripping. However, the area and depth of the SC treated by tape stripping cannot be precisely controlled. Only limited data is available regarding the safety and recovery rate of skin after tape stripping. Dermarollers offer a reasonable alternative to breach the skin barrier with excellent recovery rates.^{15,17} Pretreatment of skin with MN from dermaroller enhanced KPV skin permeation and retention levels (Figure 6.3 and Table 6.2) compared to PD. Although MN enhanced the skin permeation of KPV, this effect was small compared with ITP treatment. This result may confirm

that KPV transport across the skin under the influence of ITP is predominantly by shunt routes rather than inter- or intra-cellular pathways. Microchannels, however, offer additional pathways for skin permeation.

A synergistic effect was observed for ITP and ITP combined with MN. ITP+MN resulted in a ~19-fold higher permeation compared to 5-fold for ITP in terms of ERs (Table 6.2B). As the SC is partially disrupted, there is a gradual drop in the electric resistance of the skin. This synergistic effect for hydrophilic drugs may be the result of the newly formed aqueous channels.¹⁸ The externally applied electric current can actively push KPV ions through the channels created by MN. The synergistic enhancement of the combination was reported earlier.¹⁹⁻²¹

The effect of current application duration on KPV transport across normal and microporated skin was studied to optimize the delivery of KPV further. KPV permeation is proportional to the duration of current application. The flux remained constant irrespective of the duration for which the current is applied. This suggests that KPV may be delivered at a constant rate mimicking infusion and can be tailored to the patients needs. Microporation did not alter skin retention values for each current duration application (Table 6.3C). This suggests that microporation played no role in altering KPV partitioning across the skin but only facilitated transport across the newly created microchannels.

Confocal microscopy offers controllable depth imaging and allows collecting serial optical sections from thick specimens. This technique was used to visualize the penetration of heparin along microchannels.²² Confocal studies revealed that KPV remained in the stratum corneum region of the skin for PD. In contrast, with MN, fluorescence was observed beyond the

stratum corneum and into the dermal layer. FITC-labeled KPV followed microchannels for transport across skin.

KPV is a potent molecule and the dose for treating ulcerative colitis is 25.2 ng/day.²³ In the current experiments, high skin concentrations (5.47 ± 0.33 mg/g) of KPV were obtained under optimized conditions for ITP+MN of 10 mg/mL KPV solution at $0.5\text{mA}/\text{cm}^2$ for 6 h. This should be quite adequate for the anti-inflammatory activity for topical conditions. The results of the current study indicate the feasibility of KPV delivered via topical/transdermal route using ITP or ITP+MN. Further *in-vivo* studies in suitable allergic and irritant contact dermatitis mice models are warranted to investigate the anti-inflammatory effects of KPV.

6.6 CONCLUSIONS

The *in vitro* transport of KPV across skin without any enhancement was negligible. The permeation of KPV significantly increased with ITP and MN. ITP appears to be the most effective individual method to enhance KPV delivery. A synergistic effect was observed after combining MN and ITP. The delivery could be controlled by altering the current density and duration of application. KPV could be delivered at rates closely mimicking infusions.

6.7 REFERENCES

1. Black PH. 2002. Stress and the inflammatory response: A review of neurogenic inflammation. *Brain Behav Immun* 16(6):622-653.
2. Horn EJ, Domm S, Katz HI, Lebwohl M, Mrowietz U, Kragballe K. 2010. Topical corticosteroids in psoriasis: Strategies for improving safety. *J Eur Acad Dermatol Venereol* 24(2):119-124.

3. Kikwai L, Babu RJ, Kanikkannan N, Singh M. 2006. Stability and degradation profiles of spantide II in aqueous solutions. *Eur J Pharm Sci* 27(2-3):158-166.
4. Auriemma M, Luger T, Loser K, Amerio P, Tulli A. 2009. The antiinflammatory effect of alpha-msh in skin: A promise for new treatment strategies. *Anti-Inflammatory & Anti-Allergy Agents in Medicinal Chemistry* 8 (1):14-21.
5. Luger TA, Scholzen TE, Brzoska T, Bohm M. 2003. New insights into the functions of alpha-msh and related peptides in the immune system. *Ann N Y Acad Sci* 994:133-140.
6. Brzoska T, Luger TA, Maaser C, Abels C, Bohm M. 2008. Alpha-melanocyte-stimulating hormone and related tripeptides: Biochemistry, antiinflammatory and protective effects *in vitro* and *in vivo*, and future perspectives for the treatment of immune-mediated inflammatory diseases. *Endocr Rev* 29(5):581-602.
7. Luger TA, Brzoska T. 2007. Alpha-msh related peptides: A new class of anti-inflammatory and immunomodulating drugs. *Ann Rheum Dis* 66 Suppl 3:iii52-55.
8. Brzoska T, Bohm M, Luger A, Loser K, Luger TA. 2010. Terminal signal: Anti-inflammatory effects of alpha-melanocyte-stimulating hormone related peptides beyond the pharmacophore. *Adv Exp Med Biol* 681:107-116.
9. Getting SJ, Schioth HB, Perretti M. 2003. Dissection of the anti-inflammatory effect of the core and c-terminal (KPV) alpha-melanocyte-stimulating hormone peptides. *J Pharmacol Exp Ther* 306(2):631-637.
10. Barcellini W, Colombo G, La Maestra L, Clerici G, Garofalo L, Brini AT, Lipton JM, Catania A. 2000. Alpha-melanocyte-stimulating hormone peptides inhibit hiv-1 expression in chronically infected promonocytic u1 cells and in acutely infected monocytes. *J Leukoc Biol* 68(5):693-699.

11. Marro D, Kalia YN, Delgado-Charro MB, Guy RH. 2001. Contributions of electromigration and electroosmosis to iontophoretic drug delivery. *Pharm Res* 18(12):1701-1708.
12. Abramowitz D, Neoussikine B. 1946. *Treatment by ion transfer*. ed., New York: Grune and Stratton.
13. Schriber WJ. 1975. *A manual of electrotherapy*. 4 ed., Philadelphia: Lea and Febiger.
14. Phipps JB, Scott ER, Gyory JR, Padmanabhan RV. 2006. Iontophoresis. In Swarbrick J, editor *Encyclopedia of pharmaceutical technology*. New York: Marcel Dekker p. 2119-2132.
15. Kolli CS, Chadha G, Xiao J, Parsons DL, Babu RJ. 2010. Transdermal iontophoretic delivery of selegiline hydrochloride, *in vitro*. *J Drug Target* 18(9):657-664.
16. Brand RM, Guy RH. 1995b. Rapid transdermal delivery of nicotine by iontophoresis. *J Control Release* 33:285-292.
17. Kalluri H, Kolli CS, Banga AK. 2011. Characterization of microchannels created by metal microneedles: Formation and closure. *AAPS J* 13(3):473-481.
18. Badkar AV, Smith AM, Eppstein JA, Banga AK. 2007. Transdermal delivery of interferon alpha-2b using microporation and iontophoresis in hairless rats. *Pharm Res* 24(7):1389-1395.
19. Kolli CS, Xiao J, Parsons DL, Babu RJ. 2012. Microneedle assisted iontophoretic transdermal delivery of prochlorperazine edisylate. *Drug Dev Ind Pharm* 38(5):571-576.
20. Sachdeva V, Zhou Y, Banga AK. 2012. *In vivo* transdermal delivery of leuprolide using microneedles and iontophoresis. *Curr Pharm Biotechnol* 14(2):180-193.

21. Vemulapalli V, Yang Y, Friden PM, Banga AK. 2008. Synergistic effect of iontophoresis and soluble microneedles for transdermal delivery of methotrexate. *J Pharm Pharmacol* 60(1):27-33.
22. Lanke SS, Kolli CS, Strom JG, Banga AK. 2009. Enhanced transdermal delivery of low molecular weight heparin by barrier perturbation. *Int J Pharm* 365(1-2):26-33.
23. Laroui H, Dalmaso G, Nguyen HTT, Yan Y, Sitaraman SV, Merlin D. 2010. Drug-loaded nanoparticles targeted to the colon with polysaccharide hydrogel reduce colitis in a mouse model. *Gastroenterology* 138(3):843–853.

Table 6.1 Effect of applied current density and drug concentration on the iontophoretic delivery of KPV across dermatomed human skin

A) Steady state Flux ($\mu\text{g}/\text{cm}^2/\text{h}$)			
Current density (mA)	0-6 h	6-26 h	Total flux
0.1	5.86 ± 0.29	0.57 ± 0.20	3.22 ± 0.63
0.3	32.79 ± 1.97	3.38 ± 0.61	18.08 ± 2.17
0.5	38.66 ± 1.67	2.79 ± 0.77	20.73 ± 3.32
KPV Conc. (mg/ml)			
5	26.75 ± 2.24	1.44 ± 1.01	14.10 ± 5.52
10	39.71 ± 1.96	3.52 ± 0.91	21.62 ± 3.33
15	65.54 ± 4.62	4.12 ± 2.02	34.83 ± 9.77

B) Enhancement ratios as compared to MN (Mean \pm SEM)			
Current density (mA)	0-6 h	6-26 h	Total flux
0.1	1.33 ± 0.07	0.13 ± 0.04	0.73 ± 0.14
0.3	7.42 ± 0.45	0.76 ± 0.14	4.09 ± 0.49
0.5	8.98 ± 0.44	0.80 ± 0.21	4.90 ± 0.75
KPV Conc. (mg/ml)			
5	6.05 ± 0.51	0.33 ± 0.23	3.19 ± 1.25

10	8.98 ± 0.44	0.80 ± 0.21	4.90 ± 0.75
15	14.83 ± 1.05	0.93 ± 0.46	7.88 ± 2.21

C) Skin retention levels as compared to PD (Mean \pm SEM)

Current density (mA)	mg of KPV/g of skin
0.1	0.68 ± 0.15
0.3	0.74 ± 0.11
0.5	2.04 ± 0.26
KPV Conc. (mg/ml)	
5	0.72 ± 0.11
10	2.04 ± 0.26
15	3.06 ± 1.14

Table 6.2 Effect of MN and ITP and their combination (ITP+MN) on the permeation of KPV across dermatomed human skin

Current density = 0.5 mA and KPV concentration = 10 mg/mL

A) Steady state Flux ($\mu\text{g}/\text{cm}^2/\text{h}$)

	0-6 h	6-26 h	Total flux
PD	-	-	0.00 \pm 0.00
MN	-	-	4.42 \pm 0.11
ITP	36.66 \pm 1.59	2.87 \pm 3.17	19.77 \pm 11.32
ITP+MN	150.70 \pm 4.40	6.29 \pm 1.97	78.50 \pm 13.46

B) Enhancement ratios (Mean \pm SEM)

	0-6 h	6-26 h	Total flux
ITP	8.29 \pm 0.36	0.65 \pm 0.72	4.47 \pm 2.56
ITP+MN	34.10 \pm 1.00	1.42 \pm 0.45	17.76 \pm 3.00

C) Skin retention levels (Mean \pm SEM)

	mg of KPV/g of skin
PD	0.18 \pm 0.03
MN	0.70 \pm 0.06
ITP	2.04 \pm 0.26
ITP+MN	1.68 \pm 0.20

Table 6.3 Effect of current duration on the skin permeation of KPV across normal and MN treated human skin.

Current density = 0.5 mA and KPV concentration = 10 mg/mL

A) Steady state Flux ($\mu\text{g}/\text{cm}^2/\text{h}$)

Current duration (h)		ITP	Post ITP	Total flux
	ITP	35.64 \pm 3.96	1.22 \pm 0.71	18.43 \pm 6.37
1.5 h*	ITP+MN	84.68 \pm 5.83	7.69 \pm 0.62	46.19 \pm 3.46
	ITP	35.88 \pm 1.84	1.68 \pm 0.46	18.78 \pm 3.02
3.0 h*	ITP+MN	124.90 \pm 4.90	6.09 \pm 1.31	65.50 \pm 8.30
	ITP	36.66 \pm 1.59	2.87 \pm 3.17	19.77 \pm 11.32
6.0 h*	ITP+MN	150.70 \pm 4.40	6.29 \pm 1.97	78.50 \pm 13.46

*current was stopped at respective time points and experiment was continued for 26 h

B) Enhancement ratios (Mean \pm SEM)

Current duration (h)		ITP	Post ITP	Total flux
	ITP	8.06 \pm 0.90	0.28 \pm 0.16	4.17 \pm 1.44
1.5 h*	ITP+MN	19.15 \pm 1.32	1.74 \pm 0.14	10.44 \pm 0.78
	ITP	8.12 \pm 0.42	0.38 \pm 0.10	4.25 \pm 0.68
3.0 h*	ITP+MN	28.26 \pm 1.11	1.38 \pm 0.30	14.82 \pm 1.88
	ITP	8.29 \pm 0.36	0.65 \pm 0.72	4.47 \pm 2.56
6.0 h*	ITP+MN	34.10 \pm 1.00	1.42 \pm 0.45	17.76 \pm 3.05

*current was stopped at respective time points and experiment was continued for 26 h

C) Skin retention levels (Mean \pm SEM)

Current duration	mg of KPV/g of skin	
(h)	I TP	I TP+MN
1.5 [#]	2.18 \pm 0.33	2.71 \pm 0.30
3 [#]	2.54 \pm 0.64	2.92 \pm 0.45
6 [#]	4.95 \pm 0.66	5.47 \pm 0.33
26h*	2.04 \pm 0.26	1.68 \pm 0.20

#current was stopped at the respective time points and the experiment was terminated

*current was stopped at 6 h and experiment was continued for 26 h

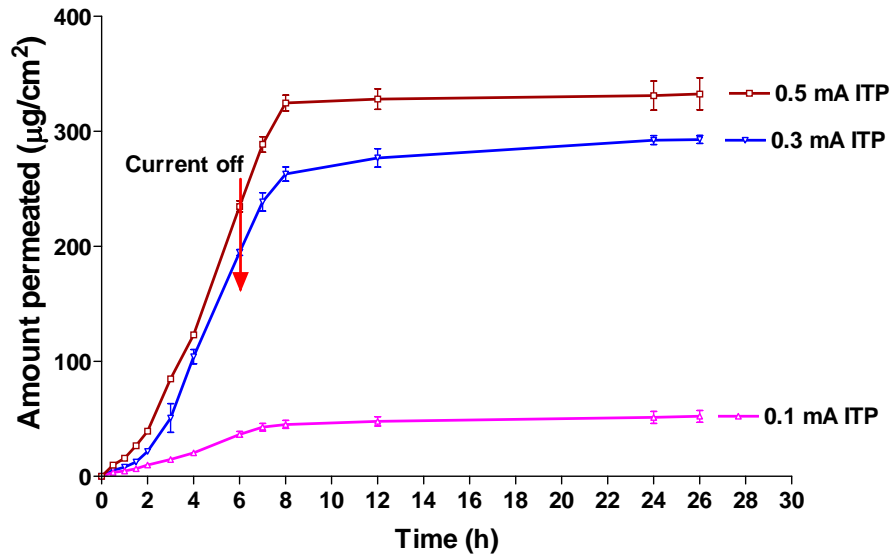


Figure 6.1 Effect of applied current density on the iontophoretic delivery of KPV (10 mg/mL) across dermatomed human skin. Values represent mean \pm SEM; n = 3

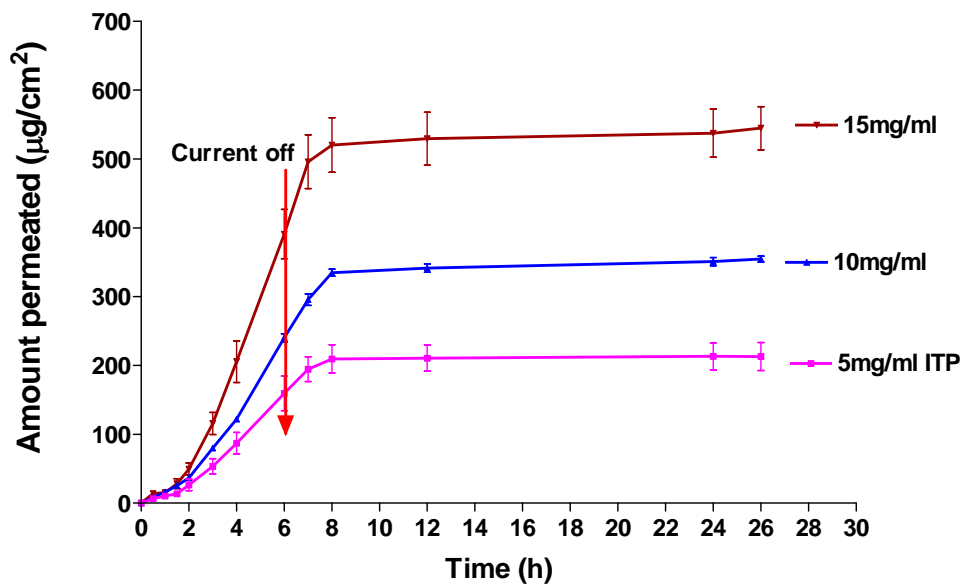


Figure 6.2 Effect of KPV concentrations on its iontophoretic delivery across dermatomed human skin. Values represent mean \pm SEM; n = 3

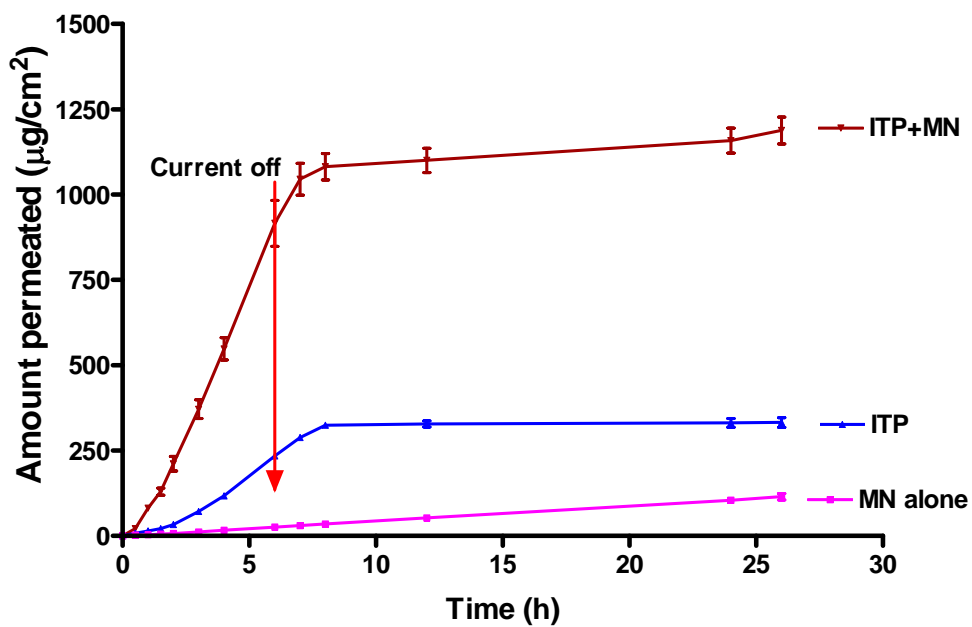


Figure 6.3 Permeation of KPV under the influence of ITP across normal and microporated skin (KPV: 10 mg/mL; current density: 0.5 mA/cm²; number of MN passes = 20)

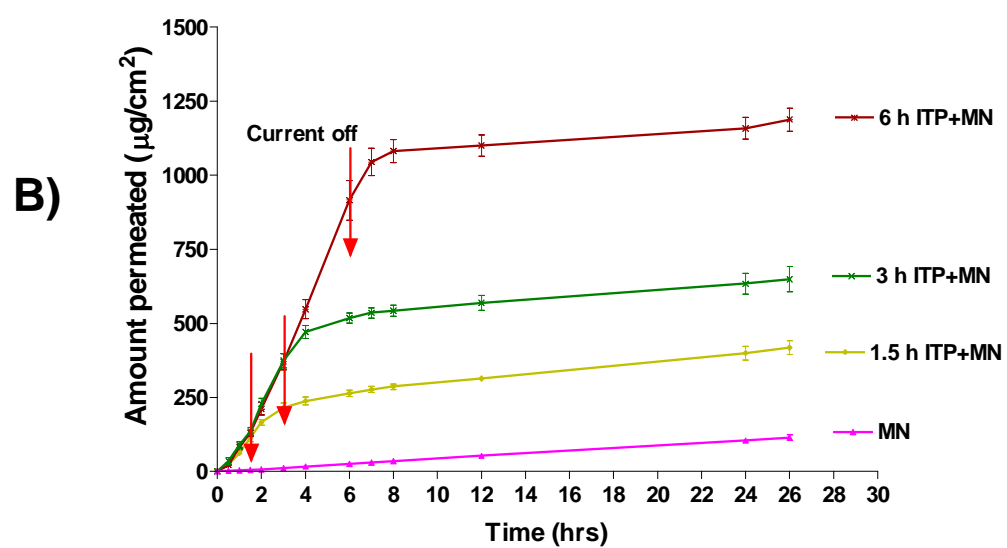
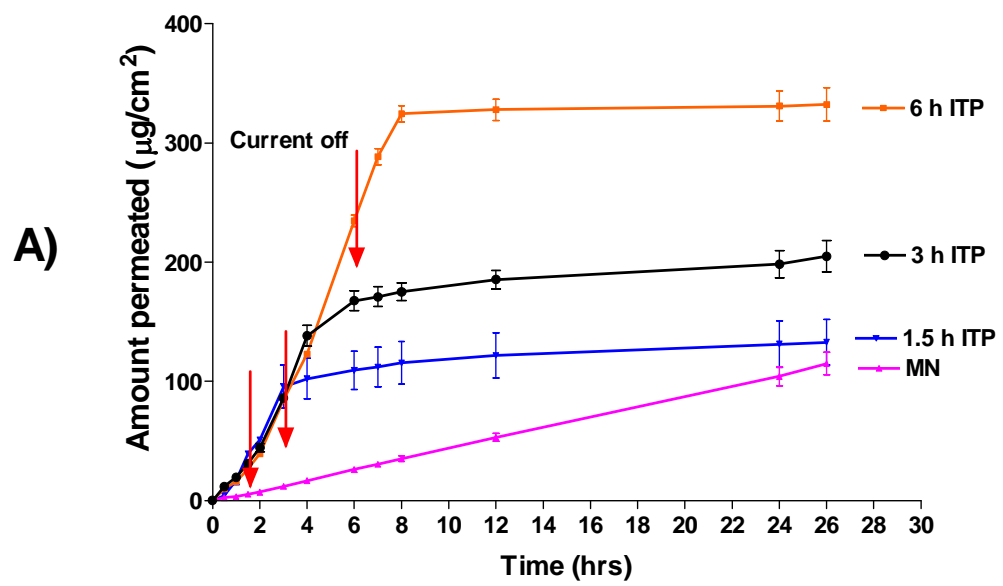
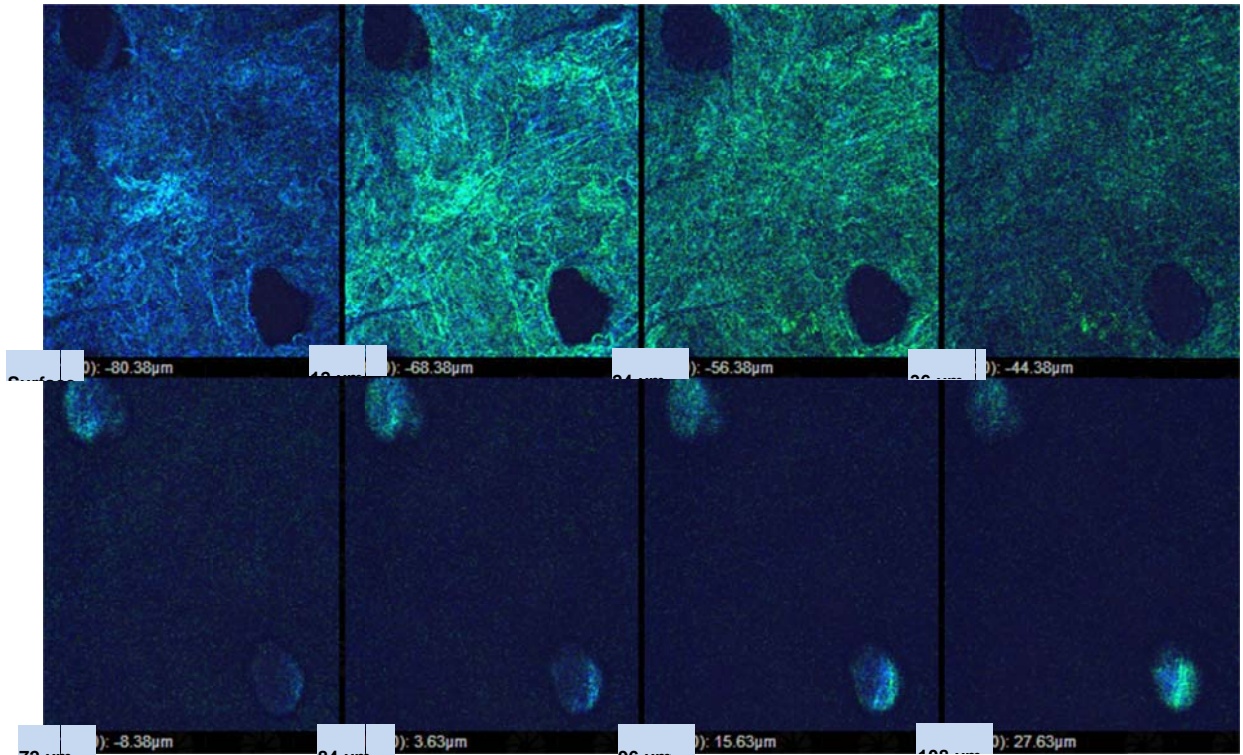
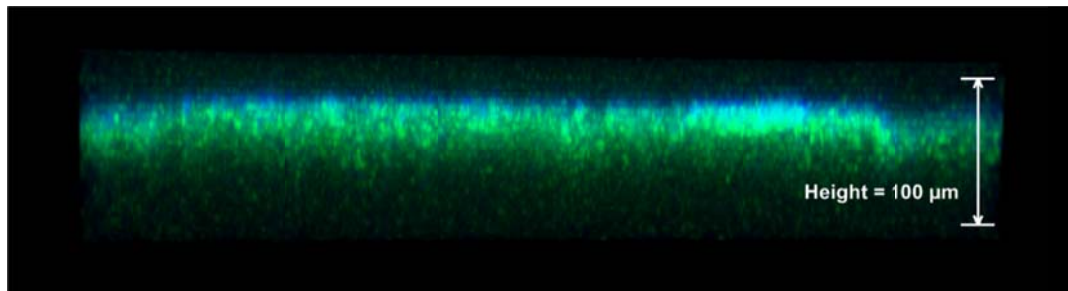


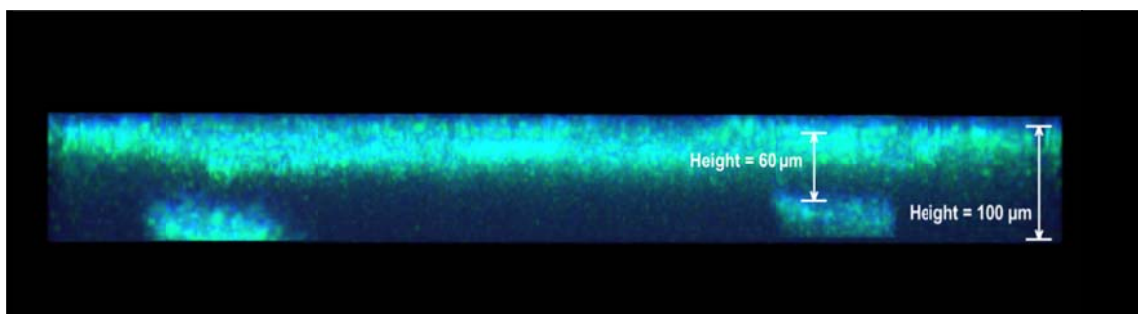
Figure 6.4 Effect of applied current duration on the iontophoretic delivery of KPV with A) ITP and B) ITP+MN, (KPV: 10 mg/mL; current density: 0.5 mA/cm²; number of MN passes = 20). Values represent mean \pm SEM; n = 3



A) Horizontal sections of the microporated skin after KPV-FITC treatment



B) Transverse section of the normal skin after KPV-FITC treatment



C) Transverse section of the microporated skin after KPV-FITC treatment

Figure 6.5 Confocal imaging of skin after treatment with KPV-FITC

7. EFFECT OF CARBON CHAIN LENGTH OF FATTY ACID IN A NANOEMULSION FORMULATION ON THE TRANSDERMAL DELIVERY OF KPV ACROSS MICROPORATED SKIN

7.1 ABSTRACT

The effect of carbon chain length of fatty acid in the nanoemulsion formulation on the skin permeation and retention of KPV across dermatomed human skin was studied. Microporation was performed on the skin with 20 passes of Dermaroller[®]. Caproic acid (C₆), caprylic acid (C₈), capric acid (C₁₀) and lauric acid (C₁₂) were used in the formulation of nanoemulsions. A parabolic relationship between the hydrocarbon chain length and skin permeation was observed across both normal and microporated skin. Microporated skin demonstrated a 3.5 to 10 fold higher skin permeation for different fatty acids as compared to untreated skin ($P < 0.05$). The most polar fatty acid, C₆ demonstrated 10 fold higher flux for microporated skin. The skin retention studies demonstrated a linear increase of KPV deposition in the skin with the carbon chain length. Microporated skin did not show any significant increase in the skin retention for C₈, C₁₀ and C₁₂ fatty acids ($P > 0.05$) as compared to the passive delivery on the untreated skin. However, C₆ showed a 2-fold increase in the skin retention for microporated skin versus normal skin ($P < 0.05$). The skin permeation and retention increases for C₆ due to microporation (10 and 2-fold, respectively) and were significantly higher than C₈, C₁₀ and C₁₂ formulations. This study demonstrates that microneedles have less significant permeation enhancement effect for the fatty acids with increased lipophilicity.

Keywords: KPV, nanoemulsion, lipids, lipophilicity

7.2 INTRODUCTION

Over the past few decades nanoemulsions have drawn significant scientific attention due to their unique advantages such as high solubilization capacity, spontaneity of formation, enhanced thermodynamic stability, ability to load both hydrophilic and hydrophobic drug molecules, enhanced stability of the encapsulated therapeutic molecule, and high diffusion/absorption rates. There have been successful applications of nanoemulsions in dermal and epidermal targeting for various conditions such as psoriasis, rheumatoid arthritis, aging, skin cancer, and dermatophytoses.¹⁻⁶ In this study, we formulated nanoemulsions for Lysine-Proline-Valine (KPV), a C-terminal peptide fragment of α -MSH that displays similar anti-inflammatory effect as the parent molecule.^{7,8} Fatty acids of varied carbon chain length ($C_6 - C_{12}$) were used as a lipid phase in different nanoemulsion formulations. The lipids used were caproic acid (C_6), caprylic acid (C_8), capric acid (C_{10}) and lauric acid (C_{12}). Microneedle based transdermal delivery is an emerging technology for local or systemic delivery for both large and difficult to deliver molecules, including proteins, peptides and vaccines. There are no literature reports to our best of knowledge on the effect of the polarity of the formulation on the skin permeation behavior of a peptide across microporated skin. The effect of carbon chain length of the fatty acid (lipid phase) in the nanoemulsion formulation on KPV delivery across dermatomed human skin was studied. These results were compared to those obtained with that of microporated skin.

7.3. MATERIALS AND METHODS

7.3.1 MATERIALS

KPV was custom synthesized from Peptides International (Louisville KY, USA). Capric acid and Caproic acid were procured from Alfa Aesar (Ward Hill, MA, USA). Lauric acid and

Caprylic acid were procured from Cayman Chemical Company (Ann Arbor, Michigan, USA) and Amresco (Solon, OH, USA), respectively. Tween 80, Acetonitrile, Trifluoroacetic acid (TFA) and potassium dihydrogen phosphate were purchased from Fisher Scientific (Suwannee, GA, USA). Dermatomed human skin (thickness ~0.35 mm) was obtained from Allosource (Cincinnati, OH, USA).

7.3.2 FORMULATION OF KPV NANOEMULSIONS

The formulation compositions of various nanoemulsions are listed in Table 7.1. The fatty acids used at 15% w/w concentration. Tween 80 and ethanol were used in 30% and 15% concentrations, respectively. Tween 80 was used as a surfactant and ethanol was used as a co-surfactant and solubilizer for KPV. KPV was added at 1% concentration of the final formula weight. KPV was dissolved in ethanol, Tween 80 and respective fatty acid was added and mixed using vortex mixer. For lauric acid based formulation, it was heated in a water bath at 70°C to melt the lipid for proper mixing of the components. Water was added to this mixture and it was mixed again using the vortex mixer. Finally the formulation was sonicated for 1 minute to obtain a clear solution.

7.3.3 VISCOSITY DETERMINATION

The viscosity of the nanoemulsion formulations was measured using a cone-plate type DV-II + Pro viscometer (Brookfield Engineering Laboratories, Middleboro, MA, USA) at 37°C. The measurement was performed with 40Z spindle (shear rate, 10 rpm) for C₆, C₈ and C₁₀ nanoemulsions whereas with 51Z (shear rate, 2.5 rpm) for C₁₂ nanoemulsion. The lower rpm was

used for C₁₂ to maintain the torque at the similar value as that of other nanoemulsions. The measurements were performed in triplicate.

7.3.4 PARTICLE SIZE AND ZETA POTENTIAL MEASUREMENT

The particle size and zeta potential of the nanoemulsion formulations were measured by dynamic and electrophoretic light scattering methods, respectively using the Nicomp 380 ZLS Particle Size and Zeta Potential Analyzer (Particle Sizing Systems, Santa Barbara, CA, USA). The particle size analyses were performed at a scattering angle of 90° and temperature of 25°C. For each sample, the mean particle diameter and polydispersity index (PDI) were calculated using multimodal analysis. The system was operated by Nicomp PSS ZPW388 software (Particle Sizing Systems, Santa Barbara, CA, USA). The zeta potential of the samples was measured after appropriate dilution using zeta mode of the Nicomp 380 ZLS Analyzer.

7.3.5 SKIN PERMEATION STUDIES

Dermatomed human skin was collected within 8 h of donor death and frozen at -70°C until use. *In vitro* skin permeation studies were performed using vertical static Franz diffusion cells (PermeGear Inc, Bethlehem, PA, USA). The skin was thawed at ambient temperature for 30 minutes after which it was cut, rinsed with water and pH 7.4 phosphate buffered saline (PBS) and sandwiched between donor and receptor cells with the epidermis facing the donor cell. The receptor cell contained 5 ml of PBS which was maintained at 37°C with a water circulation jacket that surrounded the cell. The available diffusion area of the skin was 0.64 cm². The donor cell was filled with 0.3 ml of respective KPV nanoemulsion using a syringe. The cell was covered with Parafilm[®] to prevent evaporation. The receptor cells were stirred with magnetic bars at 300 rpm during the permeation study. At regular intervals, 500 µl aliquots from the

receptor were collected and replaced with the fresh buffer solution pre-equilibrated at 37°C. The samples were stored in a refrigerator and analyzed within 24 h. All experiments were performed in triplicate.

7.3.6. DRUG EXTRACTION FROM SKIN

Residual drug in the skin was extracted at the end of the skin permeation study. The nanoemulsion remaining on the surface of the skin was removed using cotton swabs. The surface was washed with phosphate buffered saline (PBS) (pH 7.4) after which it was gently wiped with a cotton swab (Q-tips® Uniliver USA, Englewood Cliffs, NJ). 200 µL of PBS was added to the surface and dabbed with a fresh cotton swab. This process of swabbing and dabbing was repeated five times. Following the washing procedure, the active diffusion area was isolated with a biopsy punch (George Tiemann & Co, Hauppauge, NY). The collected skin was weighed, minced into pieces and transferred into a borosilicate glass vial. To each vial, 1 mL of PBS was added, sonicated for 15 min and allowed to stand overnight. They were re-sonicated for 30 min, filtered through a 0.45 µm membrane filter, and the filtrate was analyzed by HPLC.

7.3.7 MICROPORATION STUDIES

Microporation studies involved pretreatment of human skin with solid metallic microneedle arrays of a Demoroller™ (Dermaoller Deutschland s.a.r.l., Germany). The Dermaroller was passed 20 times over the epidermal surface of the dermatomed human skin and the treated skin was cut to size and mounted over Franz diffusion cells. The in vitro permeation and the skin extraction studies were conducted as described in sections 7.3.5 and 7.3.6.

7.3.8 ANALYTICAL METHOD

HPLC system (Waters Corp., MA, USA) equipped with an autosampler (model 717 plus), a pump (model 1525) and a PDA UV detector (model 2998) was used. The system was interfaced with Empower 2 software for data collection and processing. Samples were eluted on a 4.6 mm x 250 mm Luna C₁₈ analytical column packed with 5 µm silica particles (Phenomenex, Torrance, CA, USA). The method consists of 0.1% TFA in water (mobile phase A) and 0.1% TFA in ACN (mobile phase B). The mobile phases were filtered using 0.2 µm nylon filter and degassed prior to use. Chromatographic separation was achieved using a linear gradient from 1% to 30% mobile phase B in 15 min. after which the gradient was reversed to 1% in 5 min following which the column was equilibrated with 1% mobile phase for 10 min. The flow rate was 1 mL/min and injection volume was 50 µl. The eluent was monitored with a UV detector at 220 nm.

7.3.9 DATA ANALYSIS

All results are presented as mean ± standard error of mean (SEM). The cumulative amount of drug permeated through unit area of skin was plotted as a function of time. The steady-state flux was calculated from the slope of the linear portion of the plot. Analysis of variance was performed to determine the level of significance between the means. Mean differences with $P < 0.05$ were considered to be significant.

7.4. RESULTS

Various physical properties of nanoemulsions are listed in Table 7.1. The viscosity of the formulations was around 30 cps for C₆, C₈ and C₁₀ but for C₁₂ the viscosity was 1066 cps

because the semi-solid nature of C₁₂ acid which produced a viscous emulsion. The pH of the formulations was in the acidic range (3.49 to 4.45) due to the acidic nature of the lipids as expected. The mean particle size of the formulations was in the range of 10 to 20 nm. The PDI values < 0.5 and zeta potential values around -20 mV indicate physically stable state of the nanoemulsion formulations.

7.4.1 EFFECT OF HYDROCARBON CHAIN LENGTH OF LIPIDS ON SKIN PERMEATION OF KPV

The effect of microneedles on the transdermal permeation of various nanoemulsions of KPV across dermatomed human skin is shown in Fig 7.1 A and B. The steady state flux values calculated from the linear portion of the ‘skin permeation’ versus ‘time’ profiles are presented in Fig. 7.2 A and B and Table 7.2 A. As shown by the data, a parabolic relationship between the carbon chain length and the skin permeation of KPV was noted. Both cases, in passive delivery (control) and delivery across microneedle treated skin (MN delivery), a lowest amount of skin permeation was noted for C₆ and the skin permeation was peaked for C₈ and C₁₀. The skin permeation of C₁₂ was relatively lower as compared to C₈ or C₁₀ ($P < 0.05$). In passive delivery studies the KPV flux was lowest for C₆ ($0.356 \pm 0.031 \mu\text{g}/\text{cm}^2/\text{h}$) and it was highest for C₈ ($1.802 \pm 0.084 \mu\text{g}/\text{cm}^2/\text{h}$) demonstrating a 5 fold higher flux by the C₈ fatty acid (Figure 7.2 A, Table 7.2 A). Similarly, in MN delivery studies the KPV flux was lowest for C₆ ($3.728 \pm 0.192 \mu\text{g}/\text{cm}^2/\text{h}$) and it was highest for C₈ ($7.057 \pm 0.261 \mu\text{g}/\text{cm}^2/\text{h}$) demonstrating ~2 fold higher flux by the C₈ fatty acid (Fig. 7.2 B, Table 7.2 A). Microneedle application (MN delivery) significantly enhanced KPV permeation for all the formulations as compared to passive delivery ($P < 0.001$). The flux obtained for MN delivery of C₆ nanoemulsion ($3.728 \pm 0.192 \mu\text{g}/\text{cm}^2/\text{h}$)

was about 10 fold higher as compared to C₆ passive delivery ($0.356 \pm 0.031 \mu\text{g}/\text{cm}^2/\text{h}$). The MN delivery by C₈, C₁₀ and C₁₂ formulations was 3.5 to 5.0 fold higher as compared to their respective counterpart formulations of passive delivery (Table 7.2 A).

7.4.2 EFFECT OF HYDROCARBON CHAIN LENGTH OF LIPIDS ON SKIN RETENTION OF KPV

The effect of passive and MN delivery on the skin retention of various nanoemulsions of KPV across dermatomed human skin is shown in Fig. 7.3 A and B, and Table 7.2 B. The skin retention increased with increase in the carbon chain length up to C₁₀ and decreased for C₁₂. However the skin retention data of C₈, C₁₀ and C₁₂ are not significantly different from each other ($P > 0.05$). As shown in Fig. 7.3 A, the skin retention of KPV was ~4.6 fold higher for C₁₀ as compared to C₆. Similarly, MN studies demonstrate that the skin retention of KPV was ~1.6 fold higher for C₁₀ as compared to C₆ (Fig. 7.3 B). A comparison of skin retention data of passive and MN delivery in Fig. 7.3 A and B reveals that only C₆ (less lipophilic fatty acid) showed 2 fold higher skin retention by MN delivery as compared to passive delivery ($P < 0.05$). There is no significant difference in the skin retention of KPV between passive delivery and MN delivery of the respective C₈, C₁₀ and C₁₂ formulations ($P > 0.05$).

7.5. DISCUSSION

KPV is a small molecule (Molecular weight 383.49 Da) but is highly hydrophilic in nature and, thus, has poor skin penetration. An aqueous formulation of KPV in Tris buffer (pH 7.0) showed practically no detectable levels of skin permeation in 24 h. This limits its use as a topical agent for the treatment of various disorders such as rheumatoid arthritis, psoriasis, atopic

and contact dermatitis, and atopic eczema. Incorporation of KPV into a nanoemulsion formulation may enhance the skin permeation of KPV thus providing better topical delivery. There are no literature reports on the skin permeation behavior of nanoemulsions made with lipids of different polarity across microporated skin.

In this study, we formulated nanoemulsions of KPV to improve its delivery across dermatomed human skin. Further, the dependency of the chain length of various lipids was evaluated on KPV permeation across normal and microporated skin. Significantly higher delivery of KPV was observed with the nanoemulsion formulation with increased carbon chain length from C₆ to C₁₀ ($P < 0.05$). There are several reports on the effect of carbon chain length of fatty acids on the skin permeation enhancement of drugs. The enhancement effect of fatty acids on the permeation of piroxicam was studied in rat skin, and it decreases linearly with increasing carbon number of fatty acid from C₁₂-C₁₈.⁹ Similarly, the permeation enhancing effect of saturated fatty acids for melatonin through hairless mice skin decreased with the increase in the carbon chain length from C₁₂-C₁₈.¹⁰ Among a series of saturated fatty acids investigated as permeation enhancers for propranolol in rabbit skin, C₁₂ and C₁₄ saturated fatty acids were the most potent agents in increasing the permeation of propranolol from gel formulations.¹¹

A parabolic relationship was observed between hydrocarbon chain length and KPV flux with a peak permeation rate at C₈. KPV delivery increased when the chain length increased from C₆ to C₁₀, however, the permeation decreased when the chain length was further increased to C₁₂. This type of parabolic relationship between hydrocarbon chain length and melatonin skin permeation across human and porcine skin was reported.¹² Also, a parabolic correlation was observed between the diclfenac penetration enhancement and the fatty acid carbon chain length

among saturated fatty acids of C₁₂–C₂₀ units.¹³ Among C₈, C₁₂, C₁₄ saturated fatty acids, C₁₂ acid was found to be the optimum permeation enhancer for flurbiprofen across rat skin.¹⁴

Similarly, medium chain hydrocarbons (C₇ to C₁₂) showed a parabolic relationship between the flux of methyl thalidomide and the carbon chain length with peak permeation rate at C₁₀ hydrocarbon.¹⁵ It has been proposed that acids with a certain chain length possess an optimal balance between partition coefficient and affinity to the skin.¹¹ Shorter chain fatty acids would have insufficient lipophilicity for the permeation into the skin, whereas longer chain fatty acids would have much higher affinity to lipids in the SC thereby retarding their own permeation and that of other permeants. This suggests that the mode of action of saturated fatty acids as enhancers is dependent on their own permeation across the stratum corneum/skin.^{16,17}

Further, the skin retention data by passive delivery showed a ~4.6 fold increase in the skin deposition of KPV with increase in the carbon chain length from C₆ to C₁₀. The skin retention data by MN delivery also showed ~1.6 fold increase in the skin deposition of KPV with increase in the carbon chain length from C₆ to C₁₀. A comparison between passive delivery and MN delivery indicates that MN delivery did not significantly improve the skin deposition for KPV for C₈, C₁₀ and C₁₂ formulations ($P > 0.05$). Only C₆ formulation that has relatively more polar fatty acid, which increased the skin deposition of KPV by two fold as compared to passive delivery ($P < 0.05$). The data show that MN has similar skin permeation profiles as that of PD in terms of structure-permeation relationship as both methods showed a similar permeation pattern. In conclusion, microneedles have less significant permeation enhancement effect for the fatty acids with increased lipophilicity.

7.6. CONCLUSIONS

The permeation of KPV was dependent on the lipophilicity of the fatty acids and showed a parabolic relationship between the carbon chain length and transdermal flux. Further, microneedles have less significant effect on the permeation enhancement for the fatty acids with increased lipophilicity. Also, the skin retention of KPV can be enhanced by using fatty acids of higher carbon chain length.

7.7. REFERENCES

1. Fang JY, Leu YL, Chang CC, Lin CH, Tsai YH. 2004. Lipid nano/submicron emulsions as vehicles for topical flurbiprofen delivery. *Drug Deliv* 11(2):97-105.
2. Lopes LB, VanDeWall H, Li HT, Venugopal V, Li HK, Naydin S, Hosmer J, Levendusky M, Zheng H, Bentley MV, Levin R, Hass MA. 2010. Topical delivery of lycopene using microemulsions: Enhanced skin penetration and tissue antioxidant activity. *J Pharm Sci* 99(3):1346-1357.
3. Paolino D, Ventura CA, Nistico S, Puglisi G, Fresta M. 2002. Lecithin microemulsions for the topical administration of ketoprofen: Percutaneous adsorption through human skin and in vivo human skin tolerability. *Int J Pharm* 244(1-2):21-31.
4. Piemi MP, Korner D, Benita S, MartyJp. 1999. Positively and negatively charged submicron emulsions for enhanced topical delivery of antifungal drugs. *J Control Release* 58(2):177-187.
5. Rhee YS, Choi JG, Park ES, Chi SC. 2001. Transdermal delivery of ketoprofen using microemulsions. *Int J Pharm* 228(1-2):161-170.

6. Ustundag Okur N, Apaydin S, Karabay Yavasoglu NU, Yavasoglu A, Karasulu HY. 2011. Evaluation of skin permeation and anti-inflammatory and analgesic effects of new naproxen microemulsion formulations. *Int J Pharm* 416(1):136-144.
7. Luger TA, Scholzen TE, Brzoska T, Bohm M. 2003. New insights into the functions of alpha-msh and related peptides in the immune system. *Ann N Y Acad Sci* 994:133-140.
8. Brzoska T, Luger TA, Maaser C, Abels C, Bohm M. 2008. Alpha-melanocyte-stimulating hormone and related tripeptides: Biochemistry, antiinflammatory and protective effects *in vitro* and *in vivo*, and future perspectives for the treatment of immune-mediated inflammatory diseases. *Endocr Rev* 29(5):581-602.
9. Hsu LR, Huang YB, Wu PC, Tsai YH. 1994. Percutaneous Absorption of Piroxicam from Fapg Base Through Rat Skin: Effects of Oleic Acid and Saturated Fatty Acid Added to Fapg Base. *Drug Dev Ind Pharm* 20(8):1425-1437.
10. Oh HJ, Oh YK, Kim CK. 2001. Effects of vehicles and enhancers on transdermal delivery of melatonin. *Int J Pharm* 212(1):63-71.
11. Ogiso T, Shintani M. 1990. Mechanism for the enhancement effect of fatty acids on the percutaneous absorption of propranolol. *J Pharm Sci* 79(12):1065-1071.
12. Andega S, Kanikkannan N, Singh M. 2001. Comparison of the effect of fatty alcohols on the permeation of melatonin between porcine and human skin. *J Control Release* 77(1-2):17-25.
13. Kim MJ, Doh HJ, Choi MK, Chung SJ, Shim CK, Kim DD, Kim JS, Yong CS, Choi HG. 2008. Skin permeation enhancement of diclofenac by fatty acids. *Drug Deliv* 15:373-379.
14. Chi SC, Park, ES, Kim H. 1995. Effect of penetration enhancers on flurbiprofen permeation through rat skin. *Int J Pharm* 126(1):267-274.

15. Goosen C, Laing TJ, Du Plessis J, Goosen TC, Lu GW, Flynn GL. 2002. Percutaneous delivery of thalidomide and its N-alkyl analogs. *Pharm Res* 19:434-439.
16. Tanojo H, Bouwstra JA, Junginger HE, Boddé HE. 1997. In vitro human skin barrier modulation by fatty acids: Skin permeation and thermal analysis studies. *Pharm Res* 14(1):42-49.
17. Aungst BJ, Blake JA, Rogers NJ, Hussain MA. 1990. Transdermal oxymorphone formulation development and methods for evaluating flux and lag times for two skin permeation-enhancing vehicles. *J Pharm Sci* 79(12):1072-1076.

Table 7.1 Composition and physical properties of nanoemulsion formulations of KPV**A) Formulation Composition**

Ingredients	Percent Composition			
	C ₆	C ₈	C ₁₀	C ₁₂
KPV	1	1	1	1
Ethanol	15	15	15	15
Tween 80	30	30	30	30
Caproic acid (C ₆)	15	-	-	-
Caprylic acid (C ₈)	-	15	-	-
Capric acid (C ₁₀)	-	-	15	-
Lauric acid (C ₁₂)	-	-	-	15
Water	39	39	39	39

B) Physical Properties

Formulation	Viscosity (cps)	pH of Formulation	Mean Particle Size (nm)	Polydispersity Index (PDI)	Zeta Potential, (mV)
C ₆	30.20	3.49	15.20	0.53	-15.58
C ₈	35.60	4.45	11.00	0.28	-22.97
C ₁₀	31.60	4.30	9.00	0.43	-23.22
C ₁₂	1066.00	4.34	19.20	0.43	-20.55

Table 7.2 Flux and skin retention data for various ME formulations of KPV**A) Flux Data**

Formulation	Flux ($\mu\text{g}/\text{cm}^2/\text{h}$)		
	PD	MN	MN/PD ratio
C ₆	0.356 ± 0.031	3.728 ± 0.192	10.47
C ₈	1.802 ± 0.084	7.057 ± 0.261	3.92
C ₁₀	1.615 ± 0.092	5.840 ± 0.106	3.62
C ₁₂	0.904 ± 0.086	4.498 ± 0.123	4.98

B) Skin Retention Data

Formulation	Amount of KPV retained (mg/g)	
	PD	MN
C ₆	0.168 ± 0.009	0.312 ± 0.036
C ₈	0.537 ± 0.084	0.614 ± 0.034
C ₁₀	0.779 ± 0.067	0.784 ± 0.039
C ₁₂	0.768 ± 0.079	0.664 ± 0.106

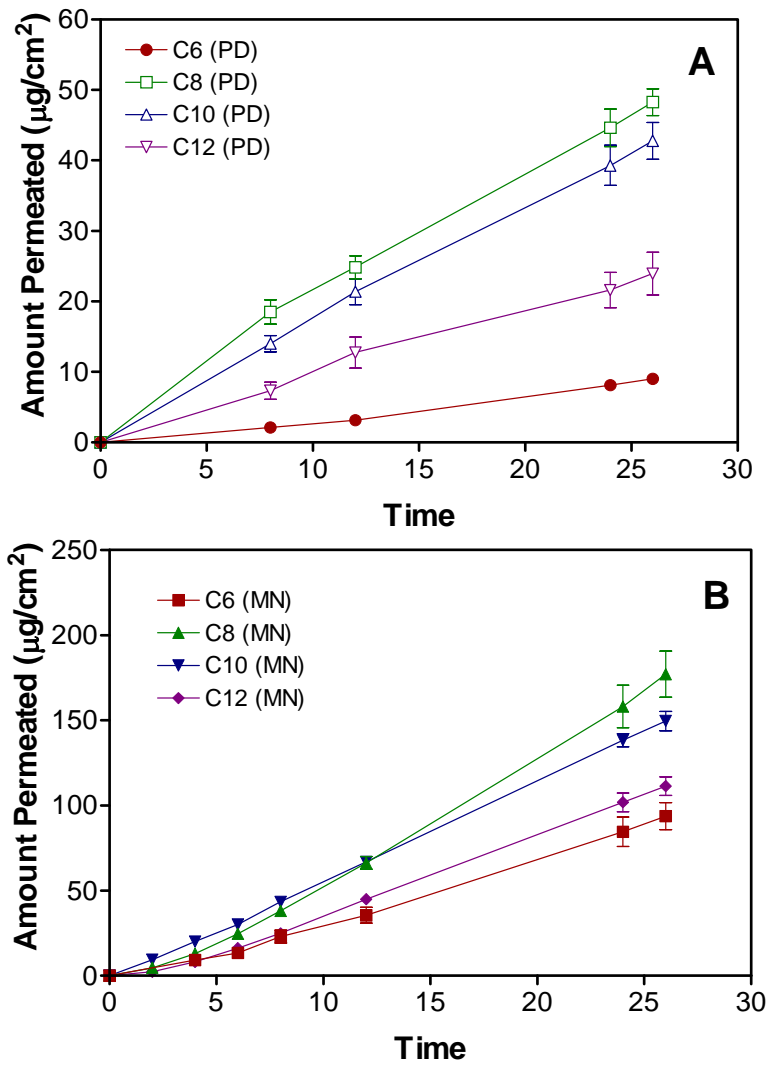


Figure 7.1 Effect of microneedles on the transdermal permeation of various nanoemulsions of KPv across dermatomed human skin. A) Delivery across Normal Skin (PD) B) Delivery across Microneedle Treated Skin (MN)

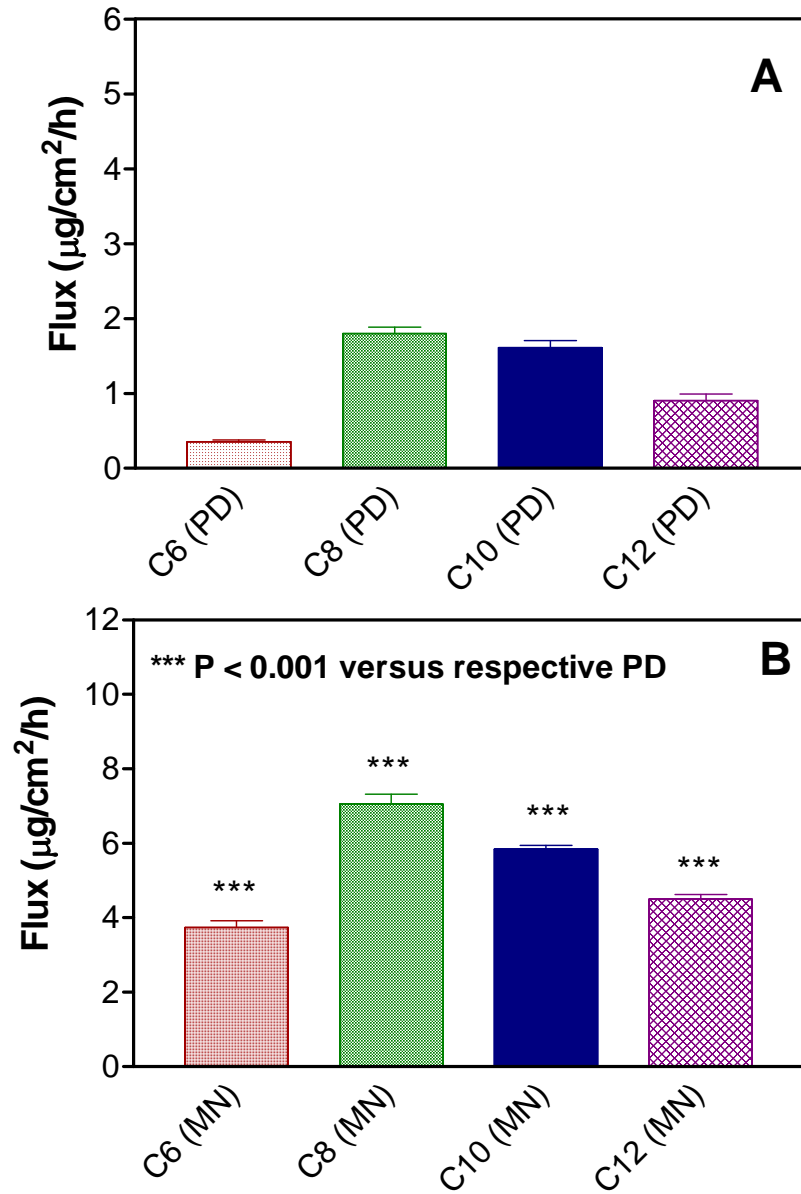


Figure 7.2 Effect of microneedles on the transdermal flux of various nanoemulsions of KPV across dermatomed human skin. A) Delivery across Normal Skin (PD) B) Delivery across Microneedle Treated Skin (MN)

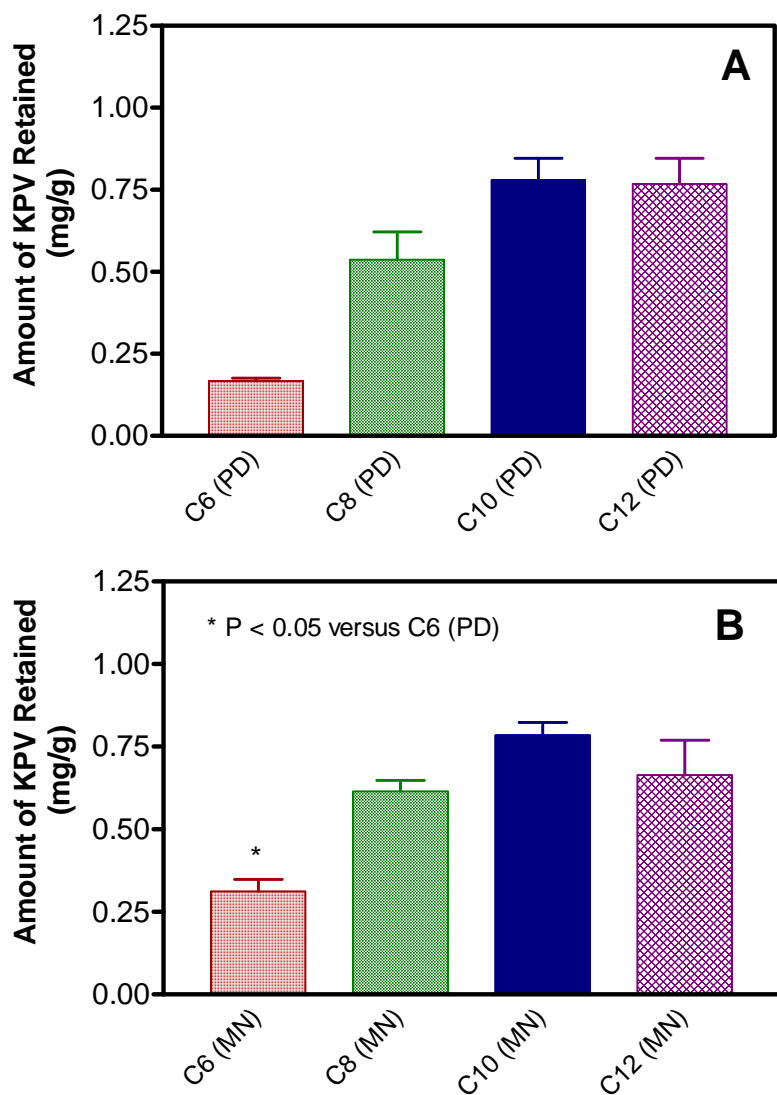


Figure 7.3 Effect of microneedles on the skin retention of various nanoemulsions of KPV in the dermatomed human skin. A) Delivery across Normal Skin (PD) B) Delivery across Microneedle Treated Skin (MN)

8. SUMMARY AND FUTURE DIRECTIONS

Delivery of drugs through the skin remains a challenge, especially for large molecular weight and hydrophilic molecules, due to the barrier nature of stratum corneum. To improve the topical and transdermal delivery of drugs, various active and passive enhancement techniques are used such as microneedles, iontophoresis, sonophoresis, magnetophoresis, thermal ablation, chemical penetration enhancers, synthesis of lipophilic analogues etc. Sometimes, more than one technique is used to achieve an additive or synergistic effect such as a combination of iontophoresis and microneedles. However, the effect of the lipophilicity of the drugs and delivery vehicles on this combination has not been reported.

This dissertation has investigated the effect of lipophilicity of drugs and delivery vehicles on the iontophoretic delivery of therapeutic molecules across dermatomed human skin. The first part of the research was to study the effect of lipophilicity of drugs on their iontophoretic delivery across skin pretreated with microneedles. For this purpose, four model beta blockers with similar pKa values but varied log P values as hydrochloride salts were selected. The selected drugs were: propranolol, acebutolol, atenolol, and sotalol. Skin permeation studies were performed on each drug: 1) passive diffusion (PD) 2) microneedle pretreatment (MN) 3) iontophoresis (ITP) and combination of MN and ITP. Anodal iontophoresis was performed as the drugs attain a positive charge below pH 7.0. It was found that MN and ITP, when used independently, increased the transdermal flux of all four beta blockers as compared to passive delivery (PD). Further, out of the two techniques, ITP was more efficient in enhancing the

delivery. However, when the combination strategy was used, the permeation enhancement was dependant on the lipophilicity of the drug molecules. Combining MN with ITP did not significantly enhance the delivery of lipophilic molecules such as propranolol and acebutolol as compared to ITP alone. However, this combination showed synergistic enhancement in the delivery of the hydrophilic molecules, atenolol and sotalol. This was attributed to the creation of aqueous pathways in the stratum corneum, which facilitate the delivery of hydrophilic drugs to a larger extent than lipophilic drugs. In the case of atenolol and sotalol, where permeation across stratum corneum is a rate limiting barrier due to their hydrophilic nature, any small disruption in this barrier would significantly enhance delivery. These observations were further substantiated by the skin retention data; an inverse relationship between the skin retention and the hydrophilicity of the drug molecule was observed. Thus, it was concluded that the combination strategy of MN and ITP indeed depends on the lipophilicity of the drug and is of more use for hydrophilic drugs than for lipophilic drugs.

Based on our previous knowledge on the the relationship between the lipophilicity of the molecule and skin permeation, we decided to study the skin permeation enhancement of a model hydrophilic peptide, Lysine-Proline-Valine (KPV) using MN, ITP and their combination, ITP+MN. KPV is a low molecular weight peptide but is highly hydrophilic in nature. No detectable levels of skin permeation were noted by passive delivery. MN and ITP, when used alone, significantly enhanced the delivery as compared to PD. Further, the combination of MN and ITP resulted in synergistic effect on the skin permeation of KPV as compared to MN or ITP. This further proves that the combination of MN and ITP results in a synergistic effect for hydrophilic drugs.

Further, to study the effect of lipophilicity of vehicle on KPV delivery, we formulated nanoemulsion with various fatty acid chain lengths (C_6 to C_{12}). It was observed that the skin permeation of KPV was dependant on the lipophilicity of the fatty acids and demonstrated a parabolic relationship between the carbon chain length and transdermal flux. Further, microneedles showed less significant permeation enhancement effect of the fatty acids with increased lipophilicity. The skin retention of KPV increased with the lipophilicity of the fatty acids. With the present results, delivery of KPV can be maximized by using the microneedles technique and fatty acid of appropriate lipophilicity.

The future work is directed to demonstrate the applicability of basic permeation study of KPV across the skin and the effect of lipophilicity of drug and vehicle on the KPV delivery.

i. Topical delivery of KPV can be maximized by formulating a nanoemulsion for its use in the treatment of contact dermatitis in a mouse model. In disease situations like psoriasis and contact dermatitis, the skin is inflamed and stratum corneum is disrupted. The skin permeability in these situations is expected to be much higher. This current work is directed to study the formulations in a disease animal model.

ii. Dermatokinetics of KPV can be studied under the effect of iontophoresis and microneedles using intradermal microdialysis across human skin. This will provide an insight on the kinetics of KPV once delivered across the skin.

iii. Lipophilic prodrugs of KPV can be synthesized using various alkyl esters to further enhance the KPV delivery. The effect can further be maximized using the microneedles, iontophoresis and the combination approach.

APPENDIX: JOURNAL PUBLICATIONS AND CONFERENCE PRESENTATIONS

PEER-REVIEWED JOURNAL PUBLICATIONS

1. **Pawar KR**, Babu RJ, Polymeric and lipid-based materials for topical nanoparticle delivery systems, *Crit Rev Ther Drug Carrier Syst*, 27,419-59, 2010.
2. Jayachandra Babu R, Dayal PP, **Pawar K**, Singh M, Nose-to-brain transport of melatonin from polymer gel suspensions: a microdialysis study in rats, *J Drug Target*, 2011
3. **Kasturi Pawar**, Chandrasekhar Kolli, R. Jayachandra Babu, Effect of lipophilicity of drugs on the iontophoretic delivery across microneedle treated human skin, Manuscript accepted in *J. Pharm. Sci.*
4. **Kasturi Pawar**, F. Smith, R. Jayachandra Babu, Development of stability indicating method for Lys-Pro-Val (KPV) peptide in topical formulations, Manuscript submitted to *Biomed Chromatogr.*
5. **Pawar KR**, Babu RJ, Lipid materials for use in topical and transdermal nanoemulsion carrier systems, Manuscript submitted to *Crit Rev Ther Drug Carrier Syst*.

CONFERENCE PRESENTATIONS

1. **Kasturi Pawar**, Nydeia Wright, Vijaya K. Rangari, R. Jayachandra Babu, Preparation and characterization of chitosan coated magnetic nanoparticles as carriers of paclitaxel, AAPS 2010 Annual meeting & Exposition, Nov 14-18, New Orleans, Louisiana (Poster presentation).
2. **Kasturi Pawar**, Patrick Dayal, Mandip Singh Sachdeva, R. Jayachandra Babu, Characterization of melatonin formulations for nose-to-brain delivery, AAPS 2010 Annual meeting & Exposition, Nov 14-18, New Orleans, Louisiana (Poster presentation).
3. **Kasturi Pawar**, Chandrasekhar Kolli, R. Jayachandra Babu, Stability and degradation profiles of Lys-Pro-Val (KPV) peptide in aqueous solutions, AAPS 2011 Annual meeting & Exposition, Oct 23-27, Washington, D.C (Poster presentation).

4. **Kasturi Pawar**, Yoon Lee, R. Jayachandra Babu, Evaluation of non-crystalline cellulose as an excipient in solid dosage forms, AAPS 2011 Annual meeting & Exposition, Oct 23-27, Washington, D.C (Poster presentation).
5. **Kasturi Pawar**, Yoon Lee, R. Jayachandra Babu, Evaluation of non-crystalline cellulose as an excipient in solid dosage forms, 22nd Annual Graduate Scholars Forum, Feb 28 - Mar 1, 2012, Auburn University, AL (Poster presentation).
6. **Kasturi Pawar**, Chandrasekhar Kolli, R. Jayachandra Babu, Microneedles-assisted iontophoretic delivery of beta blocker drugs, 22nd Annual Graduate Scholars Forum, Feb 28 - Mar 1, 2012, Auburn University, AL (Oral presentation).
7. **Kasturi Pawar**, Chandrasekhar Kolli, R. Jayachandra Babu, Effect of lipophilicity of drugs on the iontophoretic delivery across microneedle treated human skin, AAPS 2012 Annual meeting & Exposition, Oct 14-18, Chicago, IL (Poster presentation).
8. **Kasturi Pawar**, Chandrasekhar Kolli, R. Jayachandra Babu, Effect of lipophilicity of drugs on the iontophoretic delivery across microneedle treated human skin, Research Week 2013, Apr 1-4, Auburn University, AL (Poster presentation).
9. **Kasturi Pawar**, R. Jayachandra Babu, Chandrasekhar Kolli, Transdermal delivery of an anti-inflammatory peptide (KPV) across dermatomed human skin, In Vitro, AAPS 2013 Annual meeting & Exposition, Nov 10-14, San Antonio, TX (Abstract accepted for Poster presentation).
10. Diane Render, Vijay Rangari, Temesgen Samuel, Jay Ramapuram, **Kasturi Pawar** and Shaik Jeelani, Development of drug delivery system using bio based calcium carbonate nanoparticles, Nanotech Conference and Expo 2013, May 12-16, Washington, DC (Poster presentation).
11. Diane Render, Vijay Rangari, Temesgen Samuel, Madan Vig, Jay Ramapuram, **Kasturi Pawar** and Shaik Jeelani, Preparation and evaluation of 5-Fluorouracil drug delivery system for colon cancer, 2013 Southern Cell Biology Research Symposium, June 28, Tuskegee University, Tuskegee, AL (Oral presentation).
12. Diane Render, Vijay Rangari, Temesgen Samuel, Madan Vig, Jay Ramapuram, **Kasturi Pawar** and Shaik Jeelani, Preparation and evaluation of 5-Fluorouracil drug delivery system for colon cancer, 2013 Southern Cell Biology Research Symposium, June 28, Tuskegee University, Tuskegee, AL (Poster presentation).

13. Diane Render, Vijay Rangari, Temesgen Samuel, Madan Vig, Jay Ramapuram, **Kasturi Pawar** and Shaik Jeelani, Preparation and evaluation of 5-Fluorouracil drug delivery system with calcium carbonate nanoparticles, 2013 Materials Research Society Fall Meeting & Exhibit, December 1-6, Boston, MA (Abstract accepted for Oral presentation).